EFFECT OF SHEAR ON MOMENT/ROTATION CHARACTERISTICS OF CONTINUOUS REINFORCED CONCRETE BEAMS.

by

Arunchandra Mitra, M.Phil.(Lond.), D.I.C., B.E.,
C.Eng.(U.K.), M.I.C.E., M.I.Struct.E.

A thesis submitted for the Degree of Doctor of Philosophy in the Faculty of Engineering of the University of London.

Imperial College of Science
and Technology, London.

April, 1971.

ABSTRACT

The thesis is broadly divided into two parts. The first part deals with the pre-yield and post-yield behaviour of two-span continuous rectangular beams. The object of this study is:-

a) to ascertain if the prototype structural system with a uniformly distributed load can be well represented by a point load;

b) to establish which system or systems adequately models the behaviour of the critical section at the beam to column connection for a continuous system;

c) to clarify what is known as "Shear Rotation".

d) to formulate a satisfactory equation of in-elastic rotation for beams failing in flexure.

e) to derive an expression for shear strength of beams after the formation of plasticity in the concrete compressive zone.

The second part investigates the effect of curtailment of longitudinal tension reinforcement on the shear strength of restrained beams, with a view to formulating a practical approach to detailing where longitudinal tension steel is cut off.

For the first part, thirteen two-span point loaded continuous rectangular beams were tested involving the following variables: longitudinal tension reinforcement at the central support section; distance from point of maximum moment to section of zero moment;

and amount of shear reinforcement.

Virtually all the beams had high strength longitudinal reinforcement and plain mild steel shear bars. They all failed either in a "Shearing Mode" or in flexure after the yielding of longitudinal tension bars over the central support section.

To formulate expressions for the increase of ultimate strain and maximum compressive stress of concrete due to the triaxial restraint, five pairs of 100 mm diameter cylinders of varying Height/Diameter ratios were tested to destruction, and subsequently equations were derived from these test results.

For the second group of tests, six rectangular point loaded beams with overhangs on one side were tested, in which the following parameters were varied: cut-off length of longitudinal tension bars and the amount of shear reinforcement.

As in the first series of tests, the longitudinal bars were of high yield quality, and the shear reinforcement of mild steel. The beams failed either in shear or in flexure depending upon the cut-off length of tension bars and the amount of shear reinforcement.

Towards the end of the thesis, serviceability criteria are reviewed and a correlation between the author's test results and the equation formulated by Regan & Placas[78] for shear crack widths is attempted.

ACKNOWLEDGEMENTS

This work was carried out under the supervision of Professor A. L. L. Baker, D.Sc., M.I.C.E., M.I.Struct.E., to whom the author is grateful. The author is also indebted to Dr. P. E. Regan, Ph.D., S.V.R., for his valuable advice throughout the work.

NOMENCLATURE

Only the more general notation appears in the following list; additional notation being defined as it is required.

A_b - bound area of compressive concrete, i.e. area within links.

A_c - compressive area of concrete, i.e. area beyond neutral axis.

A_{sc} - cross-sectional area of longitudinal compression reinforcement.

A_{sq} - cross-sectional area of one member of shear reinforcement.

A_{st} - cross-sectional area of longitudinal tension reinforcement.

b - breadth of rectangular beam

b_r - web breadth of beam (=b in rectangular beam).

c - projection of shear crack length measured along axis of beam.

c_1 - cohesive strength of material.

c' - ultimate neutral axis depth ($=n_u d_1$).

c_t - splitting tensile strength of concrete.

d - overall depth of beam.

d_c - depth to the point at which the crack width is calculated.

d^* - depth from compressed surface to the anchorage of the shear reinforcement in the tensile zone, i.e. to the lowest layer of main steel when stirrups are used and to the layer from which the bars are bent, if bent up bars are used as shear reinforcement.

d_s - depth of flange.

d_1 - depth from compressed surface to the centroid of tension reinforcement.

d_n - depth to the neutral axis.

d_2 - depth from compressed surface to the centroid of compression reinforcement.

D - diameter of concrete cylinders.

D' - diameter of core area.

D_1 - diameter of bound area.

ϵ -apparent longitudinal tensile strain in the concrete at the point considered.

ϵ_c -compressive strain of concrete.

ϵ_{cu} -ultimate compressive strain of concrete.

ϵ_o -strain corresponding to maximum stress of concrete in compression (=0.002).

ϵ_s -steel strain.

ϵ_{st} -steel strain at commencement of strain hardening.

ϵ_y -steel strain at commencement of yield.

ϵ_{su} -strain in steel at ultimate.

E_c -Young's modulus of elasticity of concrete.

E'_s -modulus of strain hardening of reinforcing steel.

E_{st} -Young's modulus of elasticity of steel.

f' -external compressive stress in the concrete.

f_c -maximum concrete compressive stress at yield of tension reinforcement.

f_o -maximum concrete compressive stress (in stress/strain curve).

f_{cw} -compressive stress in web concrete.

f_{ct} -principal tensile stress.

f_{sc} -compressive stress in compression reinforcement.

f_{sq} -tensile stress in shear reinforcement.

f_{st} -tensile stress in tension reinforcement at service load.

f_1 -tensile stress in concrete.

f_{yc} -yield stress in compression reinforcement.

f_{yq} -yield stress of shear reinforcement.

f_{yt} -yield stress of tension reinforcement.

F -slip factor = $c_s.n_u/c_{cu}.(1 - n_u)$.

F_b -bond force per unit length dF_{st}/dx.

F_{cc} -compression force in the concrete.

F_d -dowel force in tension reinforcement.

f -axial stress.

F_i - interlock force at a crack.

F_{sc} - compressive force in compression reinforcement.

F_{sq} - force in shear reinforcement crossing a shear crack.

F_{st} - tensile force in tension reinforcement.

F_w - inclined compression in the concrete.

F_{yc} - yield force in compression reinforcement.

F_{yt} - yield force in tension reinforcement.

H - height of cylinder.

j_s - lever arm factor $=(d_1 - d_2)/d_1$.

K_B - stiffness of the member considered.

$\leq K_1$

or - stiffness of the members connected to the ends (1) or (2).

$\leq K_2$

K_1 ratio of average concrete compressive stress to cube stress of concrete.

K_2 - ratio of depth to the resultant concrete compressive force to the depth of neutral axis.

K_3 - ratio of cube stress to the maximum concrete compressive stress f_o.

K_4 - parameter for influence of type of tensile steel on plastic length.

K_5 - parameter for influence of axial load on plastic length.

K_6 - parameter for influence of grade of concrete on plastic length.

L Length of cylinder.

l_a - internal lever arm (between tension in main steel and compression in the concrete).

l_p - plastic length of the structure.

m - ratio of moduli of elasticity between steel and concrete $(=E_s/E_c)$.

M_{ult} - ultimate moment at the section.

M_{supp} - support moment.

M_s - service load moment.

M_{yield} - yield moment of the section $(=M_y)$

M - bending moment at the section considered.

n - neutral axis factor.

n_o - reference neutral axis factor corresponding to a fully developed stress-block (i.e. concrete strain reaching 0.0035) with the main steel remaining at an elastic state.

$\bar{n}$ - $n_o^2/(n_o + Q.C./M)$ = neutral axis factor at shear-compression failure.

n_u - neutral axis factor at ultimate.

n' - average neutral axis factor $(=(n_{0.002} + n_u)/2)$.

p' - ratio of the volume of binding reinforcement, i.c. one stirrup plus compressive steel to the volume of the concrete bound, i.e. area enclosed by one stirrup multiplied by the stirrup spacing.

p'' - ratio of volume of link to the bound volume of concrete between the link, i.e. bound area times the spacing of links, in the compression zone of concrete.

P_{ult} - ultimate applied load.

P_b - steel ratio at balanced ultimate strength condition in a beam without compression reinforcement.

P_L - line load along the diameter of cylinder.

q - tension reinforcement index = $r_{st} \cdot f_{yt}/U_{cyl}$.

q' - Compression reinforcement index = $r_{sc} \cdot f_{yc}/U_{cyl}$.

q_b - tension reinforcement index for balanced ultimate strength condition = $P_b \cdot f_{yt}/U_{cyl}$.

q_c - nominal transverse stress supported by concrete $(=Q/bd_1)$.

q_{cr} - average shear stress of compressive concrete at critical condition.

q_{ult} - ultimate transverse stress supported by concrete $(= Q_{ult}/bd_1)$.

Q_c - transverse force in the concrete compressive zone.

Q_{cr} - shear force causing shear cracking.

Q_{ult} - ultimate shear strength.

Q - applied shear force.

r_{sc} - A_{sc}/bd_1 = compression reinforcement ratio.

r_{sq} - $A_{sq}/b.s.\sin\alpha$ = shear reinforcement ratio.

r_{st} - A_{st}/bd_1 = tension reinforcement ratio.

Q_a - shear resistance due to arch action.

s - spacing of shear reinforcement measured along axis of beam.

t - clear concrete cover to horizontal reinforcement.

U_{cyl} - cylinder strength of concrete.

U_t - tensile strength of concrete.

U_w - cube strength of concrete.

w - width of loading plate.

w_f - flexural crack width.

$w_{s.h}$ - shear crack width

z - distance from the point of contraflexure (or zero moment) to the section of maximum moment (= M/Qd_1).

α - angle of inclination of shear reinforcement (angle between shear reinforcement and the axis of the member).

β - angle between interlock force F_i and axis of beam.

Δ_{cc} - total deformation of extreme compressed concrete fibre along shear crack.

Δ_{st} - total deformation of tension reinforcement along shear crack.

ϕ - total rotation occuring in a length of beam equal to its effective depth.

ϕ_e - elastic rotation occuring in a length of beam equal to its effective depth.

ϕ_u - rotation at ultimate (= $\psi_u d_1$).

ϕ_y - rotation at commencement of yield (= $\psi_y d_1$).

ψ - average curvature measured over a gauge length d_1, placed symmetrically about the section of maximum moment (= Maxm. Conc. compression strain/neutral axis depth).

ψ' - coefficient of internal friction.

ψ_y - curvature at commencement of yield of tension reinforcement.

ψ_u - curvature at ultimate.

η - factor of shear coverage related to shear reinforcement according to Morsch's analysis.

λ_c - crack width parameter (= f_{yt}/f_{st}).

λ_y - yield safety parameter.

θ -inelastic rotation at the section of maximum moment.

θ_{flex}-inelastic rotation for members failing in flexure.

θ_u -ultimate inelastic rotation in radians.

$\theta_u$cal-calculated ultimate inelastic rotation.

$\theta_u$test-ultimate inelastic rotation from test.

UNITS -unless stated otherwise, all quantities are expressed in S.I.

CONTENTS

Abstract 2

Acknowledgement 4

Nomenclature 5

Contents 11

Chapter 1. Introduction 16

Chapter 2. Review of Past Work 20

2.1 Shear Strength 20

2.1.1 Morsch Theory & Truss Analogy 20

2.1.2 Regan's 'Shear Compression Theory' 22

2.1.3 Placas' 'Shearing Theory' 25

2.1.4 Hill Borg's Plane of Minimum Strength Method 27

2.1.5 A.C.I.-A.S.C.E. Committee 326 on Shear & Diagonal Tension 30

2.1.6 C.E.B. Recommendations 31

2.1.7 Draft British Standard Code of Practice 32

2.1.8 Dowel & Aggregate Interlock Actions 34

2.1.8.1 Dowel Force for Beams with Shear Reinforcement 35

2.1.8.2 Aggregate Interlock Action in Reinforced Concrete Beams 36

2.2 Structural Systems 38

2.3 Rotation 39

2.3.1 Plastic Rotation 39

2.3.2 Shear Rotation 45

2.4 Curtailment of Longitudinal Tension Bars 46

2.4.1 Review of Draft British Standard Code of Practice 46

2.4.2 C.E.B. Recommendations 47

Chapter 3. Experimental Investigation 50

3.1 Series No. 1. Continuous Beams 51

3.1.1 Materials & Fabrication 51

3.1.2 Experimental Programme & Set-Up 57

3.1.3 Instrumentation 58

3.1.4 Procedure 61

3.1.5 Behaviour of Beams 62

3.1.6 Analysis of Test Results 64

3.2 Series No. 2. Restrained Beams. 68

3.2.1 Materials & Fabrication 68

3.2.2 Experimental Programme & Set-Up 70

3.2.3 Instrumentation 70

3.2.4 Procedure 71

3.2.5 Behaviour of Beams. 72

3.2.6 Analysis of Test Results 72

3.3 Series No. 3. Cylinders. 73

3.3.1 Materials & Fabrication 73

3.3.2 Experimental Programme & Set-Up 74

3.3.3 Instrumentation 74

3.3.4 Procedure 75

3.3.5 Analysis of Test Results 75

Chapter 4. Structural System 117

4.1 Moment/Shear Simulation between Pt. Load & U.D.L 117

4.2 Model Systems to Simulate Behaviour of Continuous Support Sections 119

4.2.1 Analysis of Test Results. 119

4.2.2 Review of Other Works 123

4.2.3 Compatibility between Different Findings 125

4.3 Discussion 126

Chapter 5. Rotation 133

5.1 Determination of Plastic Rotation (Flexure) 133

5.1.1 General 133

5.1.2 Determination of f_o & e_{cu} for Unbound Concrete 134

5.1.3 Determination of f_o & e_{cu} for Bound Concrete 137

5.1.4 Determination of Plastic Lengths for Continuous Beams 142

5.1.5 Determination of Plastic Rotation at Support Section 144

5.1.6 Determination of Plastic Length & Rotation for Span Sections .. 145

5.1.7 Comments on the Equation for Plastic Rotation 145

5.1.8 Determination of Rotations & Ultimate Moments in Beams. 146

5.2 Shear Rotation 147

5.2.1 General 147

5.2.2 Analysis of Test Results 147

5.3 Comparisons with Test Results. 150

5.3.1 Summary of Tests 150

5.3.2 Prediction of Results. 153

5.3.3 Comment on Shearing Rotation. 155

5.3.4 Discussion of Results 157

Chapter 6. Shear Resistance 188

6.1 Shear Cracking 188

6.2 Shear Failure. 191

6.2.1 Shear Compression Failure, ... 192

6.2.2 Shearing Failure - Equilibrium Conditions 193

6.2.3 Failure Criterion for Concrete, ... 196

6.2.4 Shear Strength of the Concrete Compressive Zone for Rectangular Beams before Yielding of Main Steel 196

6.2.5 Shear Strength of the Concrete Compressive Zone for Rectangular Beams after Yielding of Main Steel 198

6.2.6 Final Equation for Shearing Failure 199

Chapter 7. Curtailment of Longitudinal Tension Bars 210

7.1 Effect of Shear on the Forces of Longitudinal Tension Bars. 210

7.1.1 Beams Without Shear Reinforcement 210

7.1.2 Beams With Shear Reinforcement 211

7.2 Steel Force Diagram for R.C. Rectangular Beams 213

7.2.1 Beams With Vertical Stirrups 213

7.2.2 Beams With Inclined Stirrups 214

7.3 Steel Force Diagram for R.C. T-Beams 216

7.3.1 Beams With Vertical Stirrups 216

7.3.2 Beams With Inclined Stirrups 216

7.4 Analysis of Results. 217

7.5 Discussio 218

Chapter 8. Serviceability 224

8.1 Limit Crack Width 224

8.1.1 Equations for Flexural & Shear Crack Widths 226

8.1.2 Comparison With Test Results 227

8.2 Limit Deflection 228

8.3 Yield Safety 230

8.4 Serviceability Parameter. 231

Chapter 9. Conclusions, Future Research & Recommendations for Design 235

9.1 Conclusions 235

9.2 Future Research 236

9.3 Design Recommendations 237

References 239

Appendices 250

A. Determination of Stress-Block Parameters 251

A.1 Determination of K_1K_3 251

A.2 Determination of K_2 & K_2/K_1K_3 251

B. Typical calculations for Rotation & Ultimate Moment 252

B.1 Beam No. c.12 252

B.2 Corley's Test. Beam No. M.5 254

B.3 Mattock Test Beam No. D.4 256

C. Calculation of M_{ult} & θ_u for R.C. Beams by Other Methods 258

C.1 Corley's Method 258

C.2 I.C.E. Research Committee Report 264

D.1 Simplified Equation for Rotation 266

E. Expression for Bond Force with Inclined Stirrups 267

CHAPTER 1

INTRODUCTION

For limit state design, it is imperative not only to know the pre-yield and post-yield behaviour of beams, but also the effect of shear on the behaviour of a beam. Hence it is essential to ensure that a beam does not fail rather prematurely in shear during redistribution of moments due to inelastic rotation, and to know the contribution of any extra rotation due to shear to the total plastic rotation. In other words, the design of a beam should be such that sufficient shear reinforcement is provided to enable the beam to develop inelastic rotations to the extent the designer intends.

In order to study these effects, the author tested a series of thirteen point loaded two-span continuous beams, in which the cross-section and concrete strength were intended to be kept constant. Due to practical experimental problems, the applied loading was chosen as point loads. In view of this, and also due to the fact that no simply supported point-loaded systems were tested, it was essential to verify that the structural system with a uniformly distributed load could be well represented by a point load and also that a continuous system could be replaced by a simply supported system or vice versa.

Practical detailing in the design office often demands curtailment of longitudinal tension bars. Hence it was

necessary to investigate the effect of this curtailment on the shear strength of a beam which is provided with a certain amount of shear reinforcement and which needs to develop inelastic rotation to re-distribute moments from one section to another.

To study this, the author carried out a second series of tests, consisting of six point-loaded rectangular beams with overhangs on one side, in which the cross-section and the concrete strength were kept constant.

The experimental details of all the tests carried out by the author are given in Chapter 3. In addition to the two groups of tests on rectangular beams mentioned above, five pairs of cylinders of varying Height/Diameter ratios were tested, to ascertain some stress-strain properties of concrete. In all the tests on rectangular beams, the longitudinal bars were of high yield variety. This was adopted with a view to obtaining shear failures of beams with realistic percentages of longitudinal reinforcement.

Chapter 4 is concerned with the analysis of "Structural Systems". Other authors, who investigated this before, failed to agree amongst themselves. Some authors, like Corley[34] and Mattock[63], simply assumed that a continuous system could be represented by a simply supported system. To clarify this point, the author has attempted a theoretical approach to investigate whether a U.D. load system can be replaced by a point load system, and correlating his experimental results with the predictions from six other theories,

has tried to draw a definite conclusion on the subject.

Chapter 5 is divided into three parts. The first part deals with the inelastic rotation for flexure failures of beams. The second part discusses at length the effect of what is known as "Shear Rotation", and the last part is devoted to a comparison between predictions from three theories, including one derived from the present work, and test results for inelastic rotations from four different sources, including the results of the author. It may be argued that when so much work has been done on plastic rotation, this aspect of investigation by the author is unnecessary, but it should be mentioned in this connection that not many authors had previously taken into account the effect of increase of compressive stress and ultimate strain in the plastic zone of concrete due to triaxial restraint in the evaluation of inelastic rotation, nor did they attempt to check the validity of their results for both systems. The correlation between their predictions and test results were also not exemplary. Though Corley[34] and Mattock[63] somewhat improved this situation by rectifying some of the earlier mistakes of the other authors, their expressions were mainly empirical and had no sound theoretical basis.

In Chapter 6, an attempt is made to evaluate expressions for shear strengths of beams after the formation of plastic hinges. Previous author's' work was limited to behaviour before the yielding of longitudinal tension steel. To assume that the concrete compressive zone of a beam retains the same

shear strength even after the onset of plasticity, is contrary to the test results of the author. Hence, the formulation of an equation for shear strength taking account of inelastic rotation was essential.

Chapter 7 deals with expressions for cut-off lengths of longitudinal tension bars. Previous efforts on this subject were mainly empirical. The most popular approach was to shift the steel force diagram by various degrees. There was no coherent logical approach.

Although ultimate loads are the main criteria of design for shear, it is possible that considerations other than strength may determine the maximum design load in a given case. In the present context, these other considerations are those of serviceability involving control of crack widths. Though considerable attention has been paid to flexural crack widths, very little has been attempted on shear crack widths. Hence the equation promulgated by Regan & Placas[78] for measurements of shear crack widths is compared with the author's results on continuous beams. This work is presented in Chapter 8.

In Chapter 9, a summary of the theoretical and experimental investigation is presented, along with some suggestions for future research and design recommendations.

CHAPTER 2

REVIEW OF PAST WORK

This chapter is devoted to appraisal of some of the published work on the subject of shear strength, structural systems, inelastic rotation of flexural members and the effect of shear on the permissibility/curtailment of bars. In view of the enormity of the subject matter, only a few publications are dealt with.

2.1 SHEAR STRENGTH

2.1.1 Mörsch Theory and Truss Analogy

The theory proposed by Mörsch in the early years of this Century, is the basis of codes of practice in most West European countries.

In this theory, the shear stress at any cross-section in a reinforced concrete member is calculated from equation:-

$$q = \frac{Q}{b_r . la} \qquad \ldots (2.1)$$

Across a vertical section, the shear stress is assumed to be constant and at a maximum between the neutral axis and the tensile steel and to decrease to zero at the extreme compressed fibre following a parabolic path. This equation is based upon the neglect of the tensile resistance of the concrete in bending.

The theory has following limitations:-

a) At flexural cracks, a very large part of the shear force is apparently supported by interlock in the crack beyond the

depth of the neutral axis.

b) If the tensile strength of concrete is substituted in equation (2.1), an overestimate of the shear cracking strength is obtained.

c) It does not take into account the effects on shear strength of the ratio of tension reinforcement, and the ratio M/Qd_1, which other research workers have observed.

Mörsch also suggested that the internal structure of a beam containing shear cracks and shear reinforcement may be represented by an analogous pin jointed truss, in which the concrete acts as a strut and the tension reinforcement as a tie for the two horizontal parallel chords, while for the inclined chords the web reinforcement carries the tensile forces and the web concrete the compressive force. Elaborating the hypothesis, Mörsch established the following two equations.

For beams with vertical stirrups:-

$$Q = A_{sq} \cdot f_{yq} \cdot \frac{la}{s} \qquad \ldots (2.2)$$

For bent up bars inclined at an angle α, the forces are as shown in fig. 2.1 and

$$F_w \cdot \text{Sin}\,\theta_w = A_{sq} \cdot f_{yq} \cdot \text{Sin}\,\alpha$$

and $dF_{st} = F_w \cdot \text{Cos}\,\theta_w + A_{sq} \cdot f_{yq} \cdot \text{Cos}\,\alpha$.

But $$dF_{st} = \frac{dM}{la} = \frac{Q \cdot dx}{la} = \frac{Q \cdot s}{la}$$

Therefore $$Q = A_{sq} \cdot f_{yq} \cdot \frac{la}{s} (\text{Sin}\,\alpha \cdot \text{Cot}\,\theta_w + \text{Cos}\,\alpha) \qquad \ldots (2.3)$$

Putting $\theta_w = 45^\circ$ $$Q = A_{sq} \cdot f_{yq} \cdot \frac{la}{s} (\text{Sin}\,\alpha + \text{Cos}\,\alpha) \qquad \ldots (2.4)$$

This theory neglects the contribution of concrete in resisting shear through an arch action by the inclination of the main compression chord, as well as any dowel or interlock action. Thus it underestimates the shear resistance of a beam in varying degrees.

The assumption by Mörsch that all inclined compressions act at an angle of 45^{o} to the main reinforcement, or that the inclination of shear cracks is 45^{o}, is not supported by the crack patterns of the beams tested by the author as reported in Chapter 3. Placas[70] has also observed this in his series of tests.

2.1.2 Regan's[76] Shear Compression theory

Using a compatibility condition and ultimate strength precepts, Regan has formulated a theory for beams - with or without shear reinforcement - failing in shear compression.

He postulates that in analysing a beam in shear one must determine whether shear cracking would precede flexural failure, and if so, one should investigate the residual strength of the beam containing shear cracks. If the residual strength is found to be less than the shear cracking resistance, failure would occur instantaneously upon the shear cracking. On the other hand, if the strength is greater, an increase of load would take place between shear cracking and collapse. Depending upon the details of the beam, this increase could be sufficient to allow a flexural failure, or if flexural failure were not attained, then a shear-compression failure would take place by

crushing the concrete at the reduced compression zone. One of the main criticisms of this method lies in the fact that the shear failure does not always involve crushing of the compression zone of concrete, as has been observed by Placas[70] in his series of tests on T-beams, and by the author in his tests with rectangular beams, as reported in Chapter 3.

In Regan's approach the following features are significant.

i) In the determination of shear cracking loads and crack propagation, the combination of the actual longitudinal and shear stress at the point in question is used.

ii) The extent of the critical shear crack is governed by the crack propagation condition and is therefore not a fixed value.

iii) Two types of failure of concrete are considered:-

a) A tensile failure as determined by (i) above, i.e. cracking of uncracked concrete. This does not generally constitute a collapse condition, but merely a crack propagation condition.

b) A primarily compressive failure of the whole of the compressive zone by crushing. An average stress block factor of 0.667 and a cylinder strength compression criterion are used for this type of failure.

iv) The collapse load in shear compression is determined by the crack propagation conditions, compatibility conditions and minimum strength considerations.

Shear Cracking

The shear force causing shear cracking has been taken as the product of an average shear stress and the residual uncracked

concrete area at the limit state.

$$Q_{cr} = q_{cr} \cdot n_o \cdot b. d_1 \qquad \ldots (2.5)$$

The value of Q_{cr} is obtained from the known value of n_o.

Equation (2.5) has been modified in a recent paper by Regan & Placas[77] to

$$Q_{cr} = 0.25.bd_1 \left(U_w . \frac{100\ A_{st}}{b_r\ d_1} \right)^{1/3} \leqslant 0.36(U_w)^{1/3} \qquad \ldots (2.6)$$

Shear failure

The above equations give the predicted shear force at the onset of shear cracking. As the shear crack propagates, the extension of the cracks is expressed in terms of the external shear force and the stress in the shear reinforcement. At the ultimate load stage for shear compression failure,

$$Q_{ult} = q_{cr} . \bar{n}\, bd_1 + r_{sq} . f_{yq} . b . c \qquad \ldots (2.7)$$

To establish an expression for $\bar{n}$, a compatibility condition is formulated. This is based upon the fact that the inclination of the compressive force above the shear cracks causes the extreme fibre strain of the concrete to decrease more rapidly than assumed in flexural analysis. Hence considering the total deformation of the extreme compressed fibre and the longitudinal reinforcement along the length of the shear crack, $\frac{\Delta cc}{\Delta st} = \frac{\bar{n}}{1-\bar{n}}$, Regan has obtained the following compatibility relationship:-

$$\bar{n} = \frac{n_o^{\,2}}{n_o + \frac{Q . c}{M}} \qquad \ldots (2.8)$$

From the equilibrium condition for rotation, the following expression for ultimate moment is obtained.

$$M_{ult} = \tfrac{2}{3} U_{cyl}.b.d_1^2.\bar{n}(1 - \tfrac{3}{8}\bar{n}) + r_{sq}.f_{yq}.b.\frac{c^2}{2} \qquad \ldots (2.9)$$

Solutions from above equations give $\frac{Q_{ult}}{n_o.U_{cyl}.bd_1}$ in terms of $r_{sq}.f_{yq}/U_{cyl}$, Qd_1/M, n_o and q_{cr}/U_{cyl}. They are conveniently plotted as graphs of $Q_{ult}/n_o.U_{cyl}.bd_1$ against Qd_1/M, for various values of $r_{sq}.f_{yq}$ & n_o. The influence of q_{cr}/U_{cyl} & $(1 - \bar{n})$ are taken as approximately equal to $\frac{1}{15}$ and 0.8 respectively, for all charts. Graphs are also plotted for $\frac{n}{n_o}$ & c/d_1 against Qd_1/M for different values of n_o.

These charts relate to conditions at any and all sections and can thus serve as a basis for design or analysis of all types of beams containing shear cracks, provided certain detailing restrictions are observed to prevent secondary failures.

When compression reinforcement is present, this is taken into account as affecting the rotational equilibrium equation but not the compatibility conditions. Even so, there is a tendency to overestimate the strength of beams with heavy compression reinforcement and light shear reinforcement.

In a later article along with Placas[70], Regan has improved the above procedure and proposed a simplified design method by considering the rotational equilibrium from figure 6.2. Ignoring interlock action

$$M_u = M_c + M_w \qquad \ldots (2.10)$$

where M_u = Ultimate Shear Compression moment.

M_c = The moment about the main tension steel of the longitudinal compression, balancing the force in the tension steel.

M_w = The moment due to the shear reinforcement crossing the crack and - if inclined shear reinforcement is used - that due to the horizontal force in the concrete balancing $F_{sq}.\cos\alpha$.

In a previous article based upon stress-strain compatibility in the tapered block above the crack, Regan & Placas[78] expressed these terms as:-

$$M_c = M/Qd_1 \cdot d_1/c \cdot m_s \cdot bd_1^2 \qquad \ldots (2.11)$$

where $m_s = 0.8\left(U_w \cdot \frac{100A_{st}}{bd_1}\right)^{\frac{1}{3}}$.

When uniformly spaced vertical stirrups are used, the value of M_w becomes:-

$$M_w = b_r d_1 \frac{r_{sq}.f_{yq}}{2}\left(\frac{c}{d_1}\right)^2 \qquad \ldots (2.12)$$

Equating the derivative $d(M_c + M_w)/dc$ to zero gives the critical crack at which shear strength is a minimum. Substituting this critical length c in equations (2.11) & (2.12):-

$$\frac{Q_{ult}}{bd_1} = \frac{3}{2} m_s^{\frac{2}{3}}.(r_{sq}.f_{yq})^{\frac{1}{3}}.\left(\frac{Qd_1}{M}\right)^{\frac{1}{3}}.\left(\frac{b_r}{b}\right)^{\frac{1}{3}} \qquad \ldots (2.13)$$

If in the above c is greater than the length available for a crack, the latter should be used. If the crack length is less than the spacing of the stirrups, then failure on a plane unreinforced in shear should be considered.

In general Regan's method thus enables calculations to be made for failures occurring in a critical region at the head of a shear crack. Stress conditions in other parts of the beam cannot be directly analysed, but this is of no practical significance and the overall structural behaviour implied is viewed physically as being similar to that of a truss with a sloping compression chord. The inclination of this chord and that of the concrete compression members of the lattice are unknown except at the critical section where c and $\bar{n}$ are calculated. For the conditions of application of this method however, these are never critical.

This method provides a rational link between shear cracking, propagation of shear crack and ultimate failure. Its predictions are substantiated by about one thousand test results predominantly of simple-span rectangular beams, and also the author's test reported in Table 4.1. The basic weakness of this method, as mentioned earlier is its prediction of compression failures at all times and thus it does not describe accurately the physical behaviour of beams failing in other modes and its overestimation of strength of beams with heavy compression steel. It should be noted here that though it predicts not too wide scatter for the author's tests, yet all the beams tested by the author failed in 'shearing".

2.1.3 Placas' "Shearing" theory

In this type of failure the opening of the cracks is mainly due to vertical displacement. According to Placas, the interlock forces at initially steep shear cracks tend to induce additional flatter cracks until the main cracks are inclined at an angle of $\tan^{-1} 0.5$, when vertical stirrups are used and $\tan^{-1} 0.33$, when 45^{o} inclined stirrups are used. At such flat inclinations interlock forces are negligible. The cracks extend up to a height of about 0.75d* in rectangular beams and to the soffit of the flange in T-beams. Measurement of strains in stirrups show that all stirrups crossing such shear cracks

force in the shear reinforcement crossing the crack is:-

$$F_{sq} \cdot \text{Sin}\alpha = 2(d^* - t)b_r \cdot r_{sq} \cdot f_{yq} \quad \ldots (2.14)$$

for T-beams

and $$F_{sq} \cdot \text{Sin}\,\alpha = 1.5d^* b \cdot r_{sq} \cdot f_{yq} \quad \ldots (2.15)$$

for rectangular beams.

In rectangular beams the shear resistance of the concrete is provided by an inclination of the main compression. Using a Coulomb-type failure criterion - proposed by Lichtenberg(60), assuming the area of concrete involved in the failure proportional to the flexural neutral axis depth prior to yield of main steel, and evaluating the numerical constant 0.4 empirically, Placas has suggested the following formula for shearing resistance of a concrete compressive zone:-

$$Q_c = 0.4\left(\frac{100\, A_{st}}{b_r \cdot d_1} \cdot \frac{Qd_1}{M} \cdot U_w \right)^{1/3} bd_1 \quad \ldots (2.16)$$

Placas considers compression reinforcement has no effect on the above mode of failure.

For T-beams the resistance Q_c is provided by the shear stresses in the flange. The longitudinal stresses at the critical region of the flange are low. The failure criterion is expressed empirically in terms of tensile strength of the concrete and an effective flange area,

$$Q_c = 0.8 + (b_r + x) \cdot U_w^{\frac{1}{3}} \quad \ldots (2.17)$$

where x = 150 mm for the range of tests Placas considered.

Substituting the contributions of the concrete and shear reinforcement, the ultimate shear strengths of the members are as

follows:-

$$Q_{ult} = 1.5\ bd^*\ r_{sq}.f_{yq} + 0.4\left(\frac{100\ A_{st}}{bd_1}.\frac{Qd_1}{M}.\ U_w\right)^{\frac{1}{3}}.bd_1 \qquad \ldots (2.16)$$

for rectangular beams,

and $$Q_{ult} = 2b_r(d^* - t)r_{sq}.f_{yq} + 0.8(b_r + x).U_w^{\frac{1}{3}}.t \qquad \ldots (2.19)$$

for T-beams.

The predictions by this theory are compared with the author's test results in Table 4.1, and correlation seems to be within tolerable limits, though all results are unsafe to a varying degree.

The main criticism of this theory lies in the fact that it is valid for beams which fail before the formation of plastic hinges. It is shown later on, that the shear strength reduces considerably once plasticity develops at a critical section. This is why in the author's tests - where all beams developed a certain amount of plasticity - the predictions are unsafe.

2.1.4 Hillerborg's plane of minimum strength method

The empirical expressions suggested by Hillerborg[49] take into account the influence of the ratio of tensile steel as well as the concrete strength. For beams without shear reinforcement his proposals are in the form of design equation:-

$$Q_{cr} = K_1'.q_1.b.la \qquad \ldots (2.20)$$

where q_1 = permissible shear stress in Swedish Code

K_1' = factor related to the permissible stresses in

longitudinal steel in Swedish Code.

For beams with shear reinforcement, the following equation is suggested by Hillerborg:-

$$Q_{ult} = Q_c + Q_w \qquad (2.21)$$

where Q_{ult} = external shear force across any inclined plane.

Q_c = shear force supported by concrete

$$= 4.2 \sqrt[3]{U_w} \cdot \sqrt{100\frac{A_{st}}{b_r d_1}} \cdot \frac{d_1}{c} \cdot b_r d_1 \text{ , all in kgf \& cm}$$

Q_w = shear force supported by shear reinforcement

$= r_{sq} \cdot f_{yq} \cdot c\,br/2$ for vertical stirrups.

The weakest and therefore critical plane is that for which the right hand side of equation (2.21) has its least value. If this least value is a mathematical minimum, we have:-

$$\frac{d\,Q_{ult}}{dc} = -4.2 \sqrt[3]{U_w} \sqrt{\frac{100A_{st}}{b_r d_1}} \cdot \frac{d_1}{c^2} \cdot b_r d_1 + r_{sq} \cdot f_{yq} \cdot \frac{b_r}{2} = 0$$

From which $\frac{c}{d_1} = \left(\frac{r_{sq} \cdot f_{yq}}{2} / 4.2\sqrt[3]{U_w} \cdot \frac{100\,A_{st}}{b_r d_1} \right)^{\frac{1}{2}}$

which in turn gives:-

$$\frac{Q_{ult}}{b_r d_1} = \left(8.4 \cdot U_w^{\frac{1}{3}} \cdot \left(\frac{100A_{st}}{b_r d_1}\right)^{\frac{1}{2}} \cdot r_{sq} \cdot f_{yq} \right)^{\frac{1}{2}} \qquad \ldots (2.22)$$

If the value of (c/d_1) obtained as above is greater than the longest possible inclined plane - e.g. if "c" is greater than the distance from the section considered to a simple support - then the critical length is the greatest possible one. In the case of a simple point loaded beam, this is the shear span "z", then

$$\frac{Q_{ult}}{b_r d_1} = 4.2 \sqrt[3]{U_w} \sqrt{\frac{100A_{st}}{b_r d_1}} \cdot \frac{d_1}{z} + r_{sq} \cdot f_{yq} \cdot \frac{z}{2} \frac{b_r}{} \qquad \ldots (2.23)$$

In the case of a continuous beam the greatest possible crack length is taken to extend a distance equal to d_1 beyond a point of contraflexure.

Regan has shown that this theory gives rather good correlation with most test results, which has also been substantiated by the author's results presented in Table 4.1. But it has also been observed by Regan [76] and BSG Report [15] that these predictions become unreliable for beams having larger values of A_{st}/bd_1.

This method was developed for closely spaced stirrups, and only half the stirrups crossing the critical plane are taken to be contributing to shear resistance, i.e. to the stirrups crossing the part of the critical plane lying in the compressed zone of the beam are neglected.

The effects of concrete strength and ratio of tension steel have been incorporated. The loss of strength due to curtailment can therefore be evaluated by taking account of reduced value of A_{st}/bd_1.

The equation does not take into account any effect of compression steel or compression flanges on the shear strength. It can be used with good approximations in beams reinforced with bent up bars by substituting $r_{sq} = A_{sq}/b\,s\,\mathrm{Sin}\,\alpha$.

The main interest lies in the fact that this method tries to get away from the concept of a fixed crack angle, implying a fixed direct contribution of the shear reinforcement. The main criticism of this method is its implied generality in expressing the shear strength always in terms of equations of transverse forces. For

beams failing in shear compression, this principle does not hold good. This method is not applicable as such to the analysis of diagonal tension failures of beams failing upon shear cracking.

2.1.5 A.C.I.-A.S.C.E. Committee 326 On Shear & Diagonal Tension

The Committee report recommends a semi-empirical formula for evaluation of shear strength on the basis of following assumptions:-

a) The distributions of longitudinal tensile stresses and shear stresses over the cross-section are not known. The unit shear stress may be expressed by the average stress over the cross-section, i.e. $q = \frac{Q}{bd_1}$.

b) The shear cracking load should be considered as the ultimate load for the beams without shear reinforcement.

c) The shear cracking is caused by the principal tensile stress, which for any point in the beam can be evaluated as:-

$$f_{ct(max)} = 0.5\, f_t + \sqrt{(0.5\, f_t)^2 + q^2} \qquad \ldots (2.24)$$

d) The diagonal tension cracking occurs when $f_{ct(max)}$ exceeds the tensile strength of concrete.

e) The tensile strength of concrete is proportional to the square root of its cylinder crushing strength.

f) The modulus of elasticity is constant and are proportion to $(U_{cyl})^{\frac{1}{2}}$.

g) The tensile stress f_t is proportional to the tensile stress in the main steel.

From these assumptions and empirical adjustments the average critical shear stress is expressed as:-

$$\frac{Q}{bd_1} = 1.9\sqrt{U_{cyl}} + 2500.\frac{A_{st}}{bd_1}.\frac{Qd_1}{M} \lesssim 3.5\sqrt{U_{cyl}}$$

where units are in lb.inch. $\ldots (2.25)$

The values of 1.9 and 2500 are constants deduced from experiments. The following limitations are imposed on this equation.

a) If $z > 2d_1$ the equation shall not be applied within a length equal to d_1 of either end of the length z.

b) If $2d_1 \geq z \geq 0.75d_1$ the equation shall apply only at middle of length z.

c) If $z<0.75d_1$ this eqn. does not apply, but the limitation $Q \leqslant 3.5\sqrt{U_{cyl}}$ applic

The above equation has been extended to beams with shear reinforcement by adding the contribution of shear reinforcement on the basis of the Morsch truss analogy.

$$Q/bd_1 = 1.9\sqrt{U_{cyl}} + 2500 \frac{A_{st}}{bd_1} \cdot \frac{Qd_1}{M} + K.r_{sq}.f_{yq} \leqslant 8\sqrt{U_{cyl}} \quad \ldots (2.26)$$

Equation (2.26) where $K = \sin\alpha(\cos\alpha + \sin\alpha)$ is considered to be valid if the following conditions are satisfied:-

1) The inclination "α" of shear reinforcement shall not be lèss than 30°.

2) For rectangular and I sections with vertical stirrups,

$$\frac{Q}{bd_1} \not> 8\sqrt{U_{cyl}}$$

3) For T, I and rectangular sections, in which "α" is less than 70° or rectangular or I sections where $\frac{2}{3}$ of the total shear is carried by the bent-up bars,

$$\frac{Q}{bd_1} \not> 10\ U_{cyl}$$

4) $K\ r_{sq}.f_{yq} \not< 60$ psi.

5) Shear reinforcement shall not have a design value of $f_{yq} \not> 60{,}000$ psi, and shall be carried up to a distance d_1 beyond the point it is actually required.

6) Longitudinal reinforcement, terminated in a tensile zone of concrete, shall be extended a distance equal to the effective depth of the member plus an anchorage length, beyond the point at which it is no longer needed to resist flexural stresses.

The limitations of Q_{ult}/bd_1 to 8 and $10\sqrt{U_{cyl}}$ and of f_{y_q} to 60,000 psi are intended to avoid failure occurring prior to the yielding of the shear reinforcement.

The extension of the main tensile reinforcement allows for the extension of high tensile forces caused by both the arch and truss actions.

The method is entirely empirical and can only really be judged in comparison with test results (e.g. table 4.1). Theoretically it is difficult to see why the shear resistance of the concrete should remain unaltered by shear cracks which greatly reduce the area of concrete. None the less, as for the author's tests, Regan[76] has also found quite good correlation between prediction and test results.

This method does not consider the effect of compression reinforcement or the contribution of compression flanges in resisting shear and underestimates the significance of the ratio of main reinforcement.

2.1.6 C.E.B. Recommendations

For all normal beams C.E.B. requires a minimum of 0.25% of web reinforcement for plain mild bars and 0.14% for high yield bars. Provisions are given to avoid web crushing and other secondary failures, but the provisions relevant here are those concerned with web reinforcement.

The requisite shear reinforcement is calculated from the following equations:-

$$r_{sq} = \eta \, r_{sq\,m} \qquad \ldots (2.27)$$

where $r_{sq,m} = \dfrac{1.15\, q^*}{f^*_{yq}(\mathrm{Sin}\alpha + \mathrm{Cos}\alpha)\mathrm{Sin}\alpha}$

where asterisk denotes design values,

and η = reduction coefficient as follows:-

$$\eta = \frac{1 - 0.125\sqrt{U^*_{cyl}}}{q^*}\left(0.50 + 33.\frac{A_{st}}{b_r d_1}\right) \qquad \ldots (2.28)$$

where the value of the bracketed term must not exceed unity and both q^* and U^*_{cyl} are expressed in N/mm^2.

Rewriting equations (2.27) and (2.28) gives the following -

$$1.15q^* = r_{sq} f^*_{yq} (\text{Sin}\alpha + \text{Cos}\alpha) \text{Sin}\alpha + 0.575\sqrt{U^*_{cyl}}(0.5+0.33 r_{st})$$

$$\frac{Q^*}{b_1 d_1} = 0.87 r_{sq} f^*_{yq} K + 0.125\sqrt{U^*_{cyl}}(0.5+0.33 r_{st}) \quad \ldots (2.29)$$

Allowing for a partial safety factor of 1.5 on the concrete term,

$$\frac{Q_u}{b_1 d_1} = 0.87 r_{sq} f_{yq} K + 0.15 U_{cyl}(0.5+0.33 r_{st}) \quad \ldots (2.30)$$

This method is merely a more conservative version of the A.C.I.-A.S.C.E. recommendations. The manner in which the effect of the main reinforcement is taken into account is to be preferred, in as much as it is done by way of a multiplying factor and not a separate additive term. The results of the author's tests are compared with this recommendation in Table 4.1.

2.1.7 Draft British Standard Code of Practice (38)

The new shear clauses of the code (draft) are based upon the proposals of the report of the Shear Study Group of the Institution of Structural Engineers. The approach of the draft shear clause is based on the following assumptions:-

I) The reduced compression zone at the head of a critical shear crack attains its maximum resistance at failure under a biaxial state of stress, i.e. shear and axial compression.

II) The shear reinforcement crossing the critical shear crack attains

its yield stress at the ultimate limit state and is sufficiently anchored and bonded.

III) Failure by web-crushing or other secondary mode is avoided.

Based on these assumptions a semi-empirical approach, similar to that of the A.C.I.[3] has been adopted and the following equations recommended:-

$$\frac{Q_{ult}}{b_r d_1} = Kq_c + 1.1\, r_{sq}.f_{yq} \qquad \ldots (2.31)$$

where $K\, q_c$ is the nominal shear stress for the concrete taking account of the ratio of A_{st}/bd_1, & of z/d_1 if less than 2.0.

This equation is further modified to include a partial safety factor of 1.25 and for the design purposes becomes:-

$$\frac{Q_{ult}}{b_r d_1} = 0.8\, Kq_c + 0.87\, r_{sq}\, f_{yq} \qquad \ldots (2.32)$$

The following limitations are observed:-

a) The upper limit for q_{ult} is $4K\, q_c$.

b) The minimum value of $0.87\, r_{sq}.f_{yq}$ i.e. minimum amount of shear reinforcement is fixed at $0.4N/mm^2$.

c) The spacing of shear reinforcement along the axis of a beam should not exceed $0.75\, d_1$.

d) The shear reinforcement provided in the beam must be anchored adequately.

Regarding this Code, the following observations are made:-

1) The new clause is simple to use and can be applied to the majority of practical design problems.

2) The experimental investigations reported by Regan[76], Placas[70], Khan[55] & the author confirm that the shear

reinforcement does reach its yield stress before failure and hence assumption (II) is justified.

3) The upper limit of $q_{ult} = 4.Kq_c$ eliminates failures by web crushing.

4) The Code equations take account of the influence of the ratio of tensile reinforcement and the strength of concrete on the shear strength. The influence is incorporated in the values of q_c which are tabulated against concrete cube strength and the ratio of tension steel.

5) The minimum value of $0.4N/mm^2$ is necessary to facilitate redistribution of stresses at shear cracking,

6) The Code equation is used to predict results of the author's test. The results give good correlation with the recommendation. Khan[55] and Placas[70] have also observed this.

As a footnote to all the existing theories with which the author has compared his test results, it should be mentioned that the best possible correlation , and at the same time safe predictions, are obtained from the Draft British Code. None of its predictions is unsafe, and except Beams C.6 & C.11, none too conservative like the C.E.B. recommendations. This does not necessarily imply that the Draft British Code is the most logical of all the theories mentioned above. It is in a sense an empirical method like the A.C.I.-A.S.C.E. & C.E.B. recommendations.

2.1.8 Dowel and Aggregate Interlock Actions

Although they differ in the concept of the mechanism through

which shear is carried in a reinforced concrete beam - e.g. truss, tied arch, multiple arches etc. - the above theories agree that the main contributors to shear resistance are the compressed concrete and shear reinforcement. As a result the possible contributions of the dowel action of the longitudinal tension reinforcement and the aggregate interlock have been ignored. In the opinion of the writer, their influence may be of some importance in beams without shear reinforcement failing in diagonal tension, but their usefulness in beams with shear reinforcement is open to question as will be evident from the following discussion.

2.1.8.1 Dowel force for beams with shear reinforcement

Near the ultimate load stage of a beam with stirrups, it is the stirrups that resist the tearing along the main steel. A part of such a beam containing a shear crack is shown in figure 6.3. Towards the ultimate load stage, the principal shear crack is so wide that interlocking of aggregates across it may be neglected. Shear can thus be transferred across the line ABC by the following:-

i) The concrete beyond the crack;

ii) The shear reinforcement crossing the shear crack;

iii) The dowel element below the shear crack.

In solving the complex compatibility and equilibrium conditions governing the above systems, most shear theories neglect dowel forces.

Baumann[17] in 1968 tested simply supported beams with stirrups to investigate the effect of dowel action. Part of the tension zone of his test beam was cast separately from the rest of the beam and was connected only by the tensile reinforcement. The load was applied on the tension part of the beams. He presented the results

in the form of load deflection curves, where the load represents the dowel force and the deflection the displacement across the preformed crack. At the cracking stage the deflection generally increases rapidly for no increase of load. The ability of the structures to sustain increases of load hereafter is dependent on the presence of stirrups capable of supporting the vertical tension. The ability of a stirrup to do this is increased if it is close to the preformed crack and to a lesser extent, if the dowel element is stiff. The second stage of the load deflection characteristic, generally following after a considerable increase of deflection with the dowel force equal to the dowel force causing cracking, was observed to conform to a parabolic curve, a function of the distance from the preformed crack to the first stirrup. The addition of further stirrups was found to have no appreciable effect.

The general conclusion that can be drawn from Baumann's tests is that very large vertical displacements - larger than those occurring in normal beams - are required in order for a dowel force of any appreciable magnitude to be developed, with the exception of the force that can be transferred to one stirrup very close to the start of the crack.

The above indication concerning dowel action in beams with stirrups seems to be confirmed by similar dowel tests by Arroyo[9] as well as by measurement of stresses in stirrups beyond the lower end of critical shear cracks in the tests of normal beams reported by Placas[70].

2.1.8.2 Aggregate Interlock action in reinforced concrete beam

Measurements reflecting the behaviour of flexural cracks in

tests of beams subjected to bending and shear indicate that not only do the cracks open progressively as the moment is increased, but that displacements parallel to the line of the cracks also occur. Depending upon the roughness of the surface of the crack, the vertical displacements are such that parts of the opposite sides of the crack may touch and carry force across the crack.

The existence of aggregate interlock action in beams subjected to shear was first demonstrated by Paulay & Fenwick[67], through tests of a beam without shear reinforcement provided with crack initiators and by direct aggregate interlock tests on small concrete block specimens. It is of interest to note that in the tests of the concrete specimens, a diagonal crack developed when the shear force across the initial crack was sufficiently increased. The authors point out that diagonal tension cracks similar to those formed in these test specimens may be seen in tests of normal beams and are referred to by them as aggregate interlock cracks.

The results of these tests can only be termed tentative, but they indicate that prior to diagonal tension failures in normal beams 50% to 60% of the shear force may be carried by interlock actions. The authors consider that aggregate interlock depends on the following parameters, although no attempt to investigate them thoroughly was made.

a) The shear force transmitted by one aggregate particle is likely to be proportional to the contact area between the particle projecting across the crack and the concrete on the far side of the crack.

b) The contact area is reduced when the width of a crack increases.

c) The number of significant particles projecting across a crack must depend on the grading of aggregates.

d) The deformation characteristics of the cement mortar matrix will be influenced by the strength of the concrete and probably by the water and air content of the mix.

e) Different responses must be expected with respect to load application to individual particles, depending upon the direction of the applied load and the position of the particle in the freshly placed concrete.

Although the question of interlock action seems to be quite important in the formulation of any rational theory for the calculation of beams without shear reinforcement failing in diagonal tension, the research done so far in this domain does not allow this effect to be taken into account other than empirically.

No research - to the knowledge of the author - has been done in connection with beams provided with shear reinforcement, for investigating the effect of aggregate interlock. However, it is observed that the beams in this group, which fail in shear, usually induce rather large openings of cracks near the failure stage of loading. The influence of interlock for such large openings should not be nearly as significant as is observed for diagonal tension failures of beams without stirrups.

2.2 Structural Systems

Review of other works is dealt with at length in Section 4.2.2

of Chapter 4 of this thesis. Further comment in this chapter is unwarranted.

2.3 Rotation

Inelastic rotation at plastic hinges is discussed in the following paragraphs - so-called "Shear Rotation" is reviewed at the end of this section.

2.3.1 Plastic Rotation

The experimental investigations into the plastic behaviour of steel structures in the early 30's by Leibnitz and later by J.F. Baker & Others[13] laid the foundations for a rational basis of safety analysis based on the collapse state of structures. This has been later developed into the Rigid-Plastic Theory, which is also referred to as "Limit Design" due to the upper and lower bound limits of the collapse load factor.

This theory is simple in its application and for continuous beams and portal frames accurate enough for practice. However, for structures with high axial loads, the instability effects may seriously affect the limits on the collapse load factor, as the collapse mode may be altered due to the deterioration of the structural stiffness with the formation of a few local hinges before complete mechanism conditions are reached. The main difficulty in extending this method to reinforced concrete design was the uncertainty of the degree of plasticity of reinforced concrete members. It was also known in the early days that when concrete commences to crush at critical sections due to excessive strain, the strength of the section tends to

decrease, which was contrary to the basic assumptions in the plastic theory.

A method reconciling the limited plasticity in reinforced concrete was put forward by A. L. L. Baker[11] in 1949. He suggested that the classical Muller Bresleau equations for hinge rotations in a statically determinate structure could be used as a basis for an elasto-plastic method of design for reinforced concrete structures. Statical determinacy in a hyperstatic structure was attained by the introduction of suitably placed "plastic hinges".

This theory, known as "Ultimate Load Theory", is based on an elasto-plastic idealisation of the moment-rotation characteristics of reinforced concrete members. The design procedure involves trial and adjustment of the plastic hinge moments to obtain compatible hinge rotations, which must also lie within specified permissible limits.

Extensive research has been carried out on the properties of plastic hinges in reinforced concrete member by Cham[31], Soliman[89], Poolagasundaranayagam[68], Baker & Amarakone[12], Roy & Sozen[84], Szulczynski & Sozen[93], Corley[34] and Mattock[63].

Szulczynski & Sozen[93] carried out a series of tests on rectangular prisms with transverse reinforcement only. The amount of transverse reinforcement was varied by varying the diameter of the binders and the shape of the concrete cross-section; the spacing of the binders was kept constant. The effectiveness of the transverse reinforcement on the strength

was expressed by an equation as given below.

$$f_1 = f_c + \Delta f \qquad \ldots (2.33)$$

where $\Delta f = 1.8 \dfrac{p'' f_{yq}}{\left(\dfrac{b_1}{d_1} + \dfrac{d_1}{b_1}\right)}$

where f_1 = confined concrete strength

f_c = compressive strength of unconfined concrete

b_1 = breadth of bound concrete section

d_1 = depth of bound concrete section.

It is worth mentioning here that in obtaining this expression the f_1 values were calculated by dividing the maximum load by the concrete area within transverse reinforcement. Δf values were defined as the difference between the net strength, f_1, and unconfined strength obtained from a plain speciment tested with each set. Yamashiro and Siess[100] compared test results with the predictions of equation (2.33) and obtained a wide scatter. They recommended that the expression for calculating Δf values should be altered to

$$\Delta f = 1.8\, A_{sq} . f_{yq} \left(\frac{b_1 + d_1}{b_1 d_1 s}\right) = 0.9 p'' f_{yq} \qquad \ldots (2.34)$$

Roy & Sozen[84] tested a series of concentrically loaded rectangular specimens reinforced with various amounts of transverse and longitudinal reinforcement. From a consideration of their test results and the results obtained from the tests carried out by Szulczinski, Roy & Sozen[84] concluded that the effect of the rectangular transverse reinforcement on the gross

strength of the confined concrete can be neglected, but the effect on the deformation capacity is quite considerable. The ductility of the confined material is increased by increasing the amount or decreasing the spacing of transverse reinforcement. An increase in the concrete strength slightly decreases the ductility of the confined concrete. The other variables such as the diameter of the transverse reinforcement, the amount of longitudinal steel, or the shape of the concrete cross-section have little or no effect on the ductility. On the basis of these findings, they suggested that the stress-strain relationship of confined concrete can be expressed conservatively by means of two straight lines - one rising from zero to a peak value maximum compressive stress at a strain of 0.002, and then falling to reach half the value of maximum compressive stress at a strain of e_{c50} where e_{c50} is given by the following equation:-

$$e_{c50} = 0.75 \frac{p'' b_1}{s} \qquad \ldots (2.35)$$

The slope of the falling line varies depending upon the amount and spacing of the transverse reinforcement.

Chan[31] in his experimental investigation aimed to obtain information about the properties of confined concrete in flexure by testing eccentrically loaded prisms. Rectangular prisms and cylinders reinforced with various amounts of longitudinal and transverse reinforcement were tested. The following expressions were proposed relating the increase in strength and the ultimate strain observed to the amount of transverse reinforcement.

For rectangular transverse reinforcement:-

$$p'' = 0.189(K_u - K_o)^2 \qquad \ldots (2.36)$$

$$p'' = 14600(e_{cu} - e_c)^3 \qquad \ldots (2.37)$$

For circular transverse reinforcement:-

$$p'' = 0.0375(K_u - K_o)^2 \qquad \ldots (2.38)$$

$$p'' = 4970(e_{cu} - e_c)^3 \qquad \ldots (2.40)$$

where $K_u - K_o$ = Increase in concrete strength as a ratio of the cube strength.

$e_{cu} - e_c$ = Increase in ultimate strain.

Chan also proposed a theoretical stress-strain relationship for confined concrete, but no comparison was made between the proposed relationship and the results obtained from tests.

Baker and Amarakone[12] suggested the stress-strain relationship shown in fig. 5.2, i.e. reaching the maximum concrete compressive stress at a strain of 0.002. This was obtained on the basis of a statistical study of the results obtained from concrete members, subjected to pure bending or combined bending and axial load, and reinforced with different amounts of longitudinal and transverse reinforcement. In this relationship, the rising part of the curve is assumed parabolic with a maximum compressive stress equal to:-

$$f'_o = U_{cyl}\left(0.8 + \frac{0.1}{n_{ult}}\right) \not> U_{cyl} \qquad \ldots (2.41)$$

The stress then remains constant until a limiting strain value which can be calculated using the following equation:-

$$e_{cu} = 0.0015\left(1.45 + 150p'' + (0.7 - 10p'')\frac{1}{n_{ult}} - \frac{U_{cyl}}{104}\right) \not> 0.01 \qquad \ldots (2.42)$$

The effect of transverse reinforcement is accounted for by the parameter (p'') which is equal to the volume of transverse reinforcement divided by the volume of concrete under compression.

It has been observed[12] that equation (2.42) estimates the ultimate strain for bound concrete conservatively. They proposed

$$\theta_p = 0.8(e_{cu} - 0.002)K_1''K_3'' \frac{z}{d} \qquad \ldots (2.43)$$

where K_1'' = 0.7 for mild steel and 0.9 for cold worked steel

K_3'' = 0.6 for U_w = 6000 psi and 0.9 for U_w = 2000 psi.

Later Ammakone[12] modified equations (2.42) & (2.43) to following:-

$$e_{cu} = 0.0015\left(1 + 1.5p'' + (0.7 - 0.1\,p'')\frac{1}{n_{ult}}\right)$$

and $\theta_u = 2.4(e_{cu} - 0.002)$ ... (2.45)

The basic approach to the problem of inelastic rotation used by Bremner[18], Poologasundran[68], Soliman[89], etc. is similar to that enunciated by Ammakone[6], hence they are not discussed in greater detail here.

In the U.S.A., Mattock formulated equations for calculating ultimate strain and inelastic rotation which were subsequently improved by Corley. Corley's approach is discussed at length in Appendix C. It may be mentioned here that his predictions were based on test results from simply supported point loaded systems. Since Mattock's work was similar to Corley's, the details of it are not given here.

2.3.2 Shear Rotation

Rao[72] tested five simply supported single span beams. Two of the beams were tested under point loadings at third points and the remaining three had central point loading only. The percentage of longitudinal tension steel was 1.33 . The cross-section of the beams was 200 mm x 400 mm deep.. The cube strength of the concrete was 35 N/mm^2?

He concluded that:-

i) The deformation characteristics of the concrete compressive zone obtained in prism tests are consistent with the ultimate curvature observed in beam tests, if in both cases approximately equal gauge lengths were used.

ii) The moment curvature relationship for pure flexure was applicable to sections subjected to moment and shear up to the yield moment and also so long as the magnitude of the shear force was so small that diagonal shear cracks did not develop in the structure.

iii) With shear forces larger than those causing diagonal tension cracks an additional rotation occurred under the influence of the shear force much before the yielding of longitudinal tension reinforcement.

iv) The additional rotation was a function of the shear force and was of such magnitude that it could not be neglected in the deformation calculation for statically indeterminate structures under loads greater than working loads.

These conclusions are discussed further in section 5.3.

2.4 CURTAILMENT OF LONGITUDINAL TENSION BARS

Lack of published literature on the effect on shear strength of beams with stirrups due to curtailment of longitudinal tension reinforcement makes it almost impossible to discuss other works on this subject. A little information available in regard to steel force diagrams or measured strains in longitudinal tension steel - both of which indirectly relate to the effect of curtailment of tension bars - is discussed along with the main investigation in Chapter 7. Hence, the present review is limited to appraisal of the existing codes of practice in relation to cut-off of longitudinal tension steel.

2.4.1 Review of Draft British Standard Code of Practice

Except at end supports every bar should extend beyond the point at which it is no longer needed to resist flexural stress for a distance equal to the effective depth of the member or twelve times the size of the bar, whichever is greater. The points at which the reinforcement is no longer required may be taken as being where the moment of resistance of the section, considering only the continuing bars, is equal to the required moment.

In addition, no reinforcement should be cut-off in a tension zone unless one of the following conditions is satisfied.

1) the cut-off bars extend an anchorage length appropriate to their design strength (0.87 fy.) from the point at which they are no longer required to resist flexural stress.

2) the shear capacity at the section where the reinforcement is cut-off is greater than twice the shear force actually present.

3) The continuing bars at the section where the reinforcement is cut-off provide double the area required for flexure.

4) the continuing bars at the section where the reinforcement is cut-off provide double the perimeter required for flexural bond.

One or other of these conditions must be satisfied for all possible bending moment distributions corresponding to conditions at the limit state of collapse.

The above propositions which are similar to A.C.I.-A.S.C.E. recommendations, are presumably based upon test results not known to the author. Assuming these are empirical deductions; the question remains as to why such arbitrary values are chosen, e.g. Clause (2) the shear capacity must be greater than twice not three times or even two and a half times. This is also applicable to clauses (3) & (4). Research by various workers has established that the steel force diagram does not follow the bending moment diagram and any extra allowance either in the form of increasing the shear strength of beams, i.e. clause (1); or increasing the area of tension reinforcement thus reducing steel force per bar at the section of curtailment, i.e. clause (2), certainly serve to off-set the impact of curtailment. But the degree of impact for various types of applied loading is left unanswered. These limitations also singularly lack any sound theoretical basis, and do not explain the internal mechanism of beams before or after the formation of shear cracks.

C.E.B. Recommendations

As a general rule, the force in the tension steel of a beam is evaluated from the flexural moment. This tension force diagram is

translated by a distance U parallel to the absicca, where U is given by the following:-

a) If the web reinforcement is at right angles to the tension bars, i.e. $\alpha = 90^{\circ}$ or is composed of bent-up bars and perpendicular ones,

$$U = (1.5 - 1.2\ \zeta)d_1 \geq 0.5\ d_1 \qquad \ldots (2.46)$$

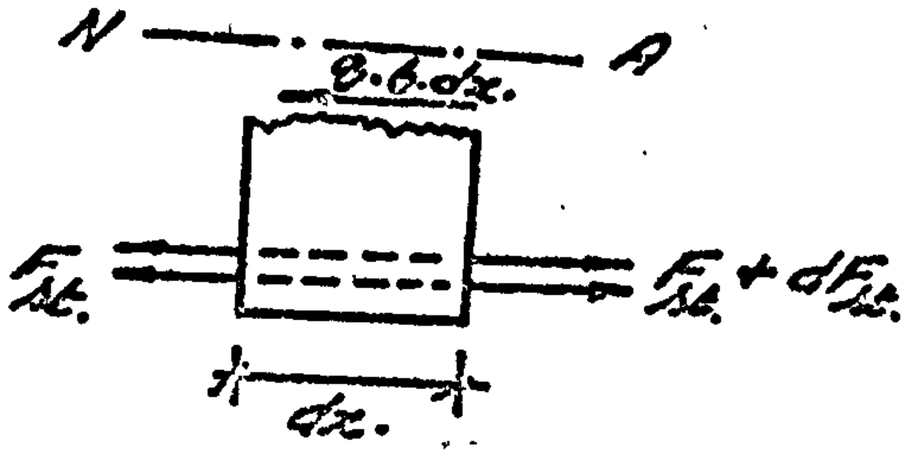
b) If the web reinforcement is inclined at 45° to the tension reinforcement, i.e. $\alpha = 45^{\circ}$,

$$U = (1.5 - 1.5\ \zeta)h \geq 0.2\ d_1 \qquad \ldots (2.47)$$

Intermediate values of U can be obtained by linear interpolation, as shown in figure 2.2. The value of ζ is as given in equation (2.28).

The C.E.B. recommendation adopts the approach suggested by Leonhardt[56] & Rusch[56]. It is presumed that the recommendation has been verified by the test results of Rusch & Leonhardt. Placas[70] observed that the majority of his tests which did not produce web crushing failures were not in agreement with the predictions of Rusch[56]. He also observed U values in the case of normal shear failures, in excess of even the maximum predicted by these theories. He therefore suggested an arbitrary value of 1.5 d* for the translation of the steel force diagram.

C.E.B. recommendations, like the Draft British Code, suffer from the arbitrary assumptions.



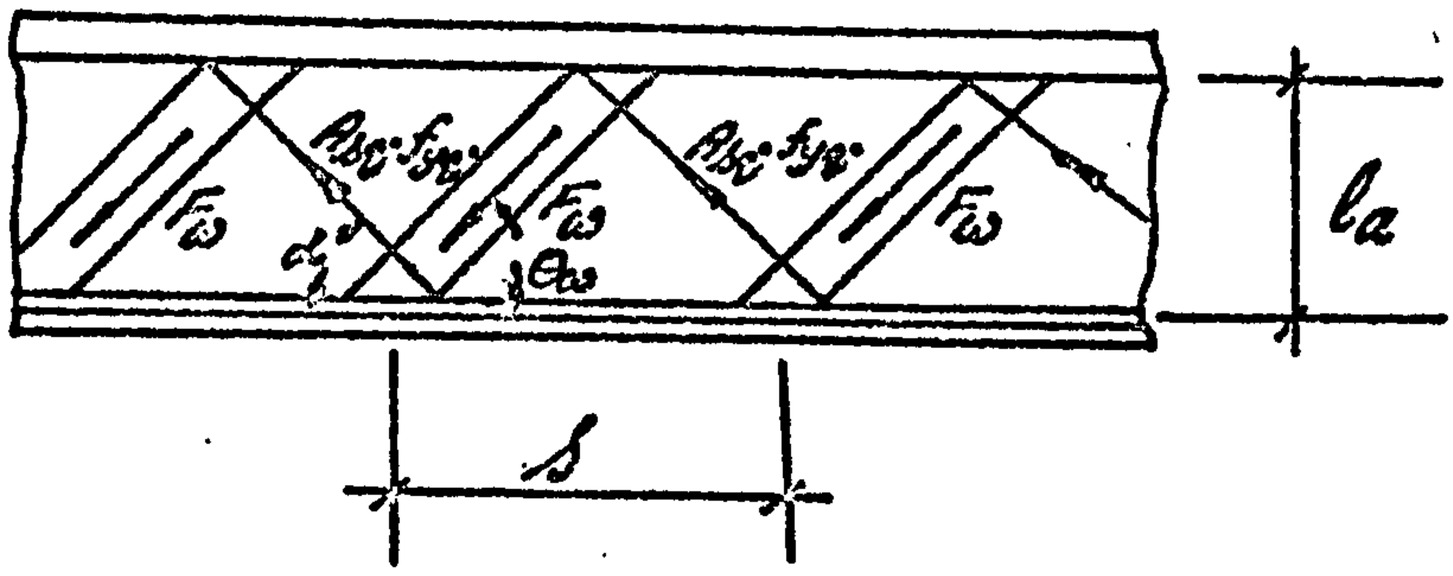


FIG. 2.1. MÖRSCH TRUSS.

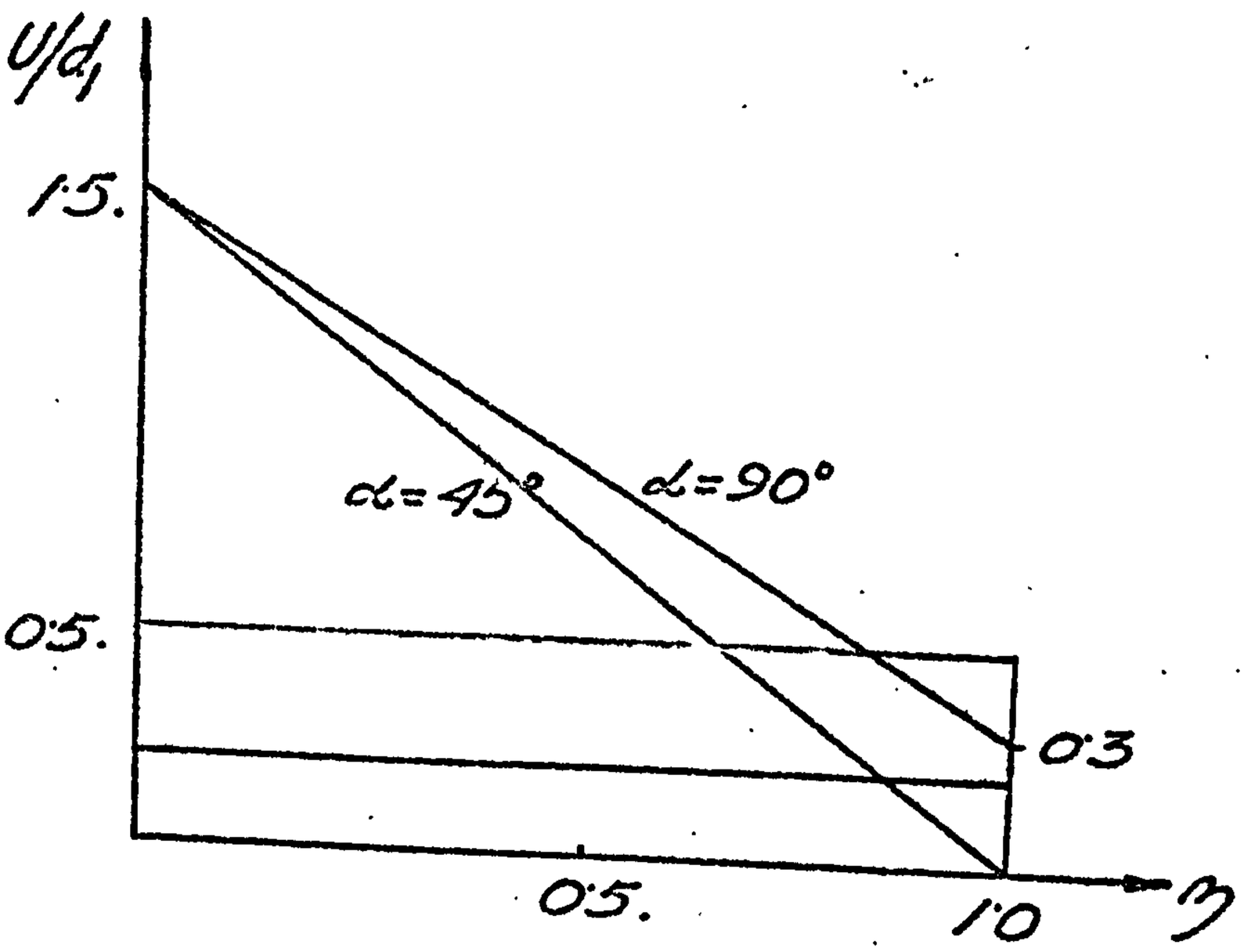


FIG. 2.2. COEFFICIENT OF TRANSLATION OF STEEL FORCE DIAGRAM.

CHAPTER 3

EXPERIMENTAL INVESTIGATION

The experimental programme was divided into three series of tests. The first group consisted of thirteen two-span rectangular beams. In the second group, six simply supported rectangular beams with overhangs were tested. The third group of tests was of concrete cylinders with varying Height/Diameter ratios.

The principal objectives of the first group were as follows:-

i) to clarify the contribution of "Shear Rotation".

ii) To study the effect of rotation on the shear strength of beams, after the formation of plastic hinges.

iii) To formulate an equation for inelastic rotation.

The object of the second series of tests was to evaluate the effect of curtailment of bars on the shear strength of beams and thence to formulate equations for curtailment.

The third series was primarily a supplement to the first. It was intended to investigate the effect of shortness of specimens on the stress-strain curve for concrete with a view to calculating the stress-block parameters at the plastic hinges of beams.

In selecting the sections and materials to be tested the rationale was as follows:-

i) The isolation of any single parameter is difficult, but the following parameters were kept constant throughout the tests for Series 1 & 2.

a) Section geometry.

b) The quality of longitudinal reinforcement.

c) The quality of shear reinforcement though different from longitudinal reinforcement.

ii) Only tied doubly-reinforced sections were considered. Singly reinforced sections without ties are rare in practice and exhibit a behaviour fundamentally different from tied sections.

The size of beams was mainly determined by the available test facilities in the laboratory, but it was considered large enough to minimise any scale effects. To provide a lesser area of longitudinal reinforcement without weakening the flexural strength in order to obtain shear failures using only moderate % of longitudinal steel, high strength Swedish steel having a yield stress in excess of 620 N/mm^2 was used in preference to British steel. Consistent with current practice, a more ductile steel (Mild Steel) was chosen for the transverse reinforcement.

3.1 SERIES NO. 1 - Continuous beams.

3.1.1 Materials & Fabrication

A. Reinforcement:-

a) The longitudinal tension and compression steel were High Yield deformed steel (KS.60).

This is a Swedish deformed steel with circular ribs at right angles to the direction of the bar. The spacing of the ribs is equal to 0.5 times the bar diameter. The bond qualities

of this steel seem to be adequate.

These "naturally hard" steels yield sharply at the yield point stress, and there is usually a definite yield plateau. Following such yielding an ultimate strength about 50% greater than the yield strength is developed. This is hot-rolled and the high strength properties are imparted by small amounts of alloy components (C, Mn, Si).

Two sizes of Swedish Steel were used: 16 mm & 12 mm. To obtain the stress-strain and yield point characteristics of this steel, two samples each of 16 mm & 12 mm diameter bars were subjected to normal tensile tests carried out in an Amsler testing machine of 500 KN capacity. Typical curves for the reinforcement are given in figures 3.1 & 3.2. Only the stress-strain curve up to yield point is shown. The complete stress-strain curve has the general form shown in fig. 3.4 in all cases. E is approximately equal to 203×10^3 N/mm^2.

b) The shear reinforcement was of plain round mild steel bars. The sizes used were 5.5 mm ($\frac{7}{32}$") 6 mm ($\frac{1}{4}$"), 8 mm ($\frac{5}{16}$") & 10 mm ($\frac{3}{8}$") diameters. The relevant average characteristics deduced from tension tests were as shown in fig. 3.3. The approximate value for E was 207×10^3 N/mm^2.

In Table 3.1 the properties of bars are given for both Swedish Steel and plain round mild steel.

TABLE NO. 3.1

PROPERTIES OF REINFORCEMENT

BAR DIA.	TYPE OF BAR	CROSS-SECTIONAL AREA:- mm^2	YIELD STRESS N/mm^2	ULTIMATE STRESS N/mm^2	REMARK
16 mm	SWEDISH	201	644	800	METRIC SIZE
12 mm	SWEDISH	113	652	930	METRIC SIZE
10 mm	PLAIN ROUND	71.5	304	472	IMPERIAL SIZE (3/8")
8 mm	PLAIN ROUND	49.5	303	493	IMPERIAL SIZE (5/16")
6 mm	PLAIN ROUND	31.7	393	521	IMPERIAL SIZE (1/4')
5.5 mm	PLAIN ROUND	24.3	280	421	IMPERIAL SIZE (7/32")

B. Concrete:-

A target strength of 40 N/mm^2 cube crushing strength at 28 days was sought. The concrete used was either supplied by Ready Mix Concrete Ltd. or obtained from a designed mix of the Imperial College Laboratory. The mix proportions(by weight) for both the Ready Mix Concrete and that prepared in the Laboratory are given in Table 3.2. It was not always easy to obtain consistent strength values for concrete in different beams. Apart from Beam c_{12}, all other beams were cast in Ready Mix concrete - the strength of which varied widely, as is evident from Table 3.3.

TABLE NO. 3.2

MIX PROPORTIONS (BY WEIGHT)

U_W = 41.5 N/mm^2 at 28 days

Maxm. aggregate size=19 mm.

PARTICULARS	DESIGN MIX AT IMPERIAL COLLEGE	READY MIX CONCRETE
Ordinary Portland Cement	1.00	1.0
Fine sand (100-25)	0.61	)
Coarse sand (25-5mm)	1.39	}2.1
Fine aggregate (5 mm-9.5 mm)	1.14	0.8
Coarse aggregate (9.5mm-19mm)	2.21	2.8
Water	0.61	to give 50 mm slump.

The sieve numbers given after the sands and aggregates, refer to the sizes given in British Standard specifications (Imperial Units). For the laboratory mix both the sands and aggregates were Thames River deposits and were batched dry. The Ready Mix aggregate was a land gravel.

C. Geometry of test beams and arrangement of reinforcement:-

The overall cross-section of all beams was 305 mm deep and 152.5 mm wide. The geometry and reinforcement of each type is discussed separately in subsequent paragraphs, but the following points are of general nature.

i) The ends of stirrups were bent 90° to form hooks, as shown in figures 3.6 & 3.7.

ii) To avoid splitting of concrete at the level of tension reinforcement under high bond stress, the deformed bars were given 25 mm clear concrete cover.

iii) When more than one layer of bars was necessary, they were grouped together in pairs as shown in figs. 3.6 & 3.7. Robinson's[81] tests proved this to be a satisfactory arrangement in the sense that the pair possesses bond qualities equivalent to those of the separate bars, provided the concrete can be vibrated around them.

(iv) The beam width was increased from 152.5 mm to 203 mm at the central support, to form a 203 mm x 203 mm column which extended 152.5 mm above and below the beam profile as shown in fig. 3.5. This was done with a view to avoiding failure occurring in the mid-support and also to simulate a typical beam-column connection.

The various details pertinent to each beam will now be examined. Depending upon the point of application of the span load, the tests were broadly divided into two groups. In group I, the point load was applied at a distance of 1.825 m away from the mid-support; whereas for group II, it was 1.37 m from the support as shown in fig. 3.5. Group I was again divided into two sub-groups depending upon the area of longitudinal tension reinforcement at the support and mid-span sections.

Longitudinal Reinforcement:-

In group I Beams c3, c4, c9 & c11 had 2-12 mm diameter KS.60 bars as tension reinforcement at the central support, against 3-16 mm diameter KS.60 bars for beams c1, c7, c8 & c12. In group II however, all the beams had 2-12 mm diameter KS.60 bars as tension reinforcement at the mid-support section. The proportions of reinforcement used are summarised in Table 3.3. Typical

arrangements of bars are shown in Figs. 3.6 & 3.7.

Shear Reinforcement:-

The amount of shear reinforcement was varied from beam to beam depending upon the mode of failure of the previous beam in the same group. For each group and also for different longitudinal tension reinforcement at mid-support section within one group, the primary objective of the tests was to ascertain the minimum amount of shear reinforcement which would avoid shear failure of the structure.

The details for various beams are summarised in Table 3.3.

D. Casting & Curing:-

The beams were cast in steel formwork which consisted of four sections, each 1.975 m long, bolted together with the joints sealed with plasticine. The central sub-column was made of 203 m x 203 m box-section in wooden shuttering. The reinforcement for each beam was made up as a cage which was located in the moulds using plastic spacers.

Four 152.5 mm cubes for compression tests and two 152.5 mm x 228 mm long cylinders for split cylinder tests were cast as control specimens for each beam. For Design Mix Concrete the four cubes consisted of the one from each batch of concrete. The concrete - either Ready Mix or Design Mix - was poured in two uniform layers in the moulds and was vibrated until full compaction. The top of each beam was then "levelled" and trowelled with a steel trowel. To ensure proper compaction, internal poker vibrators were used. To

ensure correspondence, the same procedure was followed in both halves of the same beam and the accompanying control specimens.

After concreting, the beams and control specimens were covered with wet sacking and polythene sheeting. On the third day after concreting they were removed from the forms and then cured for a further two days under wet sacking and polythene. Thereafter they remained in the normal laboratory atmosphere - relative humidity 50%, temperature 68-70°F - until the time of testing.

The beams were tested at a minimum age of 3 weeks. The accompanying control specimens were tested on the same days as the beams.

3.1.2 Experimental Programme & Set Up.

A total of thirteen continuous beams was tested. Details of all beams tested are outlined in Table 3.3. As shown, the groupings are by type of applied loading and sectional reinforcement. The cube strengths of the concrete varied widely and splitting strength values which were obtained from the following formula, did not show any consistency.

$$C_t^{(1)} = \frac{2XP_L}{\pi.D.L} \qquad \ldots (3.1)$$

The details of the test rig are shown in fig. 3.8. The reactions on the 8.103 m long beams were through tie bars at the ends and a rocker bearing at the centre. The details of these are shown in the figure, where it can be seen that the

beam was turned "upside down" before placing temporarily on two acrows - one at each end. The end cross-bridges and load cells were then placed. After correctly positioning the beams, the cross-bridges were levelled with spirit levels in two directions. The two 500 KN jacks with roller bearings on top were then floated and the acrows,on which the test beam was resting, released. The centre guide bolts were turned in to fit snugly on the side of the beams. Care was taken not to put additional load through side friction of these guide bolts.

The loading was applied in the spans by two 500 KN Amsler jacks which were coupled to loading cabinets. The size of loading platens over the rollers was 150 mm wide x 100 mm long x 16 mm thick. The size of plate over the centre support was 200 mm wide x 350 mm long x 20 mm thick. This plate was made larger than the size of stub column in order to place a climometer at the head of the stub column. One 150 mm wide x 100 mm long x 12 mm thick plate was welded to the cross bridge at each end of the beam.

3.1.3 Instrumentation

The instrumentation used to measure force, deformation, slope, strain and crack width is categorized as follows:-

A. FORCE

The applied loads from the 500 KN jacks in the two spans were measured from the loading cabinets (the points of application of the loads were varied depending on the tests, as shown in fig. 3.5.

The reactions to the applied loads were recorded by the three electrical resistance gauge type load cells placed at the central

and end supports. The load cells were calibrated before the start of the experiments. The locations of the load cells are shown in fig. 3.8.

B. DEFLECTION

Vertical deflection was always measured near the mid-support of the beams by Dial gauges which were also calibrated to 0.025 mm. Eight dial gauges were placed near the centre supports as shown in figs. 3.8 & 3.9.

To record horizontal movements of the beams, and also to spot any excessive tilting during the time of testing, four Dial gauges - two on each end, were placed horizontally as shown in Figs. 3.8 & 3.9. All these dial gauges were mounted on frames. The end frames were situated in such a way that they were independent of the main test frame. The readings of the end dial gauges were constantly watched during the progress of the tests.

C. SLOPE

Seven 100 mm base length climometers were placed at the top, i.e. tension face, symmetrically about the central support as shown in fig. 3.9. The climometers had an accuracy of $\pm 25 \times 10^{-6}$ radians. The locations of these climometers were such that one recorded the rotation at the plastic hinge near the central support, the second gave the rotation near the point of contraflexure, and the last indicated the rotation at the end support. One climometer was placed over the central support to record any tilting of the beam during testing. This tilting usually heralded the imminent failure of a beam in

one side in preference to the other.

D. STRAIN

Two types of gauges were used to measure strains - Electrical Resistance gauges and Demec points. The former were used mainly to measure the strain on the longitudinal tension and shear reinforcement. In each beam one of the tension bars was instrumented. Two 10 mm gauges were placed on diammetrically opposed sides of the bar to avoid erroneous readings resulting from the bars own bending. Seven such pairs were placed along the bar in the positions shown in fig. 39. In the case of stirrups one 20 mm gauge per stirrup was used at about mid-height of the stirrup. In addition, for earlier beams to record strains on the concrete, Demec gauges at 200 mm centres were used on the surface of the beam and 100 mm Demec gauges on the stub column, as shown in fig. 3.9. These did not give meaningful results once cracks penetrated between the points - which usually occurred at a relatively early load. Hence for later experiments, these were completely abandoned.

The least count of the Electrical Resistance gauges was ± 1 micro-strain and that of Demec gauges was of the order ± 10 micro-strain.

E. CRACK WIDTHS

After each stage of loading the cracks corresponding to that load stage were drawn on the beam and their width measured through a telescopic type crack width recorder graduated to 25 divisions to 1 mm width. The maximum widths of the shear

and flexural cracks were measured near the central supports and in the spans. Recordings for the widest flexural cracks - which usually occurred at the junction between the stub column and beam - had to be somewhat approximate since the rig, i.e. stanchions near the mid-support were in the way. As it was not a primary objective of the tests to investigate flexural crack widths, it was decided not to modify the Test Rig to accommodate the reading near mid-support. Analysis of shear crack widths is attempted in Chapter 8.

3.1.4 Procedure

Apart from occasional mishap or other variations, e.g. Beams c2 & c5; the testing procedure was essentially as described below.

After the beam was placed on the test rig any small horizontal bow was rectified with the help of central guide nuts and it was ensured that the beam, the loading platens and the load cells were in line. The loading jacks were then floated and the beam was gently lowered on to these jacks.

The zero condition for both load and deformation was taken to be the "no applied load" condition for all beams. Dead load due to the beam itself and the experimental equipment together with column load amounting to approximately 10 KN, was balanced by the jacks prior to testing and regarded as pre-load. The loading cabinets had to accommodate this additional load in such a way that from all subsequent readings 5KN was deducted to get the correct applied load. The levels of the supports were then adjusted by putting a small additional load on the jacks - usually

5 KN each, and then tightening or loosening the nuts of two end bridges and recording at the same time the load cells until correct (elastic theory) reactions were obtained for centre and end supports. These initial adjustments usually on average took 1 hour.

Loading was applied in stages and the load increment generally corresponded to an increase of 40 KN on each jack at the earlier stages of loading. Near load stages at which a significant change in the beam behaviour was observed or anticipated, the increment was reduced to 20 KN or even to 10 KN. On average each load stage required between 15 to 20 minutes before all the readings could be taken. In each of the tests, the applied loads were kept constant while the instrument readings were taken.

At each load stage the following measurements were taken:-

i) Readings of Demec points on the concrete surface (where used).

ii) Readings of strain gauges positioned on the reinforcement.

iii) Readings of dial gauges for deflections.

iv) Reading of climometers for rotations at central and end supports.

v) Cracks were drawn and their width measured.

On average the under-reinforced beams took three hours and the over-reinforced beams four hours from start to the finish of the experiments.

3.1.5 Behaviour of Beams

The behaviour of all the test beams was essentially similar.

They were either under-reinforced or balanced and failed either in shear or in flexure by concrete crushing, but in all cases the tension reinforcement had yielded by varying amounts.

After the tensile resistance of the concrete at the extreme fibre had been overcome, flexural cracks appeared first in the tension zone at the region of maximum moment. Usually this region was near the central support and the flexural cracks were first visible at between 20% and 30% of the ultimate load. Thereafter these cracks widened and extended vertically toward the compression zone slowly as the load was increased. These flexural cracks also spread from the area of the central support to the tension area of the spans and gradually to the end supports. Secondary cracks formed inbetween the existing ones. When the load was further increased, the above process continued but at some later stage an inclined crack appeared. This crack, referred to as a Shear crack, normally started by joining the heads of flexural cracks. Sometimes it formed individually. Usually it first appeared near the neutral axis and travelled in an inclined direction toward each end.

The rate of progress and the inclination of the shear cracks from this point onward depended largely on the amount of shear reinforcement and the length of shear span. The main shear crack - called the Critical Shear crack, then tended to go past the head of the highest flexural crack, its direction becoming flatter when progressing into the compressive zone. With increasing load the main steel at the central support

yielded forming a plastic concrete hinge. In the beams which failed by shearing the opening of the shear crack resulted in a tendency of the side of the beam where the load was acting to move transversely in respect to the other side. Consequently, the main steel exerted on the concrete a transverse force, which tended to tear away the concrete cover. This was a manifestation of the dowel effect. At the same time, the other end of the crack extended right through the compression zone and the beam failed by shearing. Due to yielding of the longitudinal tension reinforcement, the concrete in the compressive zone usually showed signs of distress prior to failure. Depending upon the amount of yielding, sometimes this distress produced some surface cracking and spalling of concrete.

For beams which failed in flexure, after the yielding of tension reinforcement, the flexural cracks widened rapidly and also increased in number at the level of tension reinforcement. The concrete in the compression zone started forming surface cracks and slight spalling. As the load was further increased the cracking and surface spalling in the concrete compression zone increased in severity and finally the beams failed by crushing of concrete in the compressive zone at the support and load point upon the formation of a second hinge in the span.

3.1.6 Analysis of Test Results

Analysing the beams for different groups, the following results presented in Table 3.4 are obtained. The cracked beams are shown in fig. 3.10.

It has to be mentioned in this connection that the failure of beam c.10 was achieved by flexure on left-hand span and shear at right of the mid-support. Originally the critical shear crack was the one nearest to the support. But just before failure the second crack developed and both became prominent with final stage of loading.

In the test, Beam c.2 caused the test rig to tilt dangerously sideways. The experiment was stopped and the guide bolts were introduced in the rig. Afterwards the beam was retested, but due to earlier cracking and difficulties with the strapping system used to strengthen the region of curtailment, the test results were not found to be very coherent and hence no meaningful values could be established. Final failure was achieved by loading on one span only. Beam c.2 was intended to be one of the series in Group I. Beam c.5 on the other hand, was erroneously given a lesser amount of longitudinal tension steel in the span - 3-12 mm in lieu of 3-16 mm of KS-60 bars - and hence its results could not be gainfully utilised or be fitted well with the other results of Group I beams. It failed rather prematurely in flexure at a load of 120 KN. This beam was later replaced.

To analyse the test results the following figures are drawn.

Load-Deflection diagrams

In drawing the diagrams, one beam which developed flexural capacity is taken from each group. It has been established in Chapter 5 that the rotational behaviour of beams before failure - whether they failed in shear or in flexure, is similar. Hence the beams which produced maximum rotation are considered in the analysis

and shown in fig. 3.11.

Analysis of load-deflection diagrams - which produced three distinct stages, is reported in Chapter 8.

Load-End Rotation diagrams

These diagrams - one for each group of beams (again the beams which failed in flexure) are shown in fig. 3.12. These in fact give the rotation of a beam between end support and the point of application of load. As is expected the beams having light longitudinal reinforcement in the span exhibited more plasticity than the beam with heavy longitudinal reinforcements. Therefore the former group produced more rotation at lower load stages than the latter.

Load-Mid-Support rotation

These diagrams are shown in figs. 5.13, 5.14 & 5.15. The contribution of inelastic rotation is more pronounced in the case of light longitudinal reinforcement than the group of beams with heavy longitudinal steel. There was some small deviation for beams with different strengths of concrete and also in beams which failed rather prematurely in shear towards the later stages of loading, but on the whole the behaviour of beams within the same group was similar. As on the load deflection diagrams there are three stages: uncracked, cracked elastic and plastic.

Moment-Rotation diagrams

Three diagrams representing one beam which failed in flexure for each group are shown in fig. 3.13. Like the load deflection diagrams these have also three distinct phases. The end of the initial straight part normally lies between 20%-30% of the ultimate

moment. This is the uncracked elastic phase of the structure. The next is the cracked phase where cracks reduce the stiffness of the member and the moment rotation curve changes direction. In this phase the extra rotation of the beam is solely due to the loss of flexural stiffness. The last phase is the inelastic stage. The moment-rotation diagram changes direction for the second time and the entire rotation is due to the inelasticity of the structure at the hinge section. For under-reinforced beams, the longitudinal tension steel yields at the start of this stage and the concrete reaches a strain of about 0.002.

Load-Strain diagrams

Strains were recorded in longitudinal tension reinforcement near the mid-support sections and also in the stirrups on either side of the stub column.

Studying the load-strain diagrams in fig. 3.14 for the longitudinal reinforcement, it appears that the strain profile is approximately linear at earlier stages of loading, with the strains increasing from the point of contraflexure towards the mid-supports. This behaviour, however, changes upon the formation of shear cracks. The strain profile ceases to be linear as the deformation exhibits a tendency to become uniform along the length of the main shear cracks before decreasing towards the point of contraflexure. In the stub column the strain drops, as expected, due to the increase in overall depth of the beam. The strain profile within the stub column is however not strictly as shown in fig. 3.14. It should drop near the column faces, and then follow a parabolic path depending upon the nature of bending moment over the column support.

In drawing the load-strain diagrams for stirrups, two beams from each group - one which failed rather prematurely in shear and the other which failed in flexure - are to be considered. These are shown in figures 3.15, 3.16 & 3.17. From these figures it can be seen that no appreciable strain is registered before the appearance of inclined cracks. Following the formation of inclined cracks, the strains in the stirrups increase rapidly. This is continued as the cracks cross the stirrups. Usually the first stirrups on either side of the stub column are unaffected by the shear cracks until at a very late stage of loading. In the event of a shear failure, the stirrups crossed by the critical shear crack or cracks, invariably yield, whereas for flexural failure the yielding of stirrups is unlikely, unless of course, it is crossed by a nearly critical shear crack.

3.2 SERIES NO. 2 - Restrained beams.

3.2.1. Materials and Fabrication

A. Reinforcement:-

a) The longitudinal tension and compression reinforcement was of high yield deformed KS60 Swedish Steel. The diameter of bars was 16 mm.

b) The shear reinforcement was of plain round mild steel bars to BS785. The sizes used were 6 mm & 8 mm diameter.

B. Concrete:-

The concrete used for this series was designed at the Imperial College laboratory, and details of the mix are given in table 3.2.

c) Geometry of test beams and arrangement of reinforcement.

The overall cross-section of all six beams was 305 mm deep and 152.5 mm wide. The following points are common to all beams.

i) The ends of stirrups were bent 90° to form hooks with extensions of 8 diameters beyond the bends.

ii) The clear concrete cover to all longitudinal bars was 25 mm.

iii) Vertical distance between the two layers of main bars was 16 mm.

iv) The overall length of the beams was 3.965 m.

The layout and loading system for these restrained beams are shown in fig. 3.18. The arrangement of loading was such that the moment in the span section was equal to the moment in the support section. To achieve this at every load stage, the applied load in the span was maintained at twice the value of load in the cantilever.

The beams were detailed in such a way that for each pair of beams having similar shear reinforcement, the longitudinal tension reinforcement for one beam was curtailed more than the other. Three pairs of such beams were cast. The reinforcement details of these beams are shown in figures 3.19 & 3.20. Thus beam Nos. B1, B4 & B5 had comparatively longer lengths of tension reinforcement than Beams Nos. B2, B3 & B6. For both types of beam, the size and amount of longitudinal tension steel were the same.

The shear reinforcement was varied from one pair of beams to the next. Of the three pairs cast, one pair had very light shear

reinforcement, the second moderately heavy and the last pair had very heavy shear reinforcement. The details for various beams are summarised in Table No. 3.5.

D. Casting and Curing:-

The beams were cast in steel formwork which consisted of two sections each 1.9825 m long, bolted together with the joints sealed with plasticene. The reinforcement for each beam was made up as a cage which was located in the moulds using plastic spacers.

Four 152.5 mm cubes for compression tests were cast as control specimens for each beam. These four consisted of at least one from each batch of concrete. The casting and curing was similar to the beams in Series No. 1.

3.2.2 Experimental Programme & Set-Up.

The details of test rig are shown in fig. 3.21.

3.2.3 Instrumentation

The instrumentation used to measure forces, strains and crack widths is categorised as follows:-

A. Force:-

The applied loads from the jacks in the span and cantilever support were recorded from the hollow load cells.

B. Strain:-

The electrical resistance gauges were buried into slotted holes in the longitudinal tension bars at specified locations as shown in

figure 3.22. They were not placed on the surface of the bars, in order to avoid the loss of bond of the bars. These slotted holes also avoided the strain due to bending of bars.

In addition Demec gauges were used to record the strains on the concrete surface as shown in figure 3.22. But at an early load, most of these gauges became unserviceable due to cracking. Hence though the recording of these gauges was maintained, they could not be gainfully utilised.

C. Cracks:-

These were recorded and plotted on the surface after each stage of loading and crack widths were measured by a telescope as used in Series No. 1.

3.2.4 Procedure

The beam was placed on the test rig and levelled. It was ensured before the start of the experiment that the beam was in line with the rig. The zero readings for the strain gauges were recorded and then the load was applied through the jacks - span first, cantilever support next. The loading was in stages corresponding to an increase of 40 KN in the span load. Near load stages where significant changes in the beams behaviour was observed or anticipated, this increment was reduced to 20 KN or even to 10 KN. On average, at each load stage about 10 minutes were required to take all the readings of strain gauges. The applied load was kept constant during this period. The duration of tests varied widely, taking about four hours for beams which failed at a load of 300 KN or above and only about two hours for beams which failed earlier.

3.2.5 Behaviour of Beams

The behaviour of these beams was essentially similar to the tests reported earlier for Series No. 1 - whether they failed in flexure or in shear.

3.2.6 Analysis of Test Results

Analysing the beams the following results, presented in Table No. 3.6, are obtained.

As a footnote to the table it is worth mentioning in this context that both beam s B.5 & B.6 developed very well defined flexural cracks near the ultimate stage of loading. From the readings of strains on the longitudinal tension steel, it was observed that the main reinforcement yielded.

The widths of cracks at different stages of loading are discussed in Chapter 8.

From the recorded readings of strain gauges in the longitudinal reinforcement, load-strain diagrams are drawn for the support and span sections of each beam. These are shown in fig. 3.23.

Analysing these diagrams, it is observed that for beams with longer lengths of longitudinal tension reinforcement, e.g. beams B1, B4,& B5, the strain profile is linear up to a load of between 30%-40% of the ultimate load. This is true for both span and support sections and also is valid for both layers of reinforcement. There is, of course, some erratic variation in the strain profile for successive load stages, but the general trend underlines the fact that so long as shear cracks do not materially affect the internal mechanism of the structure, the strain profile follows

the bending moment diagram of the system. This pattern, however, changes, following the appearance of what turned out to be critical shear crack or cracks. The strain profile tends to become uniform along the length of main shear cracks. However, for the other group of beams, e.g. B2, B3 & B6, the linearity of strain profile is broken at a somewhat earlier load stage, i.e. between 20%-30% of ultimate load. The main shear cracks on these beams also tended to form at a somewhat earlier load due to curtailment of longitudinal tension steel. Since the strain was recorded on only two points in the second layer of tension reinforcement, the non-linearity cannot be observed in the reinforcement of this layer.

3.3 SERIES NO. 3 - Cylinders.

3.3.1 Materials and Fabrication

A. Concrete:-

The concrete used for this series was designed in the Imperial College Laboratory with a target cube strength of 40 N/mm^2 at 28 days. The mix proportion is shown in Table 3.2.

B. Geometry of tests:-

Five groups of 100 mm diameter plain concrete cylinders - consisting of two in each group, were cast. The height of the cylinders varied from 225 mm to 50 mm as described in Table No. 3.7.

C. Casting and Curing:-

The cylinders were cast in steel formwork with varying heights. The concrete was poured in uniform layers in the moulds and was vibrated until full compaction. To ensure proper compaction a vibrating table was used. The tops of the cylinders were levelled and trowelled with a steel trowel.

The cylinders were cured in the same way as the test specimens of Series Nos. 1 & 2.

3.3.2 Experimental Programme & Set-Up.

A total of ten cylinders was tested. Details of cylinders tested are outlined in Table No. 3.7. These cylinders were divided into five groups, so that in each group two cylinders could be tested and mean value of the results obtained.

The test rig consisted of a 300 KN Amsler compression testing machine with a servo-mechanism for testing at a controlled rate of cross-head movement. Each specimen was placed on a steel plate on the lower cross-head and the reaction from the upper cross-head acted through a hemi-spherical ball joint bearing on an upper plate sitting on the specimen.

The loading was applied at a rate corresponding to a cross-head movement of 0.05 mm/min.

3.3.3 Instrumentation

The instrumentation used to measure force and deformation is categorised as follows:-

A. Force:-

The applied load was measured from the loading cabinet.

B. Deformation:-

The vertical movement of the loading plattens was recorded by transducers mounted on the sides of the bearing plates, and as close to the specimens as practicable.

3.3.4 Procedure

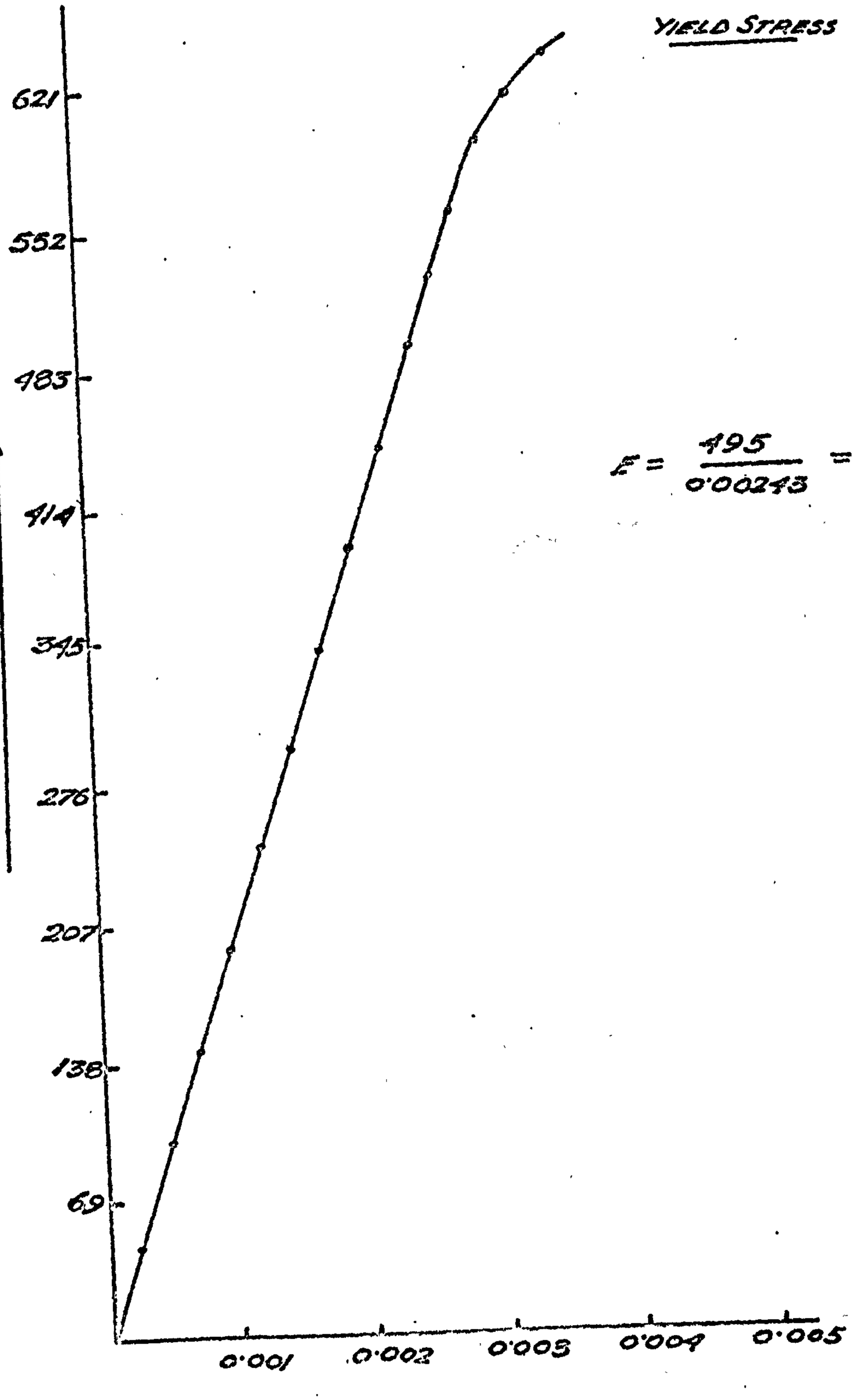
The two ends cylinders were ground level and parallel to a very smooth finish. The heights of the cylinders as cast were such that the finished size matched up to the height given in Table 3.7. The cylinder was then placed on the lower plate. The loading platten on the other end was correctly located and transducers adjusted. The loading was then applied in stages initially corresponding to load increments and subsequently to increments of deformation.

3.3.5 Analysis of Test Results

Analysing the tests for each group of cylinders the results presented in Table No. 3.7 are obtained. For cylinders in group 5, i.e. H/D = 0.5, the ultimate strain or shortening was so great that it could not be recorded. Hence the measurement for strain readings was stopped.

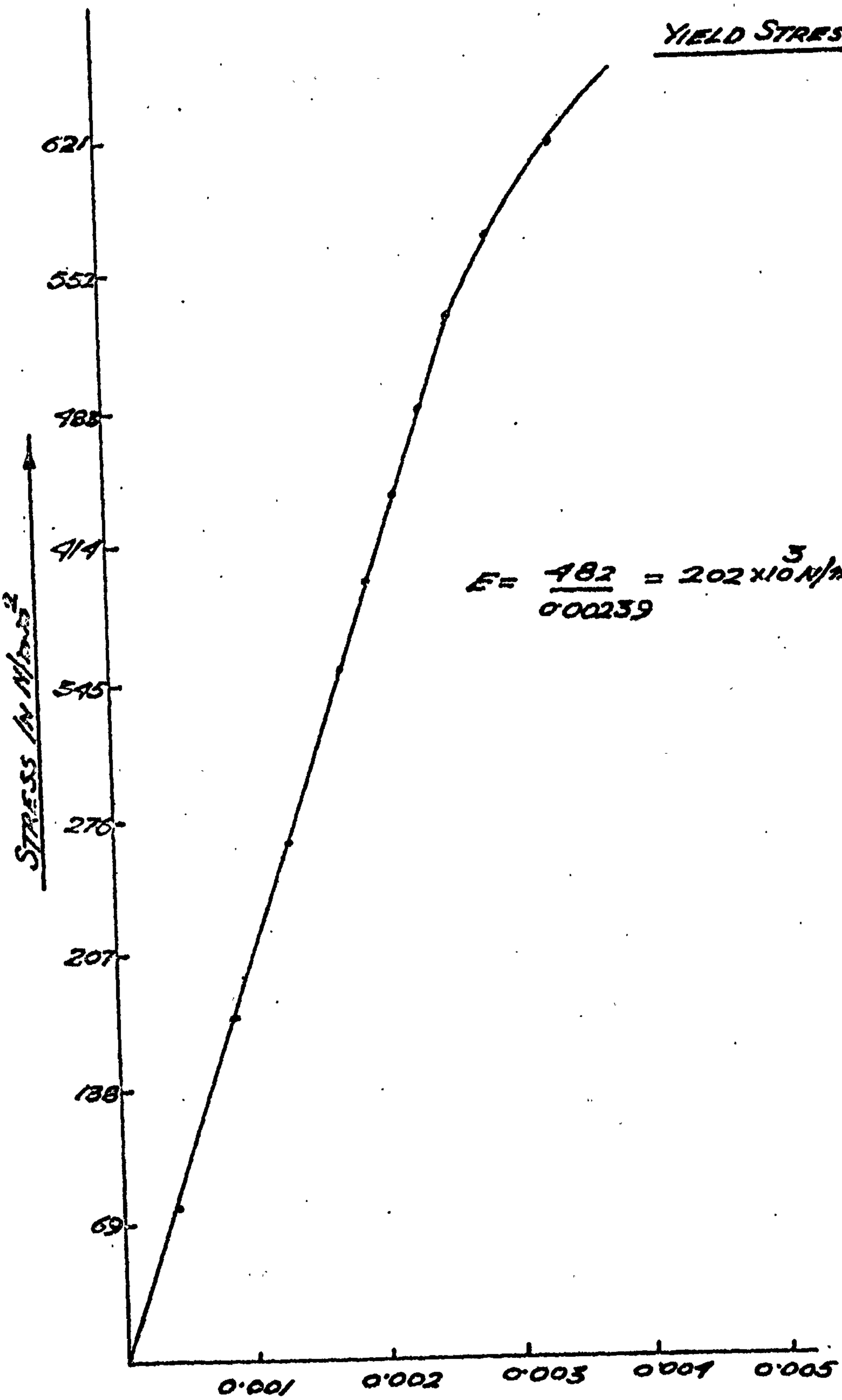
From the test results stress-strain diagrams for each group of cylinders are obtained and are plotted in figure 5.2. It is observed from the curves that the higher the ratio of H/D the more brittle the behaviour of the cylinder, and also the lower

is the strength obtained. Thus for an H/D ratio = 0.75 and lower, the profile of stress-strain diagram became flat at the top and the shortening of cylinders or ultimate strains were considerable. Whereas for H/D ratios higher than 0.75, the ultimate stresses as well as strain reduced in values. The initial part of the stress-strain diagram for every group of cylinders was similar and the significant deviations occurred at stresses greater than the normal (H/D = 2) cylinder strength.



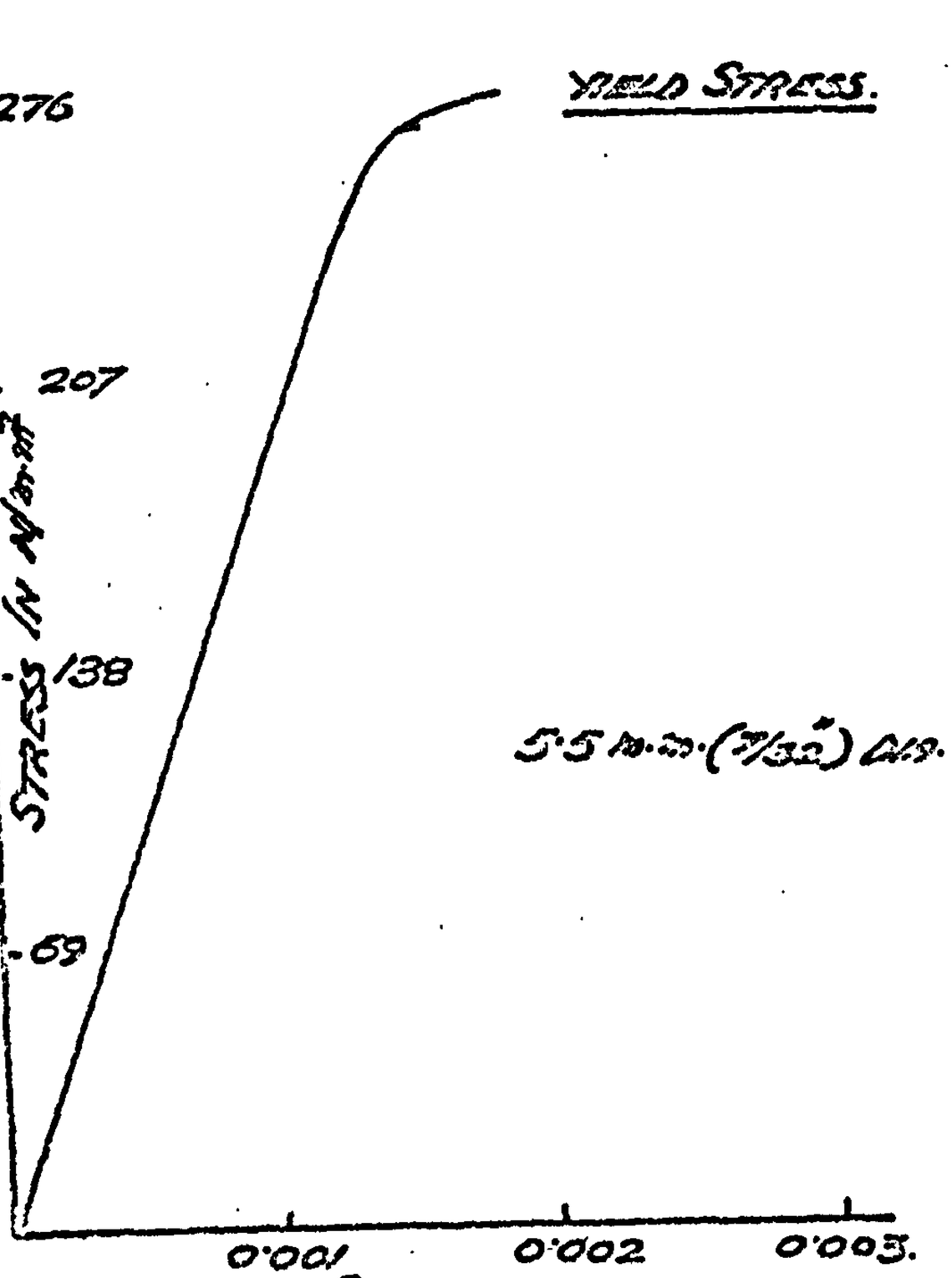
$$E = \frac{495}{0.00243} = 204 \times 10^3 \text{ N/mm}^2.$$

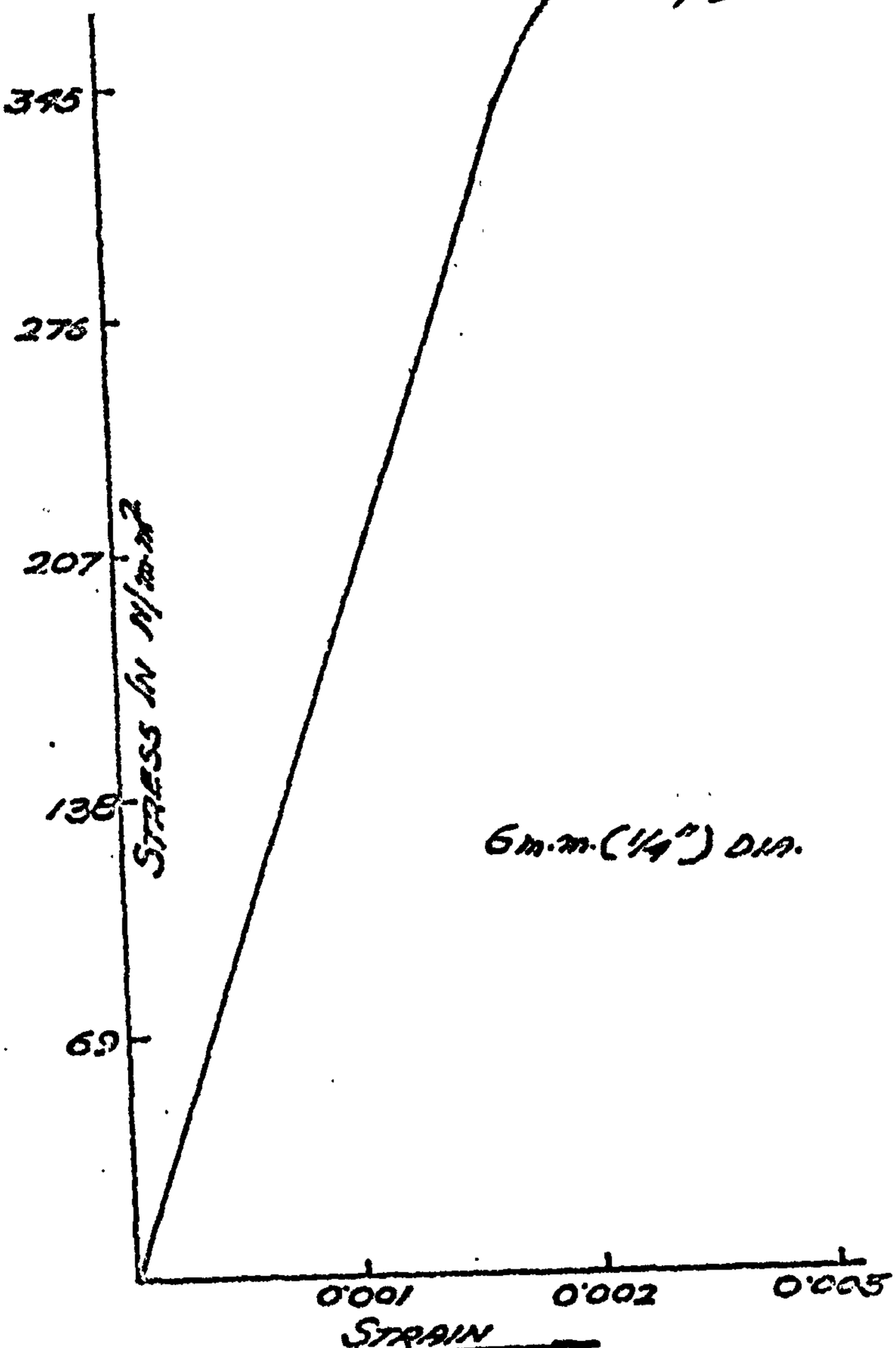
FIG. 3.1. STRESS-STRAIN CURVE FOR 16 mm. DIA. HS 60.

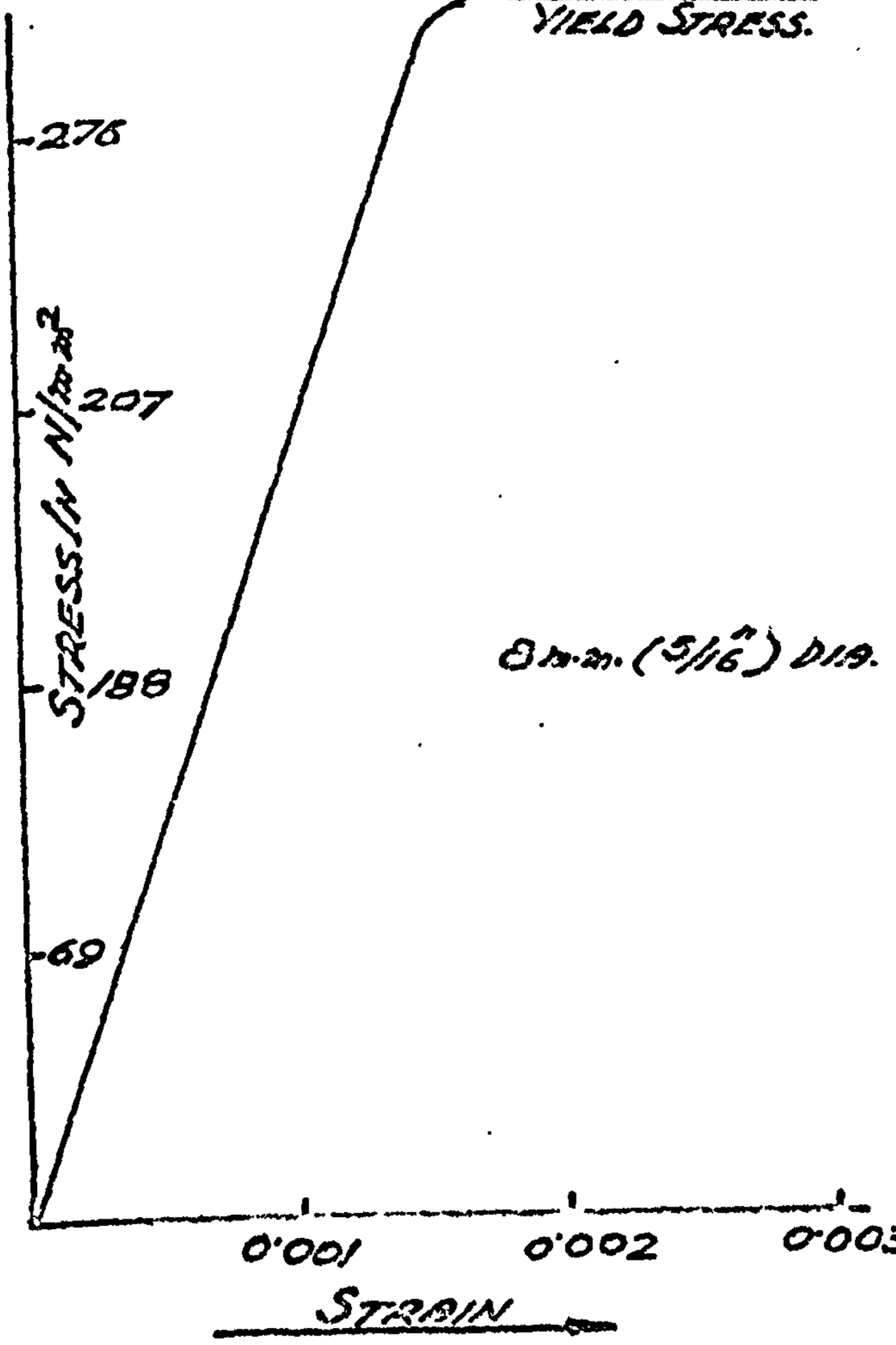


$$E = \frac{482}{0{\cdot}00239} = 202 \times 10^3 \text{ N/m.m}^2$$

FIG. 3.2. STRESS-STRAIN CURVE FOR 12 m.m. DIA. K560.







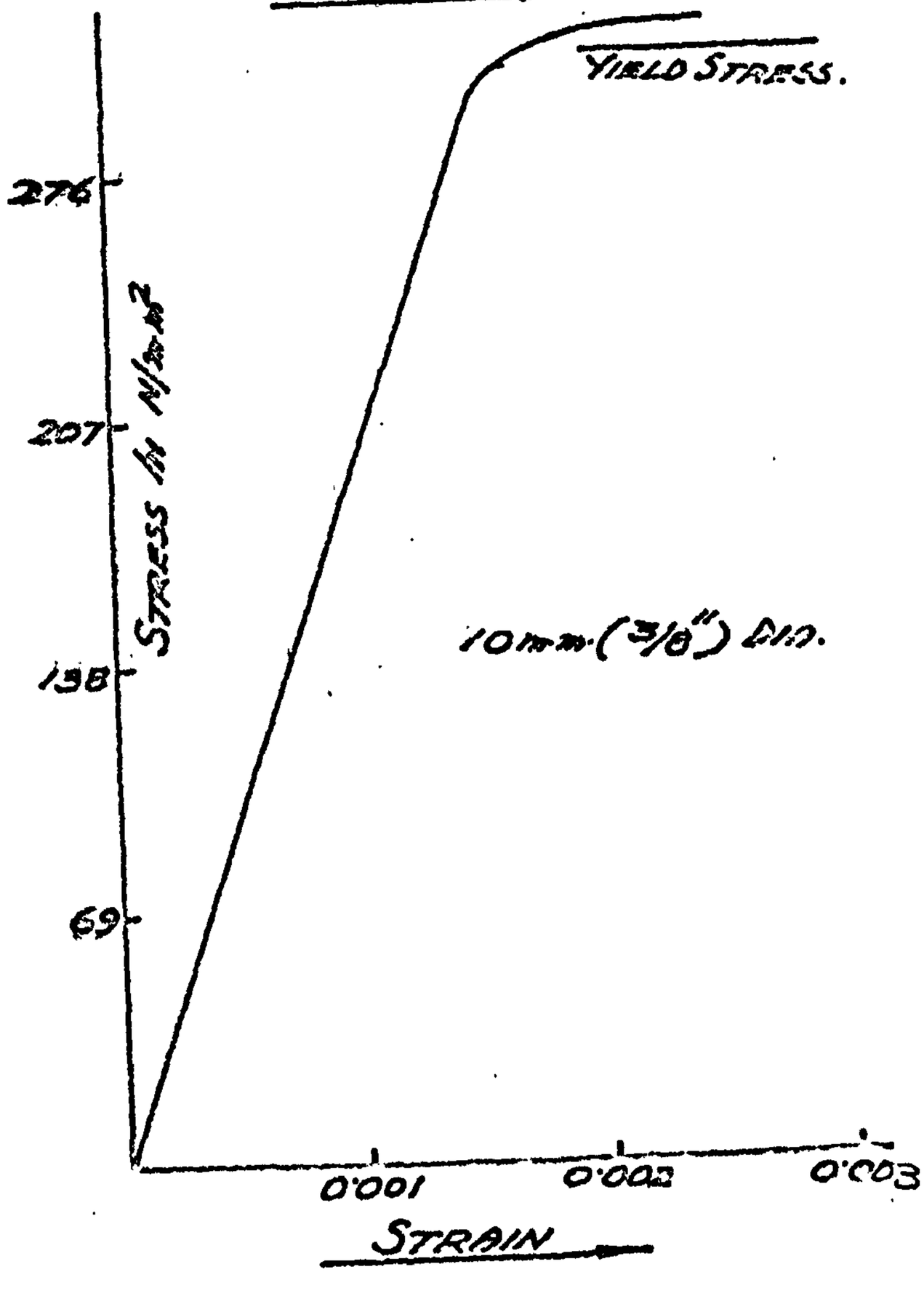


FIG. 3.3. STRESS-STRAIN CURVES FOR MILD STEEL BARS.

NOTE:- THIS FIG IS BORROWED FROM PLACAS.(70)

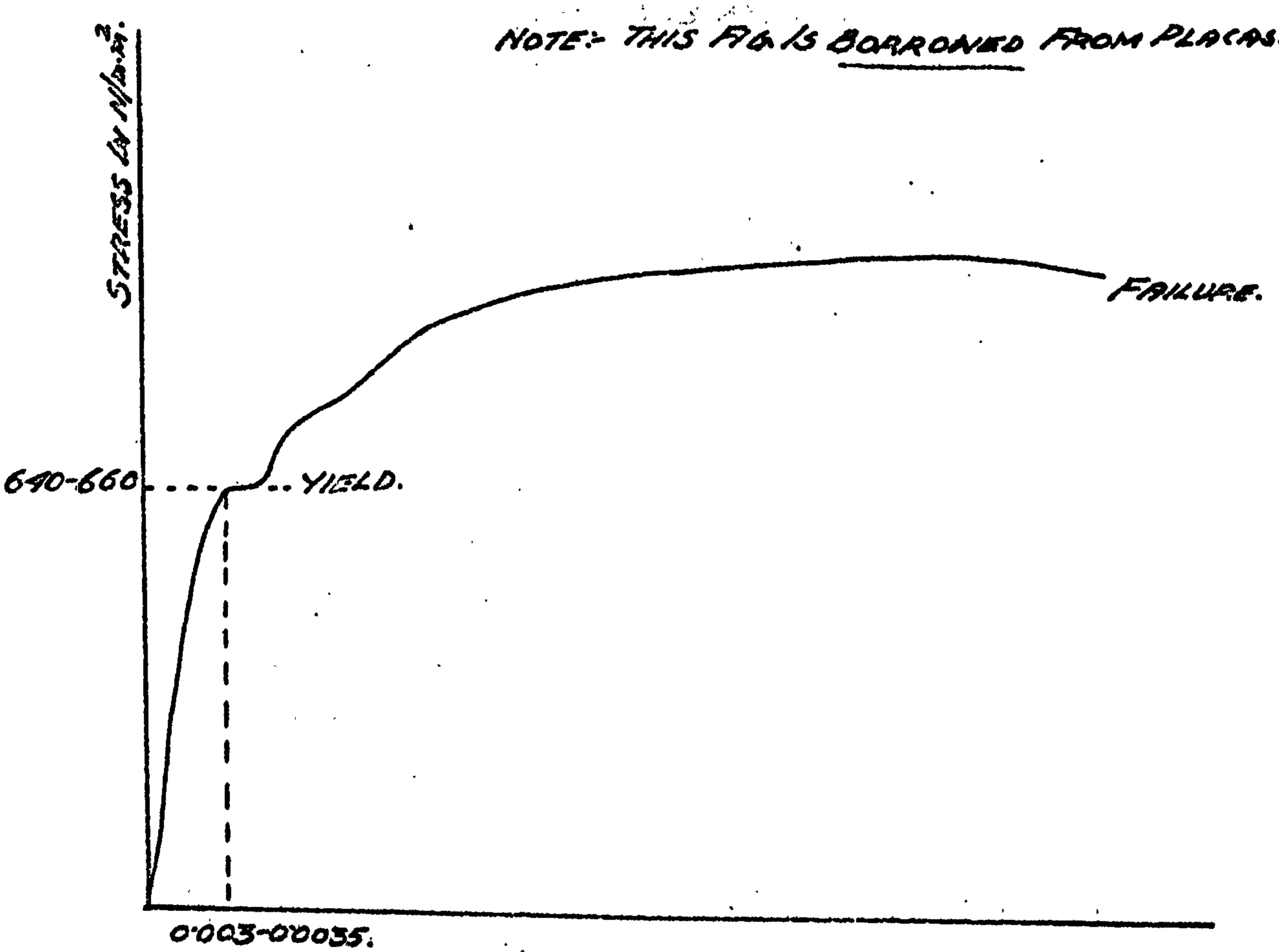
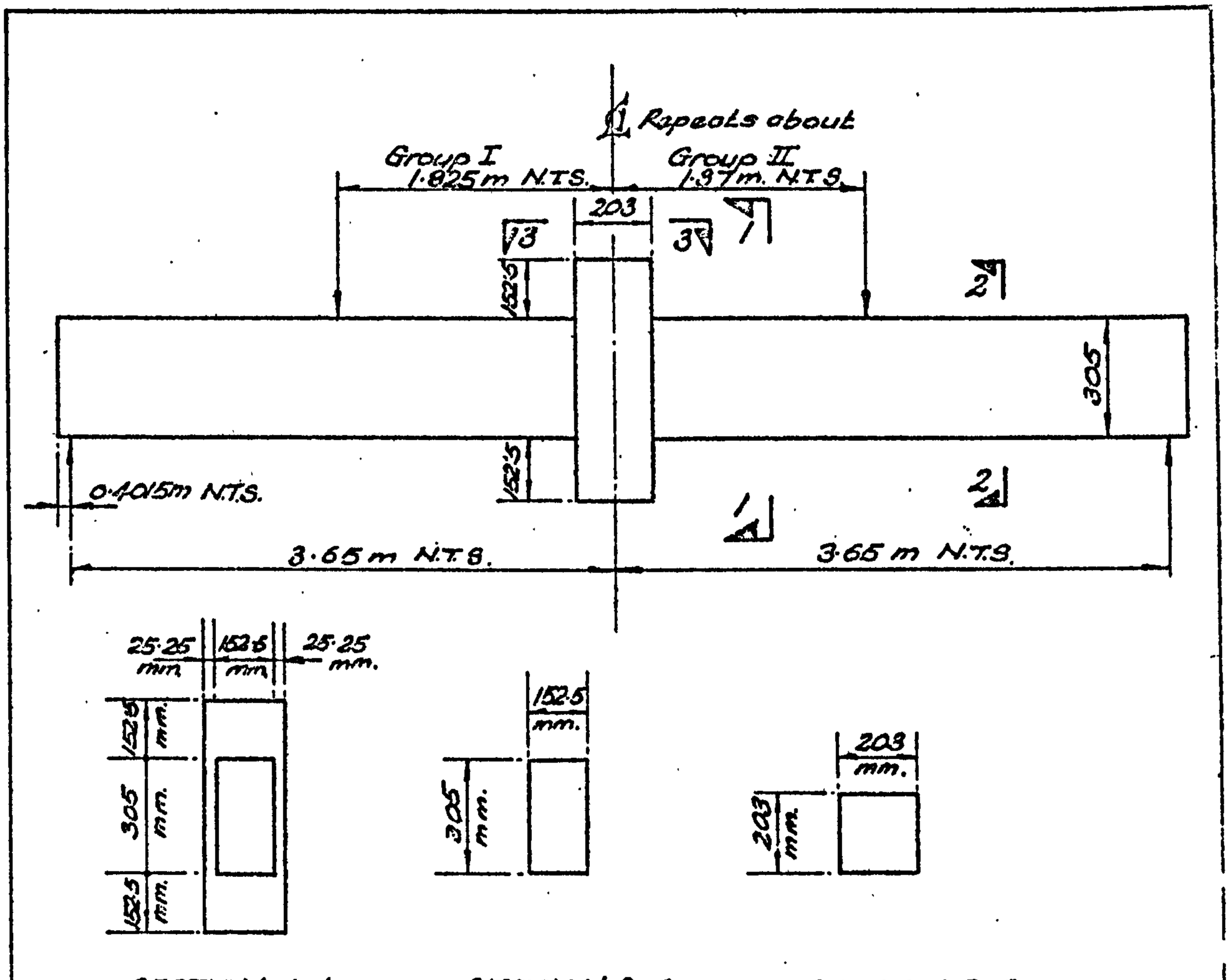
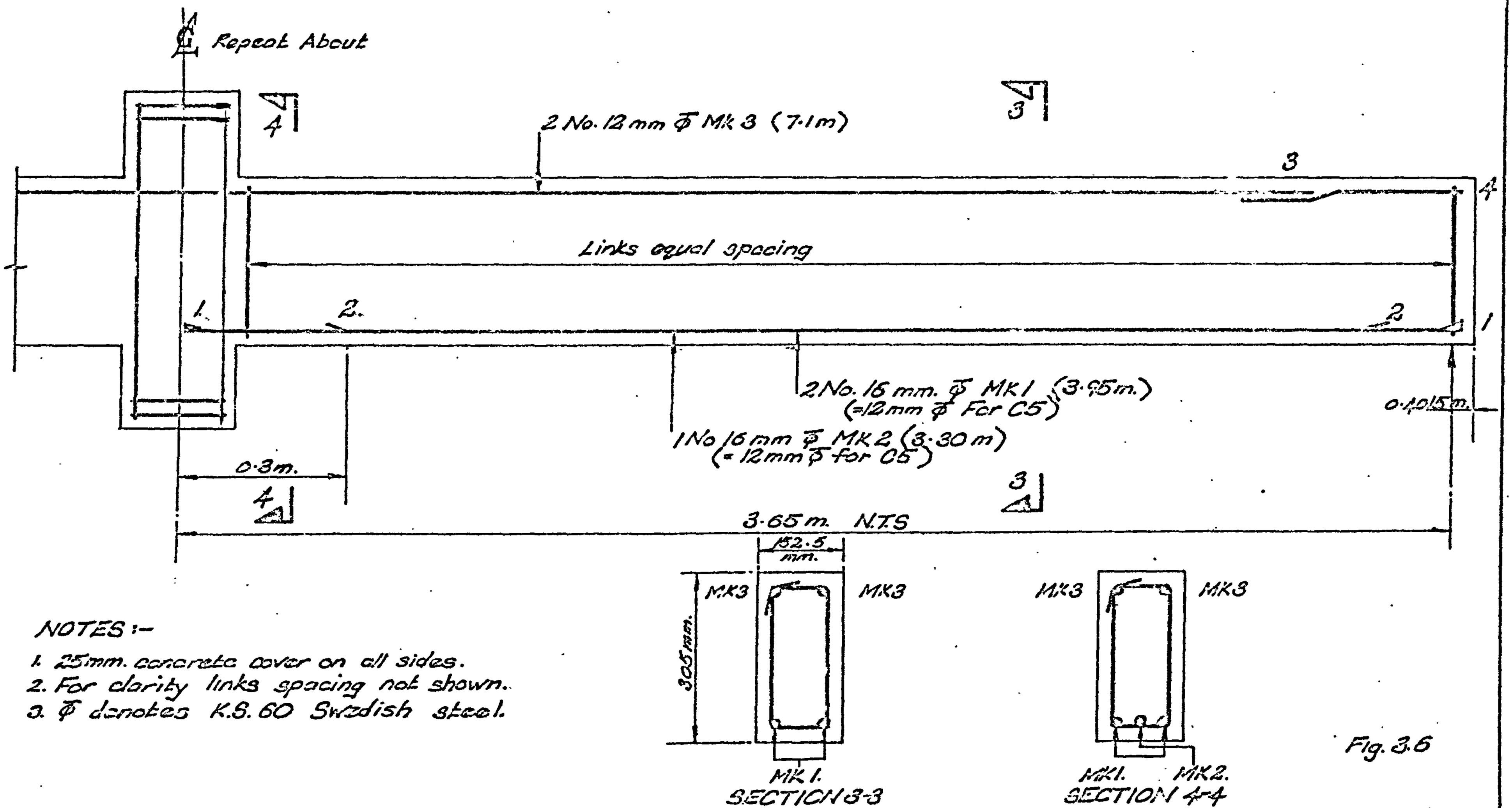


FIG. 3.4. TYPICAL STRESS-STRAIN CURVE FOR K560. BARS.



LAYOUT AND LOADING SYSTEM FOR CONTINUOUS BEAMS

Fig. 3·5



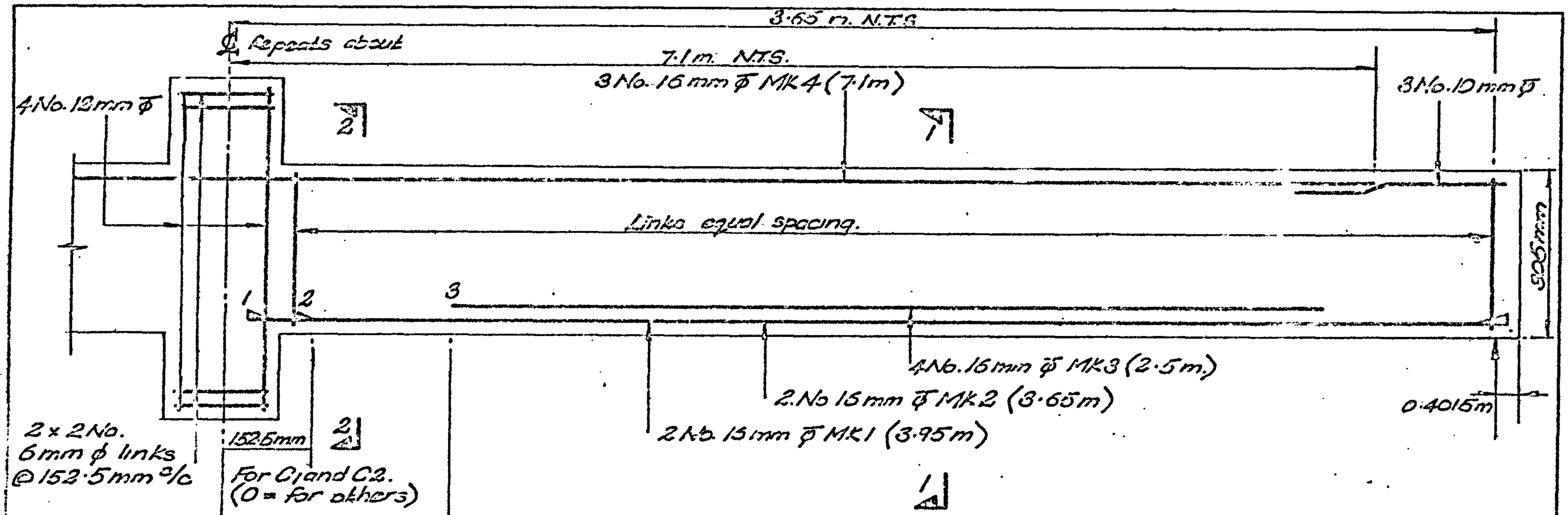
NOTES :-

1. 25mm. concrete cover on all sides.
2. For clarity links spacing not shown.
3. ⌀ denotes K.S. 60 Swedish steel.

Fig. 3.6

BEAMS :- C8, C4, C5, C6, C9, C10, C11, C13 (For links spacing see table 3.3)

REINFORCEMENT DETAILS FOR CONTINUOUS BEAMS



NOTES :-

1. 25mm concrete cover on all sides
2. For clarity links spacing not shown.
3. ϕ denotes K.S. 60 Swedish steel.

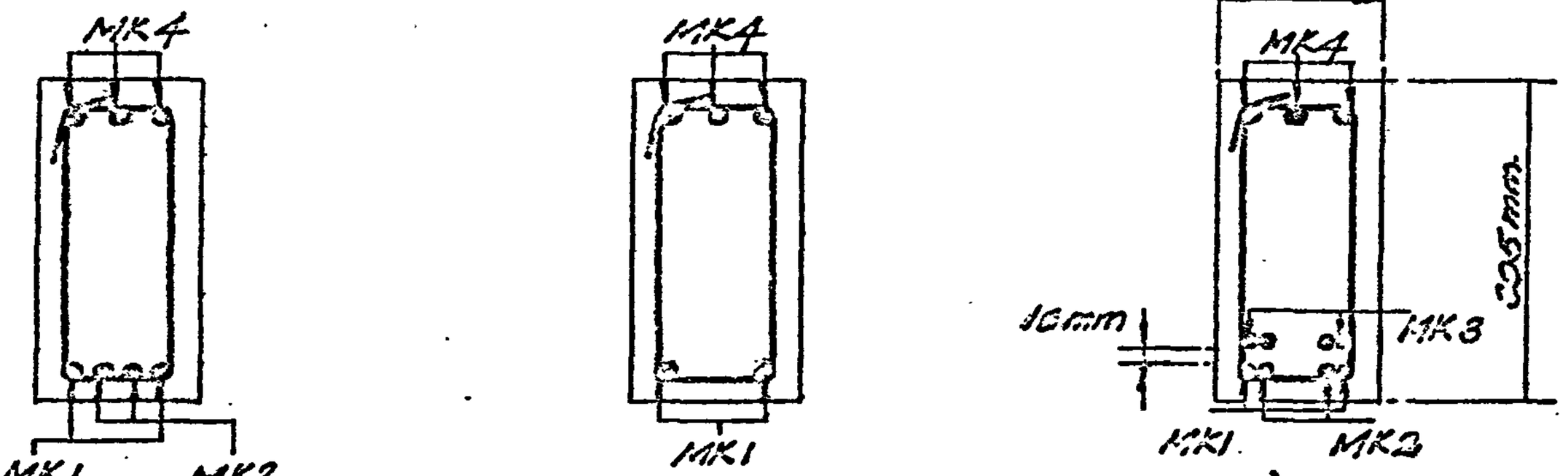


Fig. 3·7.

BEAMS C1, C2, C7, C8 and C 12 (For Links see table 3·3)

REINFORCEMENT DETAILS FOR CONTINUOUS BEAMS

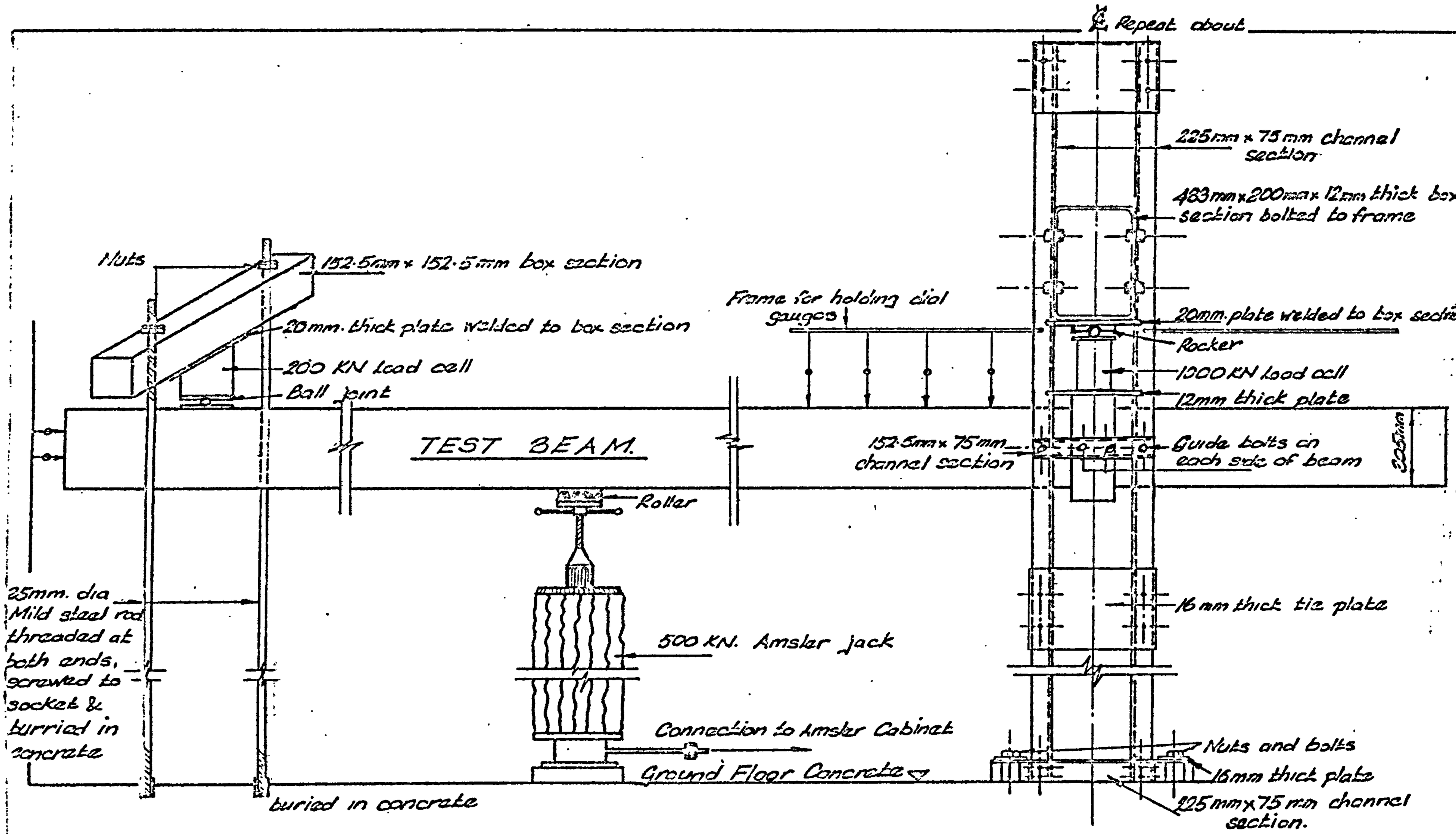


Fig. 3·8 TEST FRAME FOR CONTINUOUS BEAMS

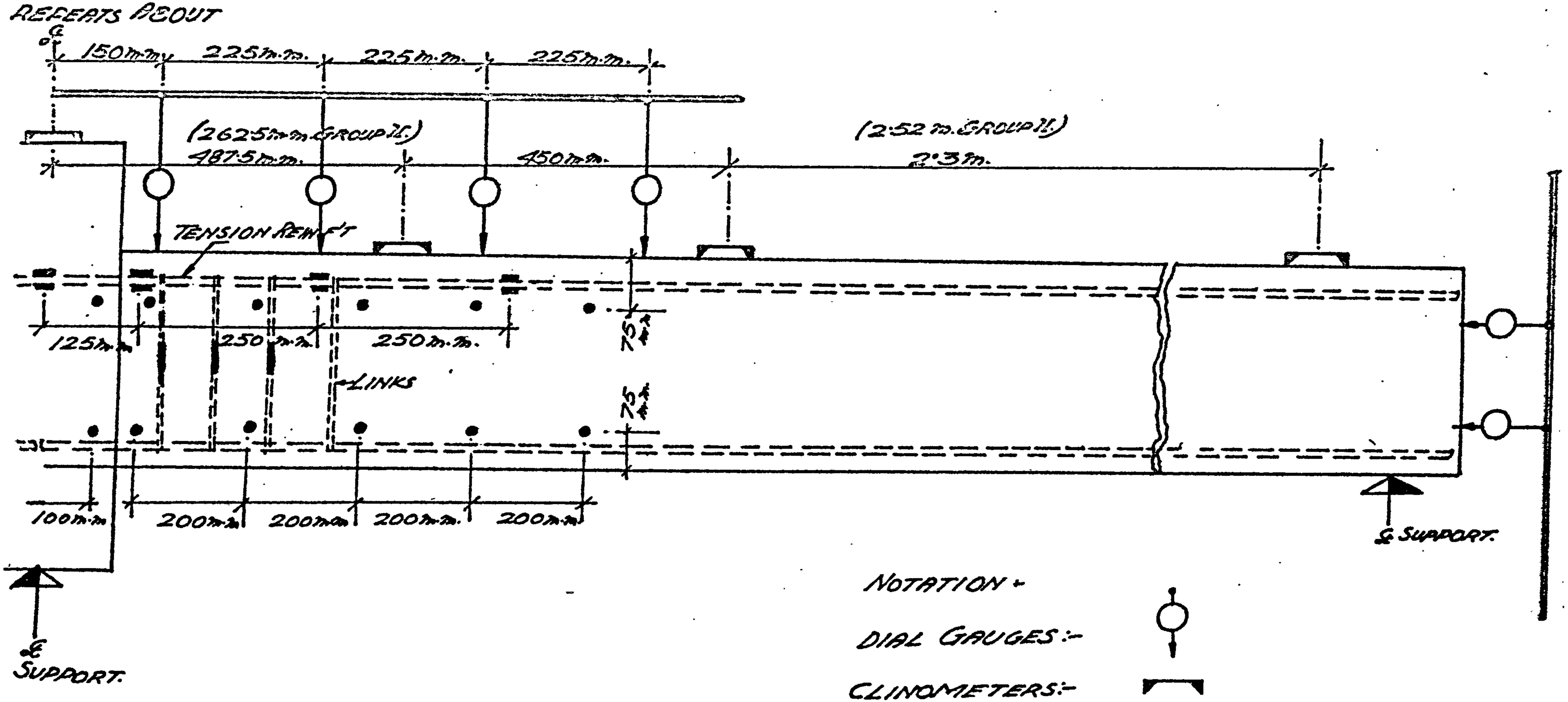


FIG. 3.9. INSTRUMENTATION.

FOR CONTINUOUS BEAMS.

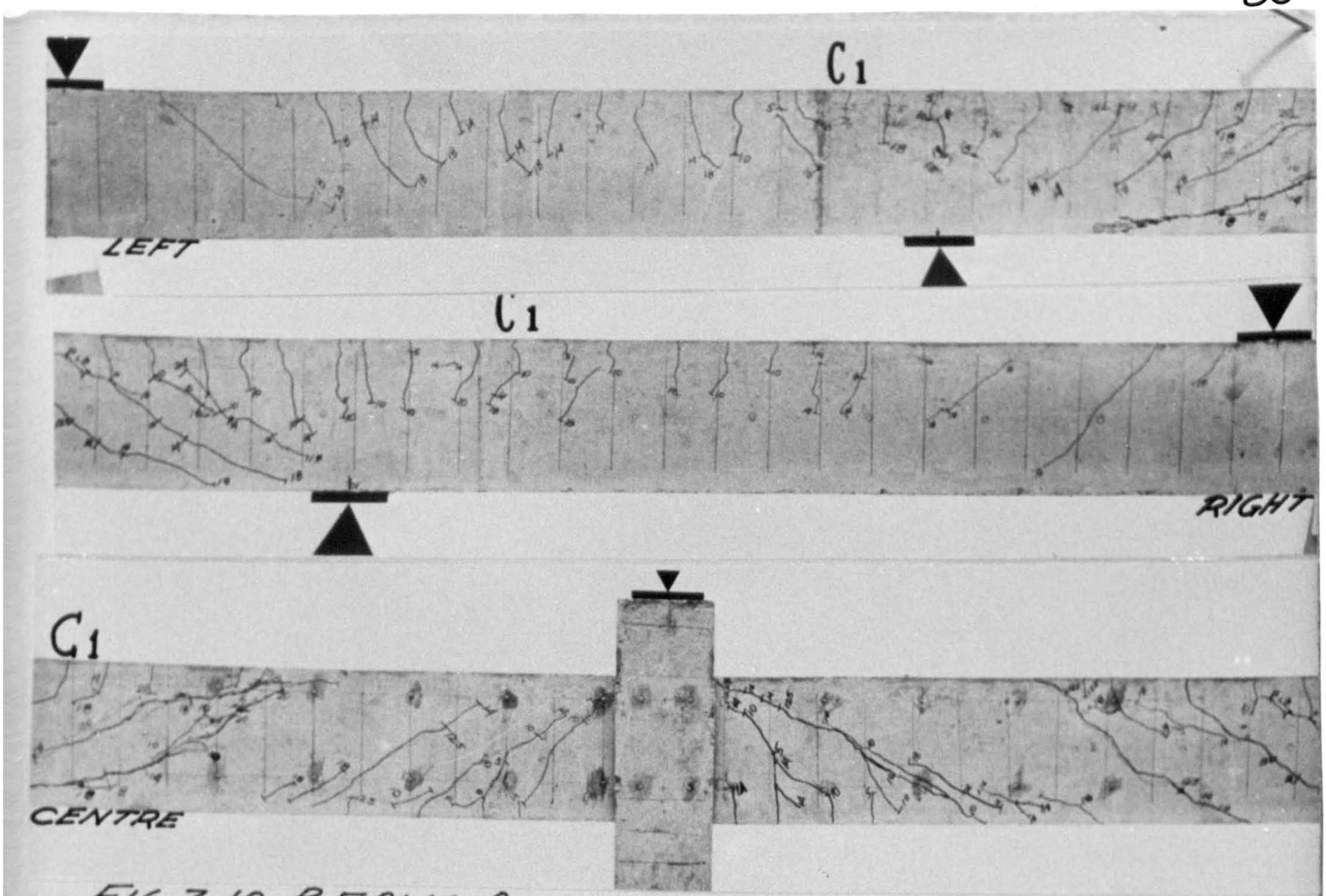
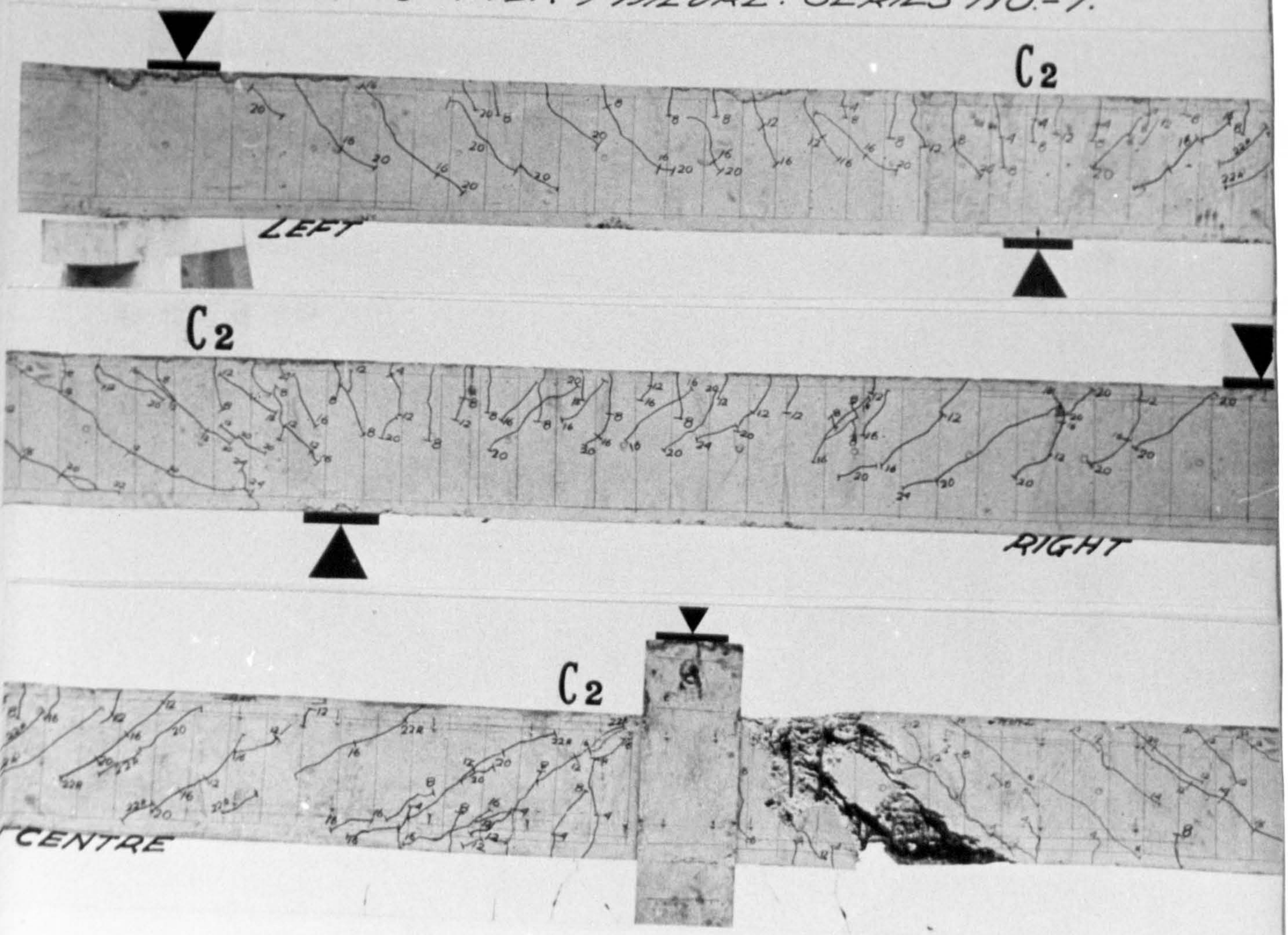


FIG. 3.10. BEAMS AFTER FAILURE. SERIES NO:- 1.



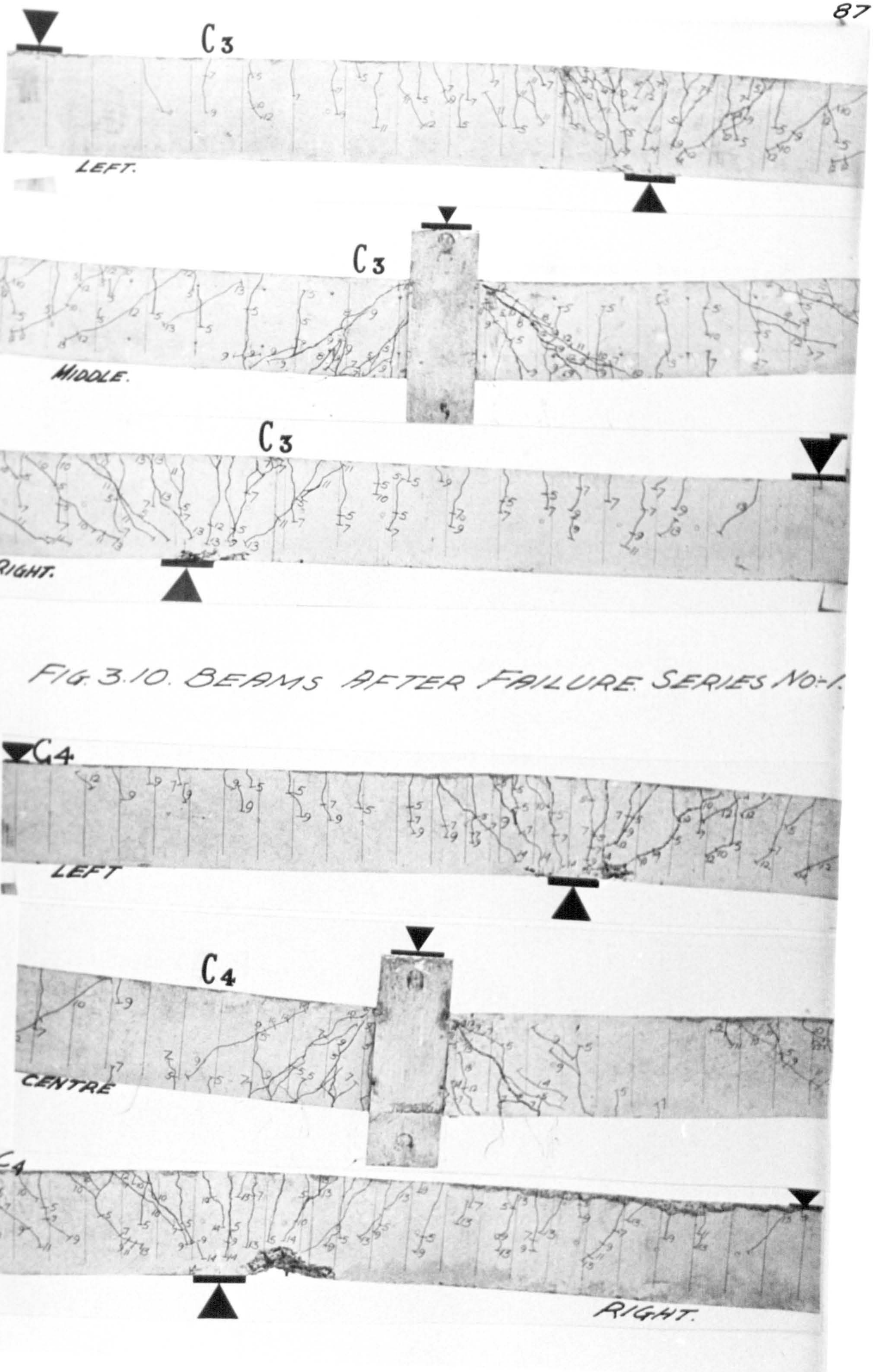


FIG. 3.10. BEAMS AFTER FAILURE. SERIES NO-1.

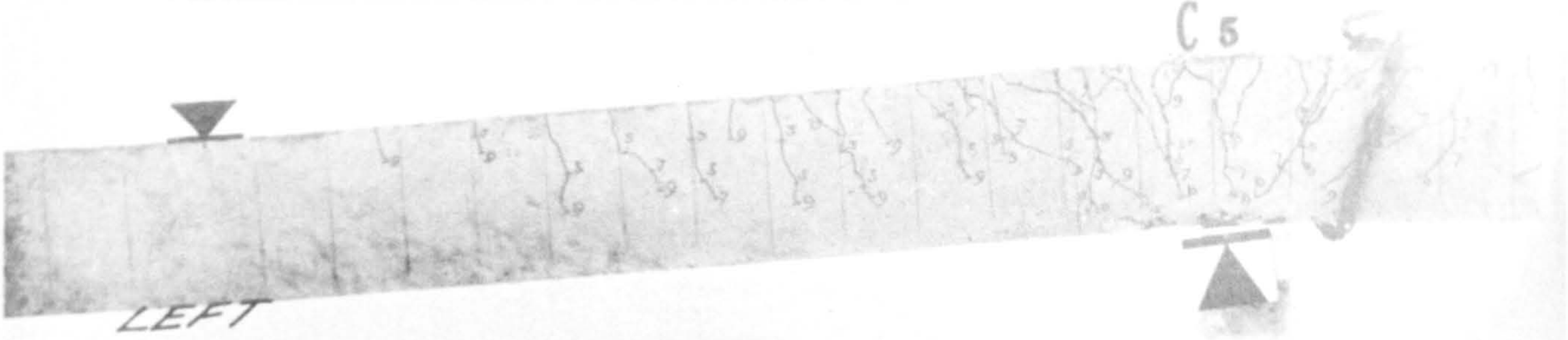
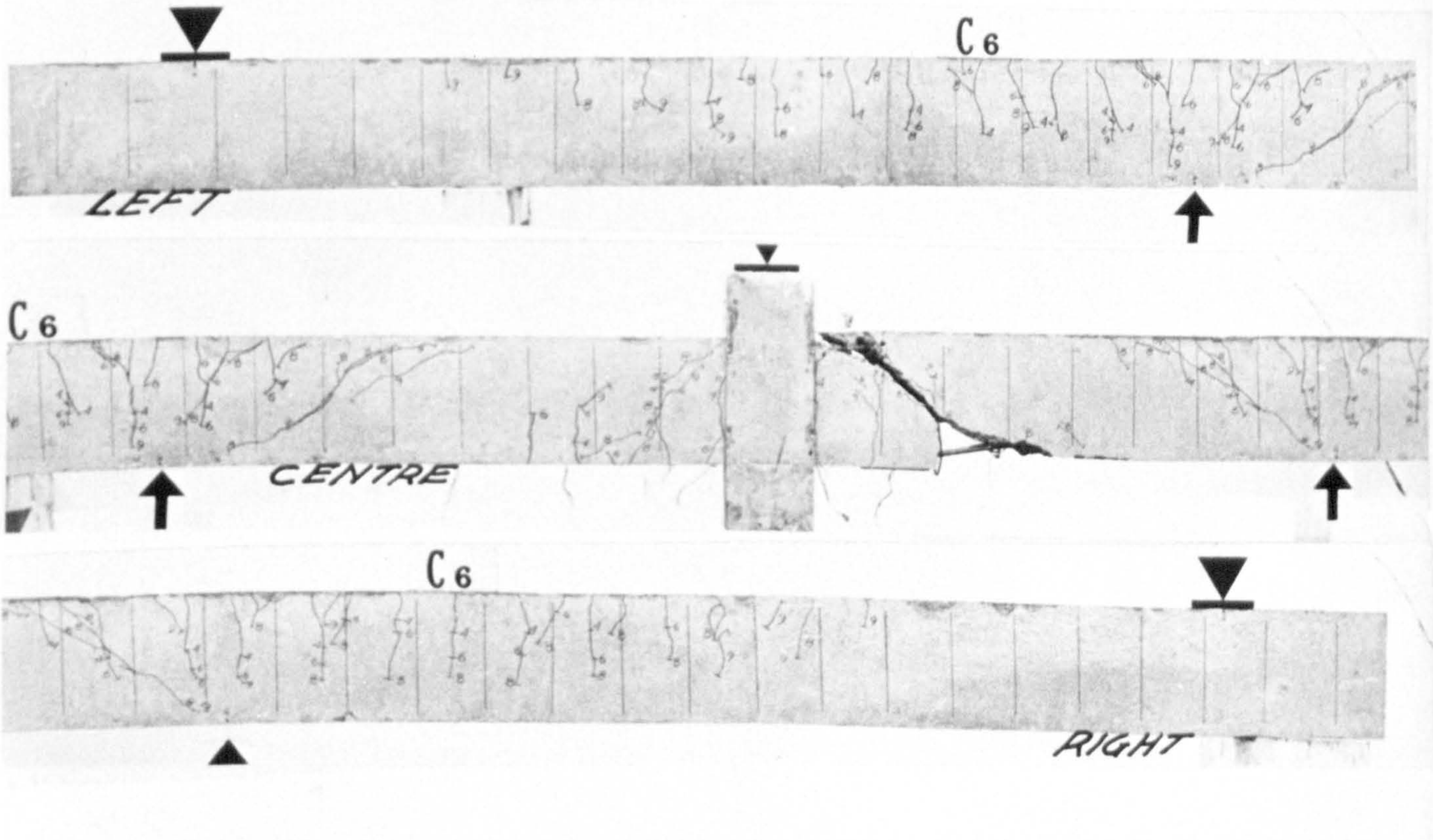


FIG. 3.10 BEAMS AFTER FAILURE. SERIES NO:-1



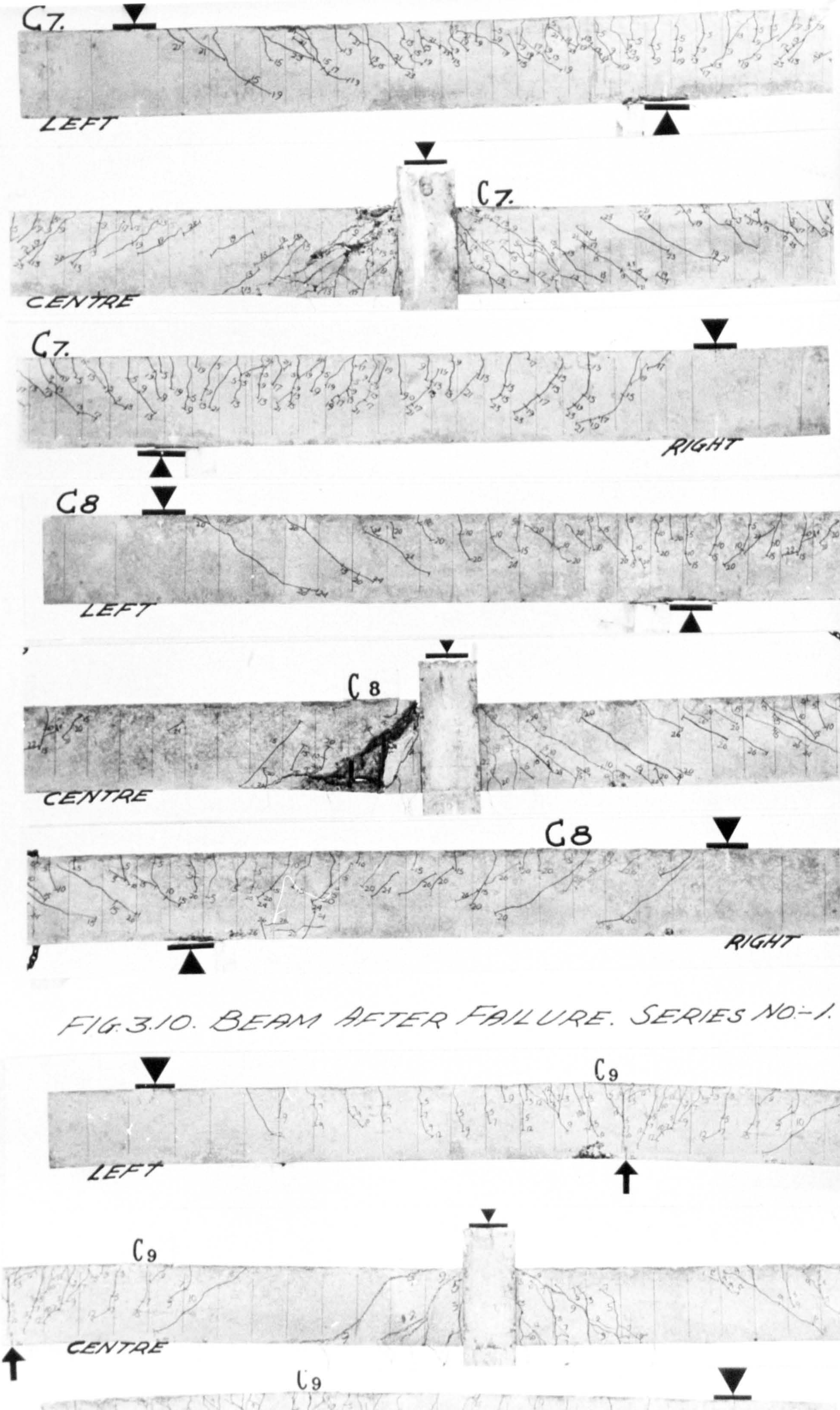


FIG. 3.10. BEAM AFTER FAILURE. SERIES NO:-1.

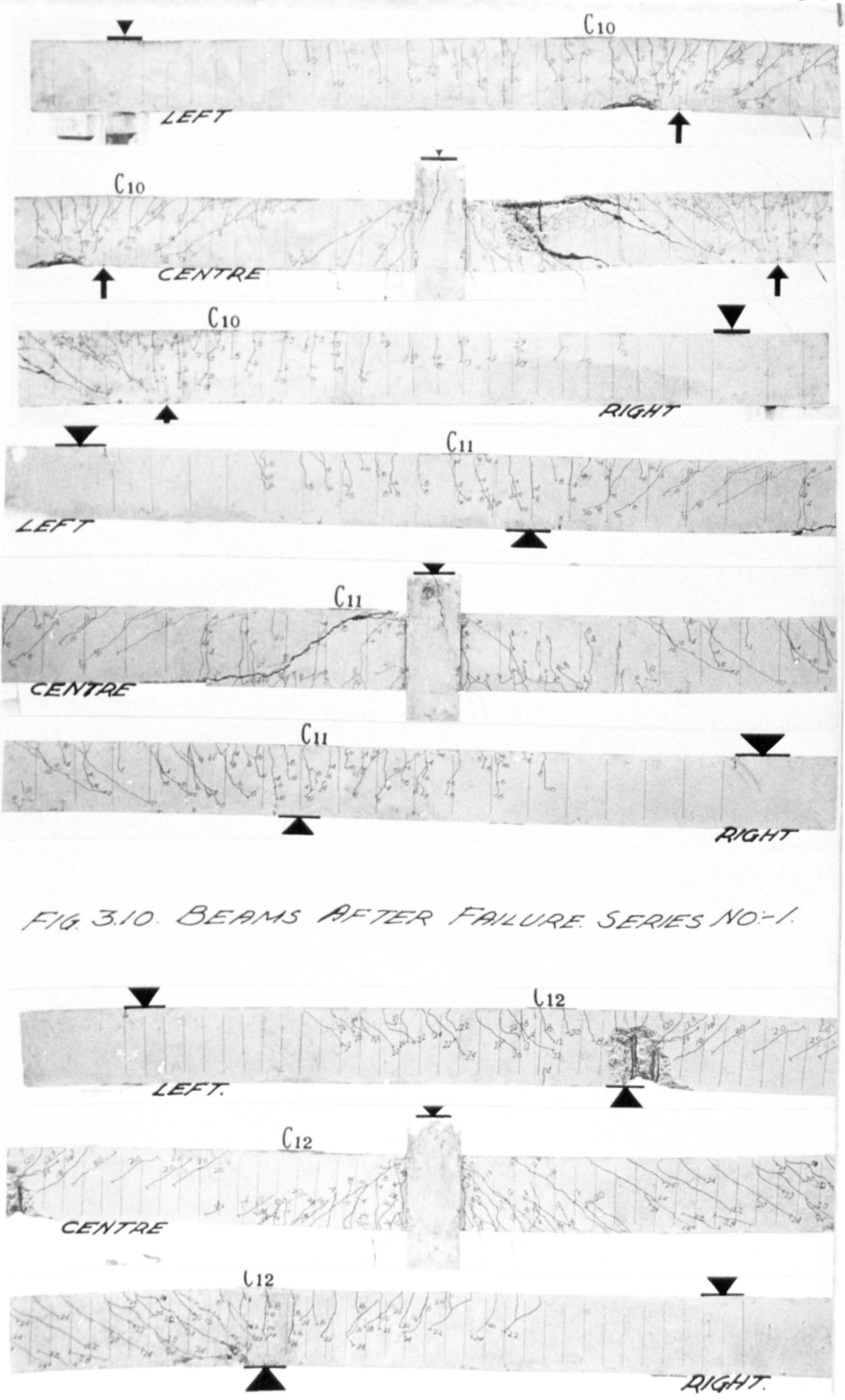


FIG. 3.10. BEAMS AFTER FAILURE. SERIES NO:-1.

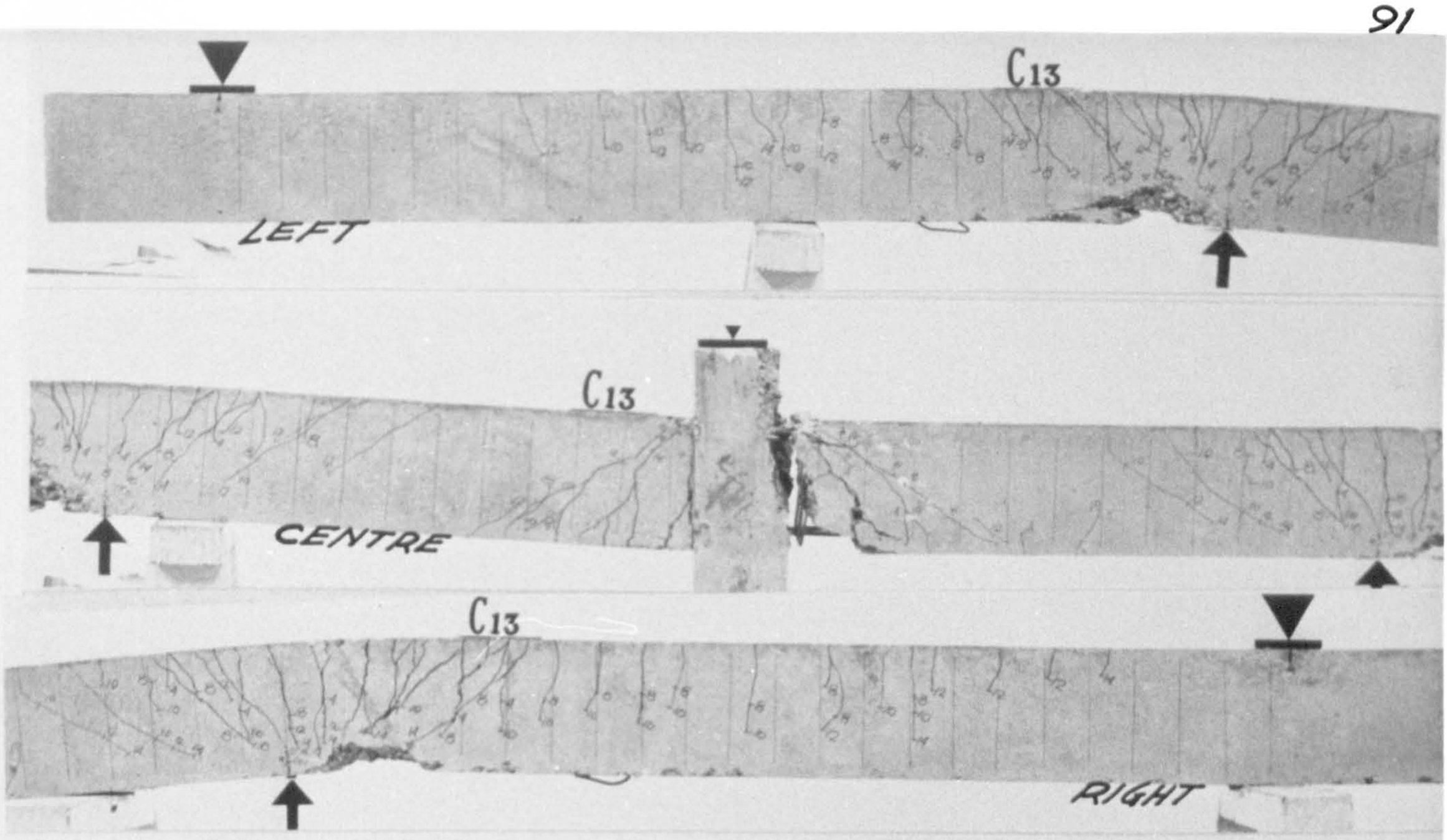
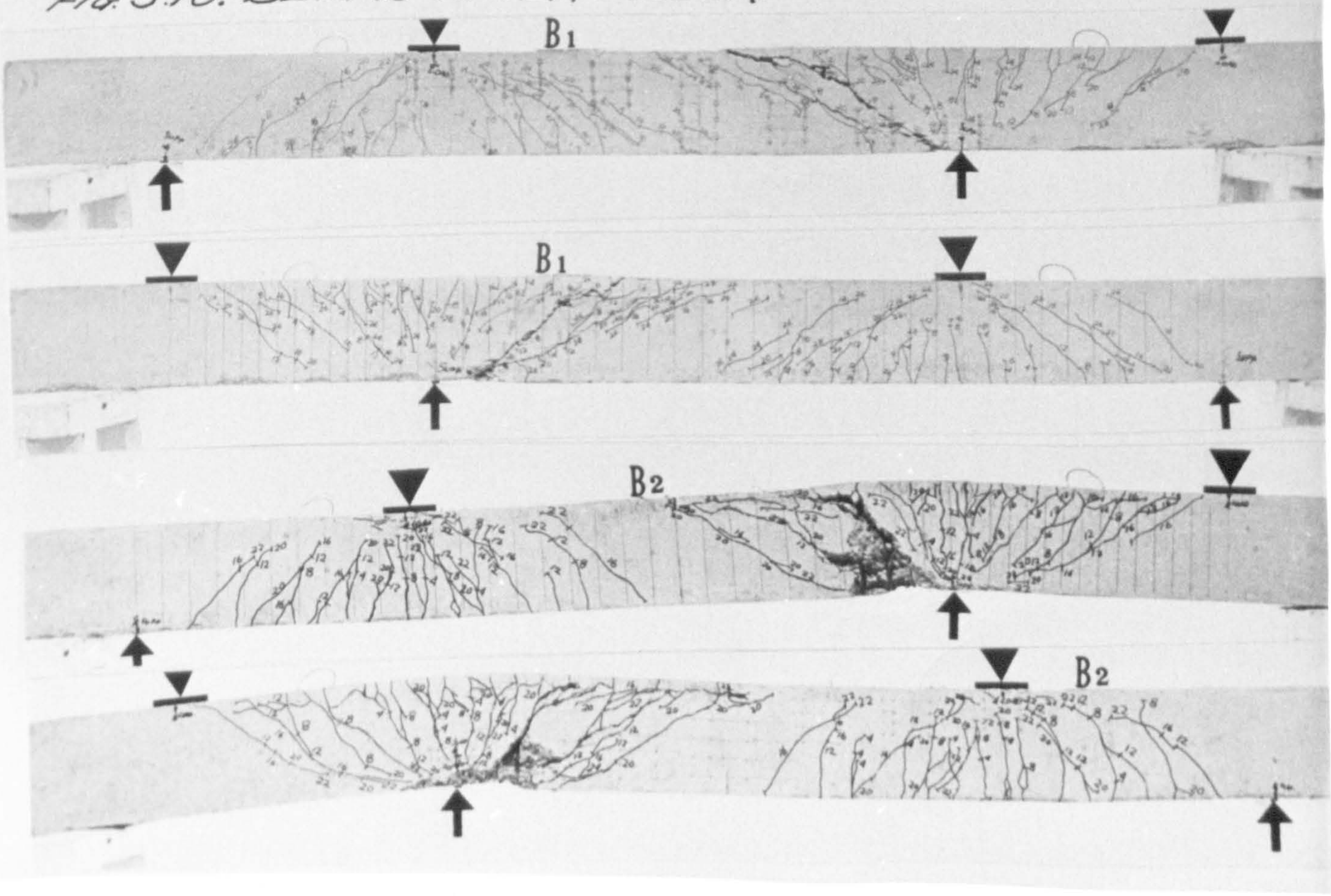


FIG. 3.10. BEAMS AFTER FAILURE. SERIES NO:- 1.

FIG. 3.10. BEAMS AFTER FAILURE. SERIES NO:- 2.



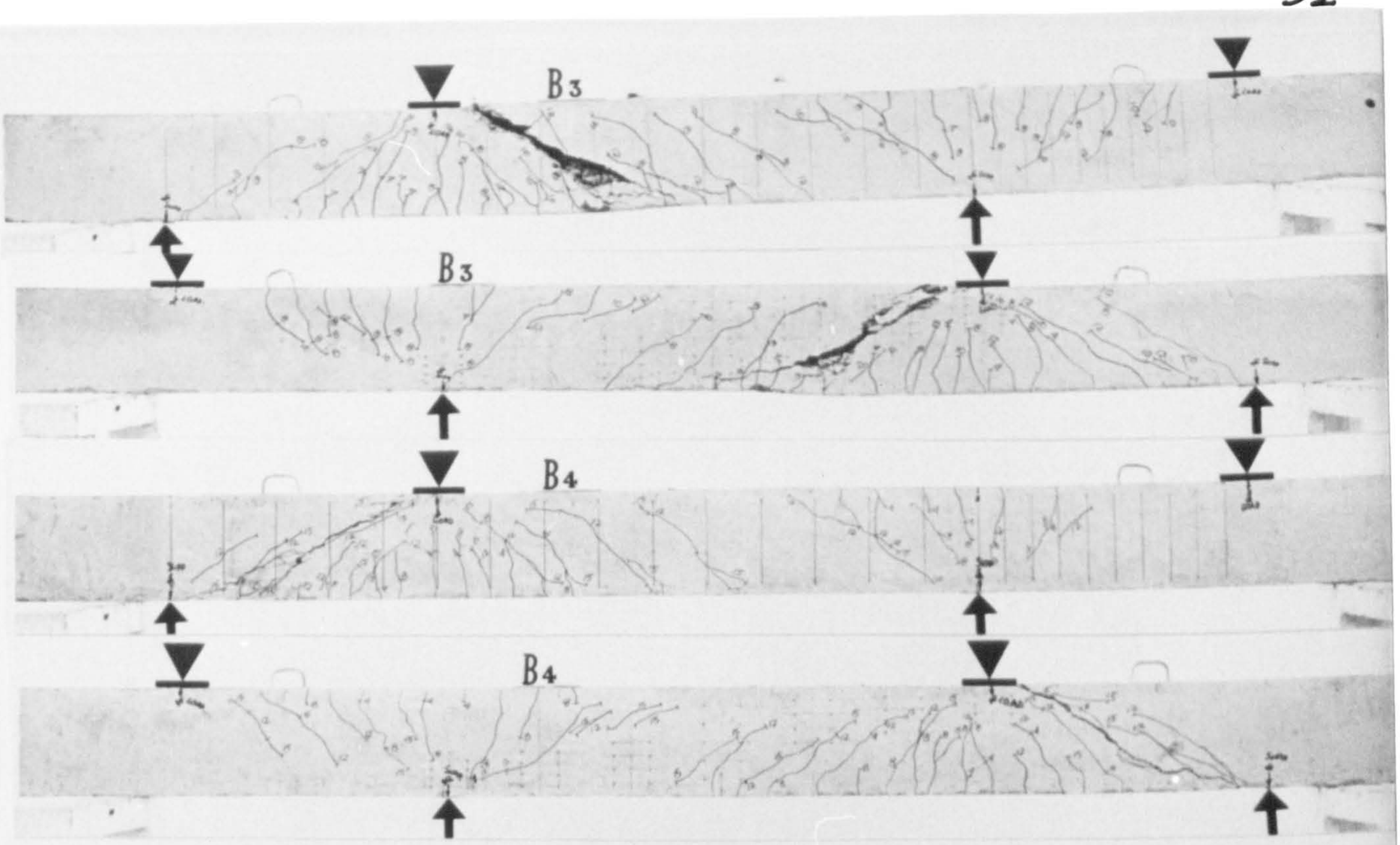
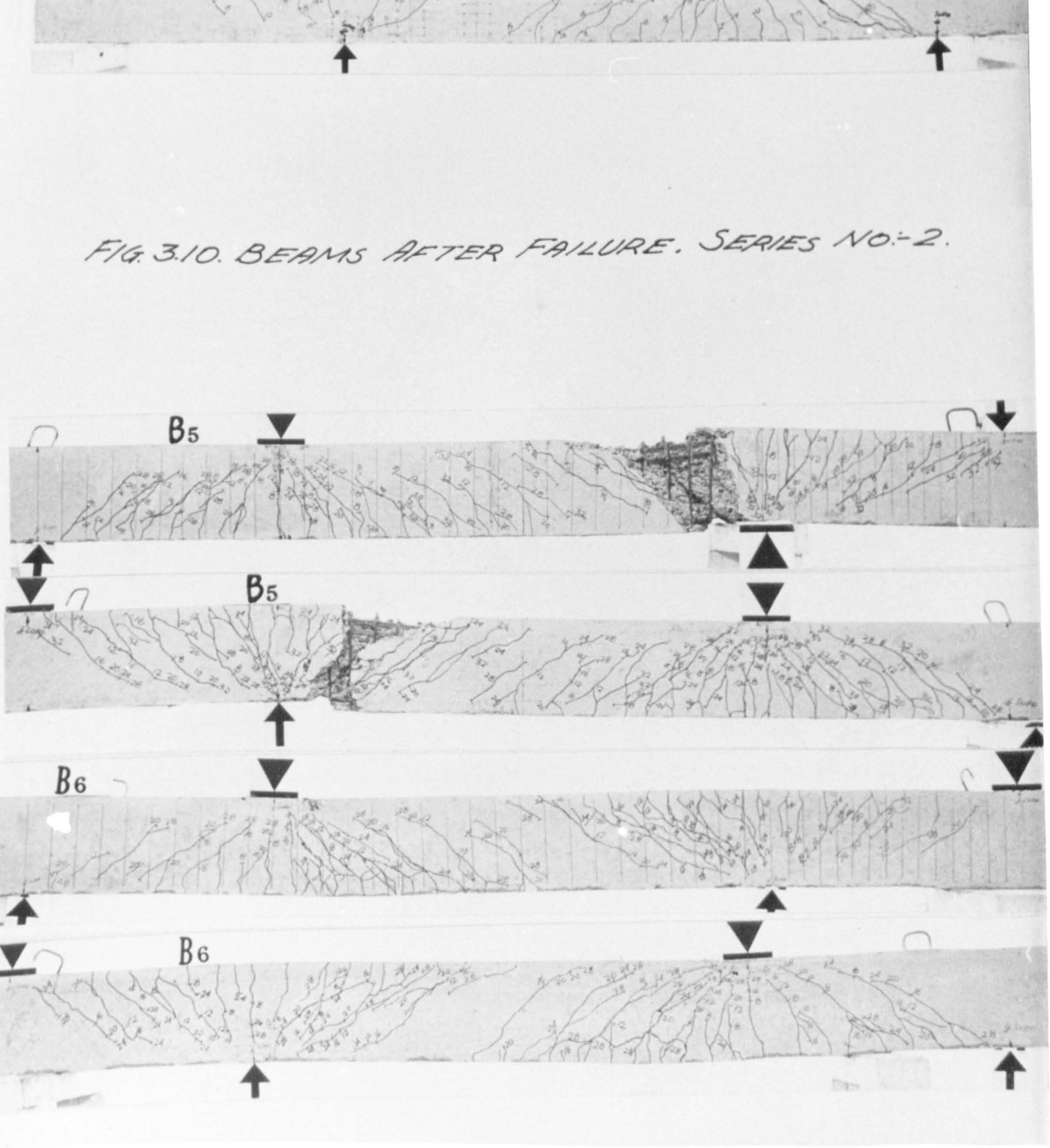


FIG. 3.10. BEAMS AFTER FAILURE. SERIES NO:-2.



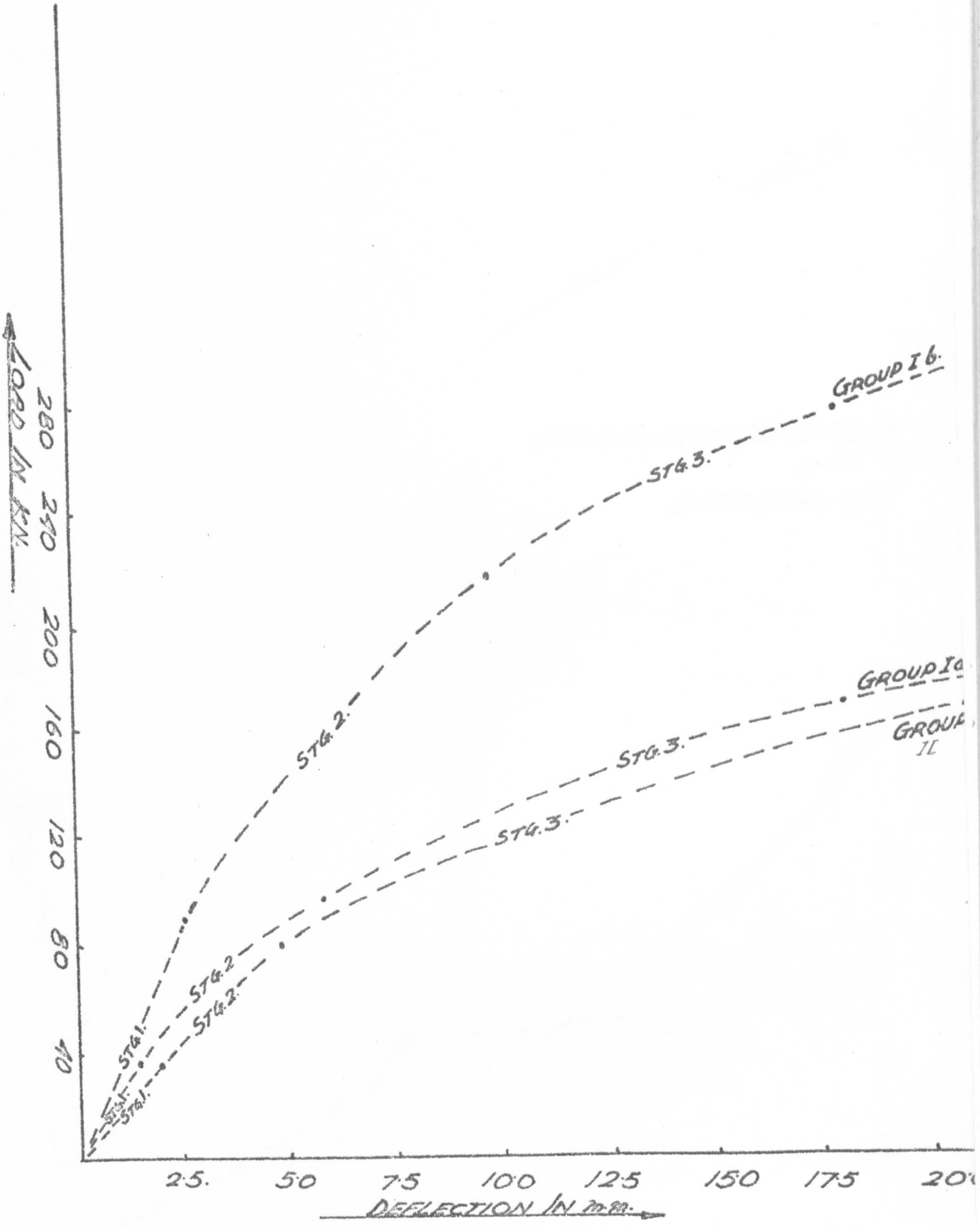


FIG. 3.11. :- LOAD-DEFLECTION DIAGRAM

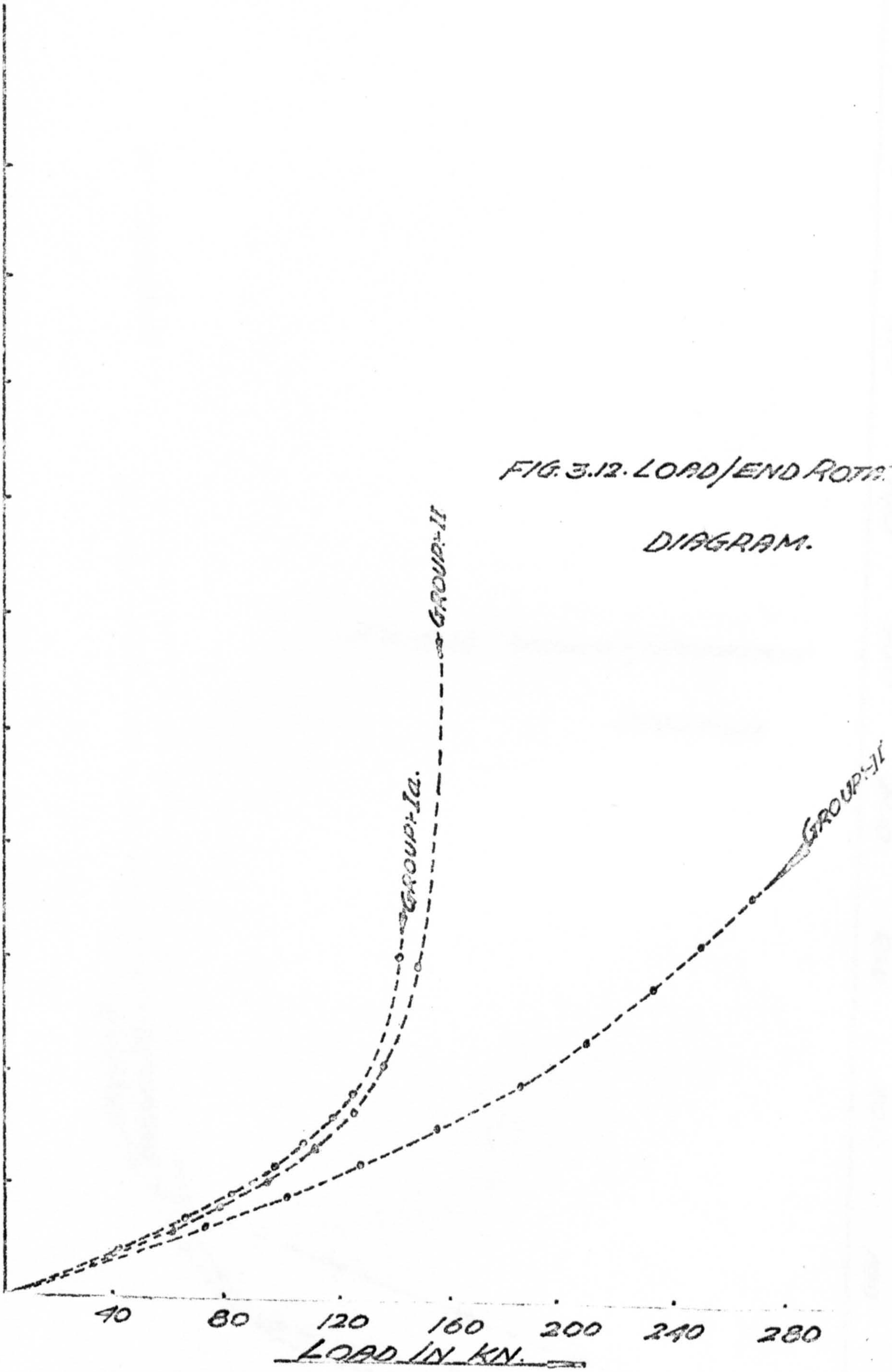


FIG. 3.12. LOAD/END ROTATION DIAGRAM.

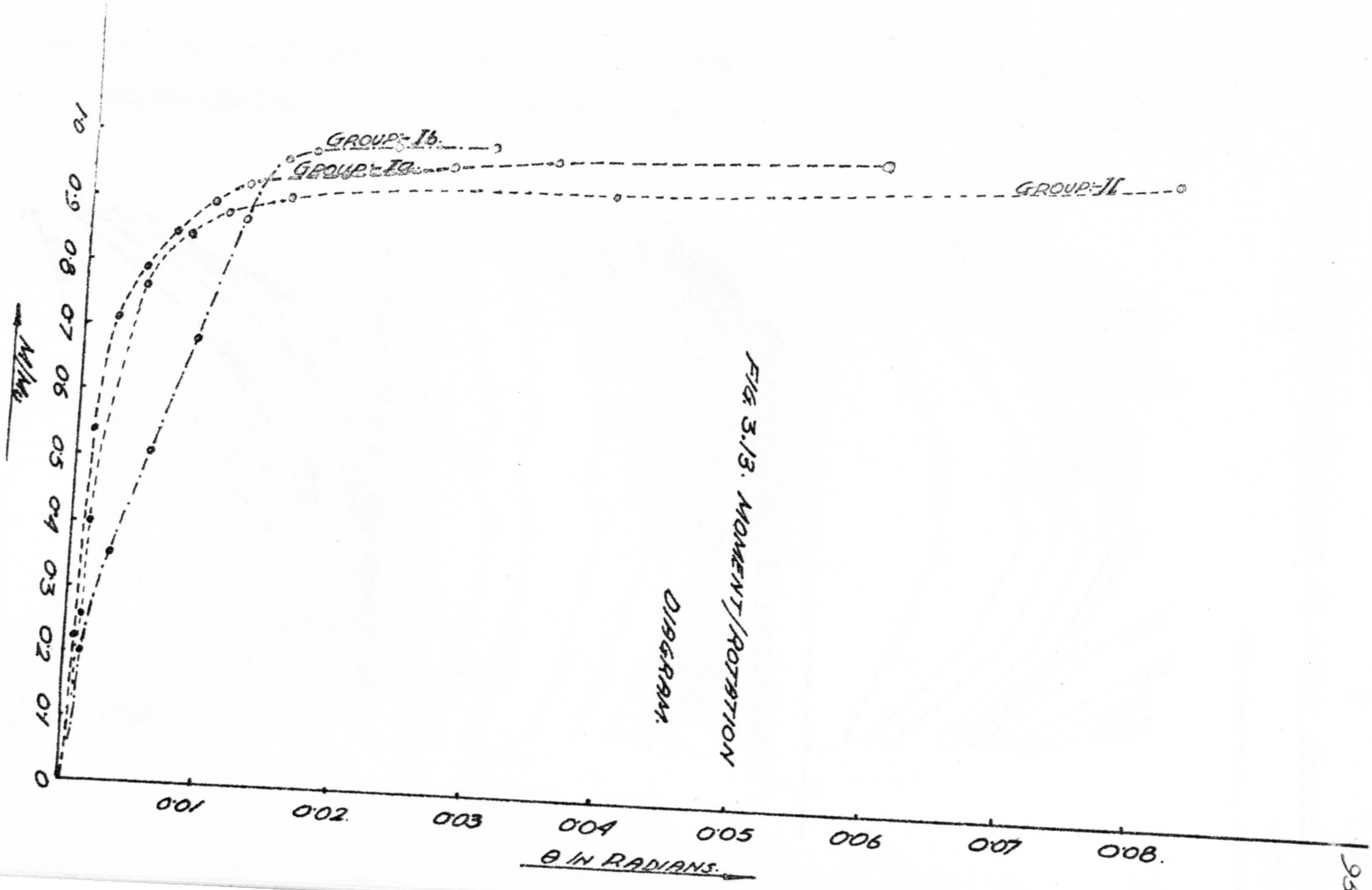
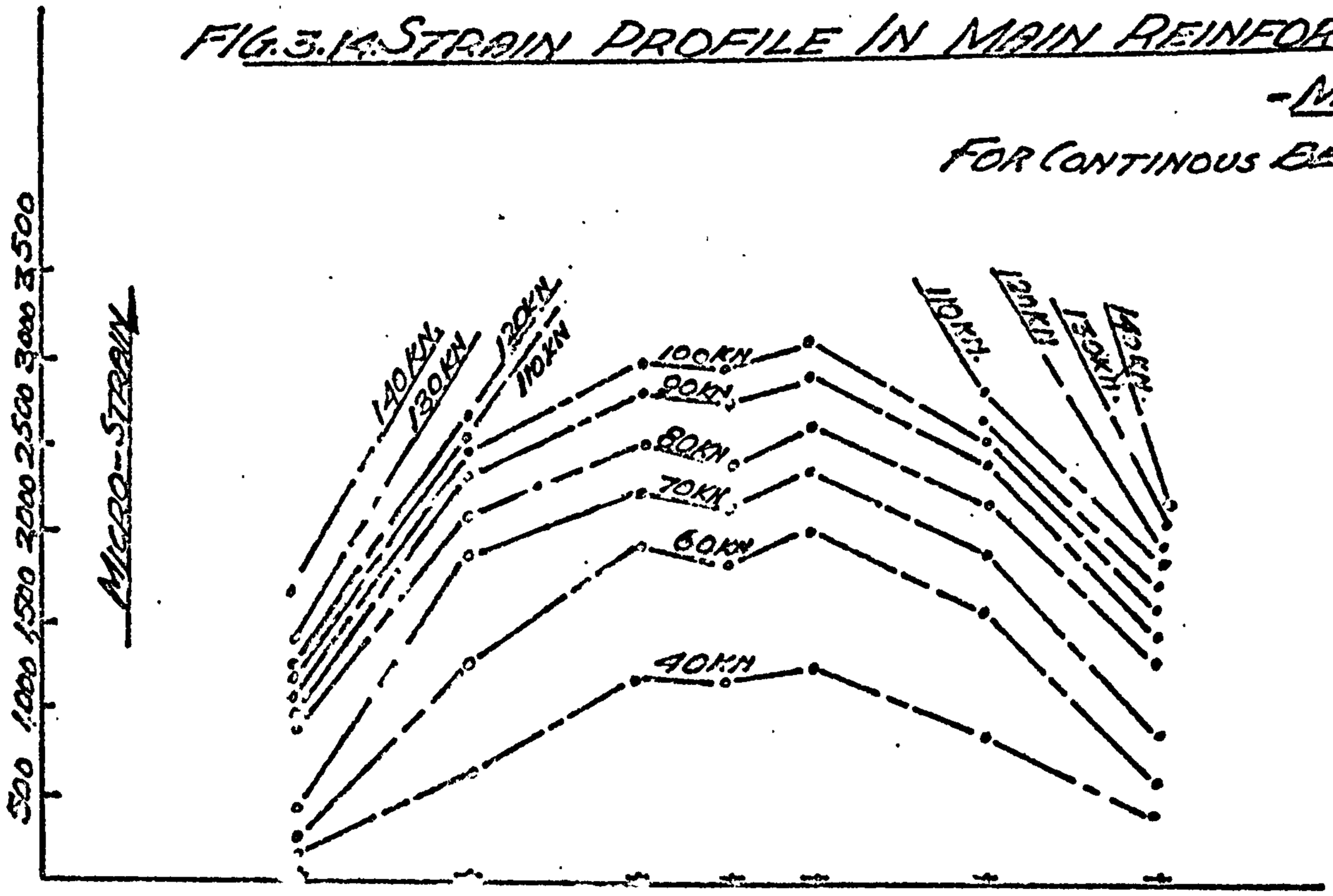
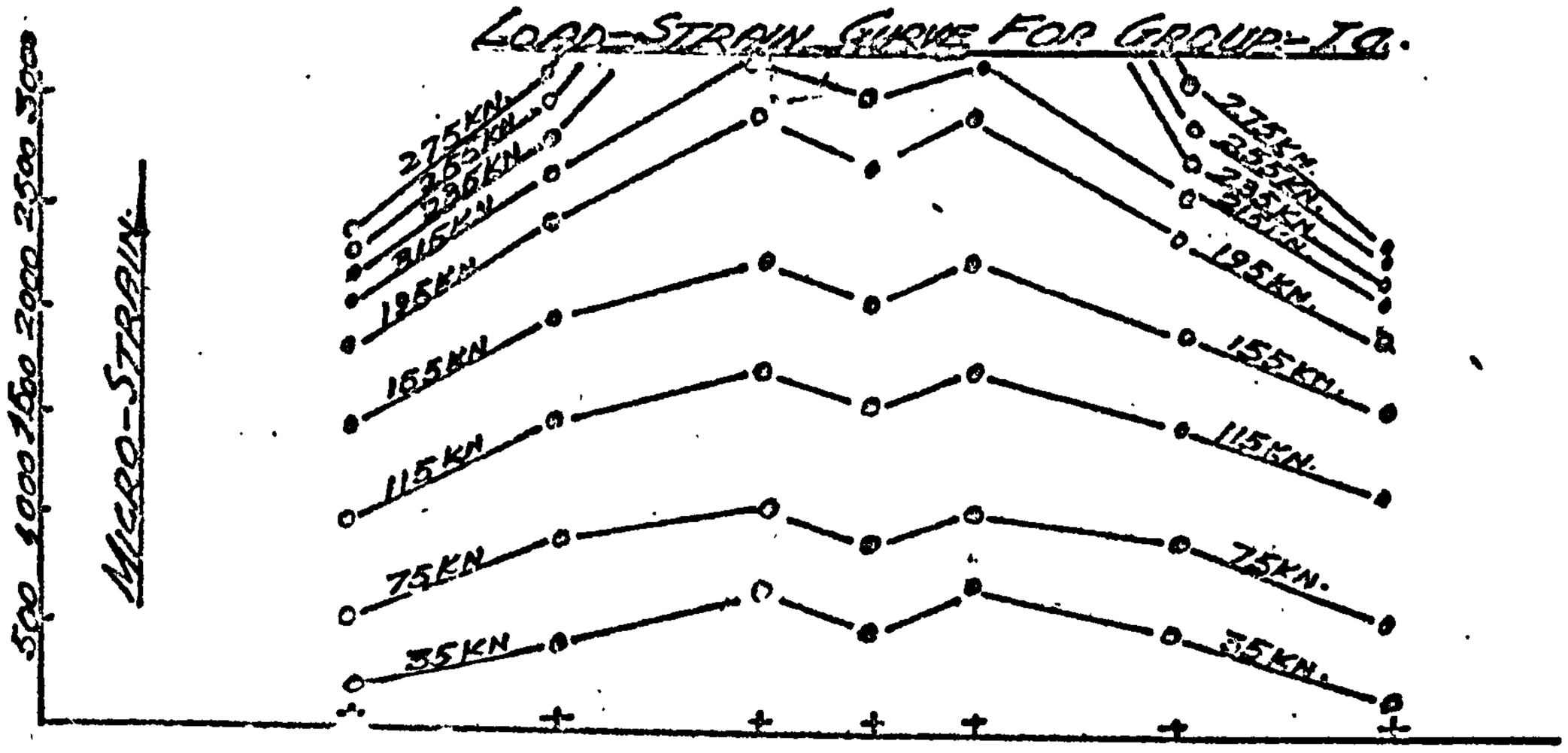

GROUP-Ib.
GROUP-Ia.
GROUP-II
0
0·1
0·2
0·3
0·4
0·5
0·6
0·7
0·8
0·9
1·0
0·01
0·02
0·03
0·04
0·05
0·06
0·07
0·08.
θ IN RADIANS.
FIG 3.13. MOMENT/ROTATION DIAGRAM.

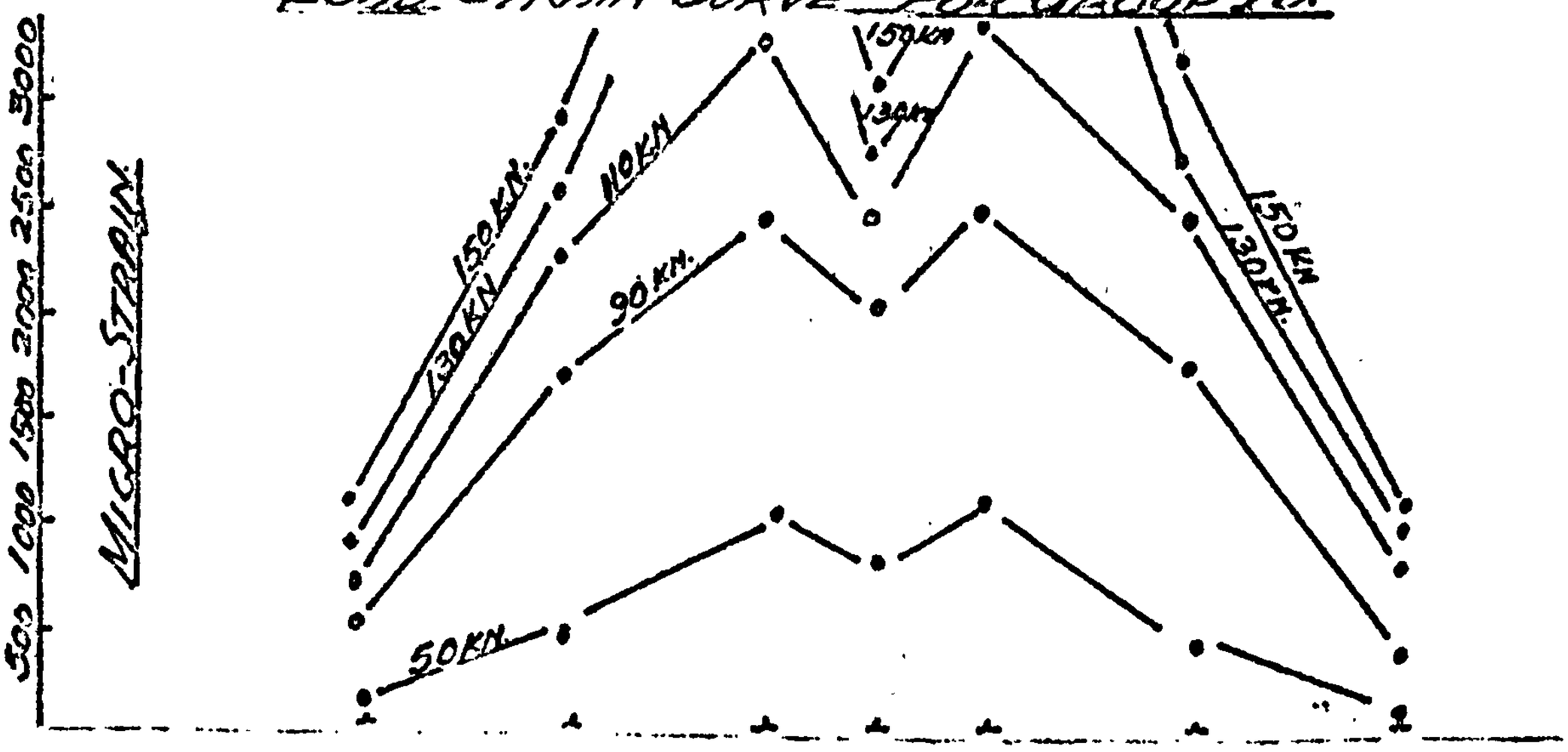
FIG. 3.14 STRAIN PROFILE IN MAIN REINFORCE-MENT FOR CONTINOUS BEAM.



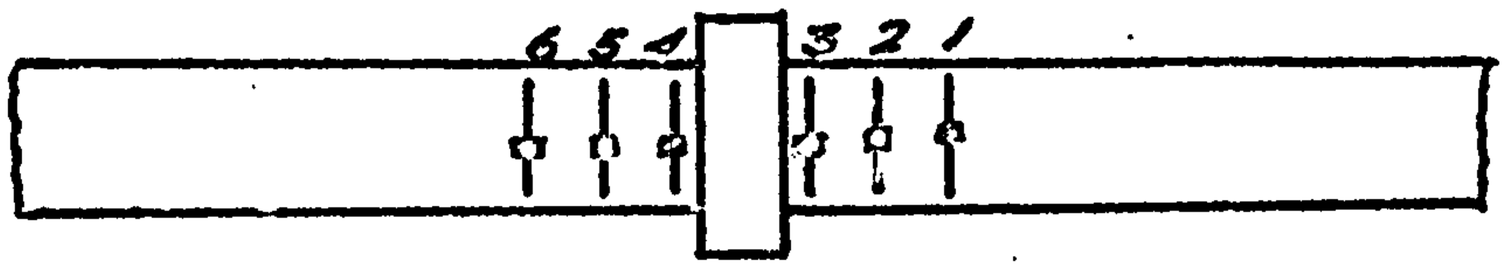
LOAD-STRAIN CURVE FOR GROUP-Ia.



LOAD-STRAIN CURVE FOR GROUP Ib.

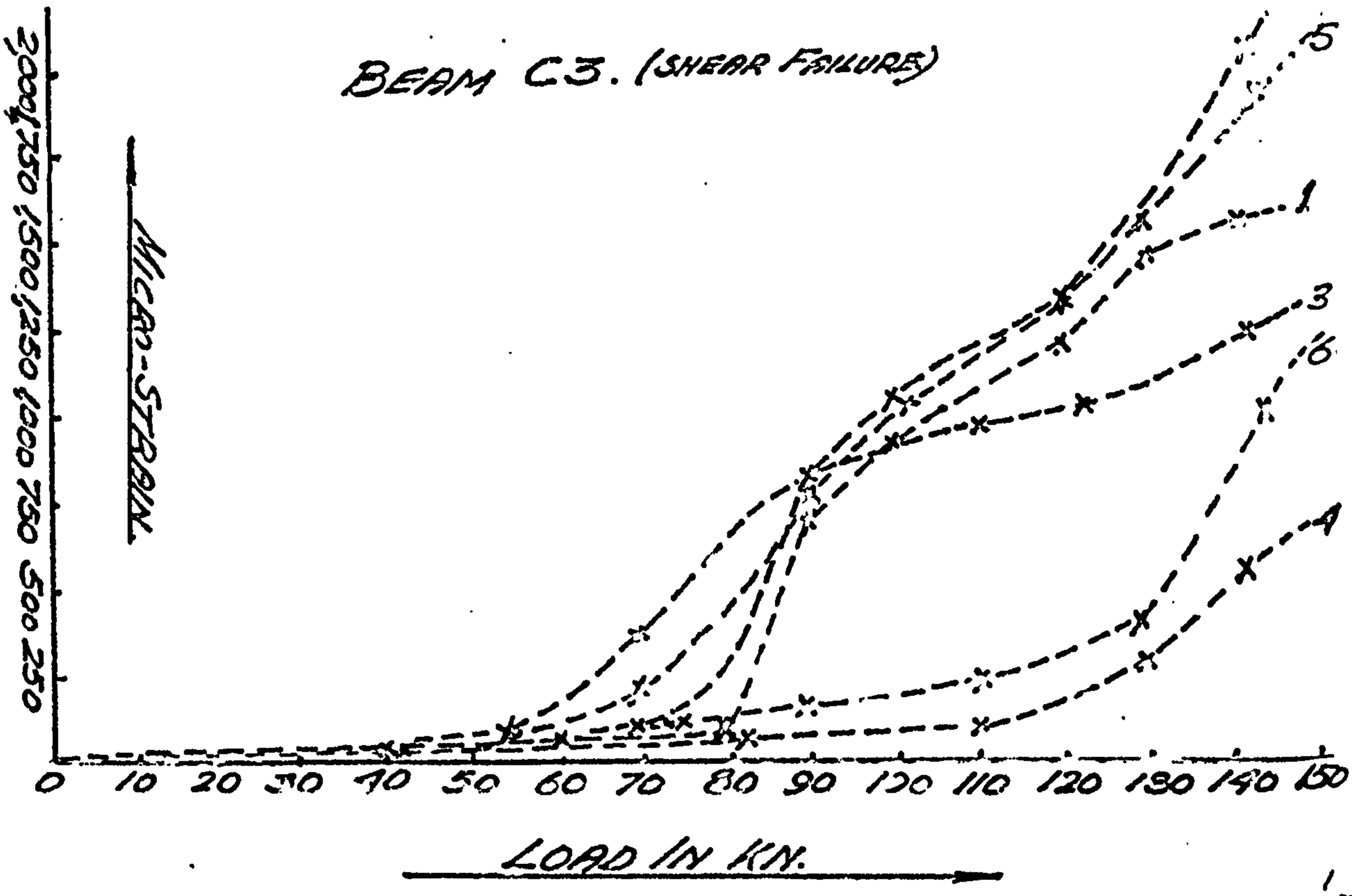


LOAD-STRAIN CURVE FOR GROUP II.



POSITION OF STRAIN GAUGES.

BEAM C3. (SHEAR FAILURE)



BEAM C4. (FLEXURE FAILURE)

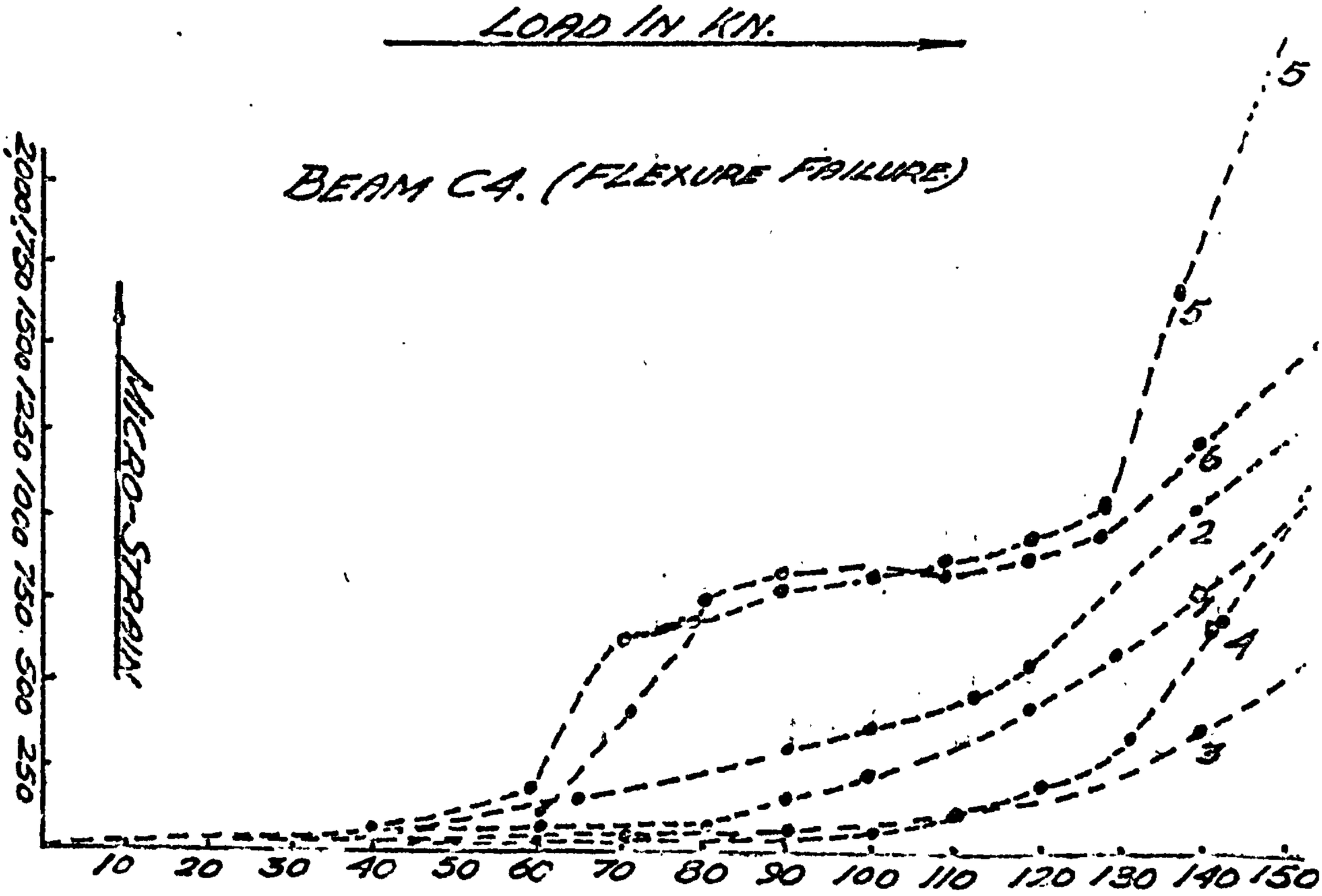
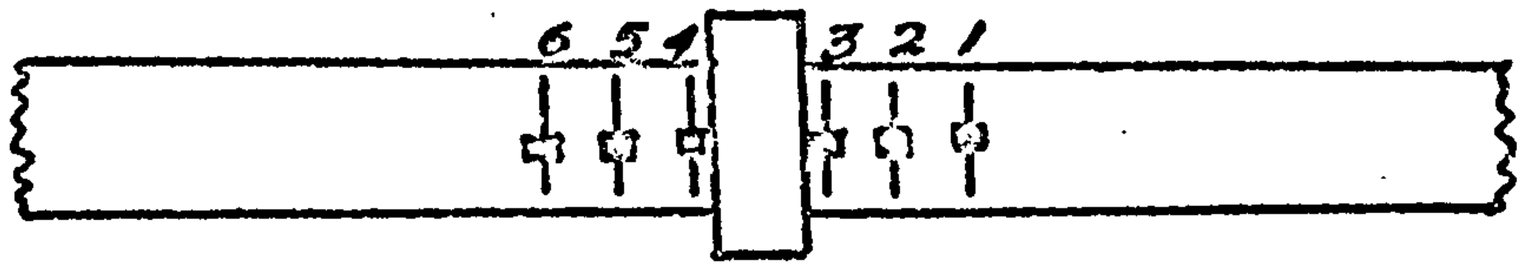


FIG. 3.15. LOAD- STIRRUP STRAIN DIAGRAM, FOR CONTINUOUS BEAM.



POSITION OF STRAIN GAUGES.

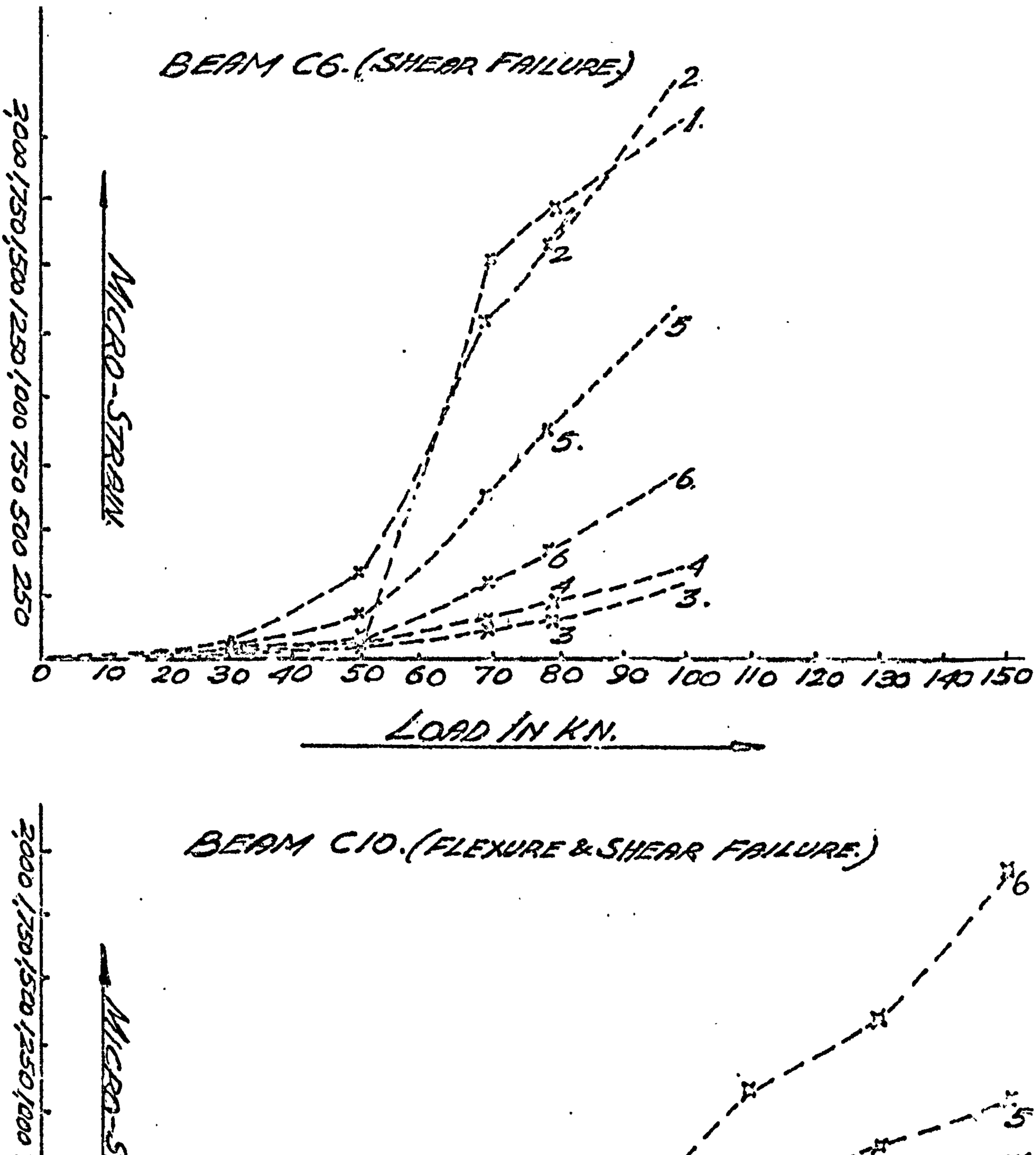
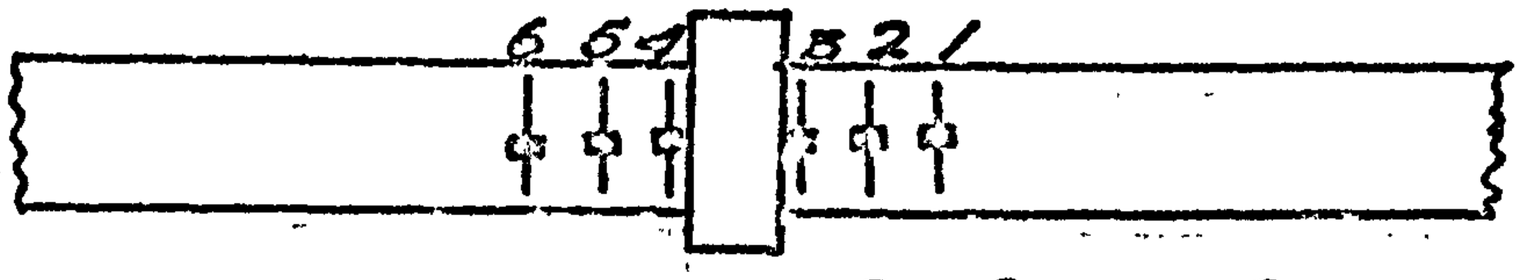
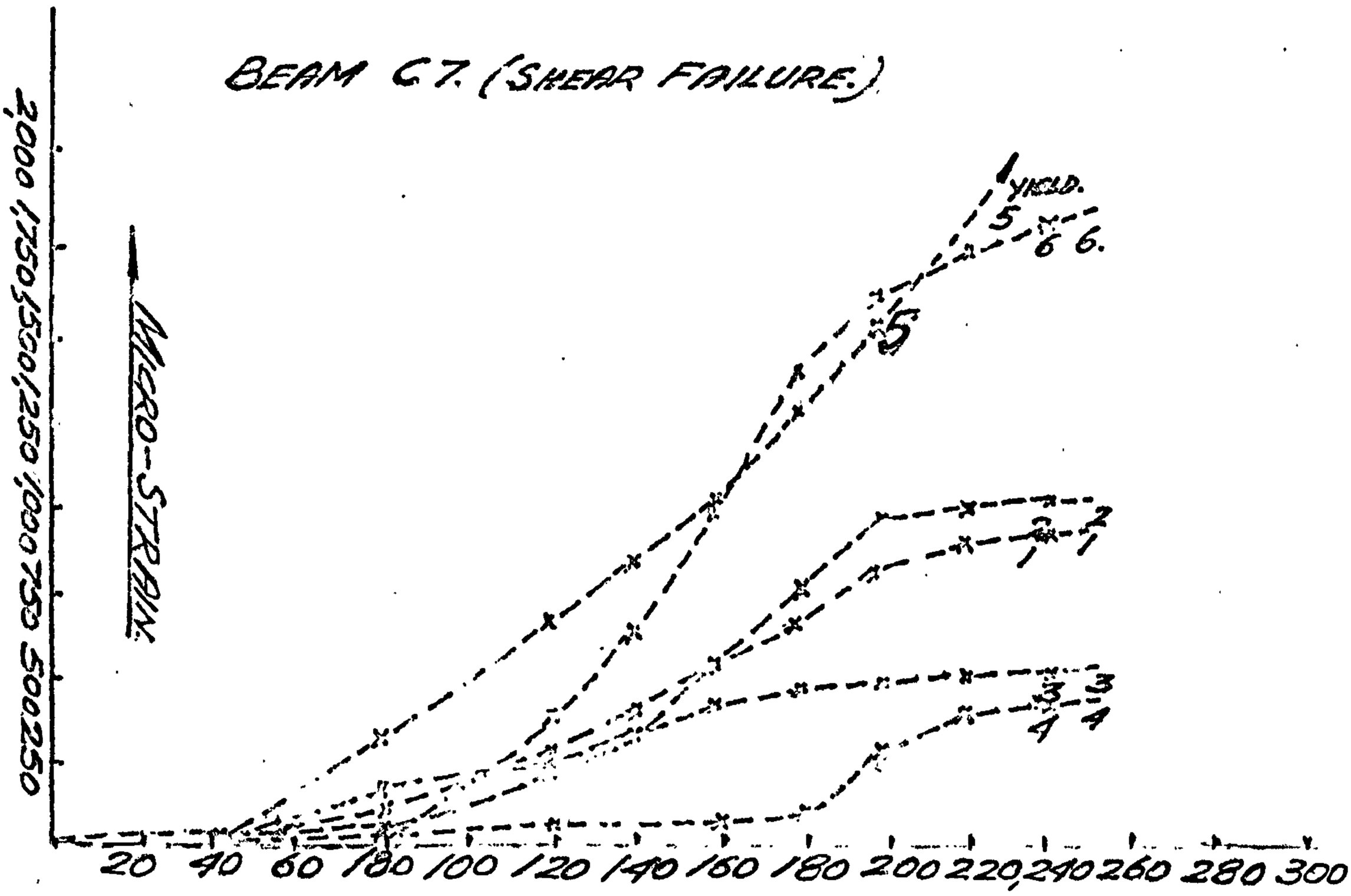


FIG. 3.16. LOAD-STIRRUP STRAIN DIAGRAM, FOR CONTINUOUS BEAM.



POSITION OF STRAIN GAUGES.

BEAM C7. (SHEAR FAILURE.)



BEAM C12. (FLEXURE FAILURE)

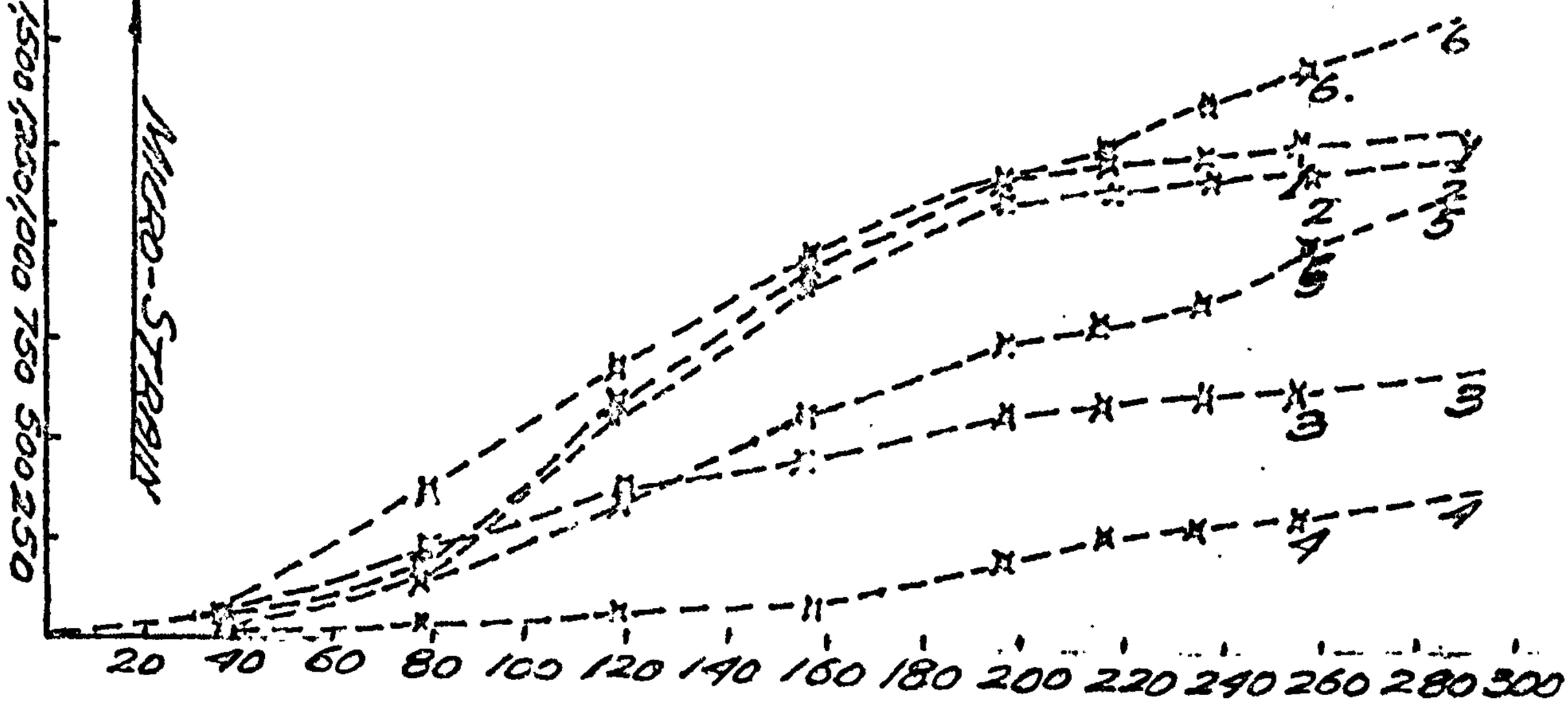


FIG. 3.17. LOAD-STIRRUP STRAIN DIAGRAM, FOR CONTINUOUS BEAM.

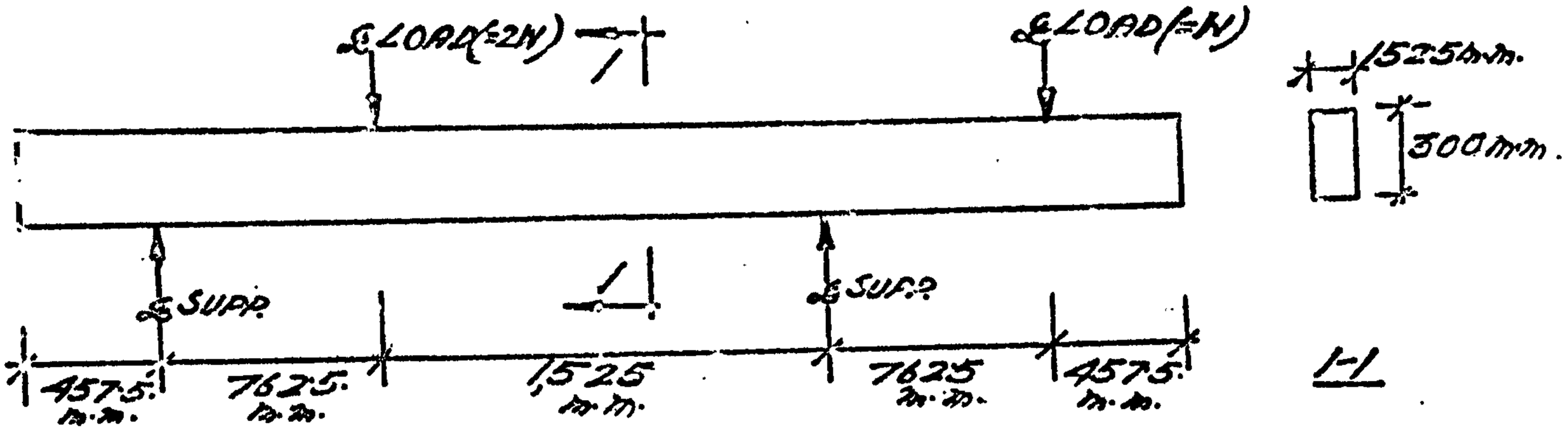


FIG. 3.18. LAYOUT & LOADING SYSTEM FOR RESTRAINED BEAMS.

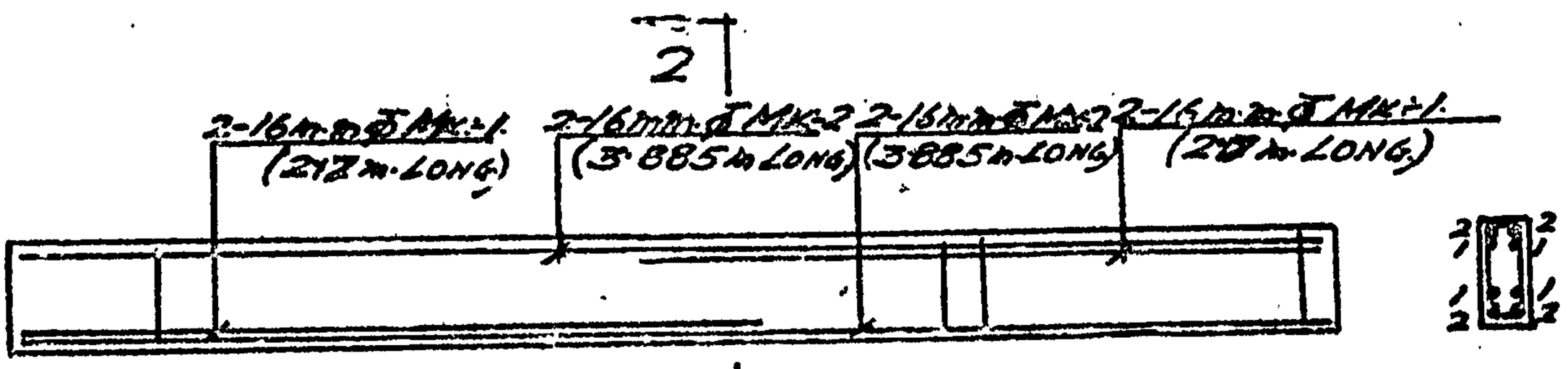


FIG. 3.19. REINFORCEMENT DETAILS FOR BEAM NOS. 4 & 5.

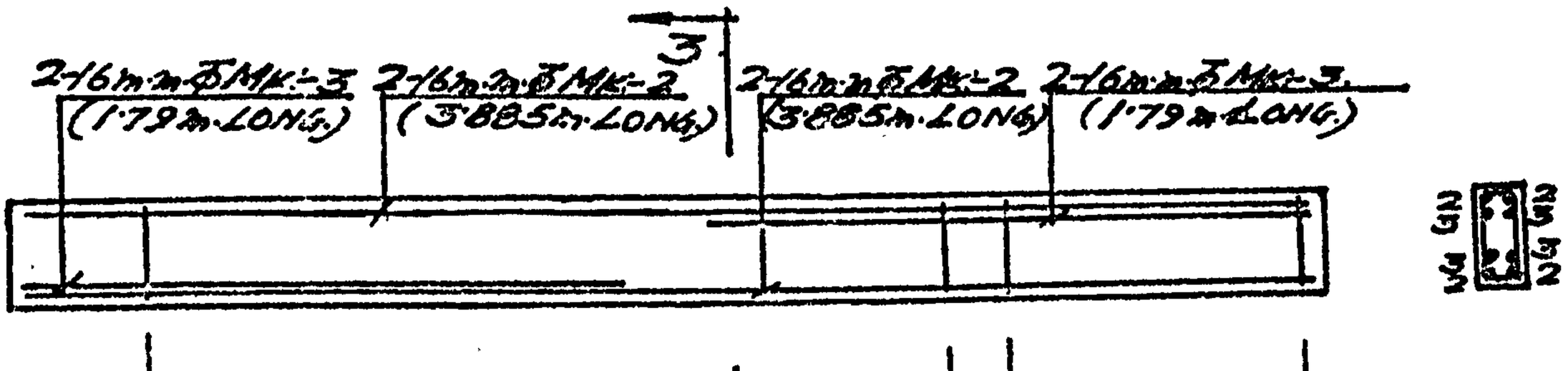


FIG. 3.20 REINFORCEMENT DETAILS FOR BEAM NO:- 2, 3 & 6.

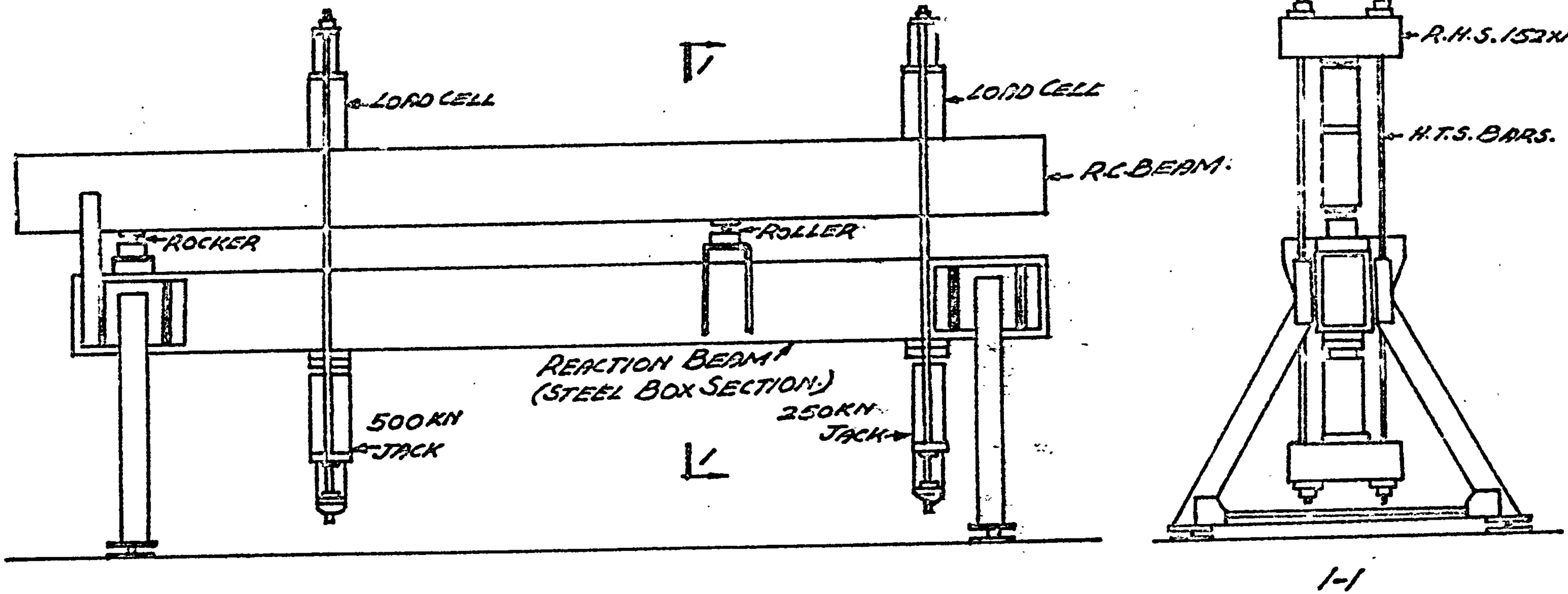
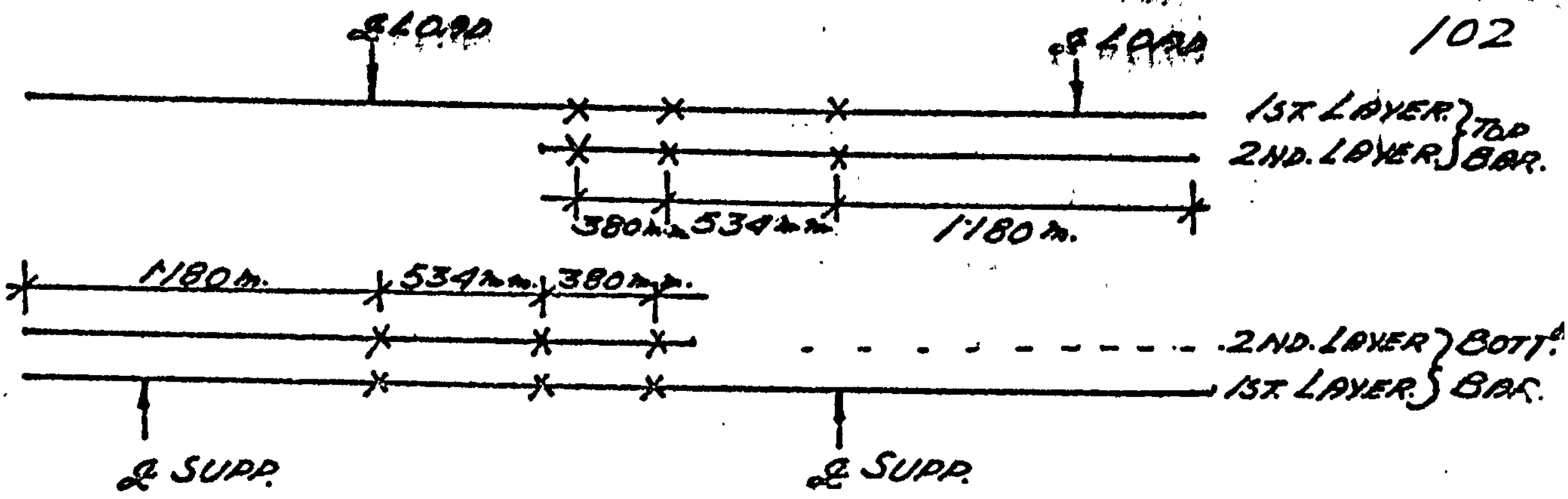
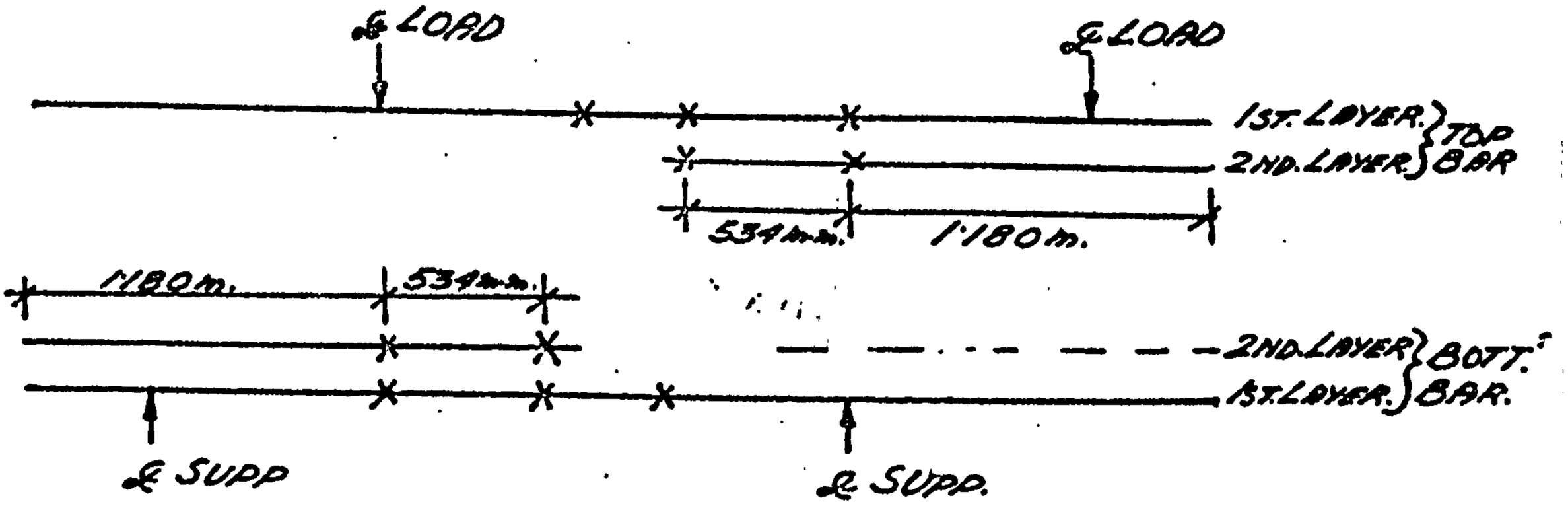


FIG.321. ARRANGEMENT FOR TESTING RESTRAINED BEAM.



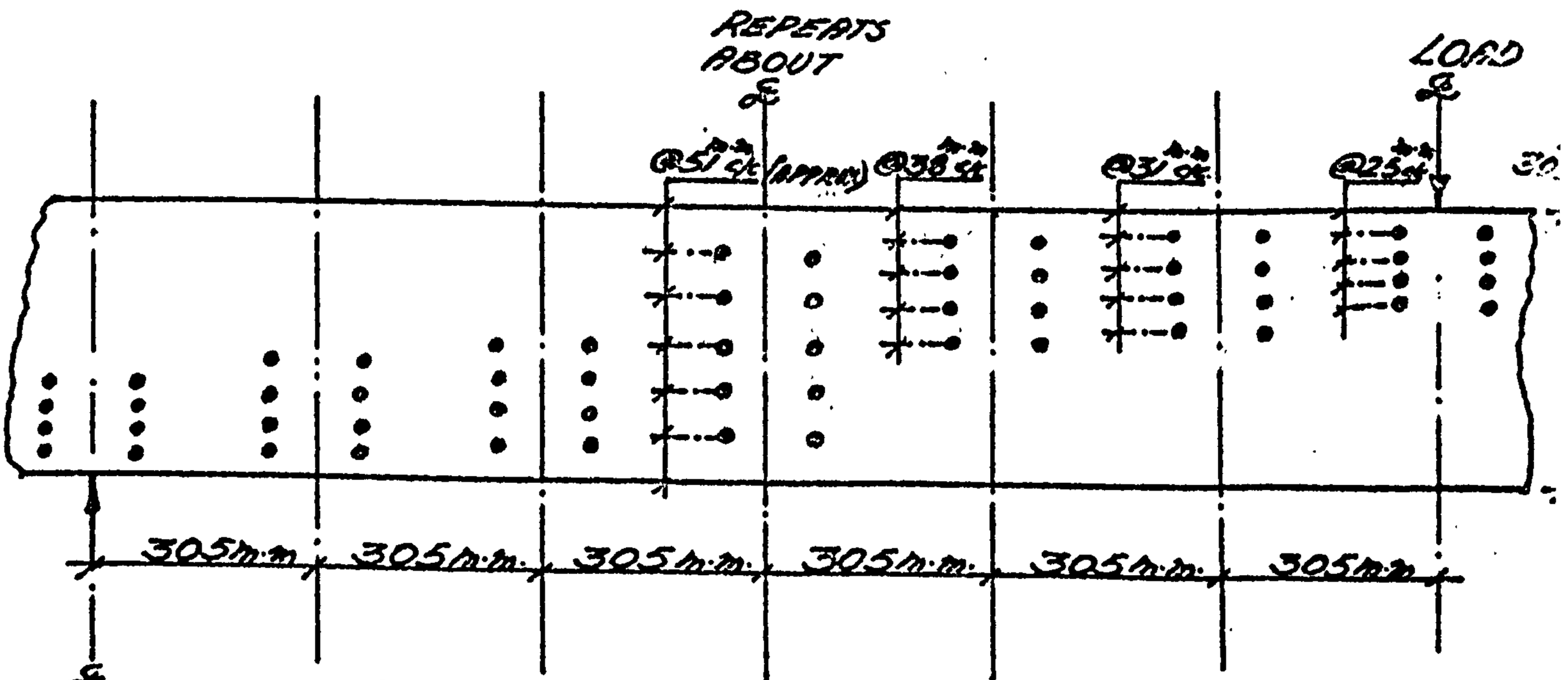
LOCATION OF SLOTTED STRAIN GAUGES

FOR BEAMS:- B1; B4; B5.



LOCATION OF SLOTTED STRAIN GAUGES

FOR BEAMS:- B2; B3; B6.



LOCATION OF DEMEC POINTS.

NOTE :-

o o SHOWS 100 m.m. DEMEC PTS.

⊢X⊣ SHOWS SLOTTED STRAIN GAUGE.

FIG. 3.22. INSTRUMENTATION FOR RESTRAINED BEAMS.

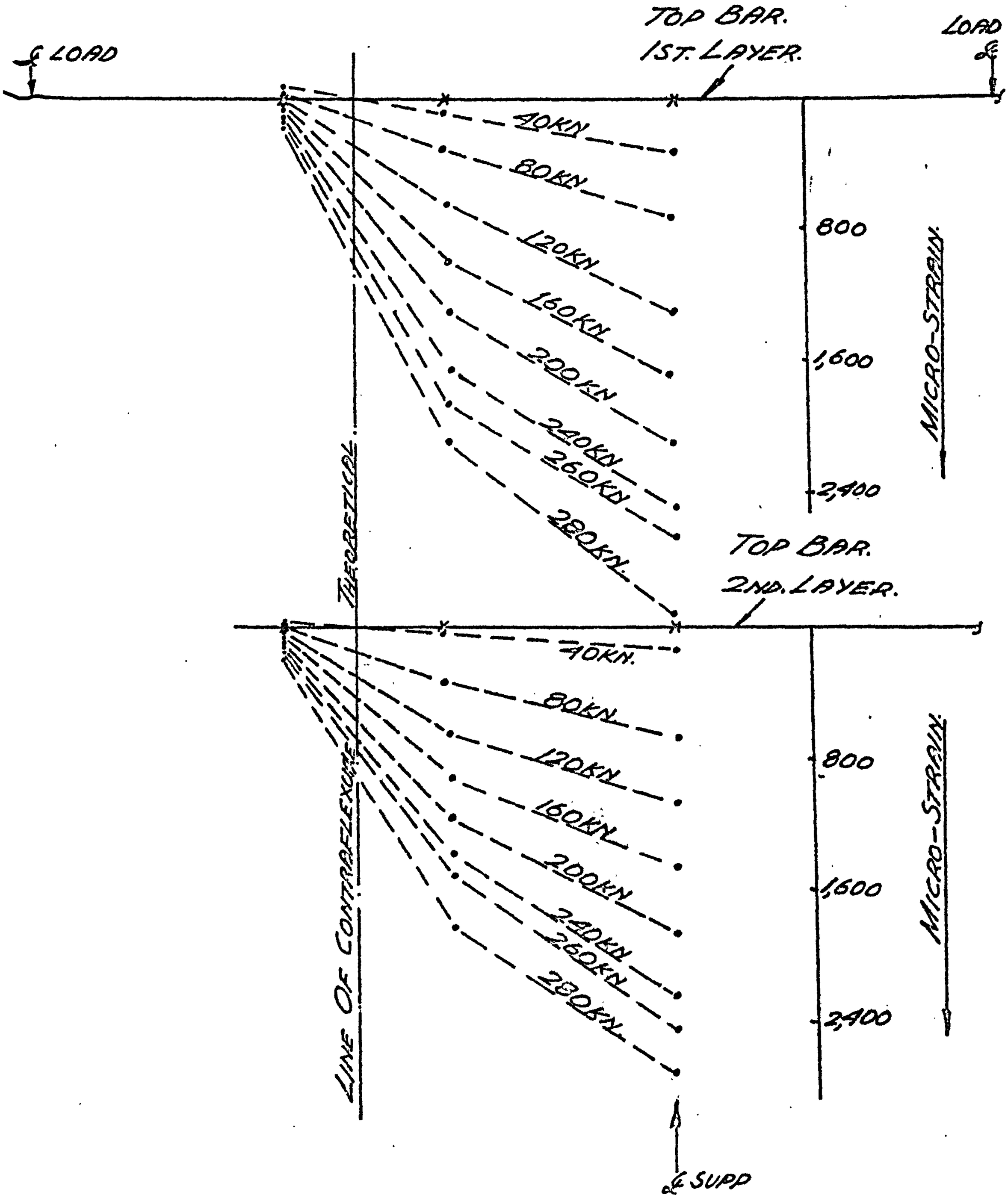


FIG. 3.23. LOAD-STRAIN DIAGRAM, FOR RESTRAINED BEAM.

BEAM NO:-1.

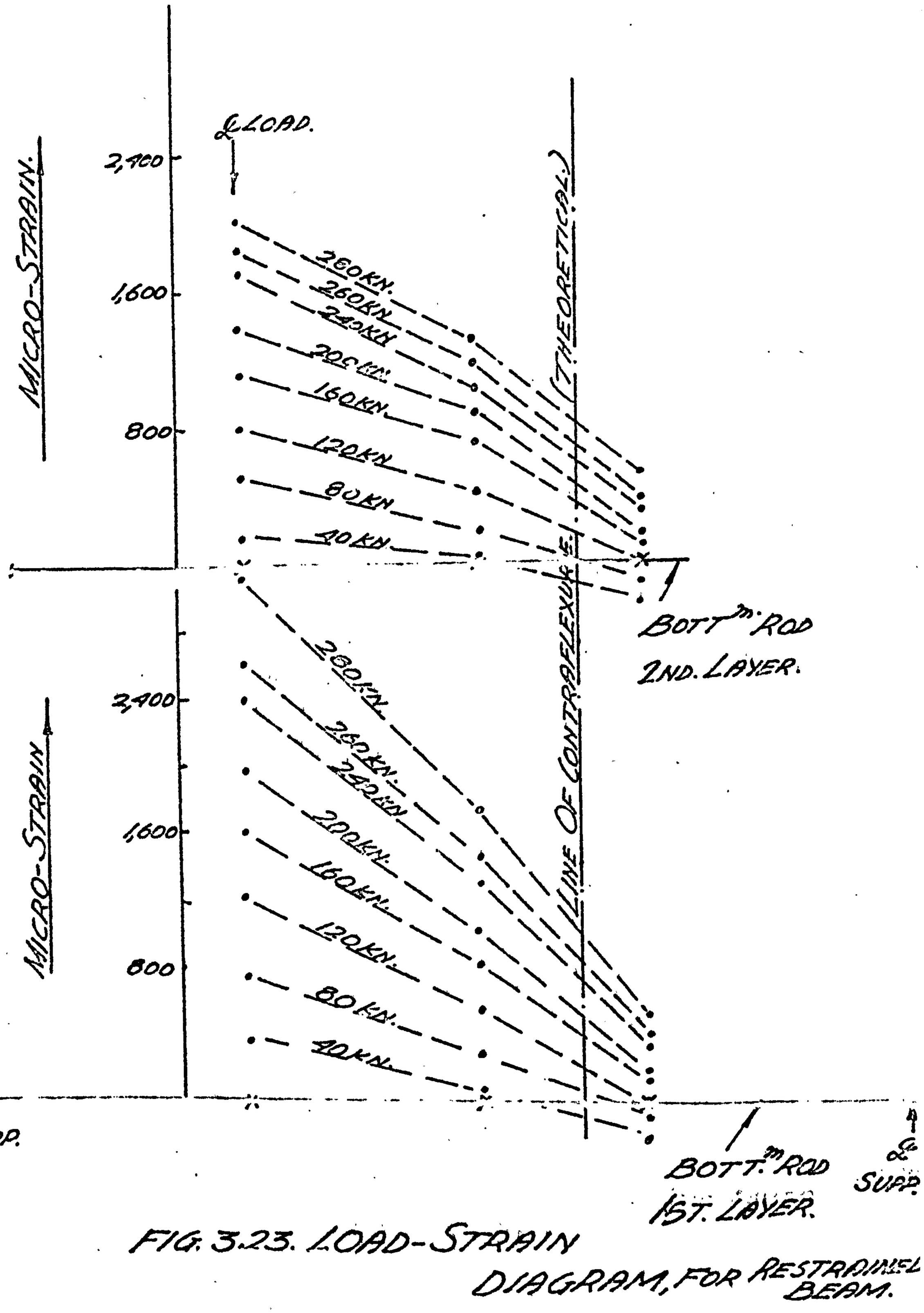
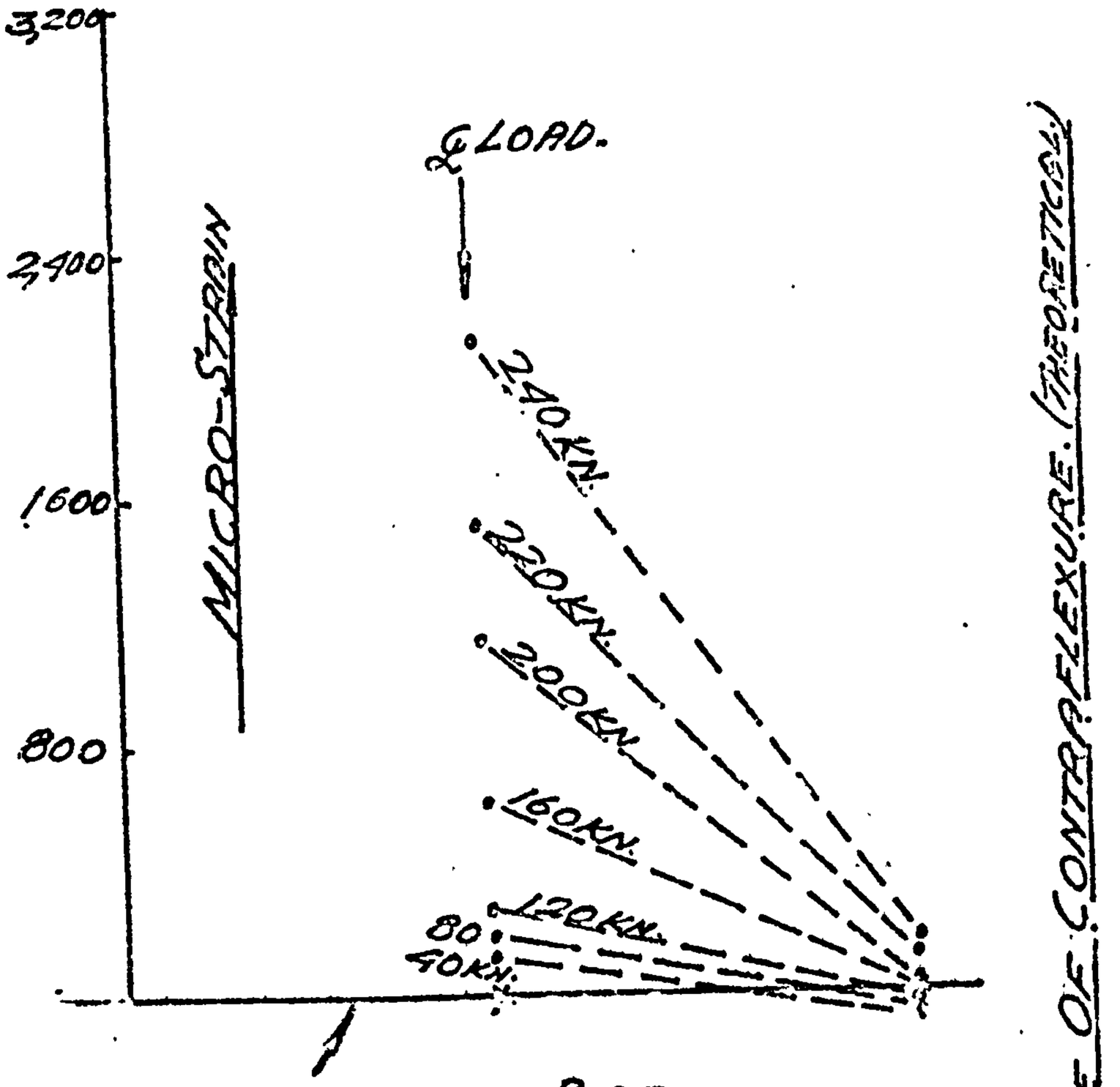


FIG. 3.23. LOAD-STRAIN DIAGRAM, FOR RESTRAINED BEAM.

TEXT CUT OFF IN ORIGINAL

BEAM NO:-2.



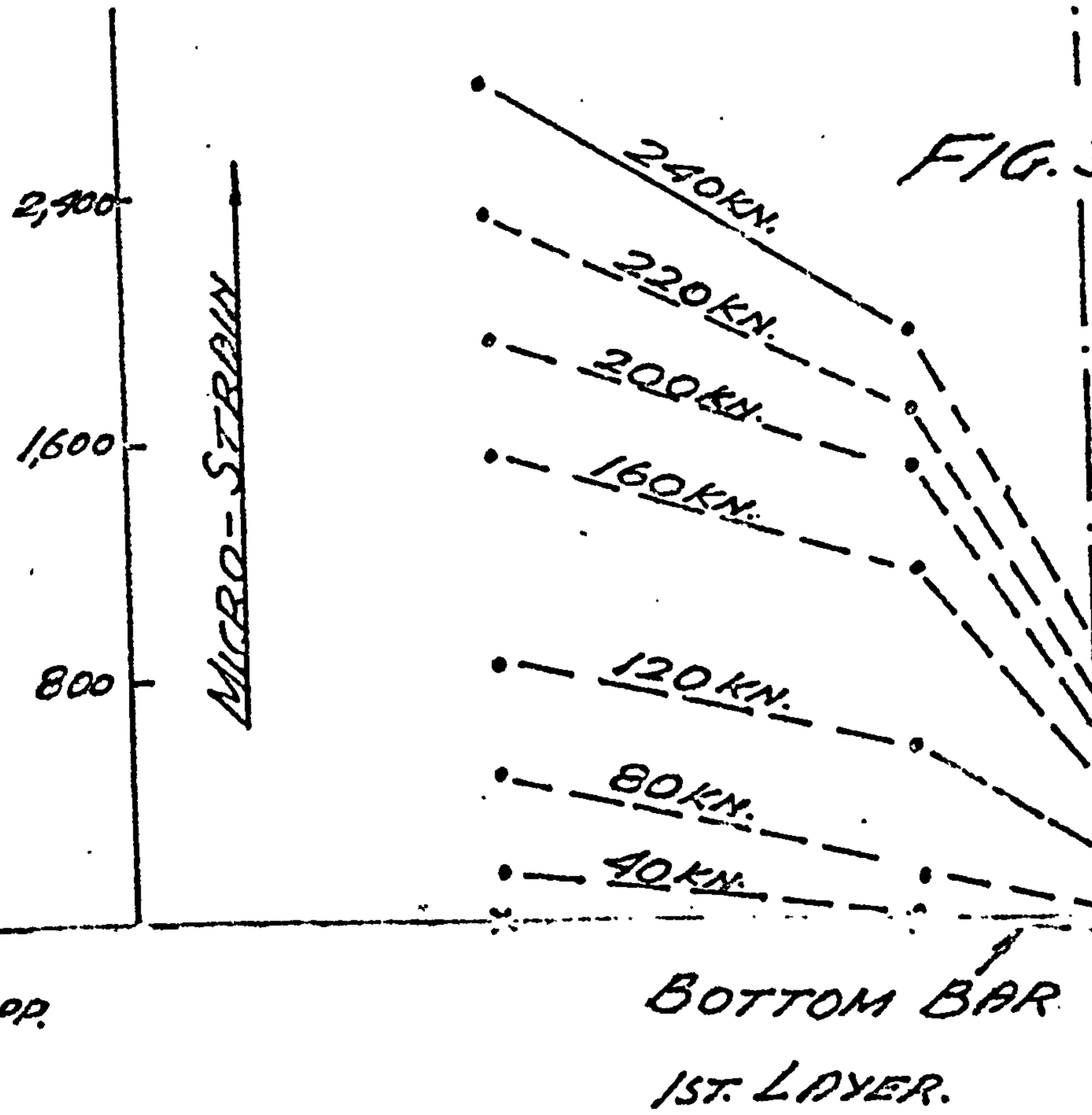


FIG. 3.23 LOAD-STRAIN DIAGRAM, FOR RESTRAINED BEAM.

BEAM NO:-2.

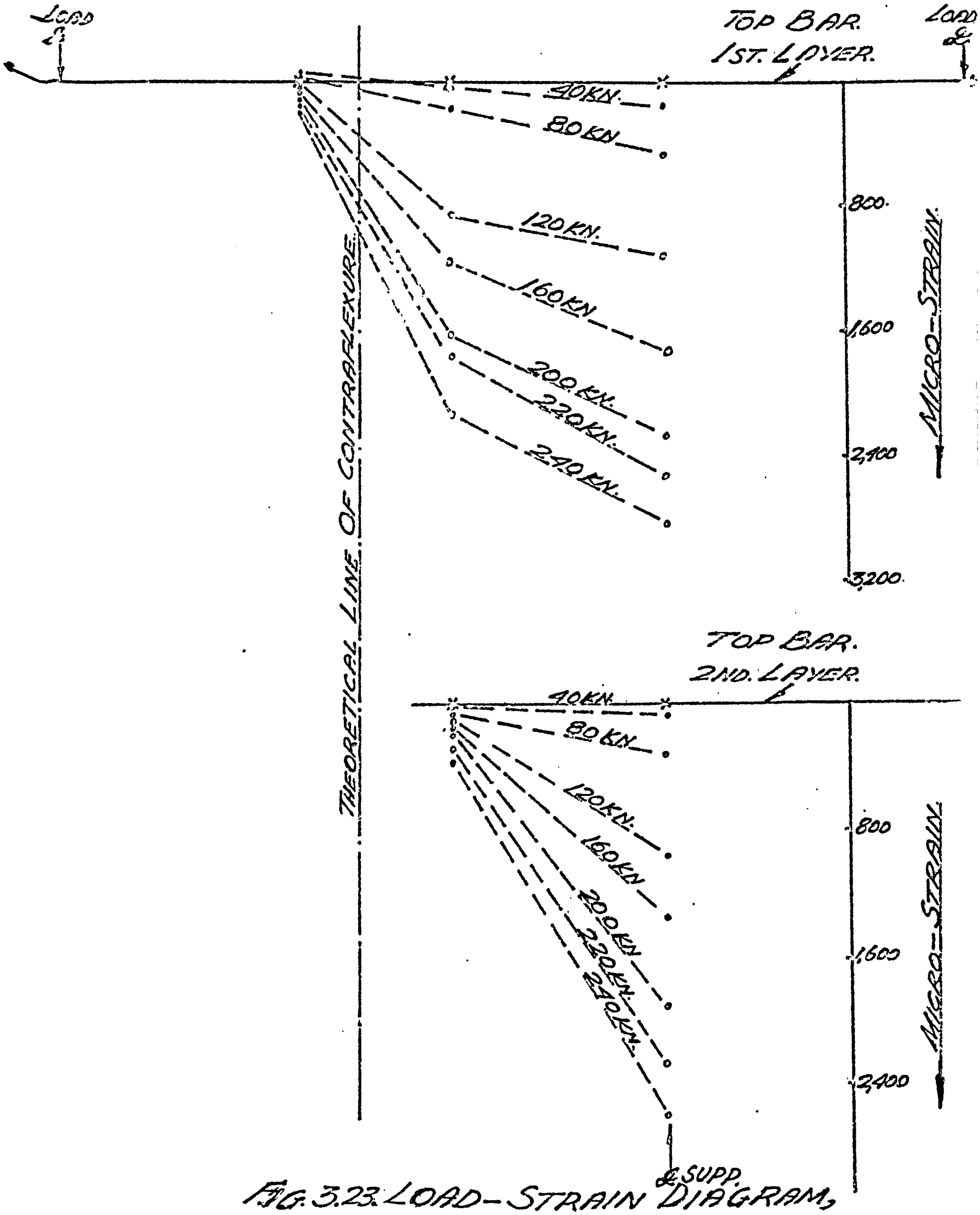


FIG. 3.23. LOAD-STRAIN DIAGRAM,

FOR RESTRAINED BEAM.

BEAM NO:-3.

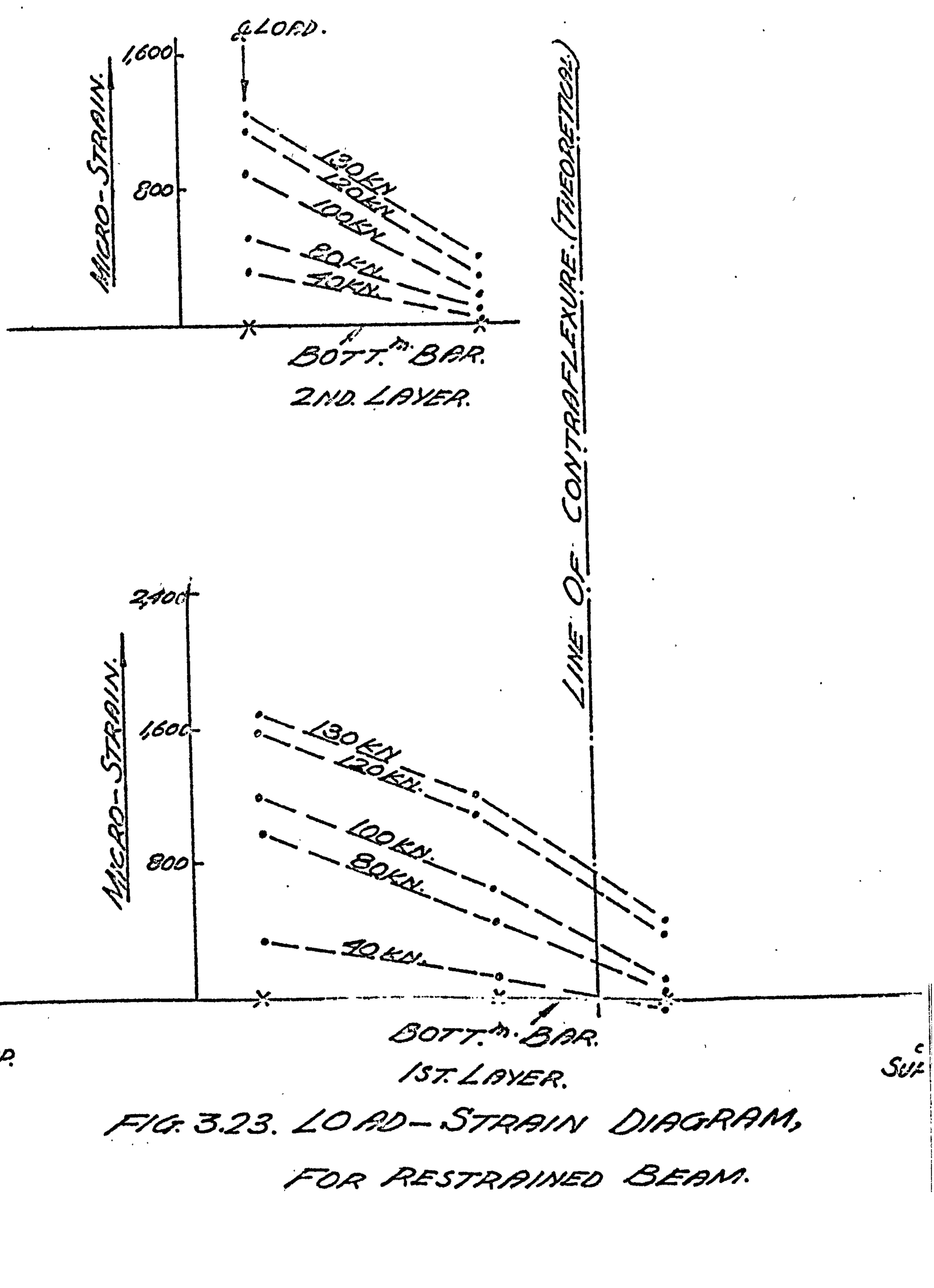


FIG. 3.23. LOAD-STRAIN DIAGRAM,

FOR RESTRAINED BEAM.

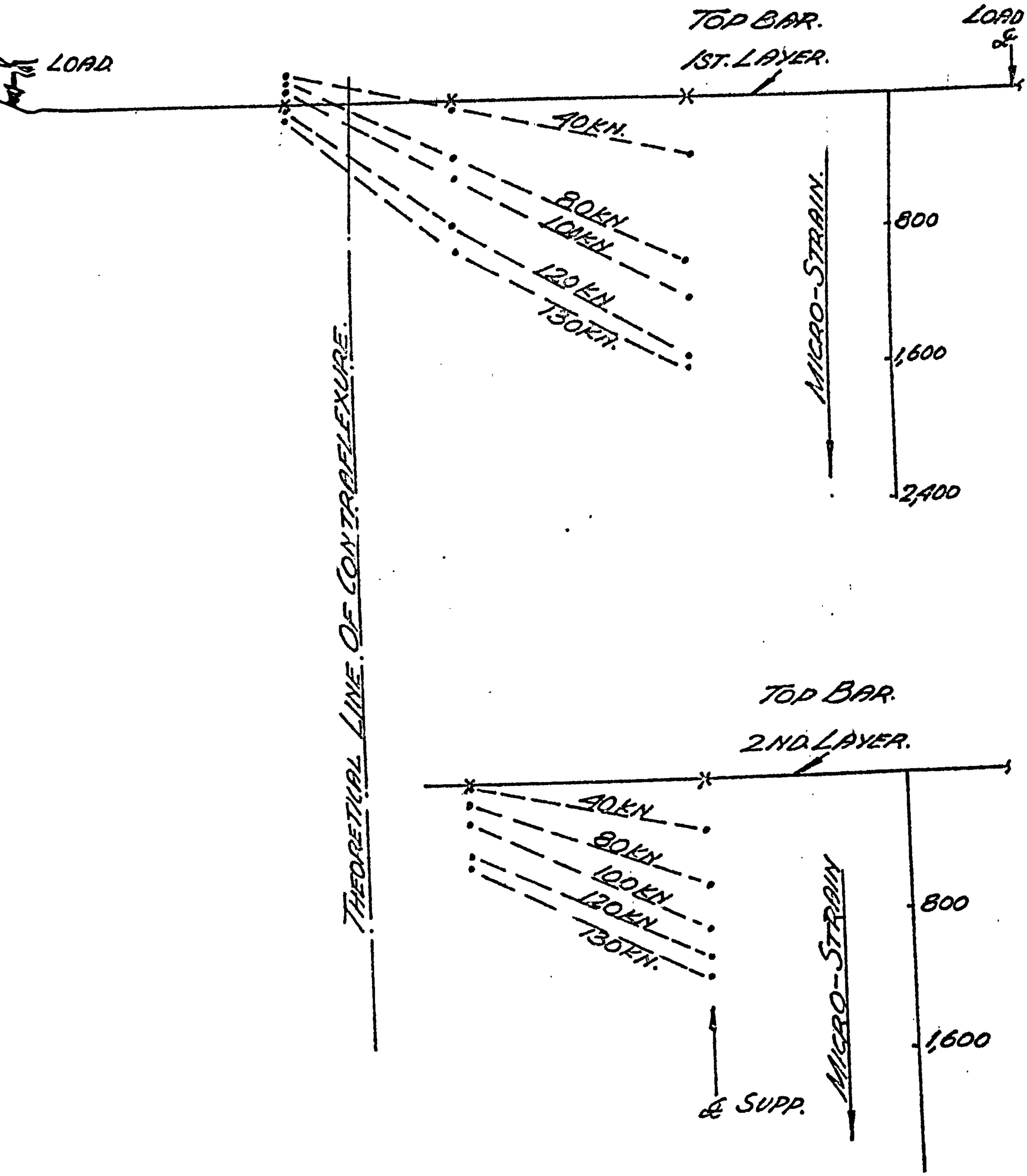


FIG. 3.23. LOAD-STRAIN DIAGRAM, FOR RESTRAINED BEAM.

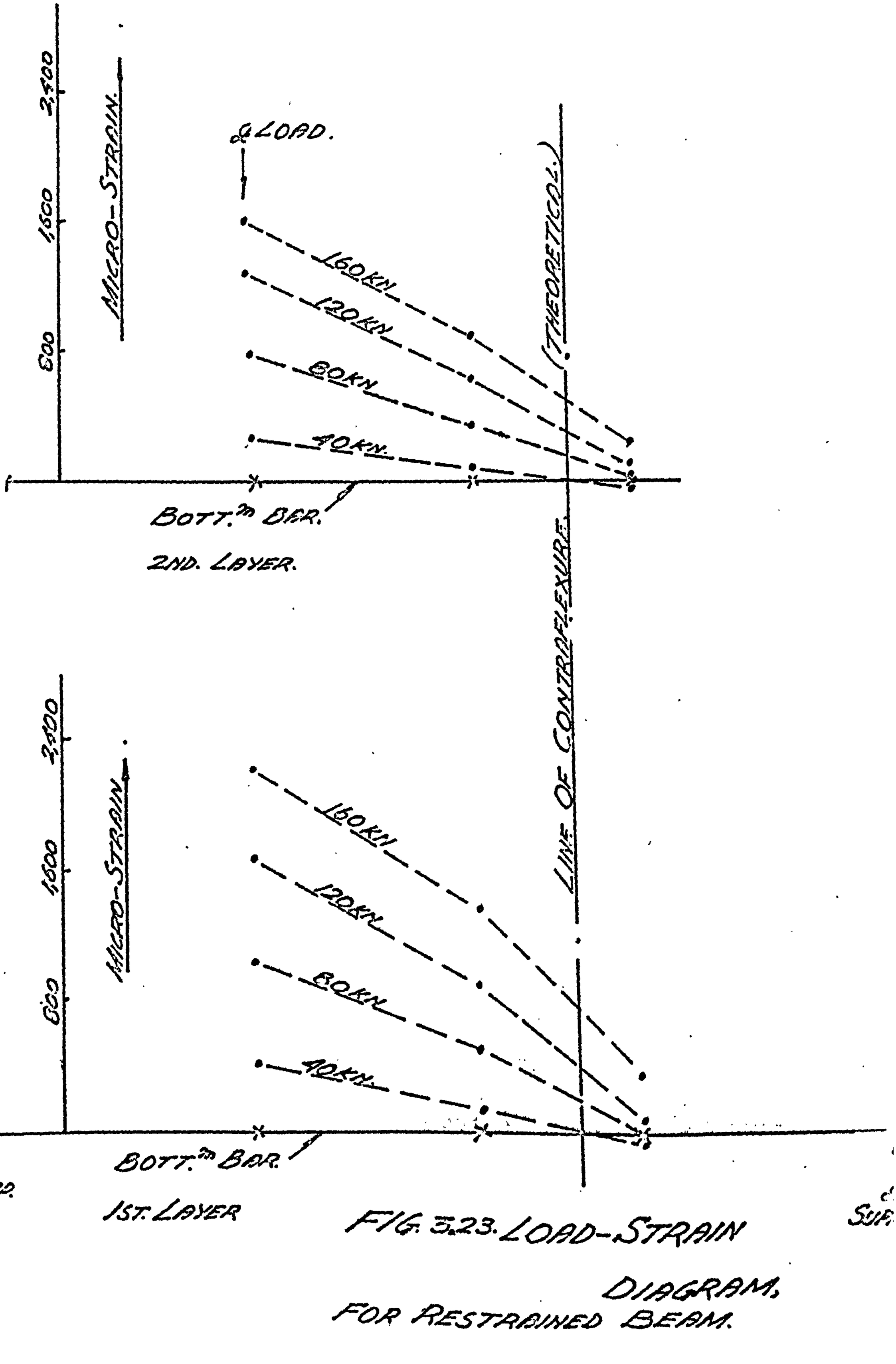


FIG. 5.23. LOAD-STRAIN DIAGRAM. FOR RESTRAINED BEAM.

BEAM NO:-4.

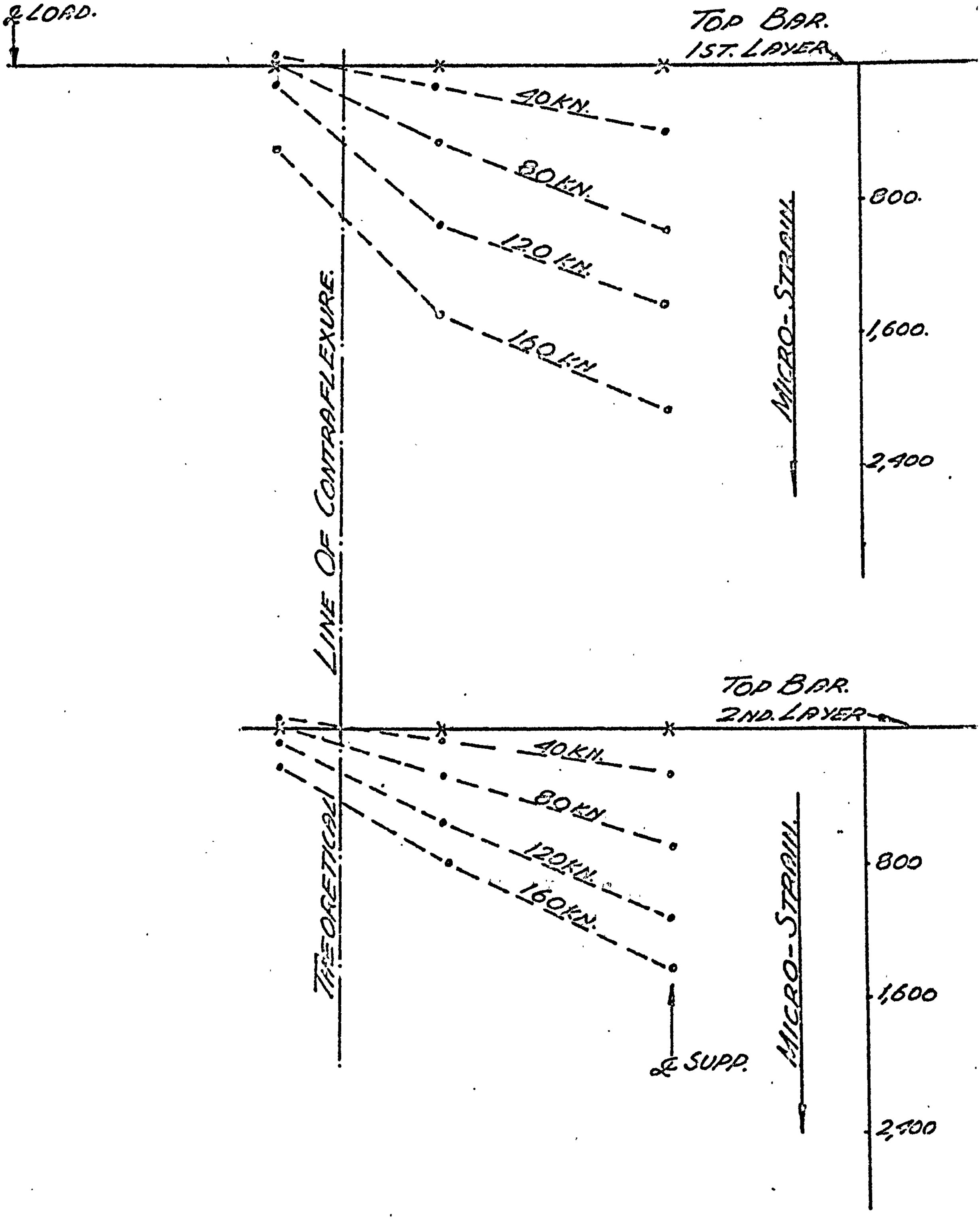


FIG. 3.23. LOAD- STRAIN DIAGRAM, FOR RESTRAINED BEAM.

BEAM NO:-5.

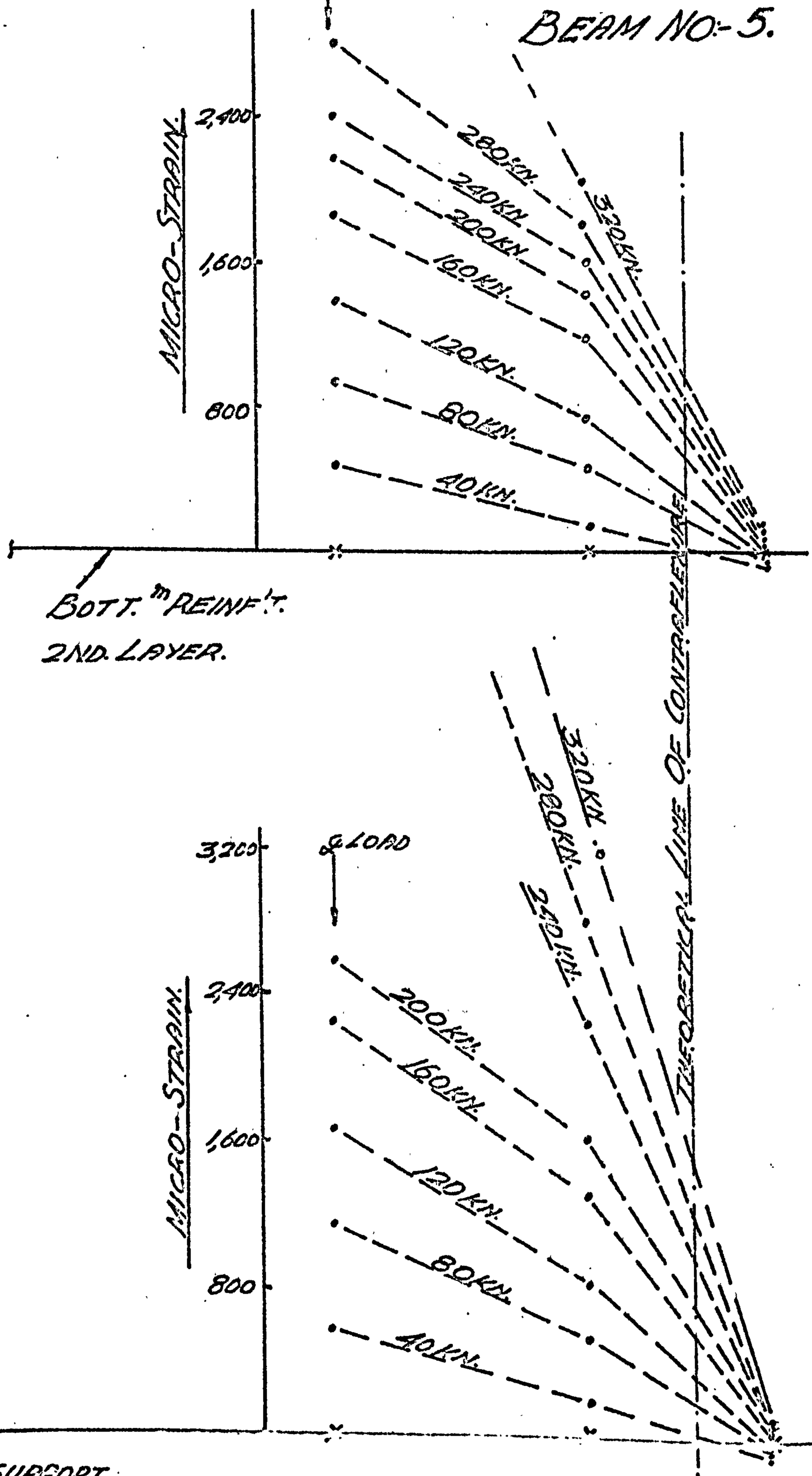


FIG. 3.23 LOAD-STRAIN DIAGRAM, FOR RESTRAINED BEAM.

BEAM NO:- 5.

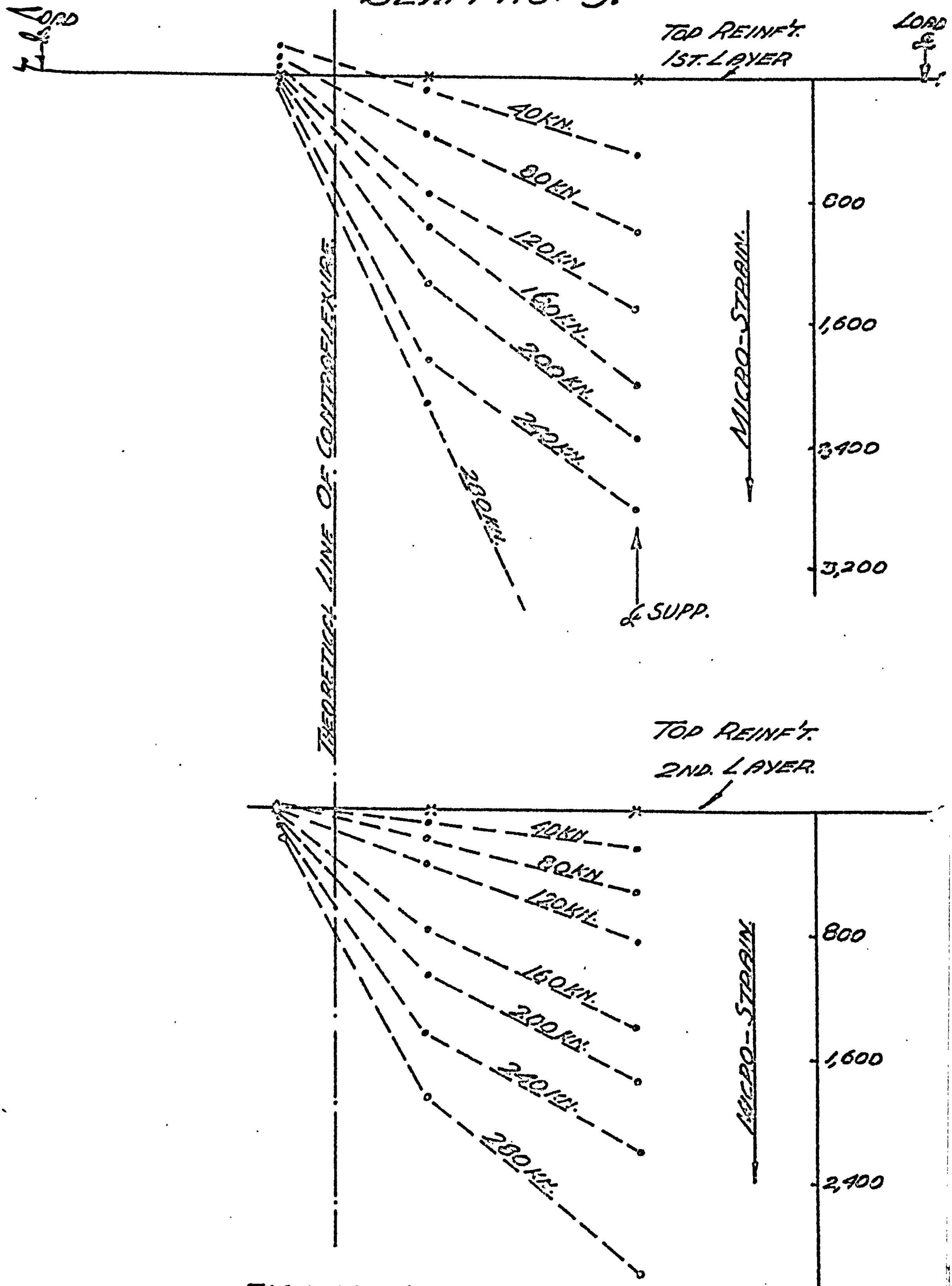


FIG. 5.23. LOAD – STRAIN DIAGRAM.

BEAM NO:- 6.

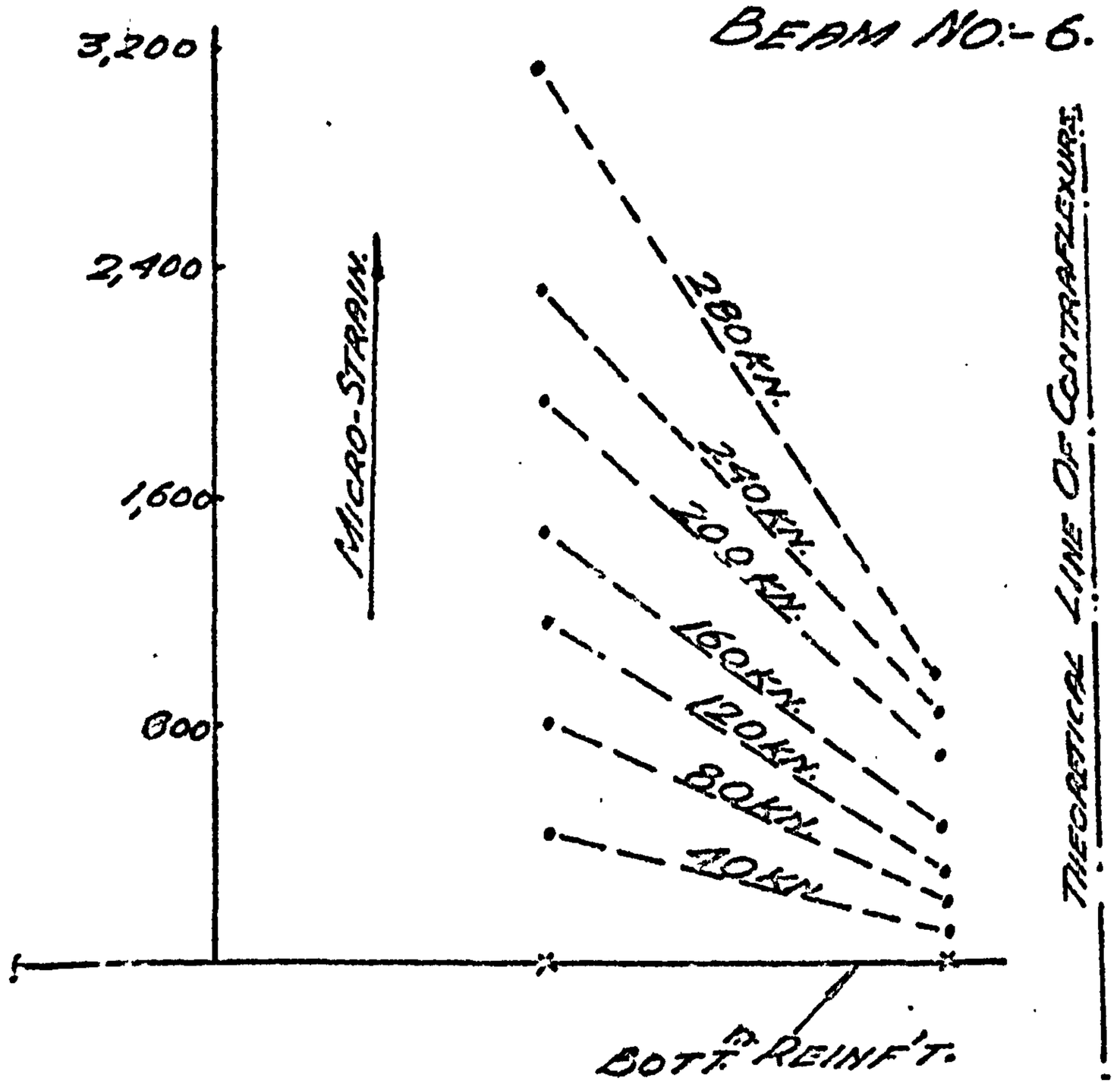
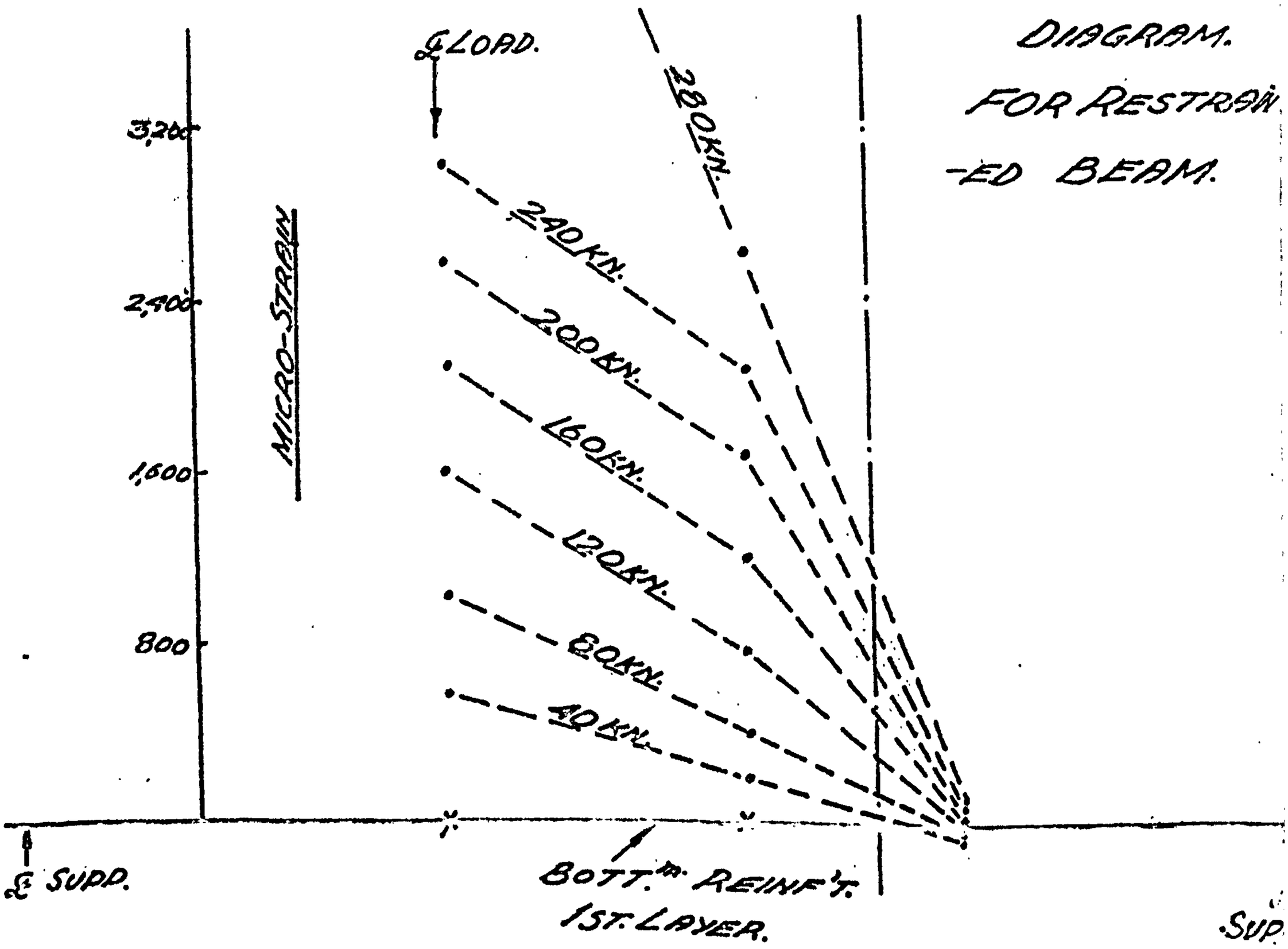


FIG. 3.23. LOAD-STRAIN DIAGRAM. FOR RESTRAIN-ED BEAM.



BEAM NO:-6.

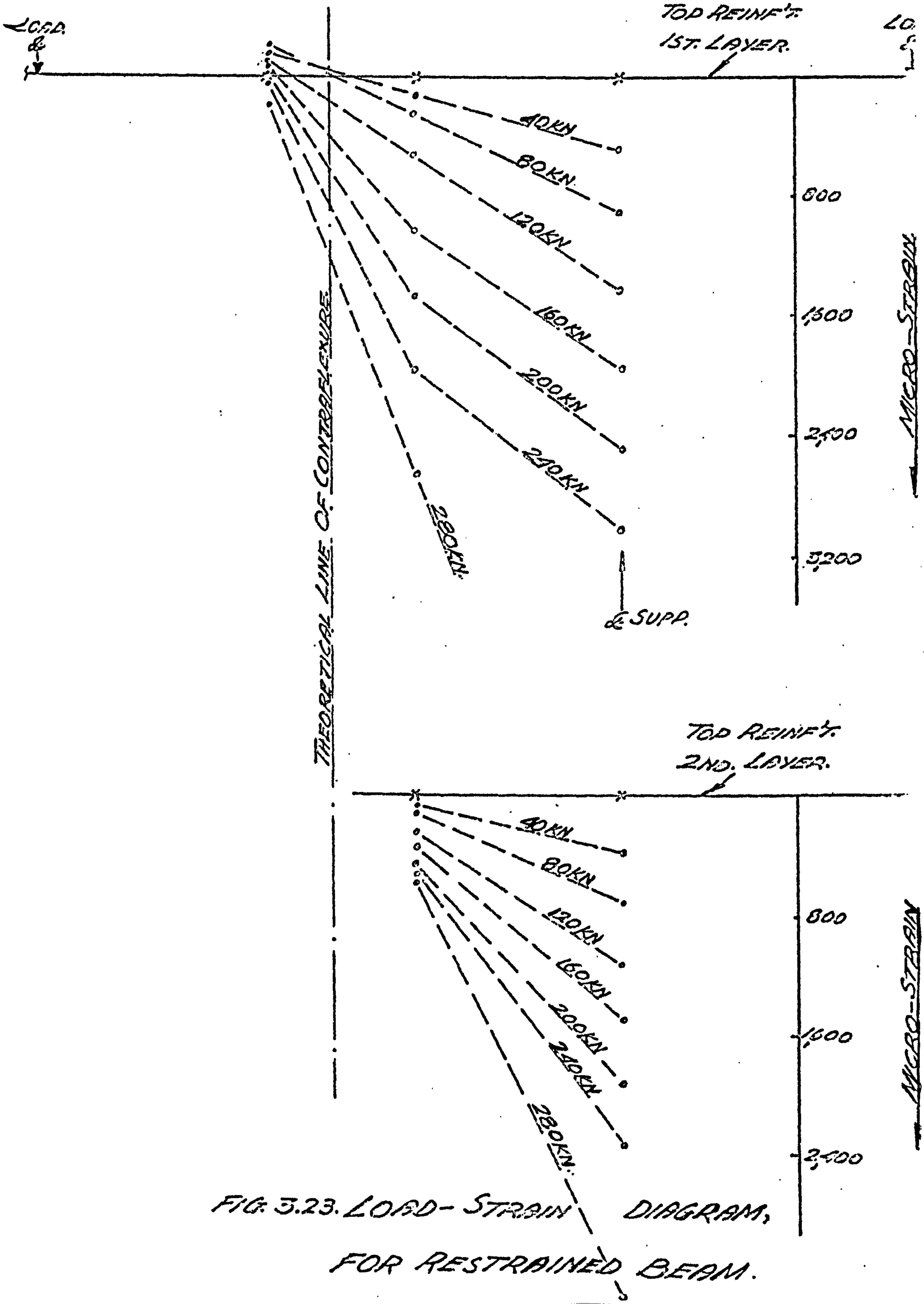


FIG. 3.23. LOAD-STRAIN DIAGRAM,
FOR RESTRAINED BEAM.

TABLE NO. 3.3

PROPERTIES OF CONTINUOUS BEAMS

Beam No.	U_w.N/m.m^2	U_{split} N/m.m^2	d_1/supp m.m	Span Reinf't KS60 Dia. Bott.	Span Reinf't KS60 Dia. Top	Supp. Reinf't Bott.	Supp. Reinf't Top	Shear Reinf't in Dia./mm Mild Steel
(c3	51.0	4.8	274	3-16mm	2-12mm	2-12mm	2-12mm	6mm @ 152.5 mm c/c
Group (c4	40.4	3.5	274	3-16mm	2-12mm	2-12mm	2-12mm	6mm @ 114 mm c/c
Ia (c9	38.8	2.4	274	3-16mm	2-12mm	2-12mm	2-12mm	6mm @ 133 mm c/c
(c11	52.5	2.9	274	3-16mm	2-12mm	2-12mm	2-12mm	5.5 mm @ 152.5 mm c/c
(c1	39.4	3.1	272	8-16mm	3-16mm	2-16mm	3-16mm	6mm @ 102 mm c/c
Group (c7	39.3	2.85	272	8-16mm	3-16mm	4-16mm	3-16mm	8mm @ 89 mm c/c
Ib (c8	41.8	2.8	272	8-16mm	3-16mm	4-16mm	3-16mm	10mm @ 114 mm c/c
(c12	40.4	3.1	272	8-16mm	3-16mm	4-16mm	3-16mm	10mm @ 89 mm c/c
(c6	46.5	3.0	274	3-16mm	2-12mm	2-12mm	2-12mm	5.5 mm @ 152.5 mm c/c
Group (c10	54.6	3.0	274	3-16mm	2-12mm	2-12mm	2-12mm	6mm @ 102 mm c/c
II (c13	57.7	3.1	274	3-16mm	2-12mm	2-12mm	2-12mm	8mm @ 102 mm c/c
c2	35.1	2.7	272	8-16mm	3-16mm	2-16mm	3-16mm	6mm @ 76 mm c/c
c5	44.5	4.1	274	3-12mm	2-12mm	2-12mm	2-12mm	6mm @ 133 mm c/c

TABLE NO. 3.4

ANALYSIS OF TEST RESULTS FOR CONTINUOUS BEAMS

Beam No.	U_w in N/mm^2	Group	$P_{ultimate}$ in KN	$Q_{ultimate}$ support in KN	$\theta_{ultimate}$ in radians	$M_{ultimate}$ support in KN.m	Failure Mode.
c3	51	Ia	145	88	0.031	56.5	Shear at R.H. support.
c4	40.4	Ia	160	95	0.053	57.0	Flexure at R.H. span.
c9	38.8	Ia	146	85	0.032	54.5	Flexure at L.H. span & shear at R.H. support.
c11	52.5	Ia	125	77	0.011	52.0	Shear at L.H. Supp & Crack on stub column.
c1	39.4	Ib	210	135	0.0035	108	Shear at curtailed bar on L.H. span.
c7	39.3	Ib	245	154	0.0060	113	Shear at L.H.supp.
c8	41.8	Ib	275	169	0.013	114	Shear at L.H. supp
c12	40.4	Ib	292	179	0.016	118.5	Flexure at L.H.spa & shear at R.H.spa
c6	46.5	II	100	76.5	0.0075	51.5	Shear at R.H. supp
c10	54.6	II	160	116.5	0.060	60.5	Flexure at L.H.spa & shear at R.H.sup crack at stub colu
c13	57.7	II	190	136	0.075	61.5	Flexure at R.H.sup Severence of beam R.H. support.
c2	35.1	-	-	-	-	-	Shear at curtailed

TABLE NO. 3.5

PROPERTIES OF RESTRAINED BEAMS

Beam No.	U_w N/mm^2	Span Reinf't. Bott.	Span Reinf't. Top	Support Reinf't. Bott.	Support Reinf't. Top	Shear Reinforcement
B1	45.0	4-16mm Ø	2-16mm Ø	2-16mm Ø	4-16mm Ø	6mm Ø Links @ 76mm c/c
B2	42.5	-ditto-	-ditto-	-ditto-	-ditto-	6mm Ø Links @ 76mm c/c
B3	51.0	,,	,,	,,	,,	6mm Ø/Links @ 152.5mm c/c
B4	47.25	,,	,,	,,	,,	-ditto-
B5	43.25	,,	,,	,,	,,	8mm Ø Links @ 76 mm c/c
B6	41.0	,,	,,	,,	,,	-ditto-

TABLE NO. 3.6

ANALYSIS OF TEST RESULTS FOR RESTRAINED BEAMS

Beam No.	$P_{ultimate}$ in Span (KN)	$Q_{ult.}$ (KN)	$M_{ult.}$ (KN)	Failure Mode
B1	290	145	110.5	Shear failure at support.
B2	250	125	95.3	-ditto-
B3	135	67.5	51.5	Shear failure at span.
B4	165	82.5	63.0	-ditto-
B5	330	165	125.5	Well defined flexural crack at span & failure by shear at support.
B6	290	145	110.5	Well developed flexural cracks & failure by shear in span.

TABLE NO. 3.7

PROPERTIES & TEST RESULTS OF CYLINDER

Cylinder	Diameter (mm)	Height (H) (mm)	H/D_{ratio}	Compressive Stress N/mm^2	Ultimate strain
Group 1	100	225	2.25	31.1	0.0058
Group 2	100	150	1.5	32.5	0.0096
Group 3	100	100	1.0	39.0	0.0137
Group 4	100	75	0.75	47.0	0.0310
Group 5	100	50	0.50	69.0	0.0970 - stopped recordings due to instability.

CHAPTER 4

STRUCTURAL SYSTEM

The primary objectives of this Chapter are as follows:-

i) to investigate if the prototype structural system with a uniformly distributed load, can be well represented by a point load.

ii) to establish which system or systems adequately model the behaviour of the critical section at the beam to column connection for a continuous system.

4.1 MOMENT/SHEAR SIMULATION BETWEEN PT. LOAD & U.D.L.

The prototype structural system is typically a monolithic reinforced concrete framework subjected to uniformly distributed dead and live loads. The critical section usually occurs at the support section of the beam-column connection. It is difficult experimentally to duplicate a uniform loading. But as is shown in fig. 4.1 that a point loaded system adequately models the hogging moment distribution.

In practice the combination of slab and beam provides a flanged section to resist sagging moment. Even for the elastic structure, the moment value at the support section in the fully loaded structure is likely to be less than two-thirds of the free span moment, i.e. 0.67 Mf; inelastic considerations are even more likely to decrease the distance between the point of contraflexure and the support section. Hence after redistribution of moment, i.e. for equal hogging and sagging moment and subject to the A.C.I. Code 318-63[2] (or C.P.114-65[28]) recommendation for deflection, i.e. $d > l/26$ (or $d > \frac{l}{25}$), it is seen that the

maximum ratio $\frac{z}{d_1}$ can be expected to be 3.41 (or 3.38). In design practice therefore, a value of $\frac{z}{d_1}$ less than three is anticipated. In the experiments with point loaded beams, the ratio $\frac{z}{d_1}$ $(M/Q.d_1)$ is always obtained as less than three, as shown in Table No. 4.1. Hence Moment-Shear-Truss simulation is maintained though actually uniformly distributed load was not applied during tests. This is illustrated clearly in figure 4.1.

It is explained in Chapter 5 that in terms of rotation, the plastic hinges form in a very small zone indeed at the section of maximum moment. This length does not alter appreciably as the process of redistribution of moments continue. In a statically indeterminate structure, these plastic zones occupy only a small fraction of the total length. Therefore the applied loads - whether uniformly distributed or concentrated - do not materially alter the shape or length of plastic zones, nor do they affect the deformation characteristics of the structure as a whole.

The shear strength of a structure prior to failure - be it a shear compression or a shearing mode of failure - depends on a very small length of concrete compressive zone, as discussed in Chapter 6. The behaviour of the structure, on the other hand, rests on parameters like M/Qd_1, f_{yq}, r_{sq}, r_{st}, U_w, **c**, etc. for shear compression and shearing mode of failures. Except **c** none of these directly or indirectly is affected by the nature of loading. As for the crack length (C) - even assuming that uniformly distributed loads might change the angle of critical shear crack slightly for the shearing mode of failure - it is difficult to imagine how the shear strength of the structure could be significantly altered. It has to be mentioned, however,

that not enough test evidence is available about the effect of crack length, viz. angle of critical shear crack for shearing mode of failure of structures under uniformly distributed load. The nearest equivalent of uniformly loaded beams are those tested by Bryant, Bianchini, Rodriguez and Kesler[25] with multiple point loading on twenty-one two-span continuous beams, none of which failed in the shearing mode of failure.

4.2 MODEL SYSTEMS TO SIMULATE BEHAVIOUR OF CONTINUOUS SUPPORT SECTIONS.

Most of our existing knowledge of post-yield behaviour derives from tests on point loaded simply supported beams. The assumption is that, provided the supports approximate the location of the points of contra-flexure, similitude is maintained. To investigate this, the author has tested thirteen two-span rectangular beams with varying r_{st} & M/Qd_1, and compared the shear strength of these beams using formulae arrived at by different codes of practices and various authors, testing mostly simply supported beams. The rotational behaviour is next compared with the ultimate values of rotation obtained by different authors, for simply supported beams. Lastly the overall behaviour of beams and the formation and nature of cracks are compared with the simply supported beams tested by Placas[70].

4.2.1 Analysis of Test Results

The shear strengths of beams are divided into three groups. The first group consists of under-reinforced beams C_3, C_4, C_9 & C_{11}, with the point of application of the load 1.8 metres away from the support. The second group C_1, C_7, C_8 ' C_{12}, are balanced sections with applied load at a distance 1.8 metres from the support, whereas

the last group of under-reinforced beams C_6, C_{10}, C_{13} had the load at a distance 1.35 metres from support. The shear strength of all these beams are compared with equations developed by Regan[75], Placas[70], Hillerborg[49], the Author, and also the codes of practice A.C.I., C.E.B., and Draft British Standard Code of Practice. Scrutinizing the test results as reported in Table No. 4.1, the following points are observed. Placas A.C.I, Hillerborg, and Draft C.P. equations predict consistent values of $q_u cal/q_u test$ with both standard deviation and coefficient of variation within tolerable limits. In the case of Placas[70], there is a small difference from group to group, which is not noticeable for the predictions of A.C.I., Draft C.P. 114 and Hillerborg. The predictions of C.E.B. are rather conservative, but they are fairly consistent, as is evident from their standard deviations and coefficient of variations. Placas[70] in comparing his test results on point loaded simply supported beams with the C.E.B. equation has also observed rather conservative nature of the C.E.B. formula. The beams which failed in shear had also been checked against the shearing equation as developed by the Author in Chapter 6. It gives also quite consistent results for each group of beams.

As a footnote to the experimental results, it must be mentioned that all the beams tested by the Author, developed yielding of the longitudinal tension steel, and those beams which failed in shear developed what is known as the shearing mode of failure. The equation of Regan[75] which fits in with the test results is based upon failure by shear compression. Beside the nature of crack at failure, the fact that the beams developed yield moments

at the support sections when they are supposed to develop shear compression moments does not speak highly of the suitability of this method in prediction of this kind.

All the methods with which the test results are compared, except the Author's equation, were basically arrived at by testing point loaded simply supported beams, as discussed in Chapter 3. The fact that they fit in almost equallly well in predicting the shear strength of continuous and simply supported systems supports the point that strengthwise the assumed simulation is justified.

The Author's test results for ultimate plastic rotation were next compared with the predicted values of Corley and I.C.E. Research Committee[48]. The results are presented in Chapter 5. Analysing the predictions of Corley, it transpires that it is no worse than the prediction of the Author. The standard deviation and the coefficient of variation are within tolerable limits. It should be mentioned in this connection that the equation formulated by Corley is an extension of Mattock's, and neither of them tested a single continuous or restrained beam. On the other hand, the Author has not tested a single simply supported beam and his equation is based entirely upon theoretical considerations and the test results of his continuous beams. The situation becomes even more clear when Author's equation is compared with the test results of Corley & Mattock, as given in Chapter 5, and is observed that his predictions are even better than the predictions of Corley on his own tests. Both these equations - viz. Author's & Corley's, are next compared with the tests of Cranston - which are on point loaded simply supported beams, and fairly good agreement is obtained between

the test results and predictions, as shown in Chapter 5. Next, the equation suggested by I.C.E. Research Committee[48] is compared with the test results of the Author. It is noted that though this formula gives rather low values of $\theta_u cal$, yet from the standard deviation and the coefficient of variations, it is noted that these predictions are not very inconsistent. The low values of θ_u are also obtained when compared with the test results of Mattock, Corley & Cranston - all of whom tested simply supported beams. Therefore, it can be concluded that, like the equations of Author & Corley, I.C.E. Research Committee formula is equally applicable for both simply supported and continuous systems. Hence from the point of view of plastic rotation, the assumed simulation seems to be justified.

The overall behaviour of the Author's beams which failed by shearing mode appear to be similar to the ones described by Placas[70] in his test series on simply supported systems, and which also failed in shearing mode. The formation of the critical crack, progress of the crack and the final failure of the beams at the support section, as described in Chapter 3, are similar to those of the simply supported systems described by Placas. Even looking closely at the nature of cracks between these two sets of experimental results, it is observed that one group is exactly a replica of the other group. There is no difference at all between the nature of cracks, though the two systems are not the same. This is shown clearly in fig. 4.2 & 4.3. It can therefore be said that, from the point of view of formation of cracks , nature of cracks and overall behaviour of beams, the simulation assumed earlier is justified.

Comparing the Author's results of beams which failed in flexure

with the equations of Corley and I.C.E. Research Committee for flexural moment, it is noted that they are fairly in close agreement. Similarly the moment equation of the Author also predicts good values for test results of Corley, Mattock and Cranston, as shown in Chapter 5. Therefore the flexural strength does not appreciably change with the change of system.

4.2.2 Review of Other Works

To obtain factual evidence from which to draw conclusions concerning the influence of systems, various other research workers have tested two span continuous beams, brief descriptions of which are given below.

Rodriguez, Bianchini, Viest & Kosler[82] tested fifty-two two-span point loaded continuous R.C. rectangular beams, and by changing the type of loading, length of support moment longitudinal reinforcement, percentage of web reinforcement and grade of longitudinal reinforcement, have arrived at the following conclusions in regard to simulation of beams.

(i) Four modes of failure were observed in these tests; diagonal tension, flexure, shear compression, and splitting failures. Ultimate loads of beams that failed by the first three modes were in reasonable agreement with the strength analyses used for simple beams and restrained beams.

(ii) The equation for diagonal tension cracking was developed from the study of simple beams with overhangs. Results of this investigation indicate that the analysis is applicable also to continuous beams.

(iii)The calculated values for shear compression strength of continuous beams are in good agreement with test results. The analysis for shear compression strength is based on the hypothesis of a limiting shear moment capacity. It was developed from theoretical considerations in connection with tests of simple and restrained beams.

(iv) The maximum flexural moment capacity of sections at which yielding of longitudinal steel was observed was in good agreement with the calculated values. The flexural moment capacity was developed from tests of simple beams, both with and without compression reinforcement.

(v) This investigation showed that the manner of diagonal crack formation and the modes of failure of two-span continuous beams failing due to shear are similar to those observed in tests of simple beams and restrained beams. However, continuity has a marked effect on redistribution of stresses in the beams. If yielding of longitudinal steel occurs at a section in a simple beam, failure has almost been reached. In a continuous beam, on the other hand, longitudinal steel at a section may yield, but the beam can still carry additional loads.

Leonhardt, Walther & Dilger[58] tested twenty-six continuous two-span beams, after extensive research on simply supported beams, with variables including (a) anchorage length of the partially cut-off longitudinal reinforcement in rectangular beams without web reinforcement; (b) M/Qd_1 ratios between one to three; (c) relative amounts and types of web reinforcement in continuous T-beams; (d) r_{st}. They have drawn the following conclusions:-

In general, the behaviour with respect to shear of a continuous beam was similar to the one of comparable single span beams, except for the poorer bond of the longitudinal tension reinforcement over the intermediate support which sometimes led to premature failure. Otherwise the continuous beams showed about the same shear strength and a similar influence of the moment shear ratio as a comparable single span beam.

Burnett[23] tested thirty-three rectangular beams of which twelve were two-span continuous beams. Apart from the system itself, he varied the parameters such as, the amount of tension reinforcement, the tie-spacing, the type of loading; the presence of columns and the column loads. He observed the following points:-

(i) The past yield flexural reserve strength of simply supported sections was greater than that for support sections in continuous systems. The presence of a column load in a continuous system reduced this reserve even further. When the number of stirrups was doubled and the effect of shear compression lessened, the reserve strength increased dramatically for all systems.

(ii) In regard to the behaviour of the beam-column support critical section, the continuous column-less model and the various simply supported models of comparable moment-shear ratio are fundamentally different in behaviour.

4.2.3 Compatibility Between Different Findings

In reviewing other works and also analysing the broad findings of the Author as discussed uner the title "ANALYSIS OF TEST RESULTS,"

it appears that there is a definite disagreement between two groups of thought - the first is represented by Burnett, and the second including the Author whose findings are broadly in agreement with the rest. It has to be seen whether these two views can be reconciled.

Burnett concludes that an increase of stirrups increases the strength of the structure and changes the load deflection curve. The Author has also observed the former effect and formulated an equation in Chapter 5, which shows that with the increase of stirrup the apparent strength of concrete increases. There is, however, an upper limit for this. As to the overall change of behaviour suggested by Burnett in his load/deflection diagram, the Author has his reservations. For identical systems with different values of $r_{sq}.f_{yq}$, the Author has plotted load against rotation at the support section, and has obtained diagrams identical in nature, as shown in Fig. 5.13, 5.14 & 5.15.

As for the additional strength in simply supported systems for comparable M/Qd_1 ratios an explanation is given in the following section 4.3 as to the cause of it. But again that would not presumably radically change the overall behaviour of the structure.

4.3 DISCUSSION

The total shear force for any structural system is carried by shear in the concrete in the compressive zone, stirrups crossing the critical crack and the arching action of the compression chord of the "truss".

$$Q_{ult} = Q_c + 1.5\, r_{sq}.f_{yq}.bd_1 + Q_a \qquad \ldots (4.1)$$

The last term Q_a is usually lumped together with the first term Q_c, and an empirical value of Q_c is established from experimental evidence. This is adopted in formulating shearing equations, as shown in Chapter 6. This arching action is shown in fig. 4.2 for beams without stirrups and its lesser significance in beams with shear reinforcement is indicated in figure 4.3.

Studying figures 4.2 & 4.3 it appears that, for a particular z value, the inclination of thrust line which determines the arching force in a beam, is steeper for a simply supported system than for a continuous system in cases where arching is dominant - i.e. where there is little or no shear reinforcement. This is why for a particular M/Qd_1 (for a point loaded beam = z/d_1) value, the simply supported system has a greater shear strength than continuous system, when $r_{sq}\ f_{yq}$ is low; on the other hand, if the arching action is eliminated or of little significance for a certain ratio of M/Qd_1, both the systems would behave in exactly the same way.

The "tied arch" action is pronounced for simply supported point loaded systems with M/Qd_1 ratios less than three, according to Walther[99] and Leonhardt[57], and a similar value of two to three, according to Dib [36]. For uniformly distributed load, the slenderness ratio is $l/d_1 \leq 12$, in accordance with the findings of Walther and Leonhardt.

Since all the beams tested by Burnett[23] as continuous systems had M/Qd_1 values below 3, the increase of shear strength for equivalent M/Qd_1 point-loaded simply supported systems could definitely be appreciable since this is the zone when the effect of arch action is predominant. For proper comparision, if however, he had used point-loaded continuous systems having $M/Qd_1 > 3$ and

compared the shear strength values with equivalent simply supported ones, he would have noted the similarity between the two. Equally if he had used simply supported systems in which arching action was eliminated by indirect loading, as shown in figure 4.4, the similarity would again have been apparent. Dib [36] has formulated equations for shear strength of short-beams, i.e. $M/Qd_1 < 3$, which are applicable to directly loaded simply supported systems on the assumption that the shearing criterion can be ignored on account of the large contribution of arch action.

For continuous systems, however, with M/Qd_1 less than 3, the shear strength can still be predicted from equations obtained for simply supported systems, so long as shearing is retained as a criterion, since, as is shown in fig. 4.2, the arching action is still minimal.

Tests by Ferguson[41] and Taylor[95] in beams without shear reinforcement and by Muto & Kokusho[26] in beams with light shear reinforcement have shown that the shear strength of short beams can be considerably reduced in the case of indirect loading and/or support conditions. An explanation of this phenomenon is given by Placas[70] and Dib [36] in their respective works, in terms of the reduction or elimination of arching effects, as shown in Fig. 4.4.

There is, however, one basic difference between the two systems, apart from the poorer load strength at the support sections in continuous systems which Leonhardt observed. This difference is the fact that a continuous system can still carry additional load even after yielding of longitudinal tension steel. On the other hand, in the simply supported system no additional load can be sustained once a hinge has formed (ignoring strain hardening effects), and failure is almost reached very soon after the yielding of longitudinal tension steel.

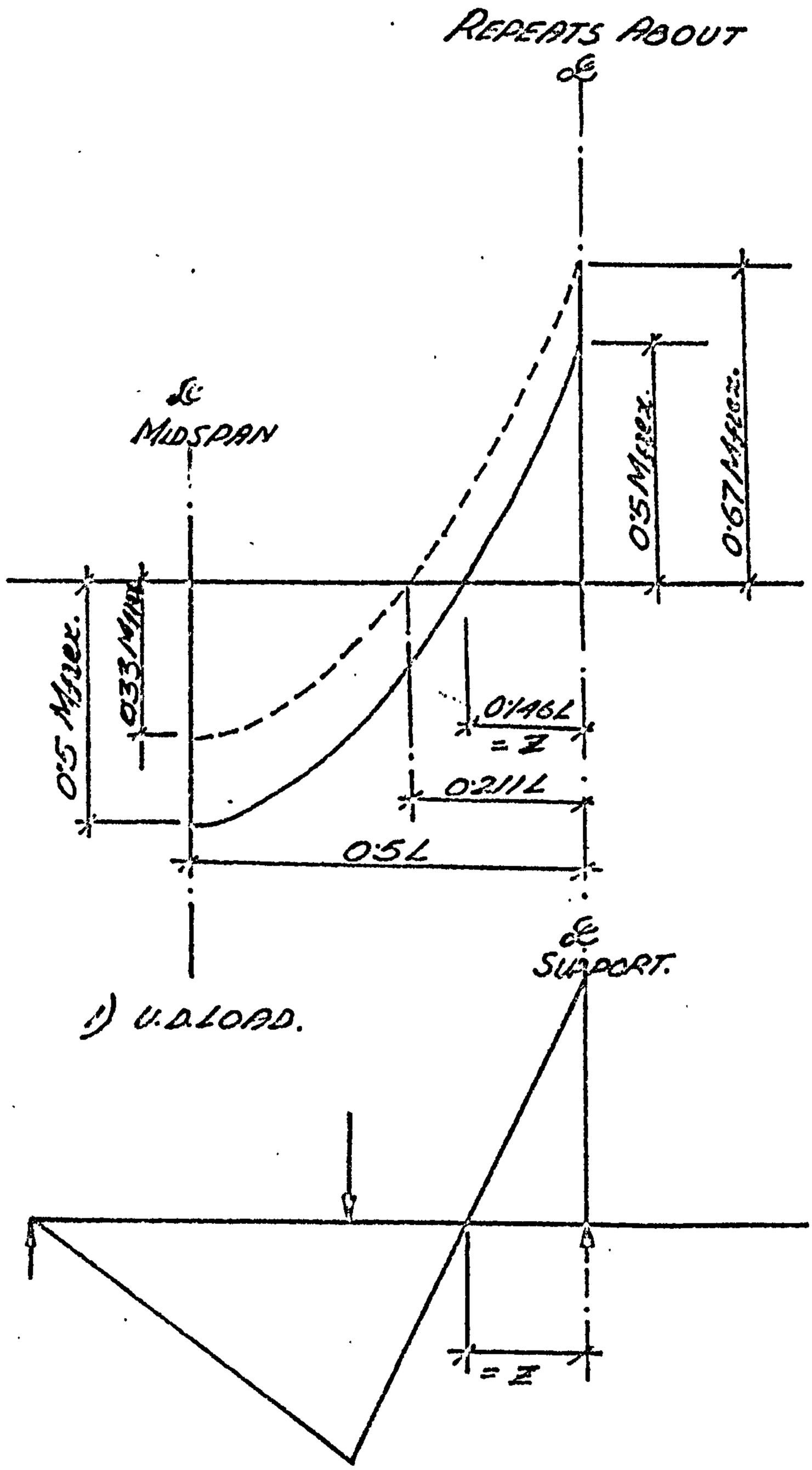
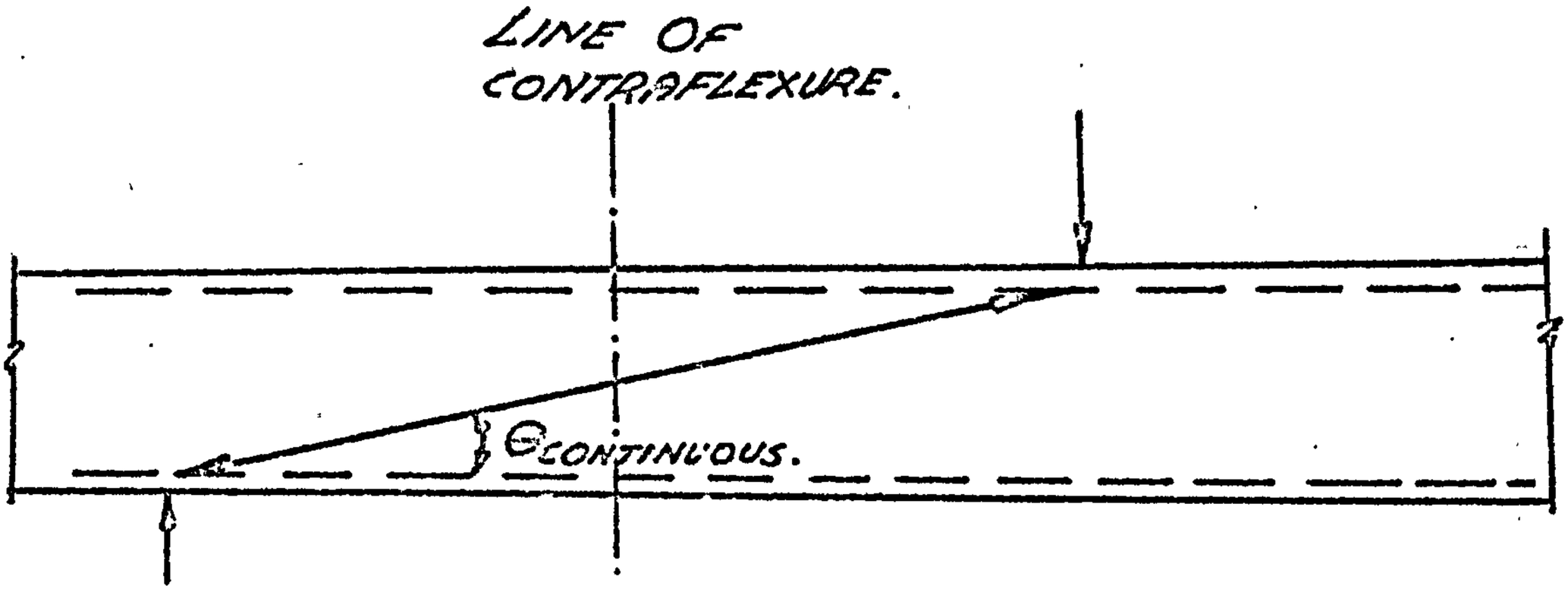
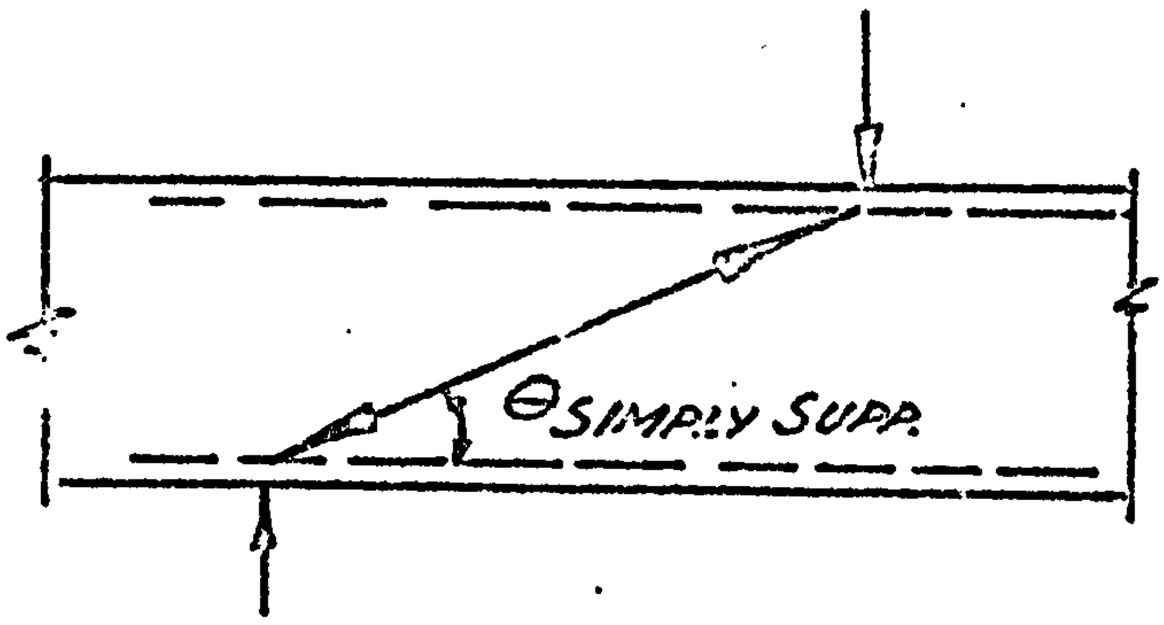


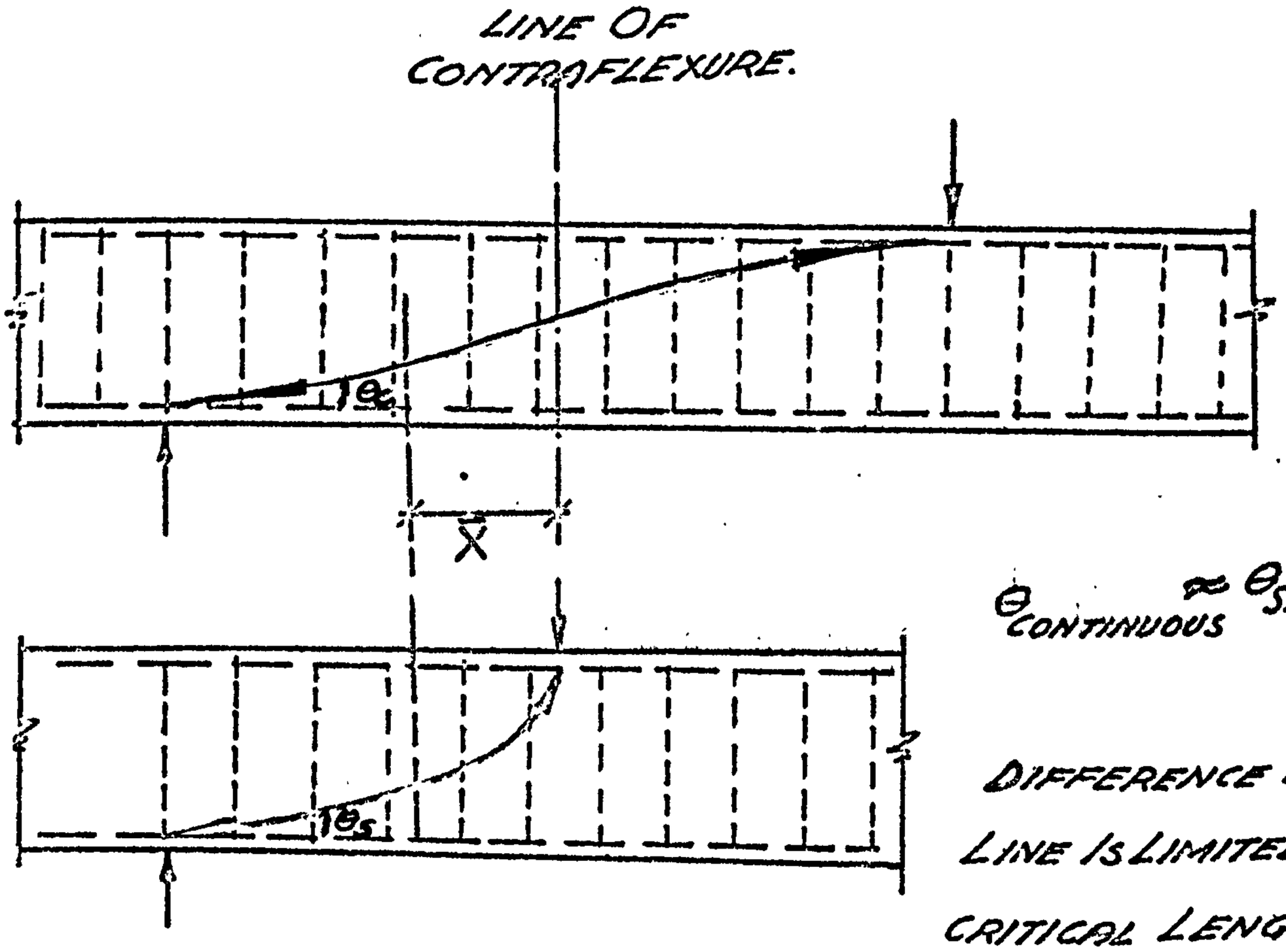
FIG. 4.1. MOMENT- SHEAR- TRUSS SIMULATION.





$$\theta_{CONTINUOUS} = 0.5\,\theta_{SIMPLY\ SUPP.}$$

FIG. 4.2. INCLINATION OF THRUST LINE FOR BEAMS WITHOUT STIRRUPS.



$$\theta_{CONTINUOUS} \geq \theta_{SIMPLY\ SUPP.}$$

DIFFERENCE IN THRUST LINE IS LIMITED TO NON-CRITICAL LENGTH $\bar{x}$.

FIG. 4.3. INCLINATION OF THRUST LINE FOR BEAMS WITH REASONABLE STIRRUPS.

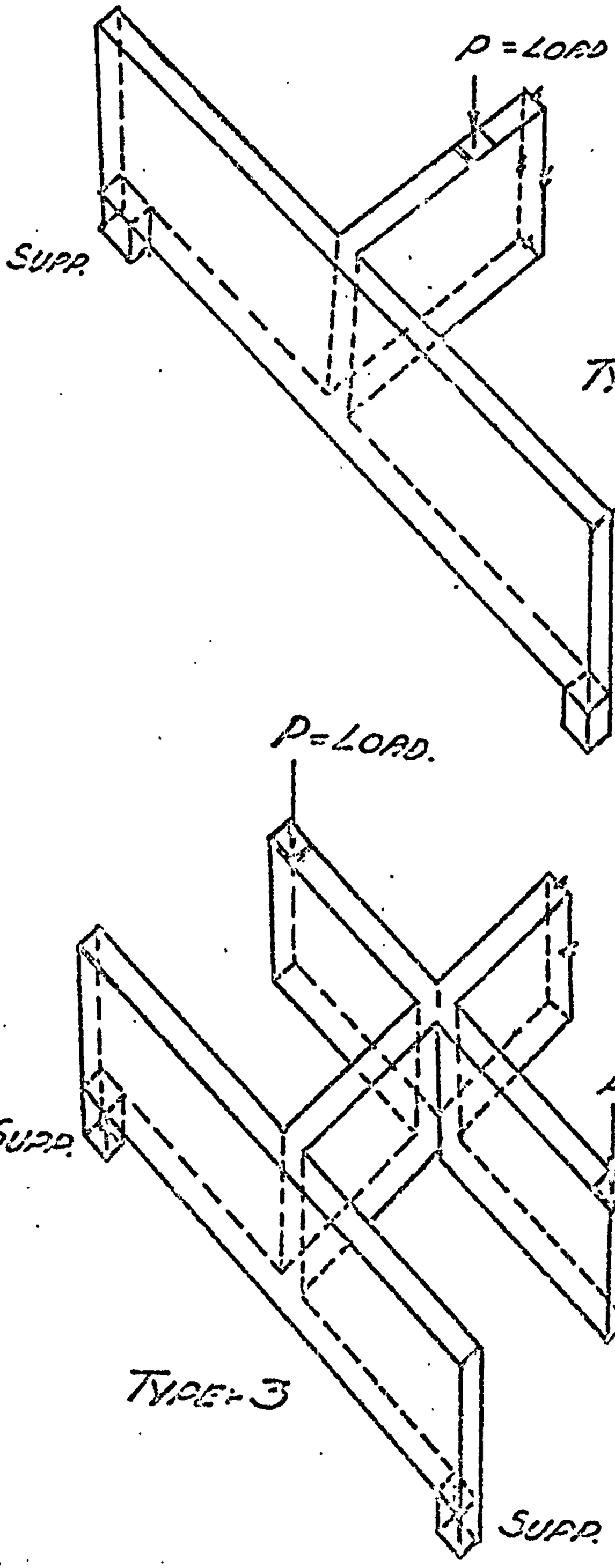


FIG. 4.4. BEAMS LOADED INDIRECTLY.

Beam Nos.	U_w N/m.m^2	r_{st}%	r_{sc}%	$r_{sq} f_{yq}$ N/m.m^2	M/Qd_1	q_u test N/m.m^2	Remark	Placas $q_u$cal/$q_u$test	Regan $q_u$cal/$q_u$test	A.C.I. $q_u$cal/$q_u$test	Hillerborg $q_u$cal/ etc.	C.E.B. $q_u$etc.	Draft C.P. q_u etc.
c3	51	0.545	-	1.073	2.0	2.11	Shear	1.21	1.14	1.0	1.08	0.85	0.89
c4	40.4	0.545	-	1.435	1.89	2.28	Flexure	1.36	1.13	1.04	1.09	0.84	0.96
c9	38.8	0.545	-	1.235	1.96	2.04	Flexure & Shear	1.37	1.17	1.06	1.12	0.89	0.96
c11	52.5	0.545	-	0.585	2.08	1.84	Shear	1.01	1.08	0.90	0.93	0.74	0.73
	S T A N D A R D		D E V I A T I O N					0.139	0.097	0.076	0.07	0.074	0.32
c1	39.4	1.465	-	1.615	2.64	3.21	Shear	1.13	0.92	0.83	1.07	0.68	0.82
c7	39.3	1.465	-	2.2	2.35	3.71	Shear	1.23	0.91	0.87	1.06	0.70	0.87
c8	41.8	1.465	-	2.49	2.22	4.07	Shear	1.24	0.91	0.86	1.08	0.68	0.87
c12	40.4	1.465	-	3.18	2.11	4.32	Flexure & Shear	1.42	0.94	0.97	1.12	0.83	0.93
	C O E F F I C I E N T		O F	V A R I A T I O N				11.4%	9.4%	8%	6.8%	9.5%	9.4%
*c6	46.5	0.545	-	0.585	2.15	1.81	Shear	1.02	1.04	0.89	0.93	0.74	0.68
*c10	54.6	0.545	-	1.615	1.85	2.79	Flexure & Shear	1.36	1.03	0.97	1.01	0.82	0.91
*c13	57.7	0.545	-	1.93	1.61	3.24	Flexure	1.24	1.01	0.95	0.97	0.81	0.92

* Denotes Series No. 2.

CHAPTER 5

INELASTIC ROTATION OF REINFORCED CONCRETE HINGES IN A BEAM.

The inelastic rotation at reinforced concrete hinge in a beam is given by:-

$$\theta_u = \int_0^{l_p} \frac{e_c}{nd_1}\, dx.$$

In the above equation l_p = plastic length of the structure at the hinging region and is defined as the length along the compressive zone of concrete where the strain exceeds the value of 0.002.

5.1 DETERMINATION OF PLASTIC ROTATIONS (FLEXURE).

5.1.1. General

In a reinforced concrete beam, the plasticity develops in a small area of the concrete compressive zone. From the length of this zone, it can be ascertained whether the concrete is bound, i.e. stirrups are present within this area to restrain the concrete laterally, or unbound, i.e. the zone is not affected by the presence of stirrups.

For both bound and unbound concrete, the stress-strain curve for concrete in the compressive zone is assumed to be parabolic at first, reaching a maximum stress f_o at a strain of 0.002, and thereafter maintains the constant stress f_o until it attains the ultimate strain e_{cu} as discussed in Chapter 3 and shown in Fig. 5.2. The stress-block parameters, e.g. K_1K_3, K_2 etc. for this type of

stress-strain curve of concrete are evaluated in Appendix A.1 and shown in Table No. A.1 .

5.1.2 Determination of f_o & e_{cu} for Unbound Concrete

It has been observed by Thaulow[96], Hansen[45], Kesler[54], Murdock[54], and Gonnermann[52] that the compressive strength of concrete increases with the reduced Height/Diameter ratio of cylinders. This has been attributed to the friction between the member and the loading plate. The effect of friction becomes minimal when the ratio of height to diameter exceeds two.

In the same way, at the ultimate state in a reinforced concrete beam, the plastic zone is also subjected to tri-axial compression. In a beam-column connection, the column provides the necessary frictional support, whereas for a simply supported beam the concrete held by the loading plate acts as a frictional base as shown in Figure 5.1 .

In the past, most investigations on short specimens were limited to evaluating the apparent increase of concrete strength of the units, and no concerted effort was made to asses the ductility of short specimens particularly with regard to the falling branches of stress-strain curves. In order to calculate the ultimate strain e_{cu} and maximum concrete stress f_o, the author tested a number of 102 mm diameter cylinders with varying Height/Diameter ratios. The details of experiments are given in Chapter 3. The stress-strain curves for concrete from these tests are drawn in Figure 5.2 .

To determine the apparent increase of concrete-compressive

strength from figure 5.2 the strength of the cylinders having Height/Diameter ratios of 2.25 is taken as unity. The relative increase of strength for other ratios of H/D are shown in Table No. 5.1.1 along with the experimental results of Thaulow[96] & Kesler[54]. A mathematical expression which gives a good correlation with these results is also given in the table.

For unbound concrete:-

$$f_o = 2.35\ U_w^{2/3} \qquad \ldots (5.1)$$

Equation (5.1) is obtained from a CIRIA report where it is used to predict flexural strengths of over-reinforced members.

When H/D < 2 the value of f_o can be found by multiplying the value from equation (5.1) by the factor given in Table 5.1.1, thus:-

$$f_o = 2.35\ U_w^{2/3}\left(\frac{2D}{H}\right)^{1/3} \qquad \ldots (5.2)$$

For long specimens (i.e. H/D ≥ 2) the generally accepted value for limiting strain is applicable.

$$e_{cu} = 0.0035 \qquad \ldots (5.3)$$

This value of e_{cu} is taken from the I.C.E. Research Committee Report[48].

To determine values of e_{cu} for short specimens, the following procedure was adopted.

The value of f_o as obtained from equation (5.2) was plotted in figure 5.2 to correspond to a strain of 0.002. This point was joined to the origin by a smooth parabolic curve. Thereafter

the stress-strain curve was extended horizontally at a constant stress f_o and cut-off at a strain such that the total positive shaded area for any particular H/D ratio became approximately equal to the total shaded negative area. The values of strain obtained from the cut-off points are entered in Table No. 5.2.

A mathematical expression was formulated to give safe values of e_{cu} for different H/D ratios as shown in Table 5.2.

$$e_{cu} = 0.0035(\frac{2D}{H})^2 \leq 0.0035 \qquad \ldots (5.4)$$

Equations (5.2) and (5.4) include terms defining geometrical properties of the section and plastic length. In the ratio H/D, H is the height of the cylinder with a diameter D. The height is measured along the line of action of the applied load. In a beam, as shown in figure 5.1, the line of action of the compressive force due to bending is along the length of the plastic zone. Therefore H = lp. The compression zone of concrete is either a rectangular or a square section with b & nd_1 as adjacent sides, and may be treated as equivalent to a section of a cylinder with a diameter equal to the average of the two adjacent sides with an upper limit for the ratio $b/nd_1 = 8$.

Hence substituting $D = \frac{b + nd_1}{2}$ & H = lp in equations (5.2) & (5.4) for unbound concrete when $b + nd_1 > lp$:-

$$f_o = 2.35\ U_W^{2/3}(\frac{b + nd_1}{lp})^{1/3} \qquad \ldots (5.2a)$$

$$e_{cu} = 0.0035(\frac{b + nd_1}{lp})^2 \qquad \ldots (5.4a)$$

5.1.3 Determination of f_o & e_{cu} for Bound Concrete.

The beneficial effects of transverse reinforcement on the strength and deformation characteristics of concrete have long been recognised. Chan[31], Rusch & Stockl[86], Soliman[88], Chinwah[32], Szulczynski & Sozen[93], Roy & Sozen[84], Vitelmo, Bertero & Felippa[98] and Macdonald[65] have all investigated the effects of transverse reinforcement with or without longitudinal reinforcement on the strength and ductility of reinforced concrete prisms, having Height/Diameter ratios greater than two. Unfortunately, not all these results can be used since the rate of loading, eccentricity of loading, concrete cover to the benders, the presence of longitudinal reinforcement etc., varied unsystematically from one experiment to another. Rusch has shown that the rate of loading has a quite noticeable effect on the ductility of concrete. Soliman[88] has observed that the effect of concrete cover, size of binders and eccentricity of loading appreciably alter the nature of stress-strain curve of concrete. Chinwah[32], Vitelmo, Bertero & Felippa[98] have shown that longitudinal bars without transverse reinforcement do not improve concrete strength or ductility. In order to formulate equations for f_o & e_{cu}, the test results on prisms from above references with concentric load and similar concrete cover and sizes of binders, are used.

Due to lack of available information on reinforced concrete specimens with Height/Diameter ratios less than two, no conclusive equations can be formulated for f_o & e_{cu}.

In order to determine the increase of compressive strength of concrete due to transverse reinforcement, experimental results from Chan[31] & Szulczynski & Sozen[93] are plotted in fig. 5.3. It shows an apparent increase of concrete stress against $p''f_{yq}$. Vitelmo, Bertero & Felippa[98] also tested prisms with concrete load and presented complete stress-strain curves for reinforced and plain concrete specimens; but due to the lack of information about the yield stress of their transverse reinforcement, these results could not be gainfully utilised for measuring increase of strength as a function of $p''f_{yq}$. Roy & Sozen[84] on the other hand have not found any significant effect of transverse reinforcement on the strength of concrete. Stockl[91] commenting on this finding of Roy & Sozen has mentioned a mean increase of 10% in strength for nine concentrically loaded prisms he tested in the Munich Laboratory, but gave no details of the transverse reinforcement.

To calculate the increase of stress, the gross-area of section is taken in lieu of the fictitious bound area suggested by Szulczynski & Sozen[93]. Accepting the argument of vertical arching action between links which increases the strength of specimens, it still remains open to question about the efficacy of choosing only the bound area and not the average of core area and bound area as shown in the figure 5.4. In any case, the gross area though a simplification can be used to give conservative results.

The scatter in the results demonstrated by fig. 5.3 and Roy and Sozen's[84] still more conservative conclusion indicate

that a numerically simple lower bound expression is all that can be justified for computing the increase of concrete stress. A lower bound value is also dictated by the need for design calculations of rotation to provide a safe limiting value. Therefore, it is proposed that the maximum compressive stress of reinforced concrete prisms can be calculated using the following equations (5.5) & (5.6).

For $lp \geq nd_1 + b$

$$f_o = 2.35\ U_W^{2/3} + 0.1\ p''.f_{yq} \qquad \ldots (5.5)$$

where $0.1\ p''f_{yq} \not> 3.5 N/m.m^2$.

For $lp < nd_1 + b$.

As stated before, increasing the concrete stress $2.35U_W^{2/3}$ by the factor $\left(\frac{b + nd_1}{lp}\right)^{1/3}$ to take care of the effect of triaxial restraint, gives:-

$$f_o = 2.35\ U_W^{2/3}\left(\frac{b + nd_1}{lp}\right)^{1/3} + 0.1\ p''f_{yq} \qquad \ldots (5.6)$$

Experimental results of Roy & Sozen[83], Vitelmo, Bertero & Felippa[98] and Szulezynski & Sozen[93] were analysed to calculate the ultimate concrete strain e_{cu} for bound concrete. Though Chan[31] has also tested some reinforced concrete prisms, it appears that he has not investigated thoroughly the falling branch of stress-strain curve of concrete. In comparing the results of the three groups, the limitations of these tests must be recognised. Szulezynski & Sozen have based their strain measurements on overall shortening of specimens after the spalling of concrete. Roy & Sozen have measured strains over gauge lengths of 102 mm, whereas Vitelmo, Bertero &

Felippa used a length of 152 mm. In a physical sense none of these measurements were true strains. Burnett[23] has shown that the gauge lengths of measuring equipments have considerable influece on the results of strain measurement, and concludes that the shorter the length of the measuring gauges the higher the recorded strains are likely to be. Hence the three groups of results, though used together for analysis, are strictly not comparable. In order to establish a lower bound equation for strain e_{cu}, the author has used the typical stress-strain curves of Roy & Sozen, and checked the equation so obtained against the stress-strain curves of Szulczynski & Sozen[93], and Vitelmo, Vertero & Felippa[98].

e_{cu} FOR $lp \geqslant nd_1 + b$.

Typical stress-strain curves from Roy & Sozen's series A, B, C, D & E, in which the prisms were without longitudinal reinforcement, are drawn in Figure 5.5 for different spacings of transverse reinforcement. The volumetric ratio of transverse reinforcement is constant. As with the unbound concrete, a parabolic curve is drawn in figure 5.5 reaching the maximum concrete stress f_o - obtained from equation (5.5), at a strain 0.002. This is then projected horizontally and is cut-off at points where the shaded positive area becomes approximately equal to the shaded negative area. The values of strain obtained from these cut-off points are plotted against H/s in figure 5.6. Writing lp in place of H, the following expression for e_{cu} is obtained, as shown in figure 5.6.

$$e_{cu} = 0.35.p''.\left(\frac{lp}{s}\right)^{2/3}.\frac{A_b}{A_c}.\frac{22.5}{U_w} \qquad \ldots (5.7)$$

where $e_{cu}^* \leq 0.0035$ for $p'' = 0$

$e_{cu} \leq 0.0050$ for $p'' = 1\%$

$e_{cu}^* \leq 0.0070$ for $p'' = 2\%$

$e_{cu}^* \leq 0.0090$ for $p'' = 3\%$

$e_{cu}^* \leq 0.010$ for $p'' \geq 3.5\%$

These limiting values of e_{cu}^* are obtained from fig. 4.3 Amarakone[6].

In order to verify the expression for e_{cu}, its values are next plotted against the experimental results of Szulczynski & Sozen[93] in figs. 5.7 & 5.8, and against the experimental results of Vitelmo, Vertero & Filippa[98] in fig. 5.9. It can be observed that, for the results of Vitelmo, Vertero & Felippa equation (5.7) predicts safe values for strains, whereas for those of Szulczynski & Sozen, the prediction is very safe for the 125 mm x 125 mm prisms, but not so safe for the 125 mm x 250 mm prisms. However, in regard to those last tests the following points have to be borne in mind:

i) Szulczynski & Sozen recorded overall deformations of the concrete prisms, as opposed to the local deformations recorded by the others. Hence the test results are not true indicators of the local deformation on which formula 5.7 is based. It is likely that had any record been kept of local strain over a short length of say 100 mm or 150 mm, the fall of concrete stress would have been much gentler. Roy & Sozen[89] have shown the discrepancy that is observed if localised strain is measured as opposed to overall deformation.

ii) The results of Szulczynski & Sozen like all the other

results under investigation are based upon prisms loaded with concentric load producing rectangular stress blocks. In the plastic zone of an actual beam, it is unlikely that the stress block could be rectangular even at the time of failure. Soliman[88] has proved that the stress-strain curve of a reinforced concrete prism produces much gentler drop of stress in the case of an eccentrically loaded specimen than is the case of a concentrically loaded prism.

iii) Authors like Rusch & Stockl[86], Roy & Sozen[84], and Vitelmo, Vertero & Felippa[98] have all observed the beneficial effects of longitudinal reinforcement along with the transverse steel, on the ductility of concrete. In the compression zones of all beams, some compression reinforcement is necessary for detailing purposes - either in the form of hanger bars for simply supported beams, or in the form of bottom reinforcement taken to the support for continuous beams. Hence some beneficial effect of these bars is inevitable in practice.

$$\varepsilon_{cu} \text{ FOR } lp < nd_1 + b .$$

Since no test results are available for reinforced concrete specimens/varying Height/Diameter ratios of, no prediction for ultimate strain is made for this group.

The strain is taken equal to the value for unbound concrete, i.e. equation 5.4.

5.1.4 Determination of Plastic Lengths for Continuous Beams

The support section of a point loaded continuous reinforced

concrete beam is shown in fig. 5.10. It is assumed that the line of action of compression thrust is linear. The inclination of main compressive force could be one of the following three cases. a) The slope of the compression thrust is unaffected by the presence of stirrups. In this case, the thrust line is straight. b) The slope of the thrust line is a straight line again, but affected by the presence of stirrups which determine its slope at the head of shear crack. c) the slope of the compression thrust is variable, changing with the amount of shear reinforcement that comes into play along its length.

Since the major part of the deformation occurs very close to the column where the main steel has yielded and the change of moment must be accommodated by a changing lever arm, errors due to the varying thrust line in the remaining less stressed part of the span must be very small and the assumption is on the safe side.

From figure 5.10, $\tan\alpha = \dfrac{l_{a1} - \frac{d}{2} + (d - d_1)}{Z}$

But $\dfrac{l_{a1} - l_{a2}}{x} = \tan\alpha' = \dfrac{l_{a1} + \frac{d}{2} - d_1}{Z} \approx \dfrac{l_{a1} - d_1/2}{Z}$

$$\frac{x}{Z} = \frac{l_{a1} - l_{a2}}{l_{a1} - d_1/2}$$

If section 2-2 is so chosen that the concrete fibre stress reaches 0.002,

$$x = lp = Z\left(\frac{l_{a1} - l_{a2}}{l_{a1} - d_1/2}\right) = Z\left[\frac{d_1\left(1 - \frac{K_2}{K_1K_3}\cdot\frac{F_{yt}}{f_o bd_1}\right)^1 - d_1(1 - K_2n)^2}{d_1\left(1 - \frac{K_2}{K_1K_3}\cdot\frac{F_{yt}}{f_o bd_1}\right)^1 - \frac{d_1}{2}}\right]$$

$$lp = Z\left[\frac{(K_2n)^2 - \left(\frac{K_2}{K_1K_3}\cdot\frac{F_{yt}}{f_o bd_1}\right)^1}{0.5 - \left(\frac{K_2}{K_1K_3}\cdot\frac{F_{yt}}{f_o bd_1}\right)^1}\right] \quad \ldots (5.8)$$

CASE I: SECTION 2-2. MAIN STEEL ELASTIC AND NO COMPRESSION REINFORCEMENT.

If the tension reinforcement at section 2-2 is elastic, with no compression reinforcement, then from the assumed properties of materials and the assumption of a linear strain distribution,

$$n = \frac{-1 + \sqrt{1 + 4K}}{2K}$$

where $E_{st} \cdot e_c \cdot \frac{1 - n}{n} \leqslant f_{yt}$ and $K = \frac{f_o K_1 K_3}{r_{st} \cdot e_c \cdot E_{st}}$.

This formula is established in Appendix B.1 .

CASE II: SECTION 2-2. MAIN STEEL ELASTIC WITH COMPRESSION REINFORCEMENT.

A trial & error solution is to be adopted.

CASE III: SECTION 2-2. MAIN STEEL YIELDED.

Section 2-2 is to be treated in the same way as section 1-1.

5.1.5 Determination of Plastic Rotation at Support Section

The rotation of a reinforced concrete hinge is given by the equation given in section 5, i.e.

$$\theta_u = \int_{\theta}^{lp} \frac{e_c \cdot dx}{nd_1} .$$

If this integral is performed in terms of values of n & e_c as defined by the thrust line given above, values of θ_u can be written as $\theta_u = \frac{K' \cdot e_{cu} \cdot lp}{n'd_1}$

where $n'd_1$ is the average neutral axis depth along the length lp. Values of K' can be obtained from curves such as that shown in figure 5.11, but can be taken to be approximately constant

and equal to 0.375.

$$\therefore \theta_u = 0.375\, e_{cu} lp/nd_1 \qquad \ldots (5.9)$$

5.1.6 Determination of Plastic Length and Rotation for Span Sections.

In deriving the formulae for plastic lengths and rotations at plastic hinges the assumptions made for support sections are also applicable to point-loaded span sections. Hence equations (5.8) & (5.9) can be used for the determination of plastic lengths and plastic rotations respectively.

5.1.7 Comments on the Equation for Plastic Rotation

In the final equation for plastic rotation, a constant 3/8 is used to take the average of the peak value of e_{cu} attained at the section of maximum moment and the lower strain at Section 2-2, as shown in fig. 5.11. In point of fact, this should strictly be $3/8(e_{cu} - 0.002)$, but it must be borne in mind that, in the derivation of the equation for e_{cu}, the values used were measured on 102 mm gauge lengths. The plastic lengths for all the author's results and also for many test results presented in Tables 5.3, are less than 102 mm. In other words, the strains are already the average for the entire plastic length. In addition, at all stages in the formulation of equation for plastic rotation, the chosen values were based upon safe lower bound solutions. Hence the constant 3/8 selected in a slightly arbitrary way can be justified on grounds of simplicity without endangering safety.

5.8 Determination of Rotations and Ultimate Moments in Beams

To determine the ultimate plastic rotation in a plastic zone, a trial & error solution is adopted. The depths of neutral axes at a strain of 0.002 and at the section of maximum moment are calculated, assuming a value of e_{cu}. From these depths the lever arm factors are known and subsequently the plastic length is obtained from equation (5.8). The plastic length and the average depth of neutral axis over this length give the ultimate strain e_{cu} from equation (5.4a). This e_{cu} is compared with the original assumed value. If the two are not in agreement, a new value is assumed intermediate between the two and the process is repeated. In this way the final ultimate strain is obtained and subsequently the average depth of neutral axis and the plastic length. Thereupon equation (5.9) gives ultimate plastic rotation in the plastic zone of the structure.

To calculate the ultimate moment of a plastic zone the lever arm (la_1) at the section of maximum moment is taken from the rotation calculation. Hence knowing la_1, and the sectional properties, the Ultimate Moment is evaluated as follows:-

i) CASE I: BEAMS WITHOUT COMPRESSION REINF'T:-

$$M_{ULT} = F_{yt} \cdot la_1 \qquad \ldots (5.10a)$$

ii) CASE II: BEAMS WITH YIELDED COMPRESSION REINF'T:-

$$M_{ULT} = (F_{yt} - F_{yc})la_1 + F_{yc}(la_1 - d_2) \qquad \ldots (5.10b)$$

Typical examples are worked out in Appendix B.

5.2 SHEAR ROTATION

5.2.1 General

Many authors, e.g. Rao[72] and Cranston[35], etc. have mentioned shear rotation. Rao[72] considers shear rotation to be considerable. If a beam fails in shear, the critical shear crack usually goes above the heads of flexural cracks as shown in fig. 5.12, or sometimes joins the heads of flexural cracks, and then proceeds into the compressive zone of concrete, as explained in Chapter 3. In either case, the critical shear crack rises higher than the flexural cracks, its direction becoming flatter when progressing into the compressive zone. As is evident, the depth of neutral axis above the head of this shear crack prior to failure, is smaller than the depth of neutral axis above the flexural cracks. Hence the rotation, which depends largely on the depth of neutral axis, would appear to be larger for beams which fail in shear. It is presumably this extra rotation, over and above the flexural rotation, which is termed "Shearing Rotation" by various authors. To study shear rotation, the complete history of beams failing in shear has to be scrutinised.

5.2.2 Analysis of Test Results

In order to evaluate the amount of shear rotation occurring in the beams tested by the author, the overall rotations of the support sections are plotted against applied load for all the beams tested, in fig. 5.13, 5.14 & 5.15. Three groups of results are presented - the first two groups

consist of balanced and under reinforced sections with a constant value of ρ; the third group consists of under reinforced sections with different values of z. In each group there is a small variation of concrete cube strength and the value of Z from beam to beam. The value of $r_{sq} f_{yq}$ has also been varied to cause different types of failure within each group. From the tests the following features are observed:

Group Ia:- Beams c_3 & c_{11} failed in shear at loads of 145 KN & 125 KN respectively. For beam c_3, it is to be noted that from the load stage of 130 KN the rotation developed is different from the flexural pattern of other beams, whereas beam c_{11} deviated at a load stage 110 KN. The small deviations may be attributed to the fact that the critical shear crack has penetrated along the tension steel - see fig. 5.16. Up to this stage, all four beams roughly follow the same line.

Group Ib:- Beams c_1, c_7 & c_8 failed in shear at loads of 210 KN, 245 KN & 275 KN respectively. In Beam c_1 the deviation from the flexural rotation curve started at a load of 185 KN, in Beam c_7 at 220 KN & in Beam c_8 at 250 KN. Again these are approximately the load stages when the main inclined crack also penetrates along the zone of tension reinforcement.

Group II:- Beam c_6 failed in shear at a load of 100 KN. The deviation from the flexural curve started at a load of 80 KN. However, it must be mentioned in this connection that Beam c_6 had much weaker concrete than the other two of the series. Hence, there was some deviation from the main flexural curve throughout its loading. This deviation became more pronounced at load stage mentioned above.

From the load/rotation curves it seems that in each group the beams which fail in shear trace the same curve as the beams which fail in flexure, until such time as the critical

shear cracks tore along the concrete in the tension zone following yielding of the stirrups, as shown in figure 5.16. The opening of the crack results in a tendency of the side of the beam where the load acts to move downwards relative to the support of the beam, thus inducing a translational movement along the crack. This movement in turn produces what is known as "Shearing Rotation" of the beam. In the load/rotation curve, the beams no longer follow the flexural line and shoot off from the main curve.

It must be admitted that there are a number of limitations of this series.

i) The readings from the last load stage are invariably extrapolated thus resulting sometimes - particularly in the case of shearing rotation - in a very tentative final section of the curve whenin some instances, only one previous reading is available for guidance. To measure behaviour in the final stages accurately, continuous recording equipment should have been used.

ii) The values of E for the different beams within each group varied.

iii) The concrete cube strengths for different beams of the same group differed.

iv) The study is limited to continuous beams. Simply supported beams were not tested.

Under the circumstances, to draw a definite conclusion about the cause and effect of shearing rotation would be futile, but it is clearly of very little significance in normal beams.

5.3 COMPARISONS WITH TEST RESULTS:-

The test results as reported by the author, Cranston[35], Corley[34] and Mattock[63] are compared with the proposed method, the method suggested by Corley[34] and the approach adopted by the I.C.E. Research Committee[48]. The comparative statement is presented in Tables No. 5.3.1 - 4 in two parts. The first half deals with the ultimate moment at the section of maximum moment - at the face of column for continuous systems and at the faces of applied loads for the simply supported systems, and the second half deals with the plastic or inelastic rotation at the sections of maximum moment.

5.3.1 Summary of Tests

In the continuous point loaded systems tested by the author, the ultimate moments were calculated from the load cell readings at the mid-support and the end supports. The inelastic rotations at the mid-support were recorded by clinometers placed near it. The final readings were always before the failure load. The rotations and failure were however obtained by extrapolation from the Load/Rotation diagram as shown in Figure 5.13. The values of z were obtained from the Bending Moments at the support and span sections. Five beams which had sufficient flexural capacity are analysed for both ultimate moments and plastic rotations and the values of z are shown in table5.31, whereas of the six remaining beams which failed rather prematurely in shear, are analysed for plastic rotation only. Details of instrumentation and the properties of sections are

given in Chapter 3 and table 5.3.1 respectively.

For point loaded simply supported systems three groups of test results are analysed. The first group consists of tests reported by Cranston & Reynolds[35]. They supported the test beams on jacks at two ends. The upward loads from these jacks were carried by a downward reaction at the span. The length Z was the portion subjected to detailed study, with the intended hinge region immediately to one side of the downward reaction. The shear in the short length of beam to the other side of the reaction was carried by heavy external shear reinforcement. Inclinometers were placed on the loading plate under the downward reaction and on the top surface of the beam 370 mm from the edge of the plate to record the hinge rotation. To be consistent with the other results presented in this thesis, the value of ultimate rotation is assumed to be that at the stage at which the section supported its maximum moment. The elastic rotation is deducted from the ultimate rotation to obtain the inelastic rotation. In the cases of beams, where the maximum moment is nearly on a plateau or falls very gently, the rotation corresponding to the average of the two successive readings starting from the value where maximum moment occurs, is taken as the limit for ultimate rotation.

Three groups of results involving ten tests are reported in this Chapter. The first two groups had comparatively light longitudinal tension reinforcement and the last group had heavy longitudinal reinforcement. The relevant information needed for computing the ultimate moments and the plastic rotations at the section of maximum moment are given in Table No. 5.3.2.

Corley, on the other hand, tested twenty-nine simply supported beams with central point loads, as detailed in Table No. 5.3.3. Some of these beams failed prematurely in shear. The results for series J are omitted from the table, since the size of beams tested - 75mm x 125 mm, is considered to be rather small and the effects of scale factors are not known. In each series the depth of beams was kept constant and the width varied. The major variables in the test programme are a) width; b) effective depth; c) span; d) amount of tension reinforcement and e) amount of binding reinforcement. The test programme of Corley was an extension of Mattock's series of tests. The rotation at mid-span over a length equal to the effective depth, was calculated from the measured lengthening and shortening near the bottom and top of both sides of each beam, by using linear differential transformers mounted 13 mm from the top and bottom. The output from these transformers was monitored by Sanborn Continuous recorders. Details of instrumentation are available in a paper by Hanson and Kurvits[44]. The inelastic rotation occuring within a length d/2 to one side of the section of maximum moment is given for each beam in the table along with the pertinent geometric and reinforcement details.

The results of thirty tests reported by Mattock[63] are given in Table 5.3.4. All his beams developed full flexural capacities. The major parameter of his tests were:-

a) concrete strength; b) yield strength of reinforcement;

c) effective depth; d) span and e) area of tension reinforcement. To obtain values of inelastic rotation in a distance $d_1/2$ to one side of the applied point load, electrical measuring devices were coupled to a set of Sanborn type 67A continuously-recording units. The measuring devices were similar to the ones adopted by Corley reported above.

5.3.2 Prediction of Results

Ultimate Moment:- To predict the ultimate moment at the column face of the support section by the proposed method, the depth of neutral axis is calculated from the principles of equilibrium of forces and the compatibility of strains. The trial and error approach is explained earlier in this chapter. The average ratios of $\frac{Mu_{cal}}{Mu_{test}}$, the standard deviations and coefficients of variation for four groups of tests are given in Table 5.3.5.

Corley - who improved the equation for maximum concrete compressive strain as developed by Mattock, also obtained the ultimate moment from the principles of equilibrium of forces and compatibility of strains as described in the Appendix. In evaluating the ultimate moments for the tests of the author and Cranston & Reynolds[35], the effect of strain hardening of longitudinal tension reinforcement is neglected. The ratios of the $M_{u\,cal}/M_{u\,test}$, standard deviations and coefficients of variation for the different tests, are given in Table No. 5.3.5.

The method of the I.C.E. Research Committee for computing

the value/ultimate moment is based upon a parabolic stress block in the concrete compression zone, the corresponding stress block parameters and the equilibrium of forces. The detailed analysis is explained in the Appendix and the values of Mu_{cal}/Mu_{test}, standard deviations and coefficients of variations, are given in Table 5.3.5.

Inelastic Rotation:- The inelastic rotations at the hinges of the beams, which failed in flexure, are calculated from the equations developed earlier in the Chapter. An iterative process is used to evaluate the plastic length, the maximum concrete compressive strain, and the ultimate depth of neutral axis. The average ratios of the standard deviations and coefficients of variation for four groups of beams are given in Table 5.3.6.

In Corley's method - which is an improvement on Mattock's, the plastic rotation over a length $d_1/2$ is calculated by determining the value of the maximum compression strain in the concrete, the yield moment and the ultimate moment at the section from various formulae described in the Appendix. The effect of strain hardening of tension reinforcement is neglected in calculating θ_u values for tests reported by the author and Cranston & Reynolds[35]. The average ratios of $\theta_{u\ cal.}/\theta_{u\ test}$, the standard deviations and coefficients of variation for the tests are presented in Table No. 5.3.6.

To determine the inelastic rotation by the method reported of the I.C.E. Research Committee, the plastic length is first calculated from the known value of z and the properties

of the section. Thereupon assuming the concrete compressive strains at yield and at the ultimate state as 0.002 & 0.0035 respectively, the inelastic rotation is obtained by dividing the product of the difference of these strains and the plastic length by the ultimate neutral axis depth. The procedure is presented at length in the Appendix. The average values of the ratio $\theta_{u\ cal.}/\theta_{u\ test}$, the standard deviation and the coefficient of variation are given in Table No. 5.3.6.

5.3.3 Comment on the Shearing Rotation

The plastic rotations for beams which failed in shear are presented in the following way.

The maximum shear strength (Q_{ult}) for the section under consideration for any beam is obtained from the test result. The apparent inelastic rotation for an otherwise similar beam which failed in flexure is also determined from tests (θ_{flex}). The shear strength of the concrete compressive zone and the stirrups are then calculated from the equations developed in Chapter 6. The rotation of any beam which fails in shear is then obtained by substituting these values in equation (6.11).

In the strictest sense this is not a direct comparison between a theoretical analysis and the corresponding experimental results. It is merely a guide to the validity of equation (6.11). The average ratio of $\theta_{cal}/\theta_{test}$ is 0.67; the standard deviation 0.279 and the coefficient of variation 0.42. The rather poor value of $\theta_{cal}/\theta_{test}$ and the coefficient

c: variation can be attributed to the following:-

i) The estimation of flexural rotation of a beam depends largely on its value of Z. In a continuous system, the value of Z is determined from the bending moments at support and span sections. Hence a beam which fails rather prematurely in shear does not redistribute its support moment to the same extent as would have been expected of an otherwise similar beam which failed in flexure. Therefore the value of Z for such a beam is somewhat different from that of an equivalent beam which fails in flexure.

ii) Fig. 6.8 shows that the equation for the reduction factor for shear strength is very much a lower bound solution. On careful scrutingy it appears that this could have been improved by choosing the other equation shown in fig. 6.8, and even more so if the results of Cranston & Reynolds tests were eliminated and the equation was formulated based upon the author's results only. However since insufficient test results are available, the rather conservative formula is justified

iii) The flexural rotation of any beam depends largely on the ductility of the concrete. The closer the spacing of the stirrups the more ductile the material becomes and consequently the flexural rotation increases. The flexural rotation of a beam is therefore not a unique value.

iv) The concrete cube strengths for different beams in each group varied. Hence flexural rotation, which depends on the ductility of concrete, varies with the cube strength.

v) The final values of flexural rotations are recorded

by extrapolation as mentioned earlier. In moment/rotation curves with flat tops or load/rotation curves with steep gradients, the determination of flexural rotations by extrapolation should themselves not be viewed as being precise.

5.3.4 Discussion of Results

In the above four groups of results presented and compared with three theories, the investigation is limited to the ultimate moment and the inelastic rotation near the section of maximum moment.

In order to check the ultimate moment, clearly the best prediction is obtained by using Corley's method, where the effect of strain-hardening of tension reinforcement is taken into account. The proposed method, though an improvement on the I.C.E. Research Committee's Report, neglects this additional strength of the tension reinforcement and predicts fairly low values of ultimate moments for the beams tested by Mattock, whereas the predictions are fairly good for beams with hot rolled British steel like Cranston's, where the effect of strain hardening is negligible. In the case of the author's tests, the reason for rather poor values of M_{ult} is due to the neglect of the effect of compression reinforcement. For most of the beams tested by Corley the influence of strain-hardening on tension steel was moderate, hence both Corley's theory and the proposed method predict good agreement with the test results.

Scrutinizing all these results, it appears that the best prediction would be obtained if the effect of strain-hardening

of tension reinforcement as suggested by Corley were coupled with the increase of strength of concrete as given by the author, but the procedure would be too involved for the small gain in accuracy.

In order to calculate the inelastic rotation at the section of maximum moment, the best method is clearly the one proposed by the author. It is true that Mattock's test gives a very wide scatter of results and rather poor ratios of $\theta_{u\ cal.}/\theta_{u\ test}$, yet in comparison with the other theories the proposed method still produces a better fit. The best agreement of results for the proposed theory is obtained for tests reported by the author and by Corley. In case of Cranston's results, it is rather difficult to fix the limit of ultimate rotation when the moment/rotation curve has very gentle slope. In spite of this difficulty, the average ratio of $\theta_{u\ cal.}/\theta_{u\ test}$ as obtained by the author's method is superior to Corley's theory and both the standard deviation and the coefficient of variation are within tolerable limits. The I.C.E. Research Committee report, however, gives such a wide scatter and low ratio for $\theta_{u\ cal.}/\theta_{u\ test}$ that it does not seem worthwhile to discuss the theory at length. One thing that appears to stand out above all other parameters considered by this Report is the wrong placement of parameter z - in the numerator instead of the denominator of the equation for plastic rotation. This has made matters worse for an already inconsistent prediction. It should be mentioned in this connection that Corley[34] & Mattock have recorded their rotation over a length of $\frac{1}{2}\ d_1$, whereas

Cranston on a length 1.5 d_1. This is the reason for low ratios of $\theta_{u\ cal.}/\theta_{u\ test}$ for Cranston's in comparison with Corley's or Mattock's results.

To study the effect of the various parameters on the accuracy for different results, $\theta_{u\ cal.}/\theta_{u\ test}$ is plotted in Figs. 5.17, 5.18, & 5.19 against Z/d_1, $r_{st}.f_{yt}/U_W^{2/3}$ and b/d_1 for the four groups of results. It is apparent that the parameters Z/d_1, $r_{st}.f_{yt}/U_W^{2/3}$ have distinct incluence on θ_u, and the effect has been taken care of properly as there is no systematic trend of errcrs with respect to θ_u. Similarly inspite of the rather arbitrary treatment of geometry used in the term $(b + nd_1)$ to formulate restraint conditions there is no systematic error with respect to the ratio b/d. Of the four groups of results, the author's and Corley's give best correlation with the predictions, followed closely by Cranston's results. Mattock's results, on the other hand, give a wide scatter.

The rate of loading plays a vital part in the formation of inelastic rotation near the section of maximum moment. Rasch[73] has shown that the slower the rate of loading the more gentle is the fall in moment/compression strain curve. In other words, instantaneous loading produces minimum compression strains in concrete whereas loading spread over a period of time increases the ultimate compression strain in concrete and consequently the inelastic rotation. The rate of loading for the author's tests was similar to Corley's & Mattock's. In the author's tests 10 KN load was applied

over a period of one minute and then holding this load for a further period of fourteen minutes before applying the next increasement of load. The complete test lasted about three hours on average. The rate of loading for Cranston's test is not known. To take care of sudden overloads, equation (5.9) for plastic rotation could be multiplied by the constants derived below. However, the following points have to be borne in mind regarding instantaneous loading:-

i) If flexural rotation is to be calculated based upon instantaneous loading, the statistical possibility of the structure facing this overload condition during its lifetime has also to be investigated properly.

ii) The instantaneous rotation is usually associated with the beams or columns in a structure. The relative importance of the members, i.e. whether they are primary or secondary members and also the function of the structure as a whole, e.g. apartments or light storage area and the economy of the structure,will have to be weighed carefully against safety.

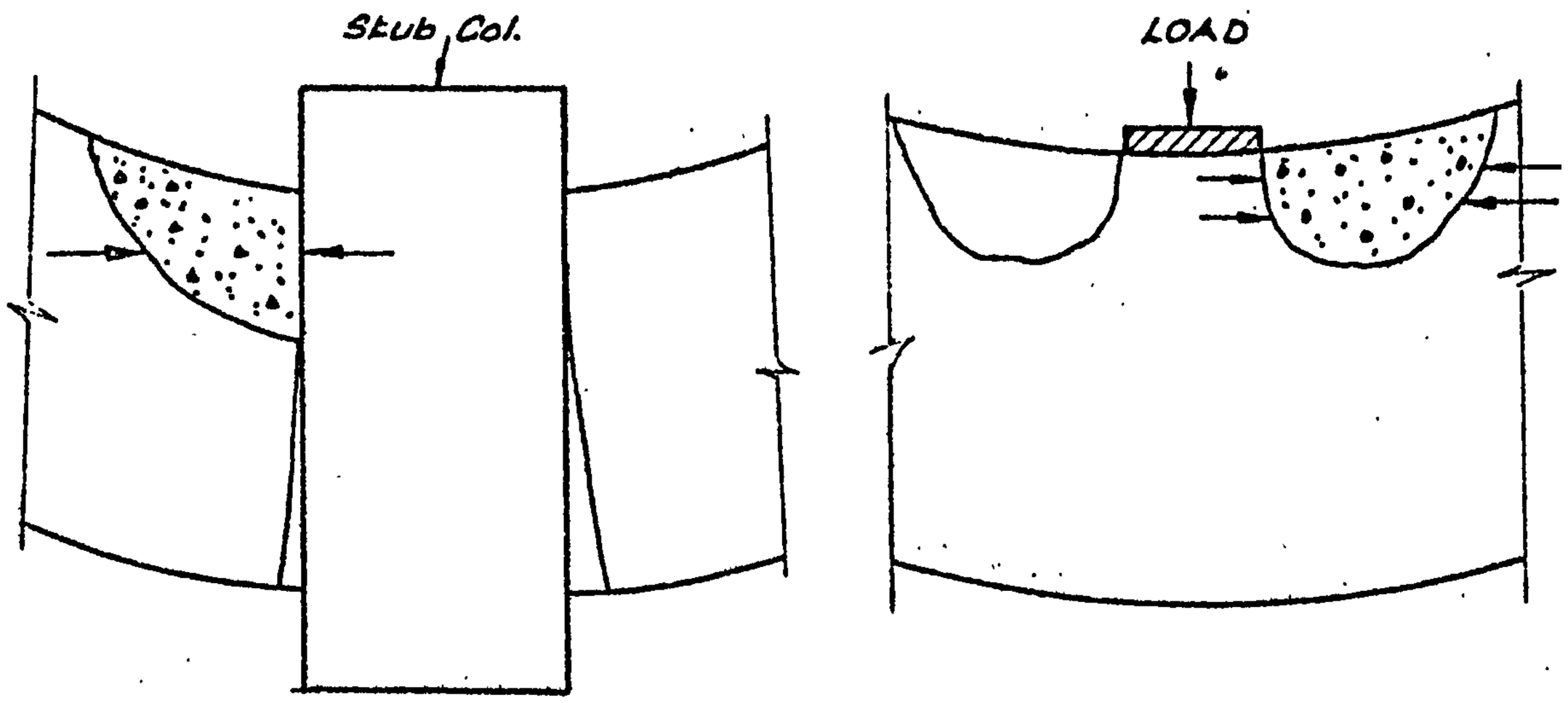
iii) Exceeding θ_{max} does not involve a total loss of strength.

In order to include the effect of instantaneous loading the author has drawn fig. 5.20 from Rasch[73]. The dotted line indicates tha value of f_o corresponding to the cube strength of the concrete used for his tests. Projecting this horizontally, the line intercepts the rate of loading line at which the author's tests were conducted in the laboratory at a strain of 0.004 and the instantaneous

loading line at a strain of 0.003. Hence if a factor of 3/4 is allowed for in the final equation for θ_{flex}, this will take care of this sudden overload condition. It has to be admitted in this connection that this is merely a guide, and proper study of this field would be desirable, but is beyond the scope of this thesis.

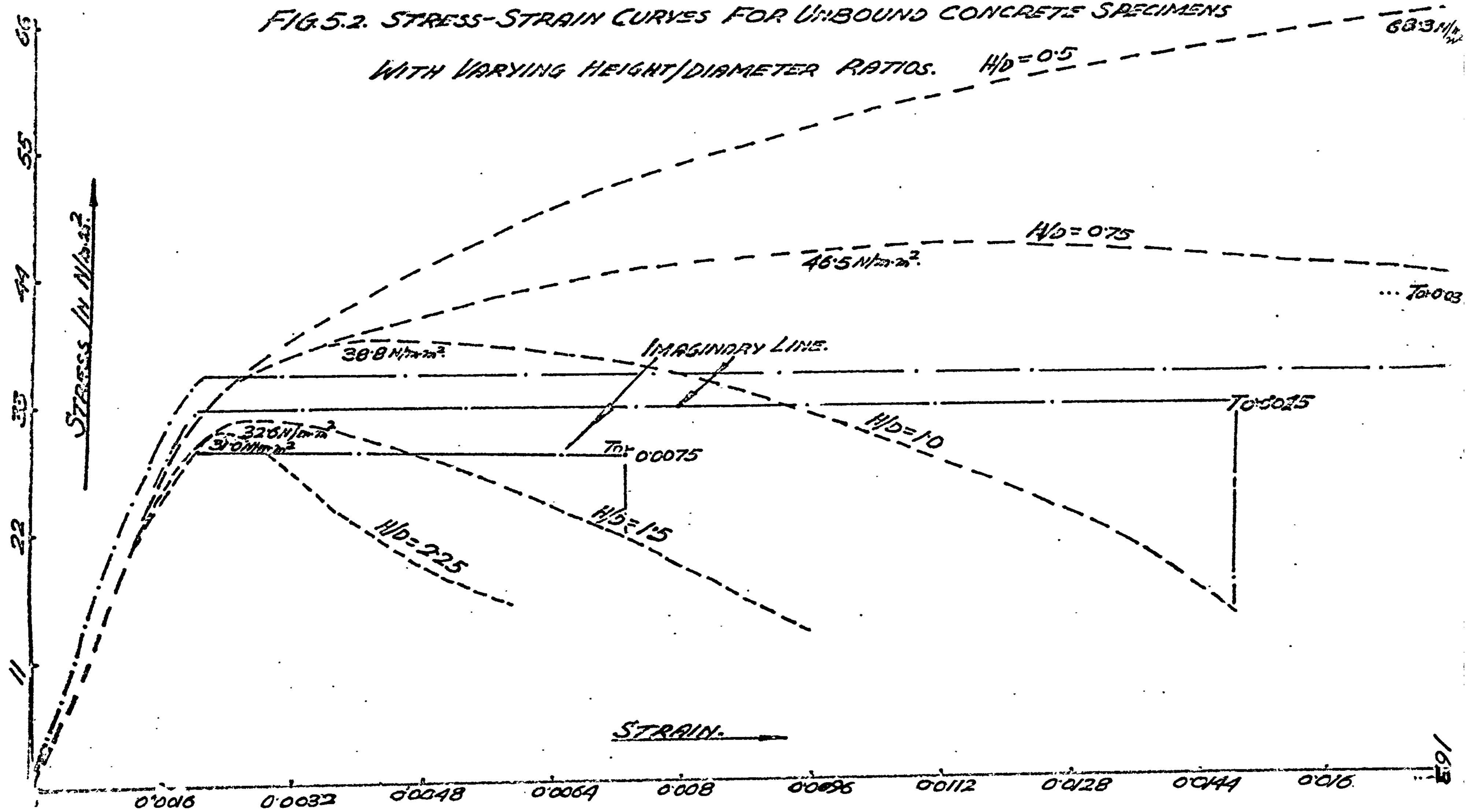
When loading is applied at a rate slower than the experimental loading, the value of $\theta_{u\ test}$ would be larger than is suggested by the present experimental study, and hence the equation suggested by the author would be safer.

Fig. 5.1.



RESTRAINT OF CONCRETE IN PLASTIC HINGES.

FIG 5.2. STRESS-STRAIN CURVES FOR UNBOUND CONCRETE SPECIMENS WITH VARYING HEIGHT/DIAMETER RATIOS.



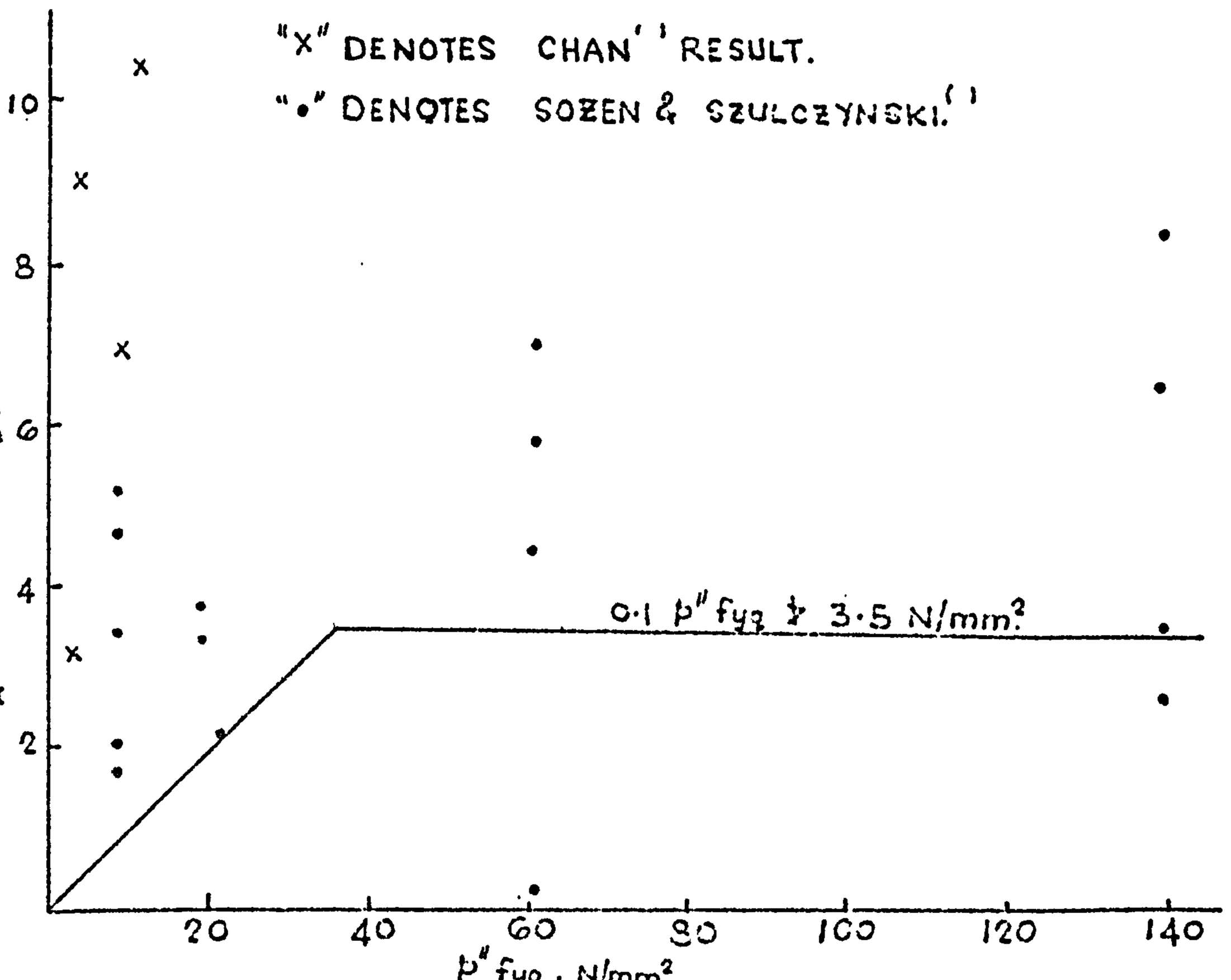
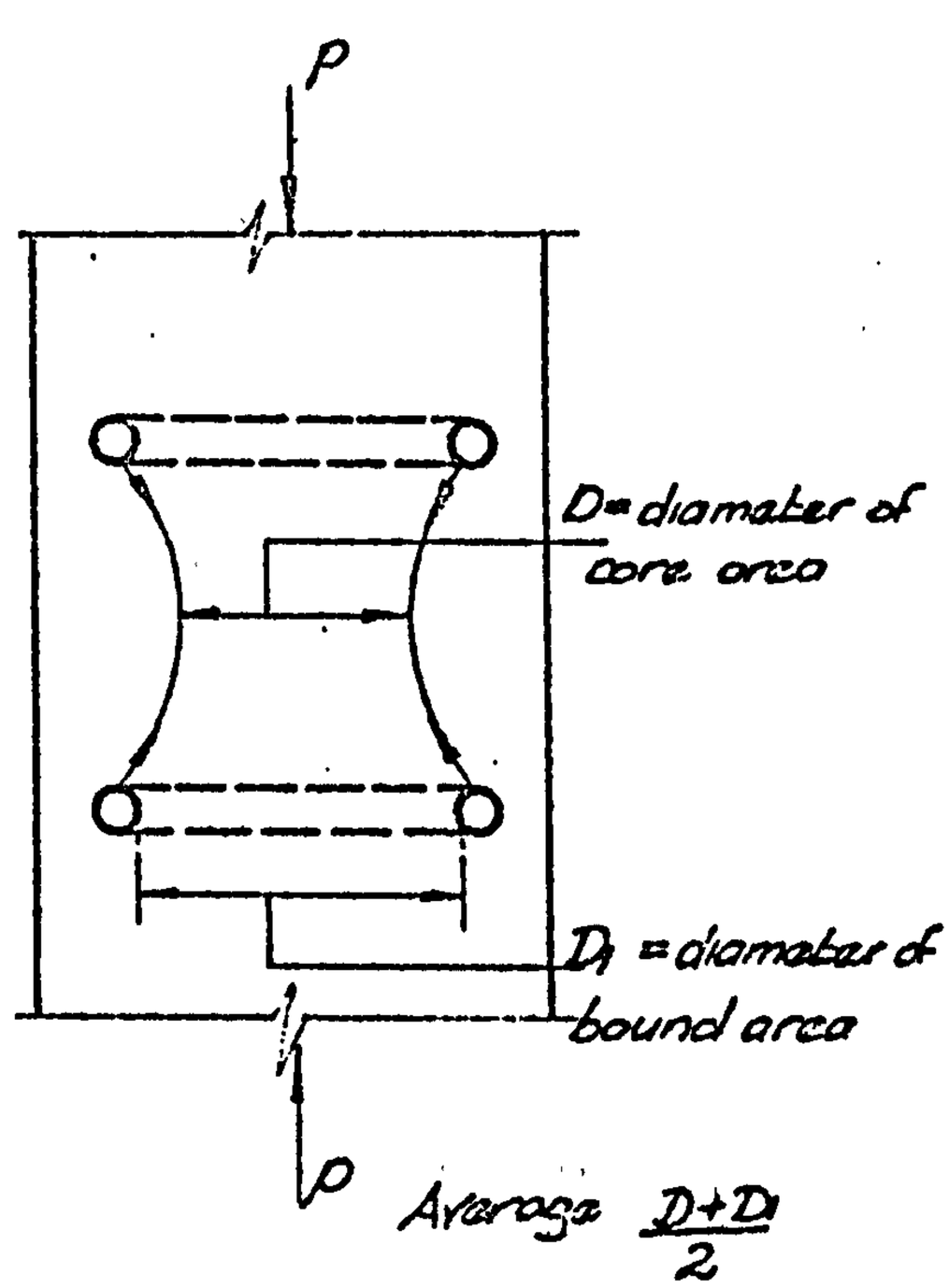


FIG. 5.3 EFFECT OF BINDING



BINDING ACTION OF TRANSVERSE REINFORCEMENT

Fig. 5.4.

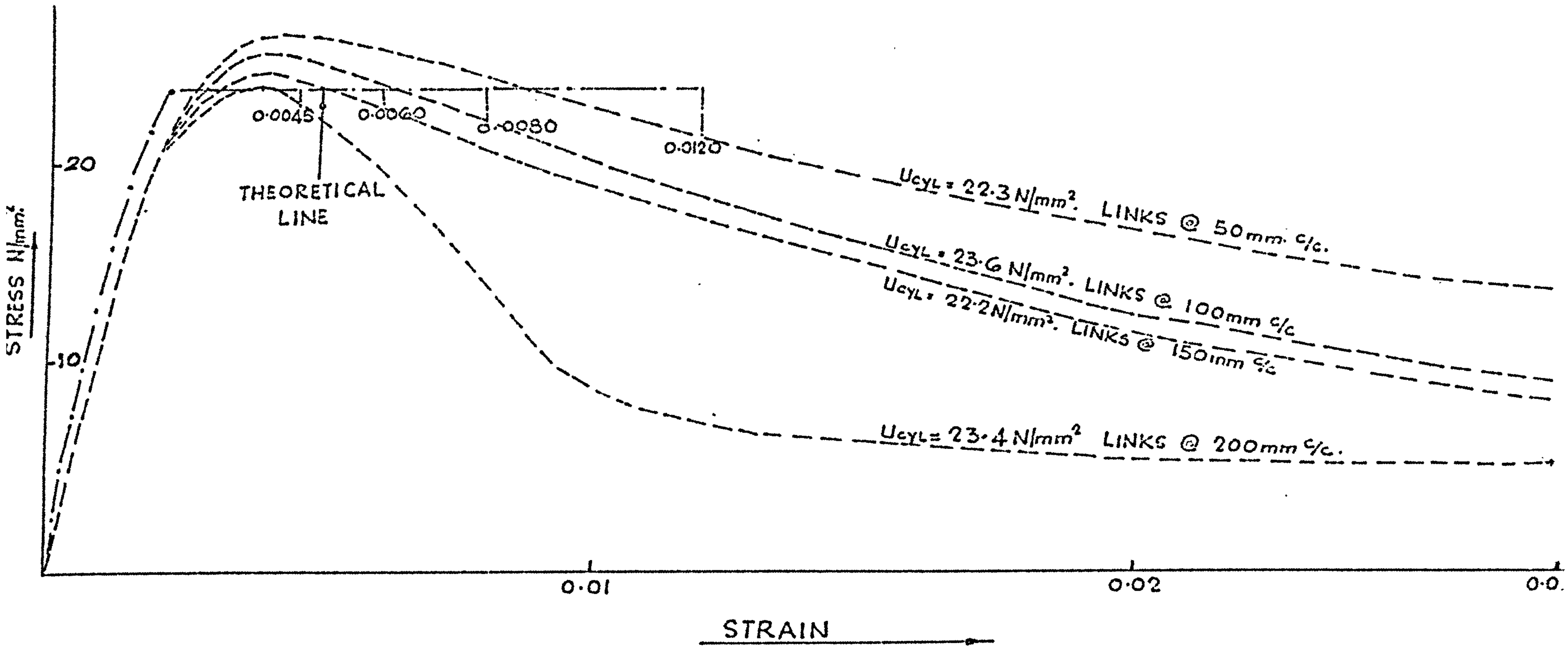


FIG. 5.5 STRESS - STRAIN CURVES FOR BOUND CONCRETE AFTER ROY & SOZEN.

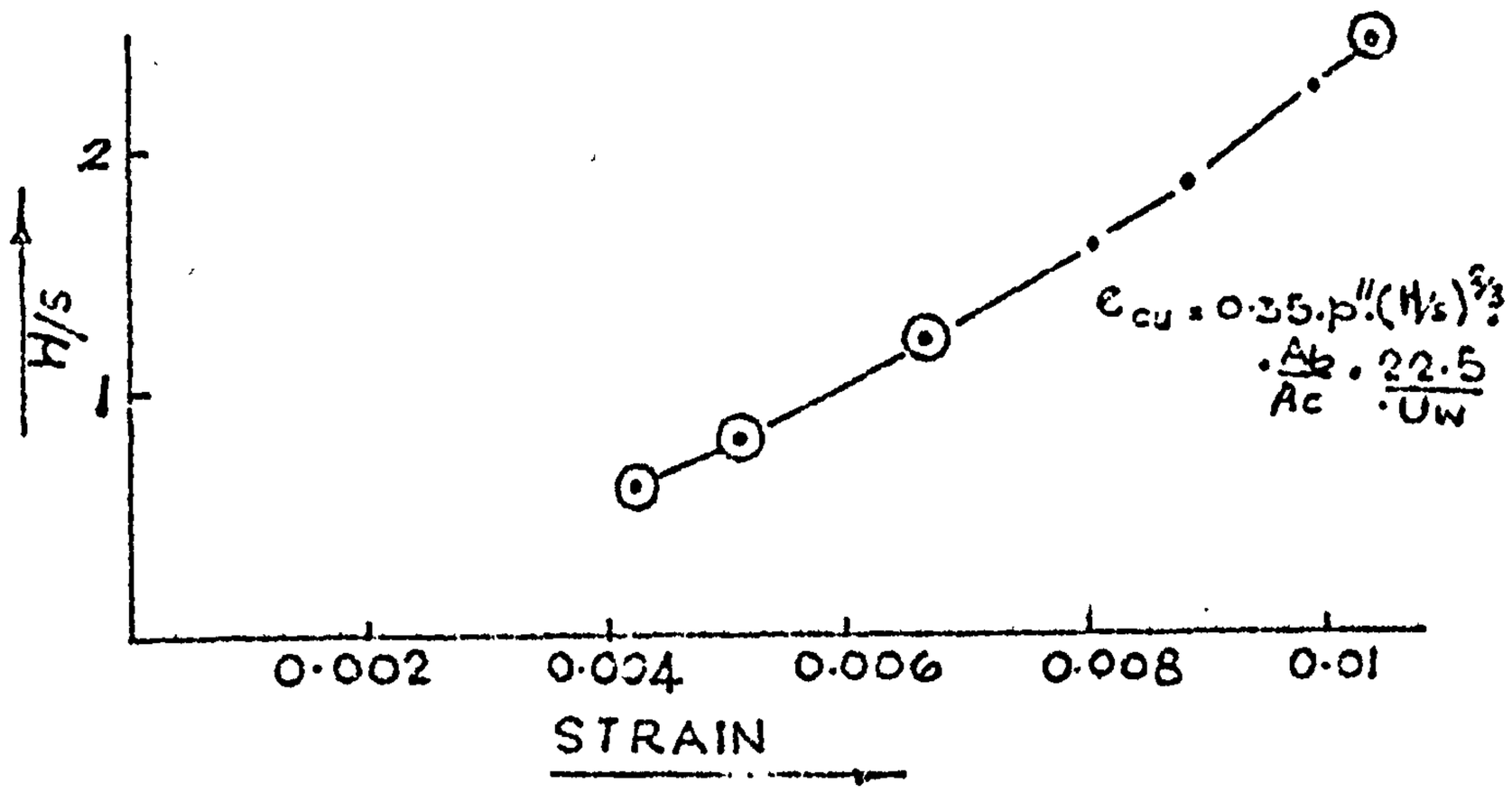


FIG. 5·6. LIMITING STRAIN e_{cu} FOR BOUND CONCRETE

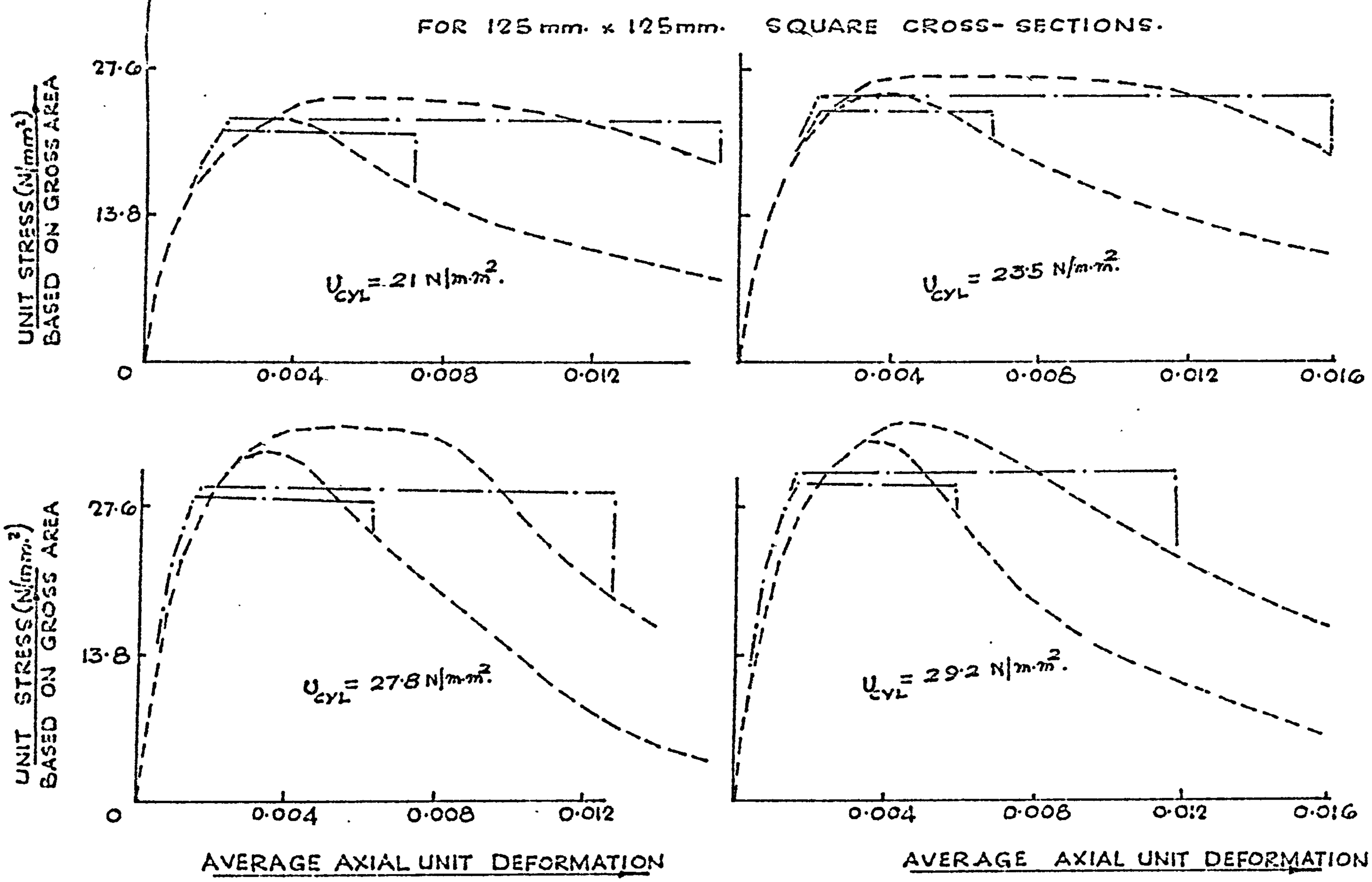


FIG. 5·7. COMPARISON OF THEORETICAL STRESS-STRAIN CURVES FOR BOUND CONCRETE WITH TEST RESULTS BY SZULCZYNSKI & SOZEN.

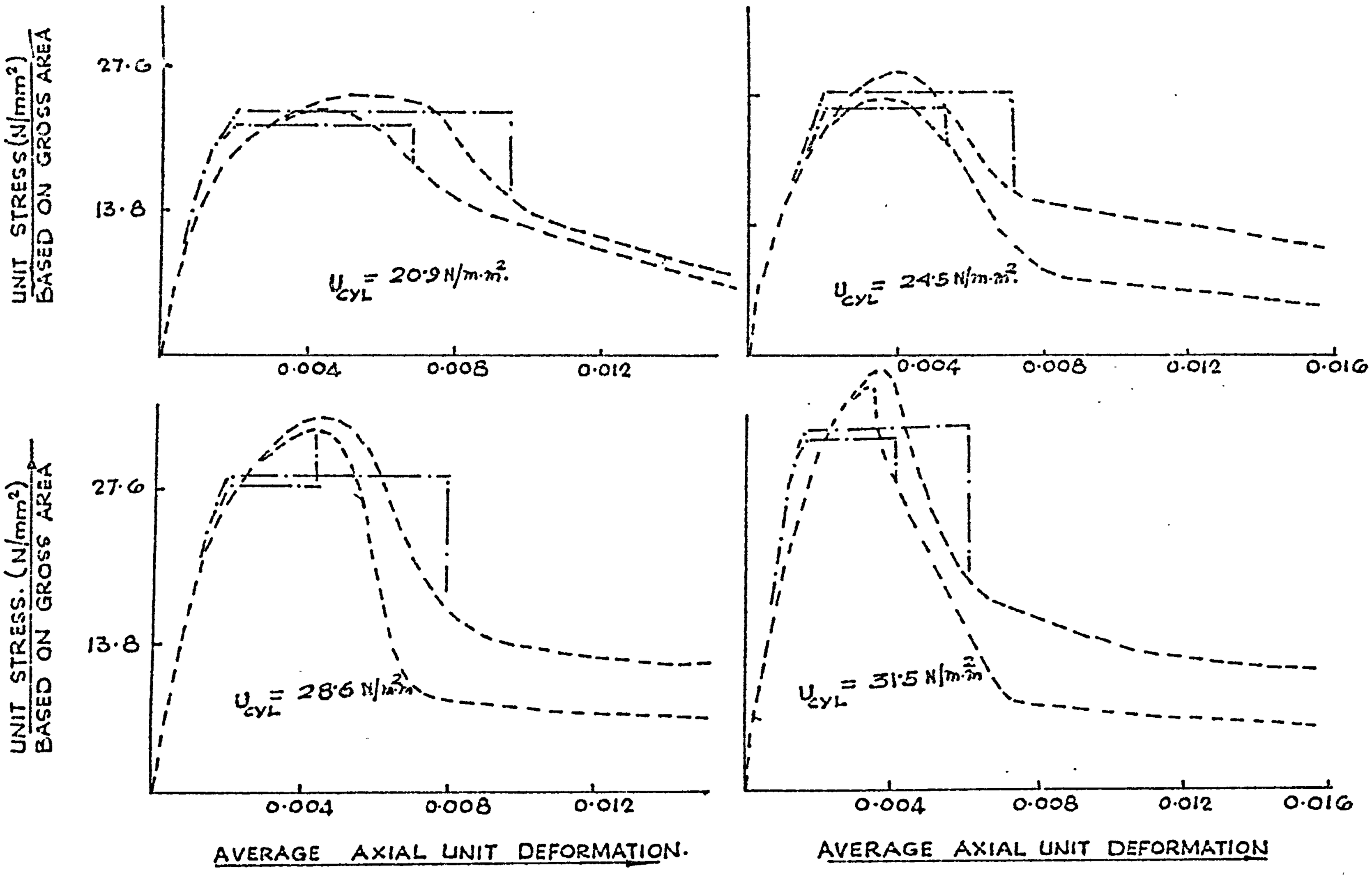


FIG. 5.8 COMPARISON OF THEORETICAL STRESS-STRAIN CURVES FOR BOUND CONCRETE WITH TEST RESULTS BY SZULCZYNSKI & SOZEN.

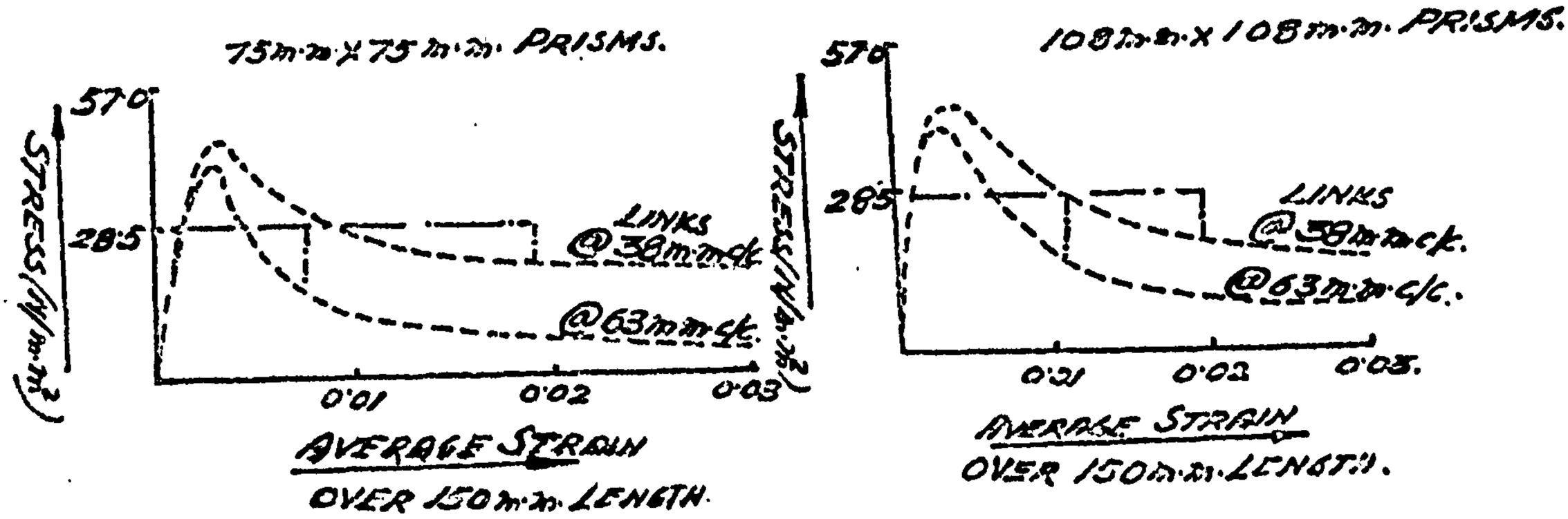


FIG 5.9. COMPARISON OF THEORETICAL STRESS-STRAIN CURVES FOR BOUND CONCRETE WITH TEST RESULTS BY VITELMO, VERTERO & FELIPA.

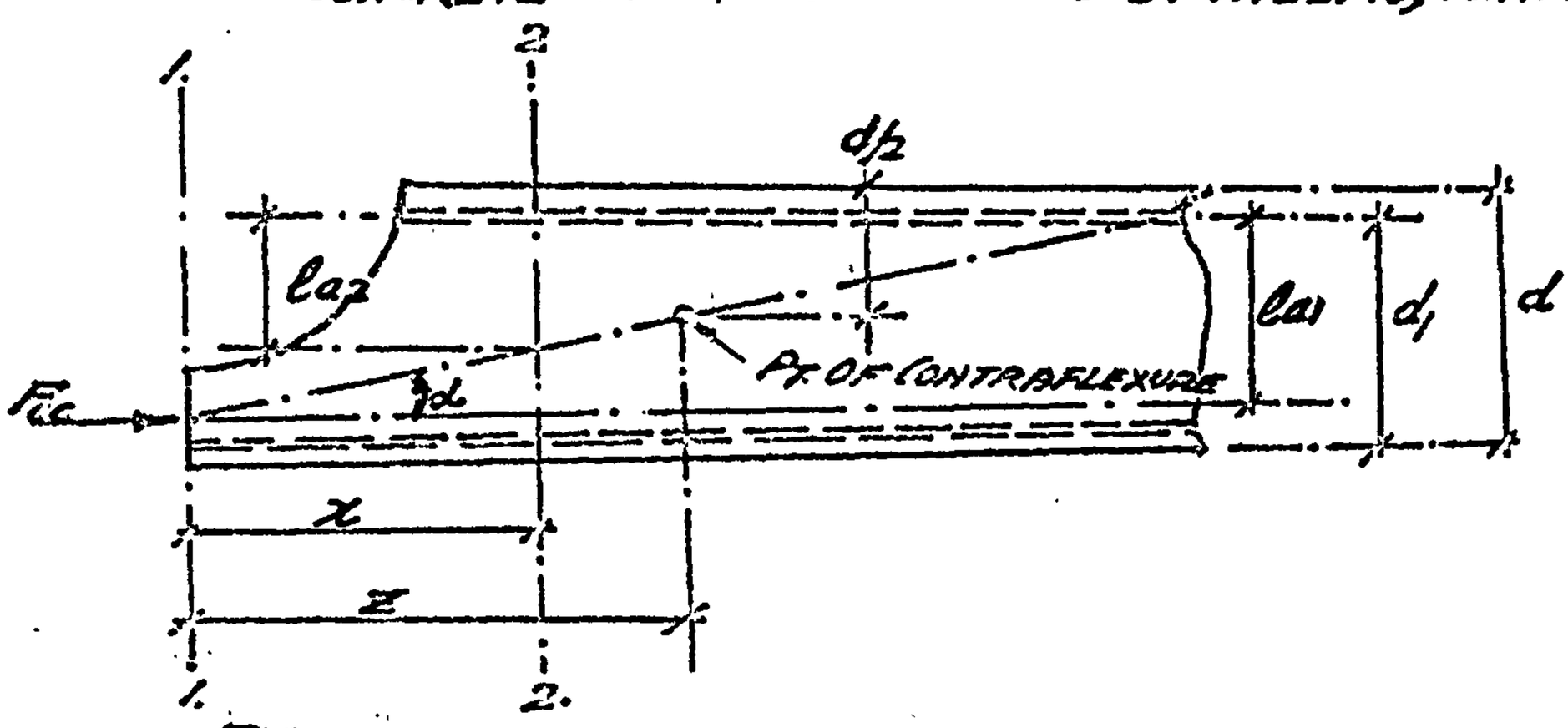
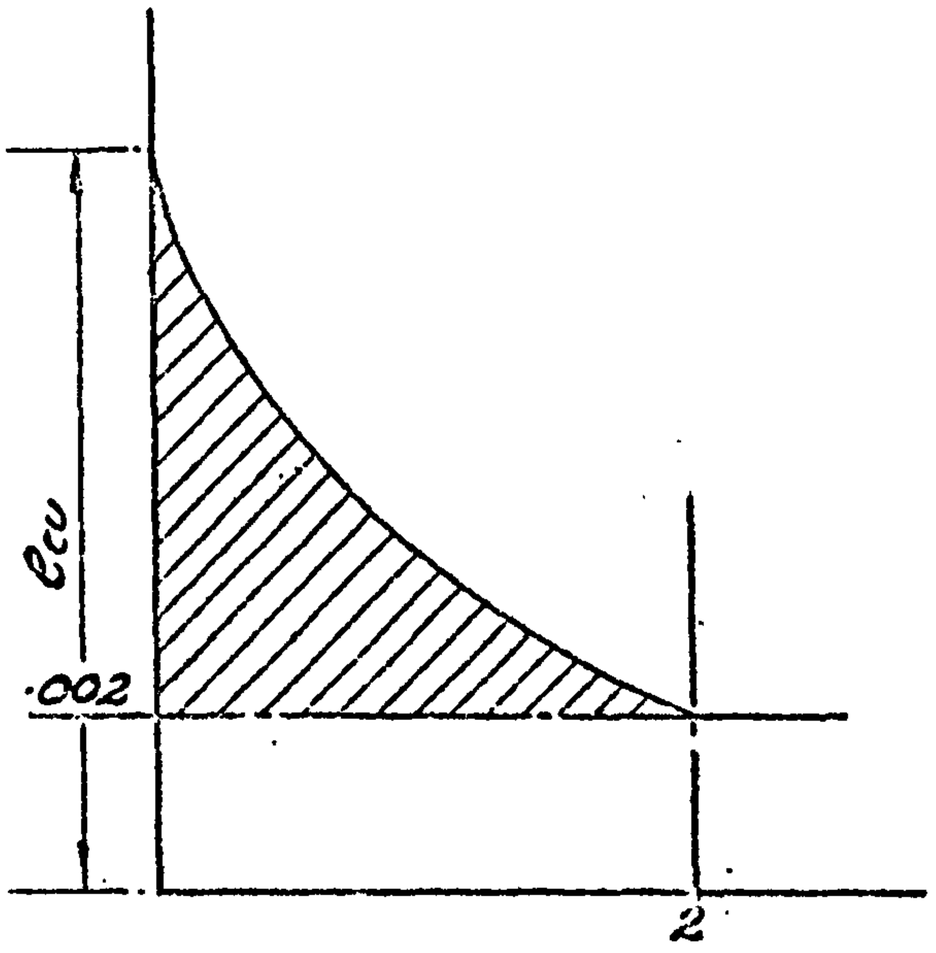
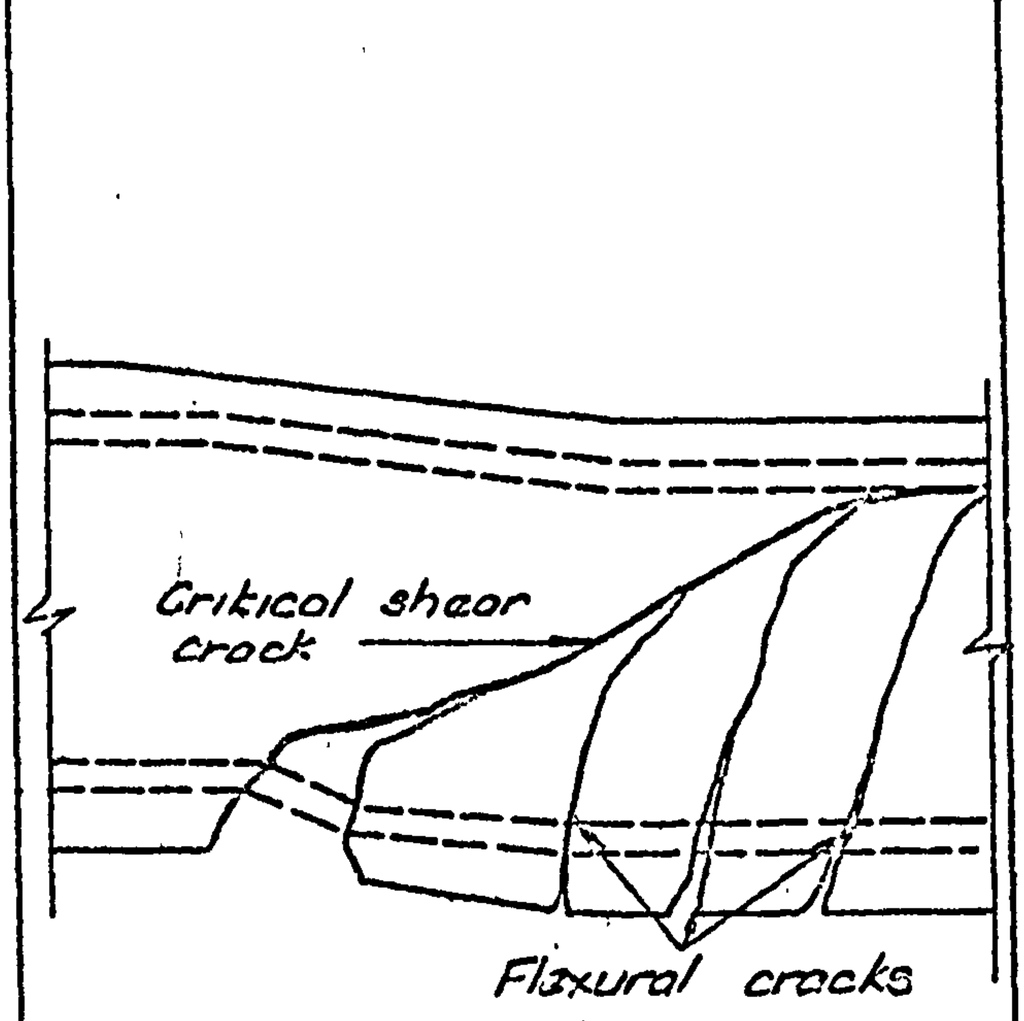


FIG. 5.10. SUPPORT SECTION OF A CONTINUOUS BEAM.



EXTREME FIBRE STRAIN DISTRIBUTION ALONG A PLASTIC LENGTH

Fig. 5·11



FORMATION OF CRITICAL SHEAR CRACK.

Fig. 5·12.

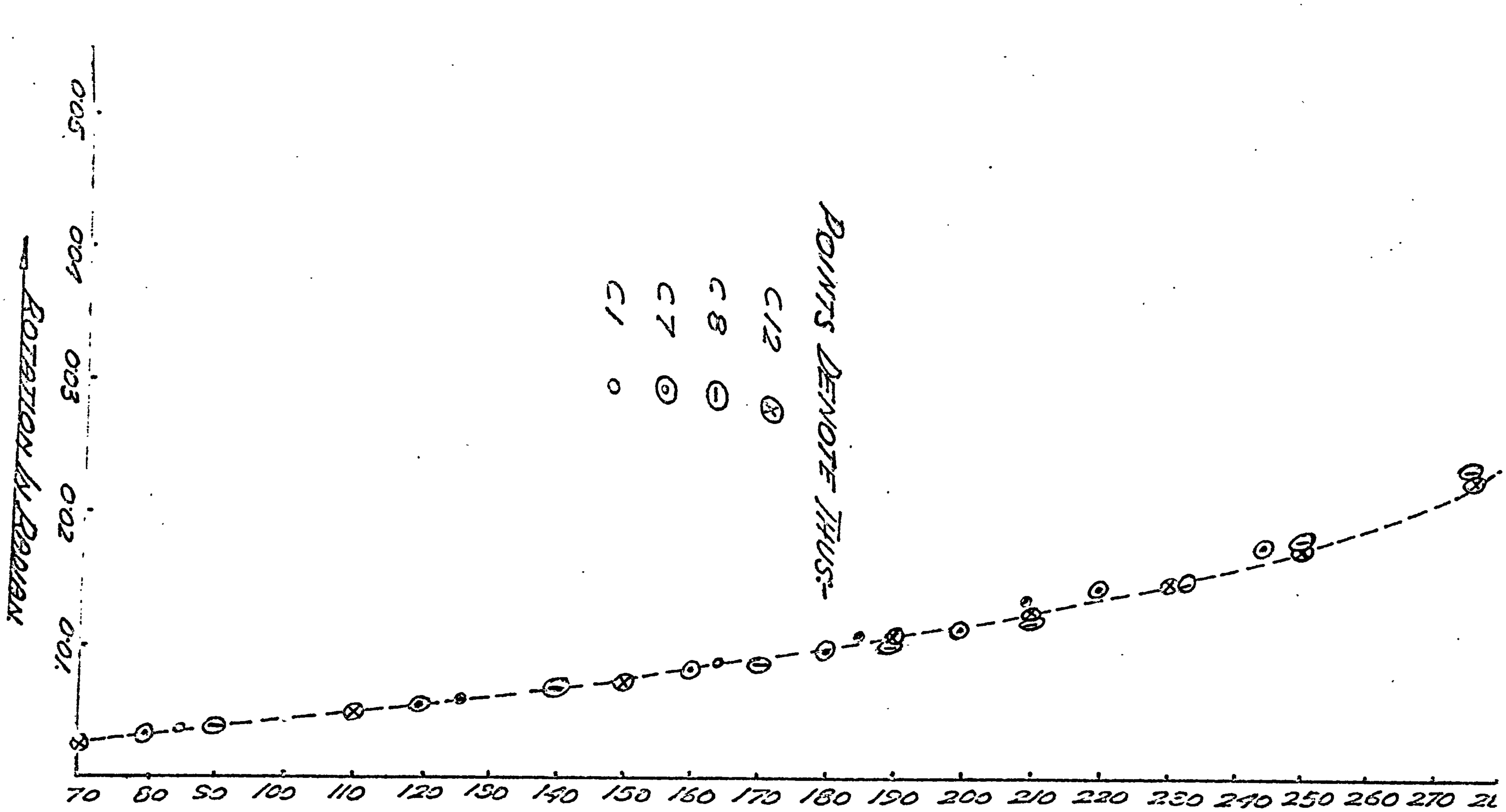


FIG. 5.13. LOAD-ROTATION DIAGRAM FOR MID-SUPPORT,

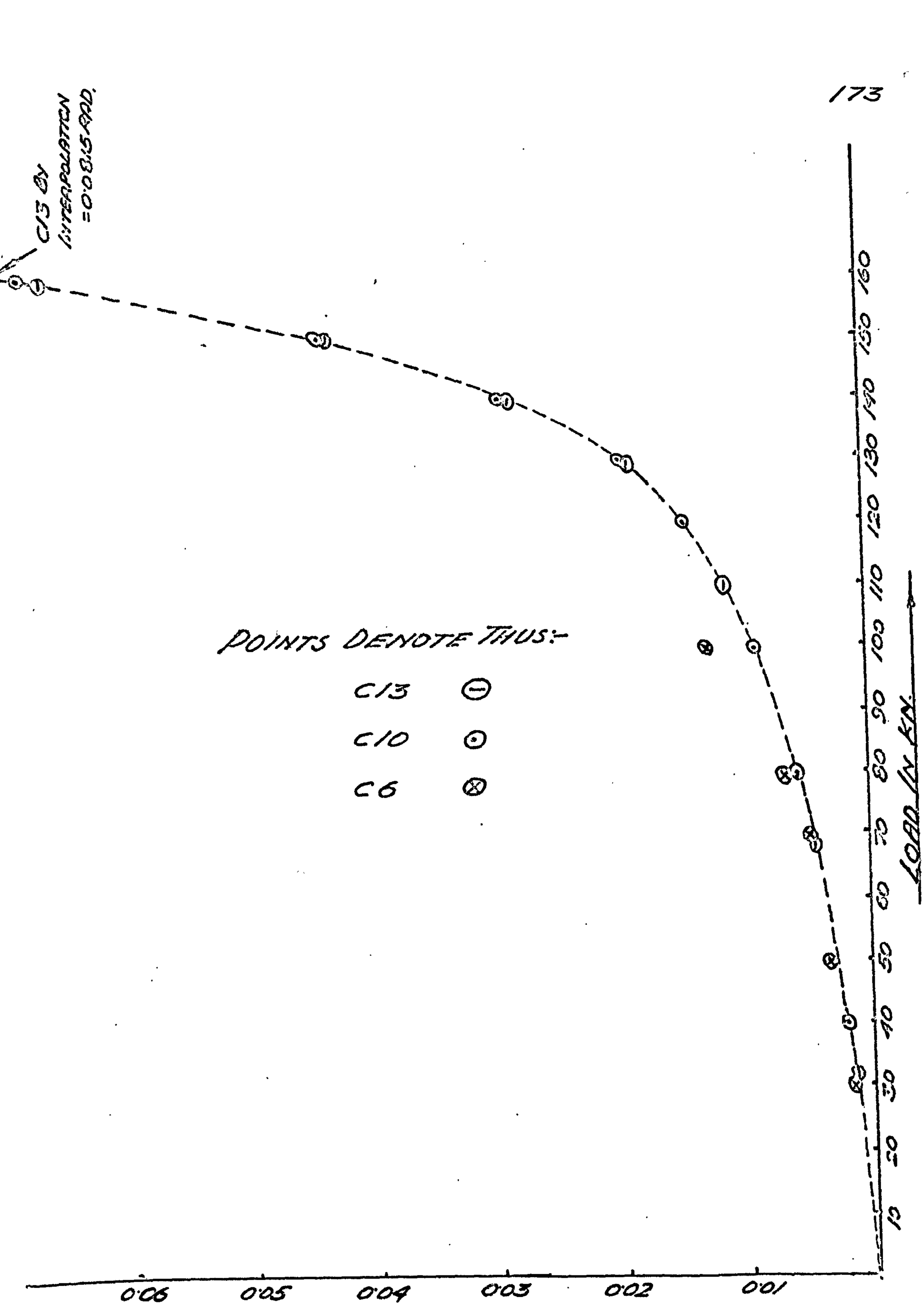
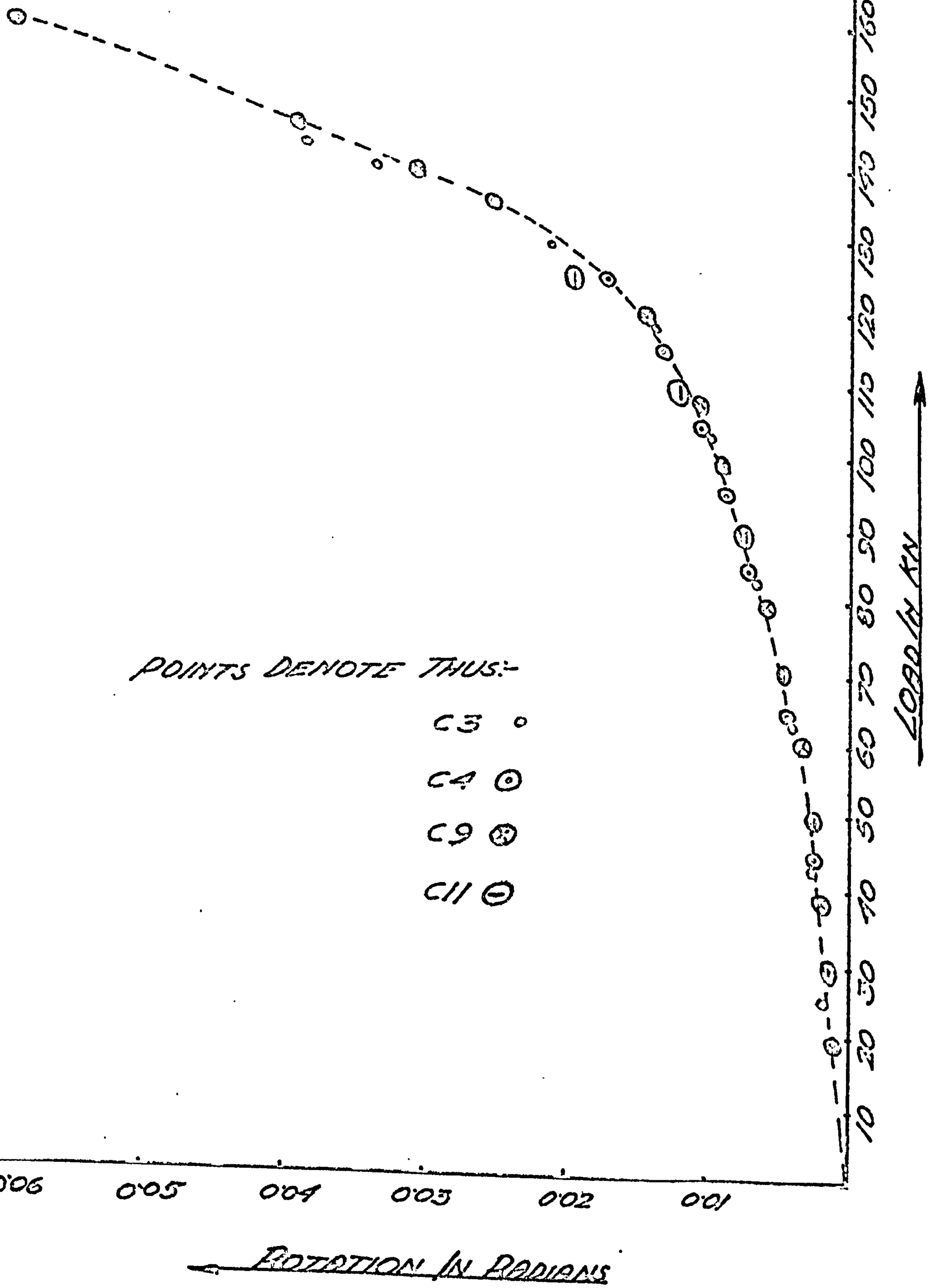


FIG. 5.14. LOAD-ROTATION DIAGRAM FOR MID-SUPPORT FOR CONTINUOUS BEAM.

FIG. 5.15. LOAD-ROTATION DIAGRAM.

FOR MID-SUPPORT,

FOR CONTINUOUS BEAM.



POINTS DENOTE THUS:-

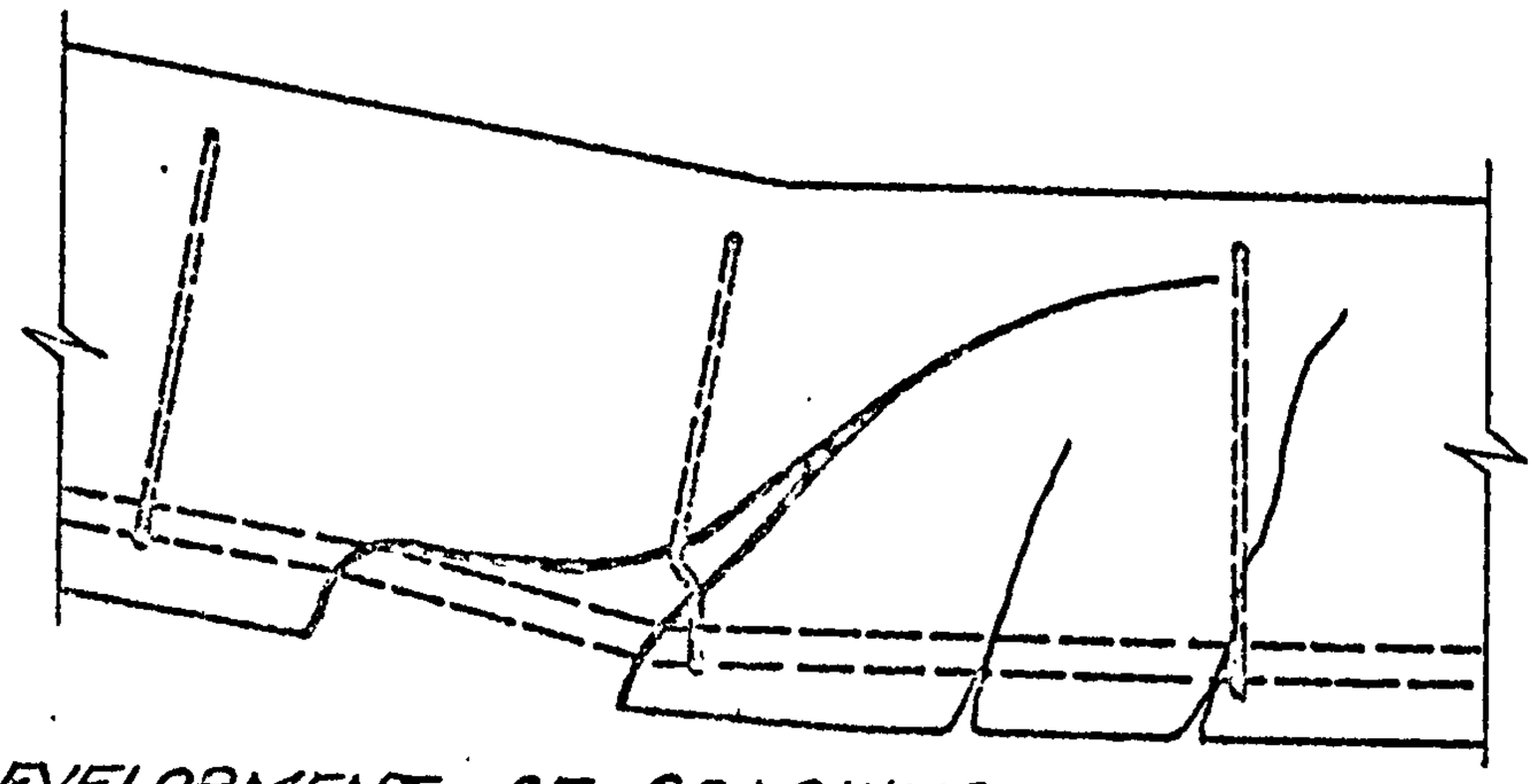
C3 ○

C4 ⊙

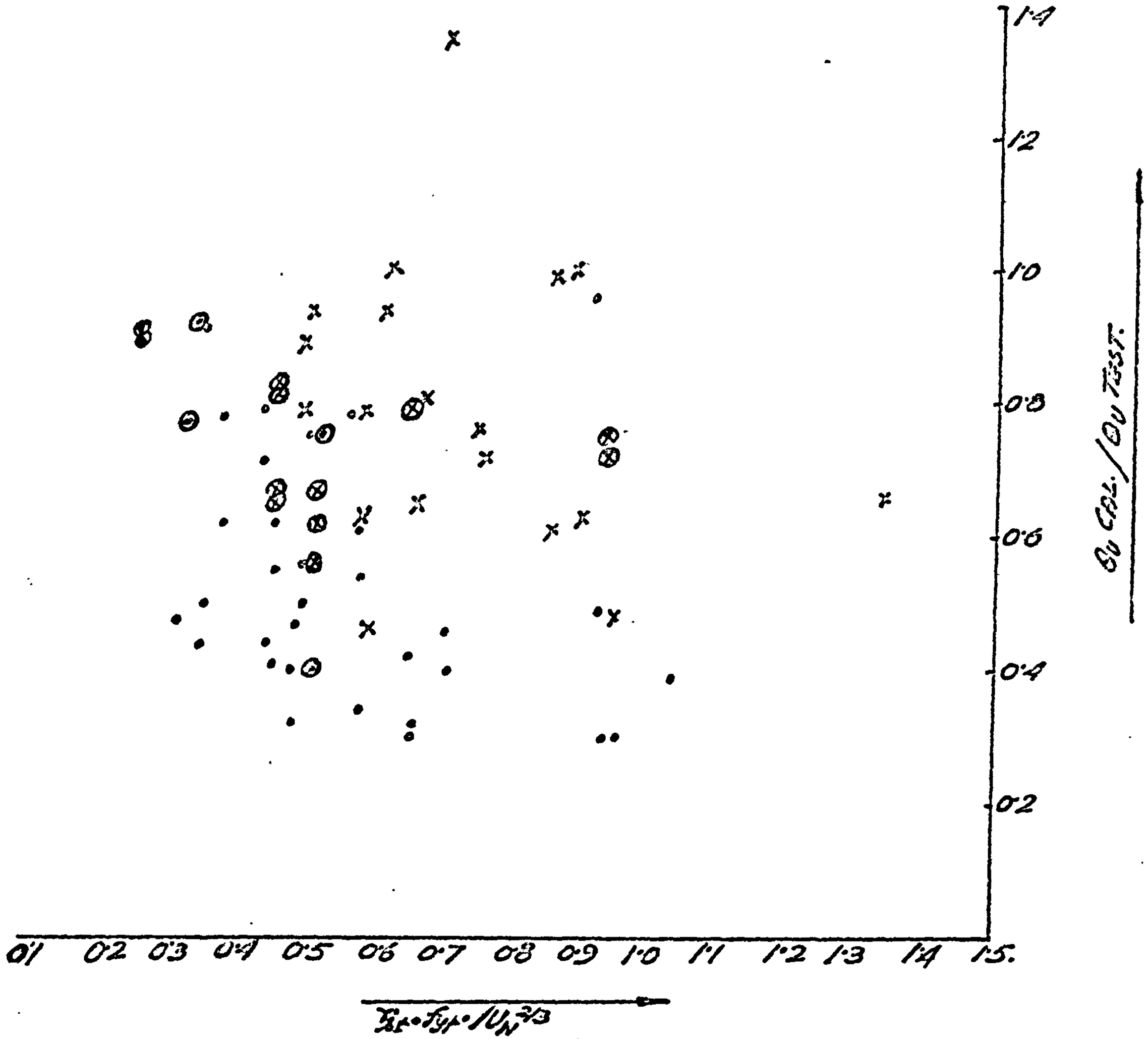
C9 ⊗

C11 ⊖

Fig. 5.16



DEVELOPMENT OF CRACKING CAUSING SHEAR ROTATION.



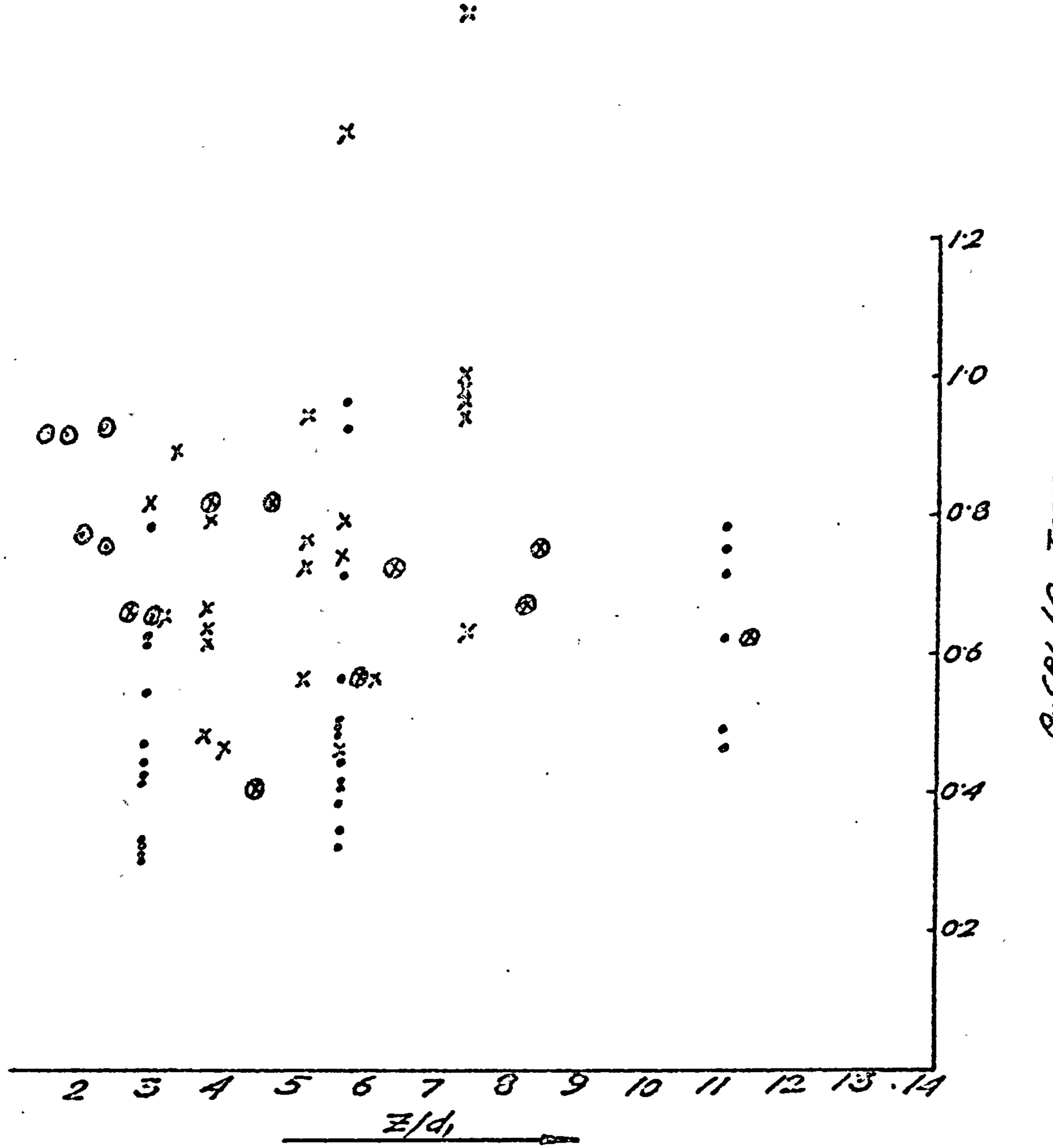
"•" DENOTES MATTOCK'S TEST RESULT.

"⊙" DENOTES AUTHOR'S TEST RESULT.

"×" DENOTES CORLEY'S TEST RESULT.

⊗ DENOTES CRANSTON'S TEST RESULT.

FIG. 5.17. θu CAL./θu TEST V/S γu·fsy/UN^2/3



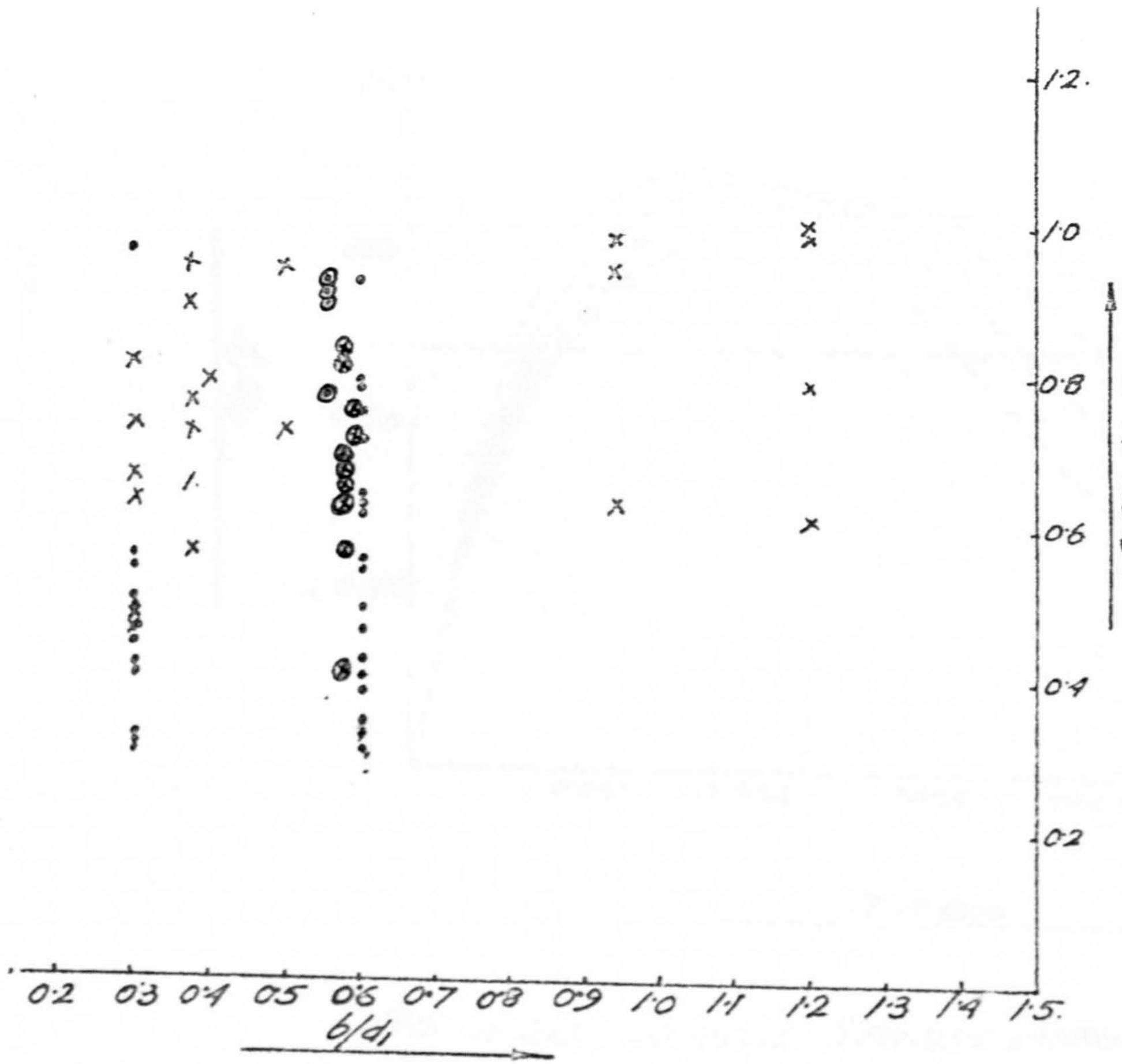
"•" DENOTES MATTOCK'S TEST RESULT.

"⊙" DENOTES AUTHOR'S TEST RESULT.

"x" DENOTES CORLEY'S TEST RESULT.

"⊗" DENOTES CRANSTON'S TEST RESULT.

FIG. 5.18. Z/d1 Vs Qu CAL/Qu TEST.



"•" DENOTES MATTOCK'S TEST RESULT.

"⊙" DENOTES AUTHOR'S TEST RESULT.

"×" DENOTES CORLEY'S TEST RESULT.

"⊗" DENOTES CRANSTON'S TEST RESULT.

FIG. 5.19. b/d_1 VS $\theta_{u\,CAL}/\theta_{u\,TEST}$.

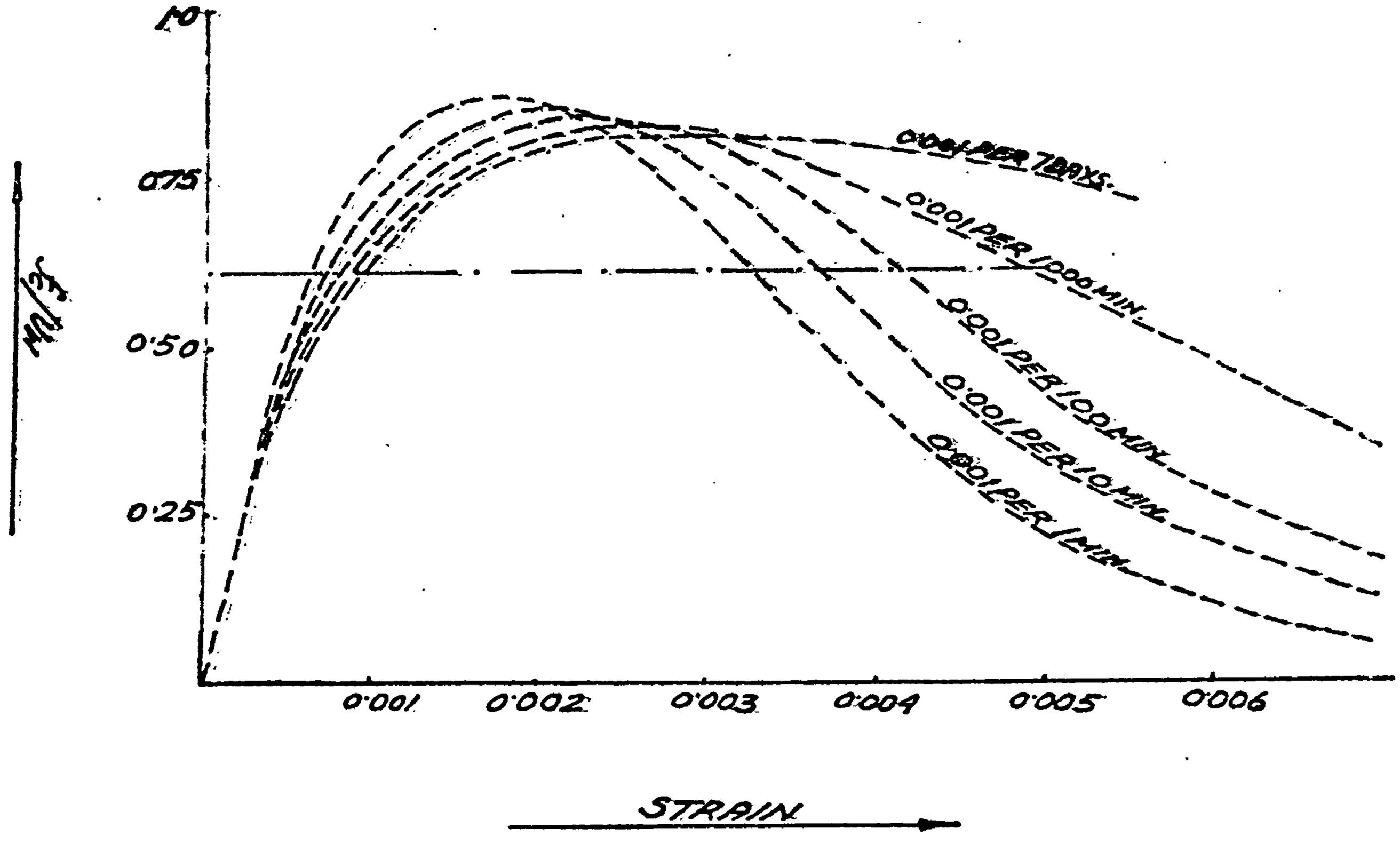


FIG. 5.20. STRESS-STRAIN DIAGRAM FOR DIFFERENT RATE OF LOADING.

TABLE NO. 5.1.1

EFFECT OF RESTRAINT ON CYLINDER STRENGTH

H/D	KESLER	MITRA	THAULOW	$(2D/H)^{1/3}$
2.25	1.0	1.0	1.0	1.0
1.5	1.06	1.05	1.15	1.1
1.0	1.15	1.25	1.2	1.26
0.75	1.25	1.5	1.4	1.4
0.5	1.47	2.2	1.75	2.0

TABLE NO. 5.1.2

EFFECT OF RESTRAINT ON DUCTILITY OF COMPRESSED CYLINDERS.

H/D	e_{cu} from fig. 5.2	Eqn. 5.4
1.5	0.0075	0.00625
1.0	0.015	0.014
0.75	0.03	0.025

Beam No.	U_w in N/mm^2	b in mm	d_1 in mm	z in mm	A_{st} in mm^2	A_{sq} in mm^2	f_{yt} in N/mm^2	s in mm	f_{yq} in N/mm^2	$M_{ult.test}$ in KNm.	$\theta_{u.test}$ in Radians	$\frac{M_u cal}{M_u test}$ New method	Corley (34)	I.C.E.(48)	$\frac{\theta_u cal}{\theta_u test}$ New method	Corley (34)	I.C.E. (48)	REMARK
c3	51.0	152	274	-	226	63.2	652	152	395	-	0.031	-	-	-	0.32*	-	-	Shear failure.
c4	40.4	152	274	482	226	63.2	652	114	395	45.2	0.053	0.86	0.85	0.82	0.77	0.66	0.23	Flexure failure.
c9	38.8	152	274	554	226	63.2	652	133	395	45.2	0.032	0.86	0.84	0.82	0.92	0.95	0.45	Flexure & shear failure
c11	52.5	152	274	-	226	48.5	652	152	279	-	0.011	-	-	-	0.48*	-	-	Shear failure
c1	39.4	152	273	-	602	63.2	645	101	395	-	0.0035	-	-	-	0.64*	-	-	Shear failure
c7	39.3	152	273	-	602	99.0	645	89	303	-	0.0060	-	-	-	1.00*	-	-	Shear failure
c8	41.8	152	273	-	602	143	645	114	304	-	0.013	-	-	-	0.56*	-	-	Shear failure
c12	40.4	152	273	592	602	143	645	89	304	101.7	0.016	0.92	0.84	0.80	0.75	0.93	0.32	Flexure & shear failure
c6	46.5	152	274	-	226	48.5	652	152	279	-	0.075	-	-	-	1.00*	-	-	Shear failure
c10	54.6	152	274	420	226	63.2	652	101	395	48.5	0.060	0.81	0.79	0.78	0.91	0.78	0.25	Flexure & shear failure
c13	57.7	152	274	343	226	99.0	652	101	303	45.2	0.075	0.87	0.79	0.78	0.91	0.88	0.19	Flexure failure

* Denotes test results which are checked by shearing equation No. 6.11 for $\theta_u$cal value.

TABLE NO. 5.3.1

ANALYSIS OF MITRA'S RESULTS

U_w in N/mm^2	Beam No.	b in mm	d_1 in mm	z in mm	A_{st} in mm^2	A_{sc} in mm^2	A_{sq} in mm^2	f_{yt} in N/mm^2	f_{yc} in N/mm^2	f_{sq} in N/mm^2	S in mm	$M_{ult.test}$ in KN.m	$\theta_{u.test}$ in Radians	$\frac{M_{u.cal.}}{M_{u.test}}$ New method	Corley (35)	I.C.E. (48)	$\frac{\theta_{u.cal.}}{\theta_{u.test}}$ New method	Corley (35)	I.C.E (48)	REMARK
24	1/1	127	220	2500	252	350	35	460	340	340	152	25.9	0.016	0.90	0.89	0.89	0.62	0.40	0.44	Flexural failure
24	1/2	127	220	1800	252	350	35	460	340	340	152	26.5	0.018	0.91	0.87	0.87	0.67	0.40	0.37	Flexural failure
24	1/3	127	220	1300	252	350	35	460	340	340	152	25.7	0.024	0.91	0.90	0.90	0.56	0.36	0.25	Flexural failure
24	1/4	127	220	950	252	350	35	460	340	340	152	27.1	0.040	0.88	0.85	0.85	0.40	0.24	0.13	Flexure & shear (ult.) failure.
30	2/1	127	220	1000	252	350	35	460	340	340	102	26.9	0.018	0.90	0.88	0.88	0.81	0.70	0.36	Flexural failure
30	2/2	127	220	800	252	350	35	460	340	340	102	27.6	0.027	0.89	0.86	0.86	0.81	0.52	0.23	Flexural failure
30	2/3	127	220	650	252	350	35	460	340	340	102	27.1	0.029	0.89	0.87	0.87	0.65	0.56	0.21	Flexural failure
30	2/4	127	220	550	252	350	35	460	340	340	102	27.1	0.033	0.90	0.87	0.87	0.66	0.53	0.17	Flexure & shear failure
35	3/1	127	215	1800	572	350	35	440	340	340	152	47	0.006	1.00	0.95	0.96	0.75	0.57	0.57	Flexure & shear (ult.)
35	3/2	127	215	1340	572	350	35	440	340	340	152	47	0.007	1.00	0.95	0.96	0.72	0.57	0.46	Flexure & shear (ult.)

N.B.:- Strain hardening of longitudinal reinforcement is ignored in Corley's method, since the value is unobtainable from published results.

TABLE NO. 5.3.2

ANALYSIS OF CRANSTON'S RESULTS

Beam No.	U_w in N/mm^2	b in mm	d_1 in mm	z in mm	S in mm	A_{st} in mm^2	A_{sc} in mm^2	A_{sq} in mm^2	f_{yt} in N/mm^2	f_{yc} in N/mm^2	f_{yq} in N/mm^2
K1	34.1	76	254	914	127	400	142	63.2	472	494	328
K2	35.6	76	254	1828	127	400	142	63.2	461	482	315
K3	34.5	76	254	914	63.5	567	142	63.2	480	483	346
K4	37.5	76	254	1828	127	567	142	63.2	465	492	315
K5	32.3	238	254	914	127	800	142	63.2	458	482	331
K51	37.1	238	254	914	127	800	142	142	472	527	531
K6	34.0	238	254	1828	127	800	142	63.2	467	486	326
K7	30.9	238	254	914	127	1134	142	142	467	482	357
K8	33.1	238	254	1828	127	1134	142	63.2	461	480	332
K9	36.8	305	254	914	63.5	998	142	63.2	481	479	333
K10	32.8	305	254	1828	127	998	142	63.2	478	487	336
K11	33.5	305	254	914	63.5	1418	142	142	478	494	362
K12	31.8	305	254	1828	127	1418	142	63.2	480	494	328
M1	39.1	229	610	1825	305	1700	142	142	448	486	486
M2	36.1	229	610	3050	305	1700	142	142	446	486	484
M3	38.4	229	610	1825	153	2320	142	142	438	485	477
M4	37.2	229	610	3050	305	2320	142	142	438	485	489
M5	36.4	305	610	1825	203	2270	142	142	448	490	481
M6	37.6	305	610	3050	305	2270	142	142	443	490	482
M7	36.2	305	610	1825	203	3480	142	142	445	487	480
M8	38.1	305	610	3050	305	3480	142	142	441	487	484
N1	39.9	229	762	2095	254	2710	142	142	429	483	468
N2	39.0	229	762	4190	381	2710	142	142	424	481	454
N3	40.4	229	762	2095	254	3060	142	254	424	483	438
N4	37.1	229	762	4190	381	3060	142	142	421	494	471
N5	34.0	305	762	2095	381	2545	142	254	425	470	440
N6	32.1	305	762	4190	381	2545	142	254	430	473	437
N7	40.9	305	762	2095	229	4080	142	254	424	483	433
N8	36.8	305	762	4190	381	4080	142	254	427	481	436

TABLE NO. 5.3.3

ANALYSIS OF CORLEY'S RESULTS

(contd. over)

Beam No.	M_{ult} test in KN.m	θ_u test in Radians	$M_u$cal/$M_u$test New method	$M_u$cal/$M_u$test Corley (34)	$M_u$cal/$M_u$test I.C.E. (48)	$\theta_u$cal/$\theta_u$test New method	$\theta_u$cal/$\theta_u$test Corley (34)	$\theta_u$cal/$\theta_u$test I.C.E.(48)	Remark
K1	47.0	0.0119	0.93	1.0	0.91	0.48	0.60	0.33	
K2	48.2	0.0099	0.88	0.96	0.87	0.63	0.62	0.50	
K3	64.7	0.0077	0.93	0.90	0.88	0.66	0.96	0.30	
K4	59.6	0.0023	0.98	0.96	0.94	1.52	1.68	1.30	
K5	95.2	0.0063	0.91	1.01	0.87	2.32	1.51	0.74	Shear failure
K51	116.5	0.0299	0.77	0.92	0.74	0.63	0.44	0.16	
K6	105.3	0.0114	0.83	0.90	0.82	0.94	0.63	0.56	
K7	130.0	0.0090	0.93	0.91	0.86	1.27	0.79	0.32	Shear failure
K8	138.2	0.0062	0.86	0.85	0.83	0.98	0.73	0.63	
K9	133.0	0.0145	0.87	1.01	0.83	0.79	0.89	0.36	
K10	129.0	0.0156	0.89	0.93	0.86	1.00	0.51	0.35	
K11	188.5	0.0259	0.82	0.86	0.77	0.61	0.44	0.13	
K12	167.3	0.0096	0.93	0.90	0.88	1.00	0.52	0.41	
M1	464.0	0.0101	0.95	1.08	0.92	0.89	0.82	0.54	
M2	471.0	0.0109	0.94	1.00	0.92	0.56	0.50	0.55	
M3	596.0	0.0098	1.01	1.02	0.92	0.65	0.45	0.41	
M4	585.0	0.0060	0.975	1.00	0.95	0.76	0.78	0.75	
M5	613.0	0.0090	0.96	1.08	0.93	1.18	1.03	0.58	Shear failure
M6	609.0	0.0090	0.98	1.04	0.95	0.74	0.80	0.60	
M7	790.0	0.0021	1.05	1.09	1.01	3.03	2.70	1.45	Shear failure
M8	843.0	0.0075	1.01	1.02	0.99	0.72	0.60	0.47	
N1	777.0	0.0047	1.05	1.19	1.03	1.36	1.35	0.82	Shear failure
N2	795.0	0.0091	1.04	1.05	1.03	0.46	0.55	0.50	
N3	881.0	0.0071	1.02	1.11	1.0	0.81	0.80	0.49	
N4	928.0	0.0048	0.98	1.00	0.96	0.73	0.79	0.84	
N5	752.0	0.0021	1.04	1.24	1.00	4.96	4.18	2.46	Shear failure
N6	818.0	0.0090	1.00	1.06	0.96	0.79	0.69	0.66	
N7	1210.0	0.0046	1.02	1.11	0.99	1.47	1.38	0.74	Shear failure
N8	1200.0	0.0030	1.01	1.03	1.00	1.35	1.40	1.30	

TABLE NO. 5.3.3

ANALYSIS OF CORLEY'S RESULTS (CONTD.)

Beam No.	U_w in N/mm^2	b in mm	d_1 in mm	z in mm	S in mm	A_{st} in mm^2	A_{sc} in mm^2	A_{sq} in mm^2	f_{yt} in N/mm^2	f_{yc} in N/mm^2	f_{yq} in N/mm^2
A1	47.7	152	254	700	127	567	142	142	315	340	340
A2	52.8	152	254	1400	127	567	142	63.2	318	340	379
A3	51.1	152	254	2800	127	567	142	63.2	337	340	384
A4	53.5	152	254	700	63	1 34	142	142	316	344	344
A5	49.5	152	254	1400	127	1134	142	142	315	333	333
A6	51.4	152	254	2800	127	1134	142	63.2	328	333	386
B1	53.6	152	508	1400	127	1 34	142	142	329	340	340
B2	52.3	152	508	2800	254	1 34	142	142	322	336	336
B3	53.5	152	508	1400	63	2268	142	142	322	355	355
B4	53.4	152	508	2800	127	2268	142	142	323	337	337
C1	34.3	152	254	700	127	567	142	142	330	342	342
C2	32.5	152	254	1400	127	567	142	63.2	330	342	440
C3	32.0	152	254	2800	127	567	142	63.2	332	342	396
C4	32.4	152	254	700	63	1134	142	142	327	342	342
C5	29.2	152	254	1400	127	1134	142	142	330	336	336
C6	34.2	152	254	2800	127	1134	142	63.2	329	334	427
D1	33.3	152	508	1400	127	1134	142	142	329	345	345
D2	32.0	152	508	2800	254	1134	142	142	316	334	334
D3	32.5	152	508	1400	63	2268	142	142	320	341	341
D4	33.6	152	508	2800	127	2268	142	142	322	319	319
E1	34.8	152	254	700	127	567	142	142	405	505	479
E2	35.4	152	254	1400	127	567	142	142	414	501	478
E3	37.2	152	254	2800	127	567	142	142	412	505	497
F1	51.5	152	254	700	127	567	142	142	405	505	471
F2	51.7	152	254	1400	127	567	142	142	415	471	481
F3	53.6	152	254	2800	127	567	142	142	415	464	500
G1	34.2	152	508	1400	127	850	142	142	414	507	480
G2	35.4	152	508	2800	127	850	142	142	413	492	492
G3	35.9	152	508	1400	127	1134	142	142	415	470	477
G4	34.0	152	508	2800	127	1134	142	142	415	504	504
G5	34.2	152	508	2800	127	567	142	142	417	507	507

TABLE NO. 5.3.4

ANALYSIS OF MATTOCK'S RESULTS

(contd. over)

Beam No.	M_{ult} test in MN.m	θ_u test in Radians	M_u cal/M_u test New method	M_u cal/M_u test Corley (34)	M_u cal/M_u test I.C.E. (48)	θ_u cal/θ_u test New method	θ_u cal/θ_u test Corley (34)	θ_u cal/θ_u test I.C.E (48)	Remark
A1	67.2	0.0360	0.67	0.93	0.65	0.78	0.48	0.16	-
A2	61.4	0.0205	0.73	0.95	0.71	0.92	0.57	0.33	-
A3	62.0	0.0168	0.79	0.90	0.77	0.62	0.53	0.44	-
A4	111.5	0.0305	0.76	0.89	0.75	0.42	0.44	0.07	-
A5	96.5	0.0207	0.89	0.89	0.88	0.40	0.41	0.14	-
A6	88.0	0.0118	1.00	0.96	1.00	0.46	0.52	0.27	-
B1	247.0	0.02777	0.75	0.93	0.70	0.44	0.47	0.38	-
B2	213.0	0.0152	0.85	0.98	0.80	0.50	0.66	0.36	-
B3	390.0	0.0218	0.87	0.93	0.85	0.30	0.47	0.10	-
B4	324.0	0.0120	1.04	1.04	1.04	0.32	0.73	0.22	-
C1	63.4	0.0718	0.72	0.88	0.70	0.32	0.22	0.07	-
C2	57.4	0.0258	0.80	0.89	0.78	0.50	0.45	0.22	-
C3	54.2	0.0187	0.90	0.90	0.88	0.75	0.51	0.36	-
C4	102.8	0.0297	0.81	0.79	0.79	0.30	0.39	0.08	-
C5	85.2	0.0130	0.96	0.89	0.92	0.38	0.42	0.18	-
C6	77.5	0.0125	1.03	1.00	1.02	0.49	0.37	0.24	-
D1	206.0	0.0202	0.86	0.94	0.83	0.47	0.54	0.22	-
D2	199.0	0.0144	0.91	0.91	0.88	0.40	0.55	0.36	-
D3	334.0	0.0147	0.95	0.91	0.92	0.30	0.51	0.13	-
D4	316.0	0.0079	1.01	0.96	0.99	0.96	0.48	0.30	-
E1	71.7	0.0277	0.77	0.96	0.75	0.61	0.56	0.16	-
E2	71.5	0.0279	0.80	0.94	0.78	0.34	0.46	0.18	-
E3	65.3	0.0155	0.91	1.02	0.90	0.78	0.63	0.40	-
F1	80.5	0.0366	0.70	0.98	0.68	0.62	0.54	0.17	-
F2	75.6	0.0258	0.76	0.96	0.75	0.55	0.60	0.26	-
F3	75.6	0.0228	0.81	0.96	0.80	0.71	0.63	0.35	-
G1	224.0	0.0227	0.77	0.95	0.75	0.41	0.65	0.28	-
G2	229.0	0.0243	0.78	0.92	0.76	0.44	0.55	0.31	-
G3	250.0	0.0142	0.90	1.01	0.88	0.54	0.83	0.31	-
G4	249.0	0.0123	0.93	0.99	0.90	0.56	0.86	0.43	-
G5	180.0	0.0342	0.67	0.94	0.66	0.48	1.30	0.39	-

TABLE NO. 5.3.4

ANALYSIS OF MATTOCK'S RESULTS (CONTD.)

TABLE NO. 5.3.5

STATISTICAL ANALYSIS FOR $M_{ULT.}$

TESTS	AVERAGE $\frac{M_{ult.}\ Cal.}{M_{ult.}\ Test}$			STANDARD DEVIATION.			COEFFICIENT OF VARIATION.		
	PROPOSED METHOD	CORLEY	I.C.E. RESEARCH COMMITTEE	PROPOSED METHOD	CORLEY	I.C.E. RESEARCH COMMITTEE	PROPOSED METHOD	CORLEY	I.C.E. RESEAR COMMIT
MITRA	0.86	0.82	0.80	0.039	0.030	0.020	0.045	0.036	0.025
CRANSTON	0.92	0.89	0.89	0.044	0.034	0.039	0.048	0.038	0.043
CORLEY	0.96	0.98	0.90	0.078	0.072	0.073	0.081	0.074	0.081
MATTOCK	0.84	0.94	0.82	0.106	0.050	0.107	0.126	0.053	0.131

TABLE NO. 5.3.6

STATISTICAL ANALYSIS FOR ρ_u

TESTS	AVERAGE $\frac{\theta_u\ Cal.}{\theta_u\ Test}$			STANDARD DEVIATION.			COEFFICIENT OF VARIATION.		
	PROPOSED METHOD	CORLEY	I.C.E. RESEARCH COMMITTEE	PROPOSED METHOD	CORLEY	I.C.E. RESEARCH COMMITTEE	PROPOSED METHOD	CORLEY	I.C.E. RESEAR COMMIT
MITRA	0.85	0.83	0.29	0.084	0.113	0.102	0.099	0.136	0.353
CRANSTON	0.67	0.49	0.32	0.123	0.133	0.143	0.184	0.272	0.448
CORLEY	0.82	0.74	0.55	0.257	0.301	0.298	0.314	0.407	0.542
MATTOCK	0.52	0.56	0.25	0.181	0.229	0.111	0.349	0.409	0.444

CHAPTER 6

SHEAR RESISTANCE

6.1 SHEAR CRACKING

The term "shear cracking" means the stage at which a shear crack effectively transforms the mode of action of the beam. This can be taken to happen when an inclined crack rises above the flexural neutral axis. The first such cracks usually appear either independently in the concrete .. above the flexural cracks or by the inclination of existing flexural cracks. In either case, they tend to extend towards the top and bottom edges of the beams, joining the heads of flexural cracks in the process.

Recent research, reported in Chapter 2, has shown that the following components resist the shear force prior to the shear cracking:-

i) The uncracked zone above the flexural cracks.

ii) Interlocking of aggregate across the flexural cracks.

iii) Dowel action by the main reinforcement.

iv) Forces in any inclined bars.

In the absence of any inclined bar the last becomes zero.

A thorough analytical treatment of the three actions does not seem possible at present, mainly because of the uncertainty concerning the extent of the interlock action and to a lesser degree that of the dowel force. The semi-empirical approaches to these actions by various authors however, are discussed in Chapter 2. From the present knowledge on dowel action, it is estimated that

between 20% and 30% of the total shear force can be carried by the dowel force. The generally small widths of flexural cracks at the shear cracking stage allow the transfer of some force by aggregate interlock. It would therefore be wrong to assume that all the shear force is resisted by the uncracked zone above the flexural crack, although it is a failure of this zone that occurs when the inclined crack forms.

The influences of concrete strength and the ratio of main reinforcement on the uncracked zone above the flexural cracks, on the aggregate interlock and the dowel actions, are explained in the following way. An increase in steel area increases the area of the compressive zone of concrete above the flexural cracks, decreases the width of the flexural cracks and also stiffens the dowel action, lengthening thereby the concrete zone supporting the dowel. The concrete strength on the other hand increases the unit strength and presumably the interlocking force and the unit tensile resistance, but reduces the area of compressive zone and the length of concrete supporting the dowel force.

The regions near the central column of the author's beams invariably sustained shear cracks at a load earlier than the failure load. Oi the various theories, that due to Placas gives reasonable agreement with the Tests results as described in Chapter 3. He states that the shear cracking load Q_{er} is equal to:-

$$Q_{cr} = n\, q_{cr}\, bd_1 \qquad \ldots (6.1)$$

where "q_{cr}" is the average shear stress in the compression zone at the cracking stage, and "n" is the neutral axis factor at the section in which the shear crack enters the uncracked concrete. Since the difference in flexural neutral axis depths is not very significant beyond an early load stage, n is taken approximately equal to n_o, the neutral axis factor, when the concrete reaches its limiting compressive strain prior to yield of main steel.

Assuming a uniform distribution of shear stress in the compressive zone of concrete, Placas postulates that for sections under low direct stress, i.e. direct stress less than 0.5 U_{cyl}, the value of q_{cr} is as follows:-

$$q_{cr} = 1.02\ U_{cyl}^{2/3}$$

Substituting the value of q_{cr} and writing n_o in place of n, equation (6.1) reduces to

$$\frac{Q_{cr}}{bd_1} = n_o\ 1.02\ U_{cyl}^{2/3} \qquad \ldots (6.2)$$

From the fig. 6.1, $\frac{e_{cu}}{e_{st}} = \frac{n_o}{1-n_o}$ or $e_{st} = e_{cu}\left(\frac{1-n_o}{n_o}\right)$

$$F_{cc} = bn_o d_1 K_1 K_3\ U_{cyl} \quad \text{and} \quad F_{st} = A_{st}\ f_{st} = A_{st} \cdot E_{st} \cdot e_{st}$$

$$= r_{st} \cdot E_{st} \cdot e_{cu}\left(\frac{1-n_o}{n_o}\right) bd_1$$

But $F_{cc} = F_{st}$

therefore $bd_1\ n_o \cdot K_1 K_3\ U_{cyl} = r_{st} \cdot E_{st} \cdot e_{cu}\left(\frac{1-n_o}{n_o}\right) bd_1$.

Writing $e_{cu} = 0.0035$,

$$\text{or} \quad \frac{n_o^2}{1-n_o} = \frac{0.0035\ r_{st} \cdot E_{st}}{K_1 K_3 \cdot U_{cyl}} ,$$

the expression $\frac{n_o^2}{1-n_o}$ is approximately equal to $2.83\ n_o^{5/2}$.

Therefore $2.83\, n_o^{2.5} = \dfrac{0.0035\, r_{st}.E_{st}}{K_i K_3\, U_{cyl}}$

or $n_o = \left(\dfrac{0.0035\, r_{st}.E_{st}}{2.83.K_1 K_3\, U_{cyl}} \right)^{0.4}$

Substituting the value of n_o & q_{cr} in equation (6.2), above,

$$\frac{Q_{cr}}{bd_1} = 1.02\, U_{cyl} \cdot \left(\frac{0.0035\, E_{st}.r_{st}}{2.83\, K_1 K_3\, U_{cyl}} \right)^{0.4}$$

Writing $K_1 K_3 = 0.67$

$$\frac{Q_{cr}}{bd_1} \approx 0.25 (100 r_{st}.U_w)^{1/3} \qquad \ldots (6.3)$$

6.2 SHEAR FAILURE

If the shear cracking load is exceeded, shear reinforcement is generally required for a beam to reach its full flexural capacity. If the shear reinforcement or web section is insufficient for the attainment of full flexural capacity, but sufficient to prevent a diagonal tension failure immediately upon shear cracking, then the failure due to shear will be one of the following.

i) Shearing failure of the concrete in the compression zone.

ii) Compression failure of the concrete compressive zone - the area of which is reduced by the shear cracking - shear compression.

iii) Web distress.

Besides these three main failures, there are other secondary modes of failure, e.g. dowel, bond or instability of the concrete compressive zone.

All the shear failures of the Author's beams appeared to be

of the "shearing" type. Apart from the nature of the failure pattern of the beams, the moment needed to develop shear compression for beams tested by the Author are calculated in Chapter 4 (table 4.1), and shown to be generally greater than the yield moments - which the support section developed in all the beams.

6.2.1 Shear Compression Failure

The mechanism of shear compression failure is explained in the following way. In shear compression failure, the movement is one of rotation at the crack, not involving displacements parallel to the crack. Neglecting the interlock forces from figure 6.2 and also any direct dowel term (see section 6.2.2),

$$M = F_{sc}.E_{sc} + F_{cc}.Z_{cc} + \Sigma F_{sq}.Z_{sq} \quad ,$$

the stirrups crossing the main shear cracks causing failure, yield, thus making F_{sq} the yield force in the stirrups. From this basic equation, Placas[70] has established the following equation for shear compression moment for beams with vertical stirrups and no compression reinforcement.

$$M_{ult} = \frac{M}{Qd_1} \cdot \frac{d_1}{c} . m_s b d_1^2 + r_{sq} f_{yq} . b . \frac{c^2}{2}$$

where $m_s = 0.8 \left(U_w . 100 r_{st} \right)^{1/3}$

differentiating M_{ult} w.r.t. c for the minimum moment of resistance at a given crack head, i.e. $\frac{\delta M_{ult}}{\delta c} = 0$

and expressing the resulting equation in terms of Q_{ult}:-

$$\frac{Q_{ult}}{bd_1} = 1.5(m_s)^{2/3} . (r_{sq} . f_{yq})^{1/3} . \left(\frac{Qd_1}{M}\right)^{1/3} \qquad \ldots (6.3)$$

6.2.2 Shearing Failure - Equilibrium Conditions

This type of failure involves primarily transverse deformation. If the crack angle is such that any transverse displacement across the crack brings a considerable interlock force into action, then this causes a flatter crack to appear. Thus progressively flatter cracks are formed as the principal shear crack gets wider and wider with higher loads. Due to the large opening and flat angle of the final crack, the interlock across it becomes extremely small. According to Regan & Placas[77] the value of this critical angle is $\tan^{-1}0.5$ for vertical stirrups and $\tan^{-1}0.3$ for inclined stirrups. The tests discussed in Chapter 3 corroborate this statement for vertical stirrups.

It appears from the test results discussed in Chapter 3 that the general mode of shear failure was as shown in figure 6.3 for a reinforced concrete continuous beam. Most of the critical shear cracks follow the line ABDE. The main elements supporting the shear force are therefore the following:-

i) The concrete at the head of the crack at A.

ii) The shear reinforcement crossing the crack along the length AB.

iii) The shear reinforcement crossing the dowel crack BD.

iv) The dowel force at DE.

Fig. 6.2 shows the force resultants at the failure plane of a reinforced concrete beam, which is failing in shear.

The following forces are effective in maintaining the equilibrium of the system.

i) The longitudinal and transverse forces in the concrete

compressive zone (F_{cc} & Q_c).

ii) The interlock force at an angle β to the horizontal (F_i).

iii) The force in the shear reinforcement crossing the crack and inclined at an angle α (F_{sq}).

iv) The longitudinal forces in the main reinforcement - both tension and compression (F_{st} & F_{sc}).

v) The dowel force F_d.

To include the dowel force in the equilibrium equation, its mode of behaviour has to be studied first. In a reinforced concrete beam with shear reinforcement failing in shear, most of the dowel force is transferred from the main reinforcement to the stirrup situated just beyond the main inclined crack. Normally only the stirrup nearest to the shear crack is affected in this way. Arroyo[9] & Bauman[17] have, however, shown that stirrups further beyond the main shear crack may also be strained. Some of the test results discussed in Chapter 3 also support this theory. In order to take the dowel force into account, the stirrup just beyond the main shear crack is indirectly included by considering the numbers of vertical stirrups crossing the shear crack as c/s, i.e. in effect taking the contribution of an additional stirrup over and above the minimum possible number.

From the condition of equilibrium (fig. 6.2),

$$Q = Q_c + F_i \text{ Sin } \beta + \Sigma F_{sq} \text{ Sin } \alpha \text{ .}$$

In the failure stage, the contribution of interlock force is zero, hence the equation above reduces to,

$$Q = Q_c + \Sigma F_{sq} \text{ Sin } \alpha \qquad \ldots (6.4)$$

Hence re-writing equation (6.4) in terms of ultimate strength,

$$Q_{ult} = Q_c + \Sigma A_{sq} . f_{yq} . \text{Sin } \alpha \qquad \ldots (6.5)$$

In his series of tests on rectangular beams, Placas[70] has noticed that if failure is by the "shearing mode" in place of "shear compression", the critical shear crack generally rises higher than in the case of shear compression failure. In view of this observation, to determine the amount of shear reinforcement crossing the crack, he has suggested that the highest of the main inclined cracks should be taken as 0.75d*, for shearing mode of failure. The symbol d* represents the depth from the compressed surface to the anchorage of the shear reinforcement in the tensile zone, i.e. to the lowest layer of the main reinforcement when the stirrups are used, and to the layer from which the bars are bent when bent-up bars are used as shear reinforcement.

It has been noted earlier that the inclination of the final shear crack for a reinforced concrete beam with vertical stirrups is $\emptyset$ arc.tan 0.5. Therefore equation (6.5) becomes:-

$$Q_{ult} = Q_{ct} + 1.5\ bd^*\ r_{sq} . f_{yq} \qquad \ldots (6.6)$$

The shear resistance of the concrete compressive zone above the main inclined crack depends primarily upon the area of concrete resisting the shear, and its ultimate unit resistance to shear. In rectangular beams a large part of the resistance is offered by the inclination of the compressive force towards the main steel in the direction of decreasing moment, as shown

in fig. 6.4.

In order to calculate this value of unit shear stress, a clear idea of the failure criterion of concrete is necessary.

6.2.3 Failure Criterion For Concrete

In order to predict the strength of any concrete structure, a failure criterion has to be postulated. Across the failure plane, the stresses active in maintaining equilibrium with the longitudinal compressive force F_{cc} and the transverse shear Q_c are shears and compressions. Various methods of approach to this problem of a failure criterion have been proposed, some theoretical, e.g. Baker[10], Anson[8]; some empirical, McHenry & Karni[66], Bresler and Pister[19] ( ), and Guralnick[43]; and some semi-empirical, e.g. Lichtenburg[60]. The problem, however, is not solved yet. In order to formulate a shearing equation for the shearing failure of beams tested at Imperial College, Placas[70] adopted a failure criterion in an approximate manner, to satisfy the mode of shear failures observed during the tests, i.e. a plastic shear rather than a brittle tensile failure. Before attempting further simplifying assumptions, the internal mechanism of the failure of concrete compressive zone is to be studied first.

If two adjacent stones are considered, the failure at the junction can take place in two ways: i) The stones will separate and move in the direction of the tensile stress, when the applied tension overcomes the tensile strength of the joint; ii) the stones will slide transversely. This latter type of failure

occurs when

$$q \geqslant c_1 + \varphi' f$$

Concrete is a heterogeneous material and the strengths of the joints between the aggregates vary. In that case, the two ways of failure mentioned above can be interpreted in the following way.

i) The tensile stress at the weakest joint reaches its limiting value U_t, the joint fails and the load supported by that joint is passed on to other joints. A chain reaction is thus initiated which causes failure of the concrete without any increase of the external load above the level at which the tensile strength of the weakest joint is reached. This type of failure is known as "brittle tensile failure".

ii) With higher ratios of compression to tension the limiting strength of the most loaded joint is governed by the frictional equation and the chain reaction described in i) above does not take place. An increase in load is necessary to produce failure in the next joint. The frictional force continues to act while the displacement at the weak joints increases and causes neighbouring joints to take up the excess load, till the load reaches a value approximately equal to the number of joints times the average joint strength. Consequently the value of the cohesive c_1 in the equation $q = c_1 + \varphi' f$ is an average value, greater than U_t. This type of failure is known as the plastic shear mode.

In these terms Lichtenberg[60] has developed a theory based

on Coulomb & Conard's work on Soil Mechanics. To construct a failure envelope, he has drawn a line tangent to the circle representing uni-axial compression, with a slope $\varphi' = 0.9$. An arc of a circle tangent to this line and intercepting the normal stress axis at the uniaxial tensile strength is then drawn to complete the envelope. He has assumed a value of $U_t = \frac{U_{cyl}}{10}$. Regan & Placas[71] have also used this failure criterion based on Coulomb's method, but with different constants for predicting stresses at failure. Although the strict application of this criterion gives a curved interaction between shear and compression of vertical planes through a compressive zone, within the range of practical stresses in beams, the ultimate value of q is sensibly independent of f and this fact is used in the following section.

6.2.4 Shear Strength of the Concrete Compressive Zone for Rectangular Beams Before Yielding of Main Steel.

The results of tests of specimens subjected to compressive and shear stresses are shown in fig. 6.5. It is evident from these results that though there is a wide scatter, there is a definite trend over a wide range of compressive zone as shown by the horizontal line drawn with $q_c = 0.33\ U_w^{2/3}$. This range of compression covers all practical combinations of average ultimate stresses in the compressive zones not undergoing plastic rotations. Assuming the maximum shear stress to be 1.5 times the average, the average shear stress at failure $= \frac{2}{3}\ 0.33\ U_w^{2/3}$.

Therefore $Q_c = 0.22\ U_w^{2/3} bnd_1$ ... (6.7)

where "n" is equal to the neutral axis fartor at the section in which shear crack enters the uncracked concrete. Since the difference in flexural neutral axis depths is not very significant beyond an early stage of loading, n is taken approximately equal to n_o the neutral axis factor when the concrete reaches its limiting compressive strain prior to yield of main steel.

The value of n_o is obtained from figure 6.1, thus:-

$$F_{cc} = F_{st} = f_o . K_1 K_3 . bnd_1 = A_{st} . E_{st} . e_{cu} \left(\frac{1 - n}{n}\right)$$

writing $f_o = 2.35\ U_w^{2/3}$ $E_s = 200 \times 10^3 N/m^2$ $e_{cu} = 0.0035$ and $K_1 K_3 = 0.81$ (from Table A.1):-

$$\frac{n^2}{1 - n} = \left(\frac{A_{st}}{bd_1}\right) \left(\frac{200 \times 10^3}{1.9\ U_w^{2/3}}\right) \times 0.0035.$$

As established before $\frac{n^2}{1 - n} \approx 2.83 n^{2.5}$ and

$$n \approx 1.1 \frac{r_{st}^{0.4}}{U_w^{0.27}} .$$

Substituting this value of n in equation (6.7), it reduces to

$$q_c = \frac{Q_c}{bd_1} = 0.24 (r_{st} . U_w)^{0.4} \quad \text{... (6.8)}$$

This is valid so long as the main longitudinal reinforcement does not yield.

6.2.5 Shear Strength of the Concrete Compressive Zone for Rectangular Beams after Yielding of Main Steel.

In a reinforced concrete beam undergoing rotation, the formation of a plastic hinge reduces the shear carrying

capacity of the concrete compressive zone. Cranston & Reynolds[35] suggest that this may be due to severe deformation of the concrete compressive zone. Whatever may the be the reasons, the author has observed from his tests reported in Chapter 3, and presented in Table 6.1, that with the same longitudinal reinforcement and similar Z values, there is a definite trend of a reduced contribution by the concrete compressive zone towards the shear resistance of the section, as the rotation is increased. The concrete resistance to shear is arrived at by deducting the contribution of vertical stirrups - which invariably yielded at the main inclined crack - from the applied shear at the section of failure. There is some variation of cube strength of concrete. But this effect, though significant in some cases, is not present when comparison is made between beams C3 & C11, and C4 & C9 in group Ia; C7 & C1 in group Ib; and C6 & C10 in group II.

It is therefore necessary to make a reappraisal of the failure pattern of beams which failed in shear, as reported in Chapter 3. All the beams tested developed plastic hinges in the concrete compressive zone before failure. Examination of failure zone reveals that at failure the final shear crack goes through an area of elastic zone before crossing the plastic zone as shown in the figure 6.6.

Unfortunately insufficient test results make it almost impossible to draw any definite conclusion based upon factual evidence about the length of crack in the plastic and elastic zones of concrete. The three groups of tests of the author

were made with varying longitudinal reinforcement and Z values, and each comprised three or four beams. No other published work is available to the knowledge of the author of which results can be gainfully utilised for comparison and predicting the length of shear crack at the plastic and elastic zone of concrete just before failure.

To overcome this difficulty and utilise the test results of Cranston & Reynolds[35], an indirect method of approach is attempted. In this method the test results of Cranston & Reynolds are transformed by interpolation in such a way that direct comparison can be made with the Author's results. The method adopted is as follows.

Cranston & Reynolds[35] tested three groups of beams. The first two groups were of under reinforced beams with two different concrete cube strengths and stirrup spacings. The last group consisted of over-reinforced beams. In each group of tests they varied the parameter Z and recorded rotations and shear forces at various stages of loadings.

To achieve correlation between the Author's results and Cranston's, the measured rotations of Cranston & Reynolds( ) are plotted against Z for each group of beams as shown in fig. 6.7. The points representing flexural rotations are then joined and the resulting lines are extended. It is thus possible to predict the flexural rotation of any beam from these extended lines if its Z value is known.

In order to determine the reduction of the shear carrying capacity of the concrete compressive zone due to rotation, the

theoretical shear stress q_c, as calculated from equation (6.8), is compared with q_c obtained by deducting $1.5\ r_{sq}.f_{yq}$ from q_{ult}. The value of n chosen here is based upon $e_{cu} = 0.0035$. As described before in the final stage of loading, the shear crack covers a large part of elastic zone of concrete. The ratio of $\frac{q_c test}{q_c cal}$ - a Reductor Factor, is plotted against $\frac{\theta_{test}}{\theta_{flex}}$, θ_{flex} being the value obtained by the method described above. The results of the tests of the Author and the tests of Cranston & Reynolds are presented in Table No. 6.1, and figure 6.8.

Studying figure 6.8, it appears that there is a definite pattern amongst the scatter of results. Both the curves for Reduction Factors shown in the figure, give lower bound solutions. One is, however, slightly safer than the other. The two equations for Reduction Factors are:-

$$R.F_1 = 1 - \left(\frac{\theta}{\theta_{flex}} \cdot 1{:}11 - 0.11\right)^{1/3} \qquad \ldots (6.9)$$

$$R.F_2 = 1 - \left(\frac{\theta}{\theta_{flex}} \cdot 1{:}11 - 0.11\right)^{\frac{1}{2}} \qquad \ldots (6.10)$$

It is to be noted in this connection that the number of results on which the above two equations are based are by any standard very few indeed. Therefore unless more is known about this it is advisable to use the more conservative equation (6.9) in lieu of the slightly more accurate equation (6.10).

6.2.6 Final Equation for Shearing Failure

From equation (6.6) $Q_{ult} = Q_c + 1.5bd^* r_{sq}.f_{yq}$.

Substituting the value of Q_c from equation (6.8) and modifying it by the Reduction Factor from equation (6.9), equation (6.6) reduces to:-

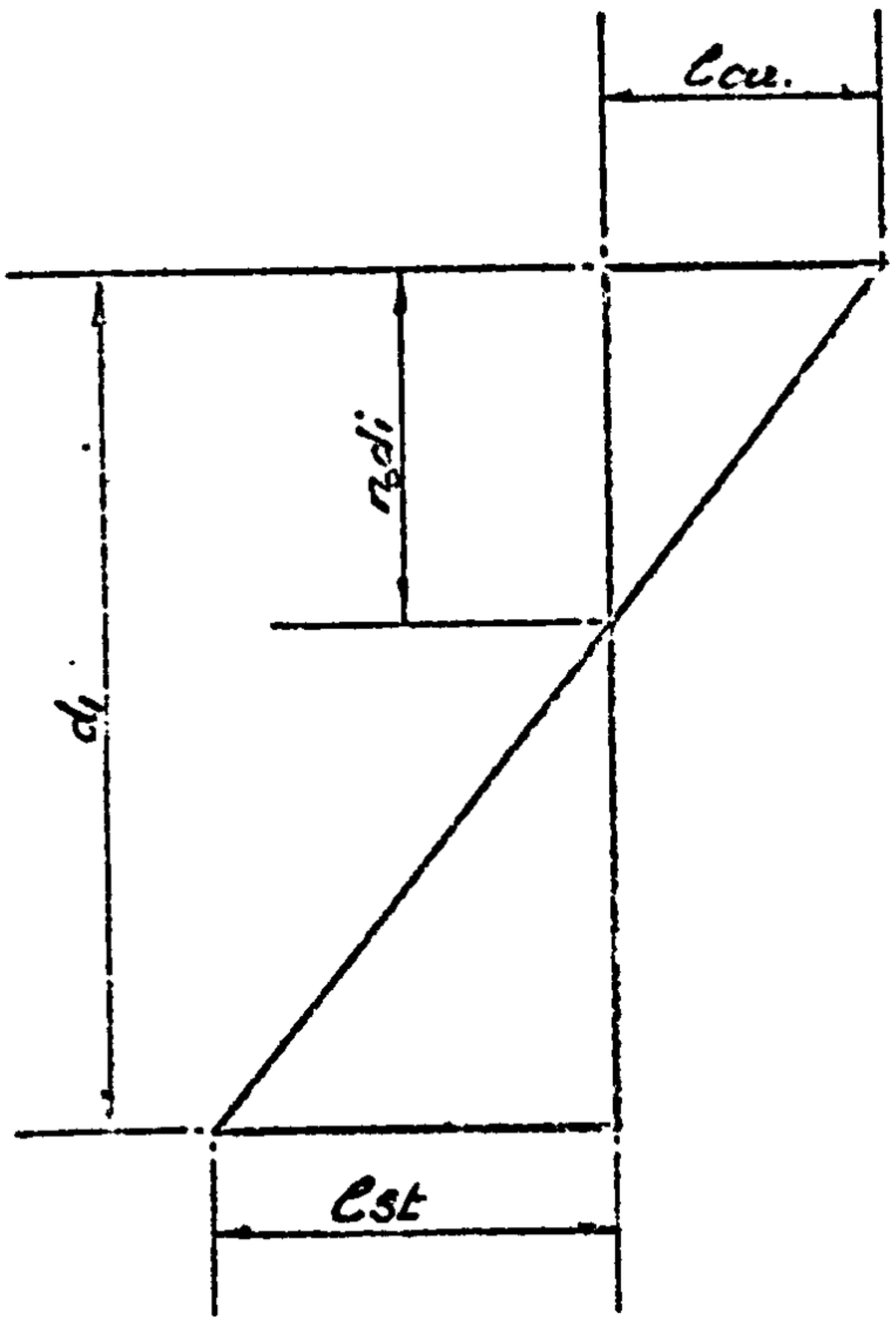
$$Q_{ult} = 0.24(r_{st}.U_w)^{0.4}\left\{1 - \left(\frac{\theta}{\theta_{flex}} \cdot 1.11 - 0.11\right)^{1/3}\right\} bd_1$$

$$+ 1.5\, r_{sq}.f_{yq}.bd^* \qquad \ldots (6.11).$$

Unlike the other equations for the "Shearing mode of failure" for R.C. rectangular beams, equation (6.11) does not give the shear strength directly from the properties of section. It depends largely on the overall deformation of the beam and in particular on its local rotation at the plastic hinge. Hence in order to predict the shear strength of a beam, its rotation at the critical shear section must be known. In the absence of this information, the rotation at which the beam is likely to fail can be predicted from equation (6.11). This procedure for predicting ultimate inelastic rotation at shear failure is adopted in presenting results of beams which failed in shear in Table 5.3.1. On the other hand, in order to predict the shearing strength of beams, as given in Table 6.2, the actual flexural and shear rotations are taken from the test results and shear strength is calculated from equation 6.11.

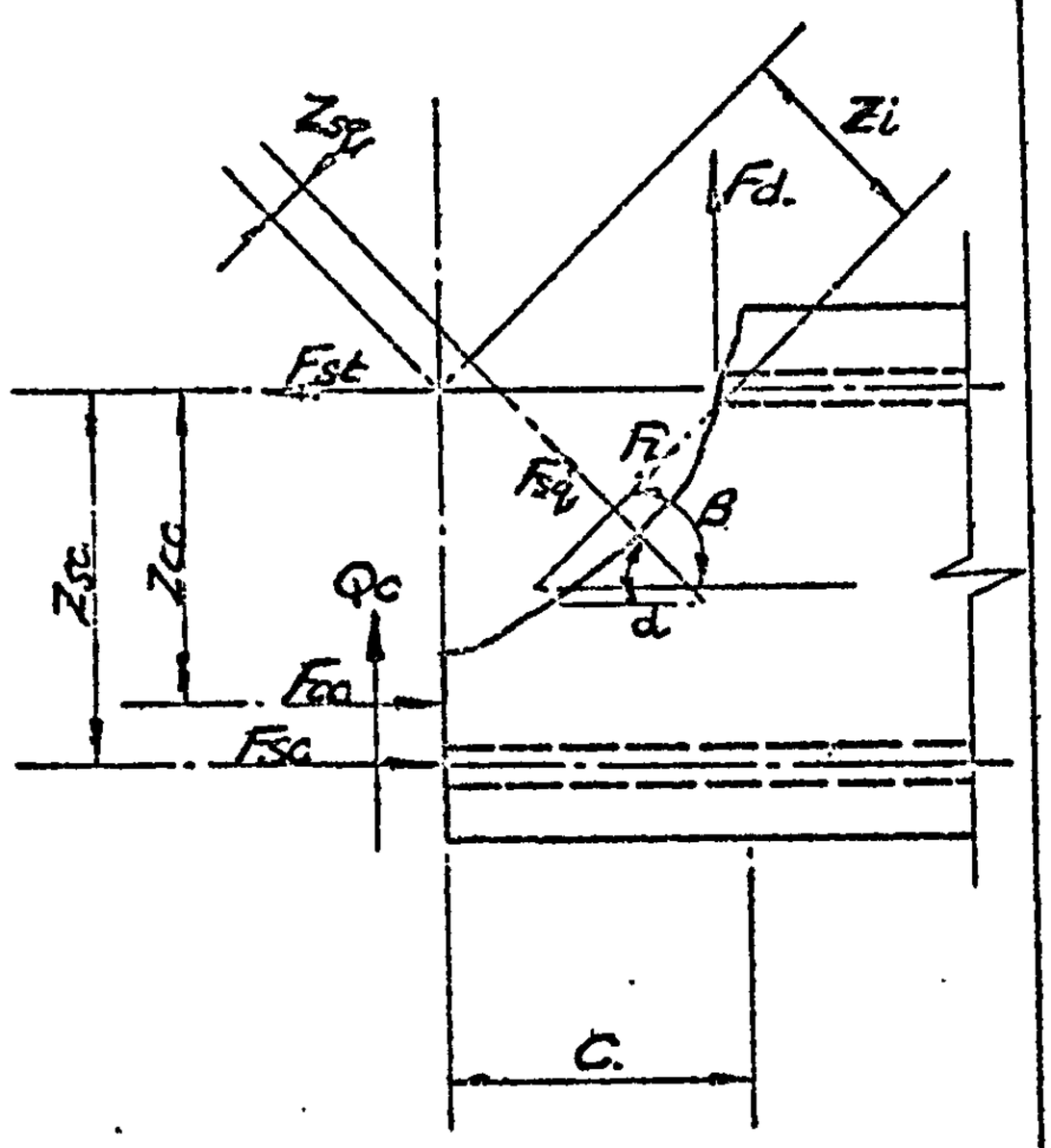
As can be seen, the shearing strength equation gives safe values and is perhaps a little oversafe in the absence of plastic rotations, but is none the less of acceptable accuracy. The predictions of rotations at shear failure are much less accurate as could be expected in view of the

scatter of all rotation results and the continual use of lower bound rotation rather than best fit curves. In practice there can be little need to predict rotations at shear failure and the approach is sufficiently accurate for determining the shear reinforcement necessary to ensure the safety of designed plastic hinges.



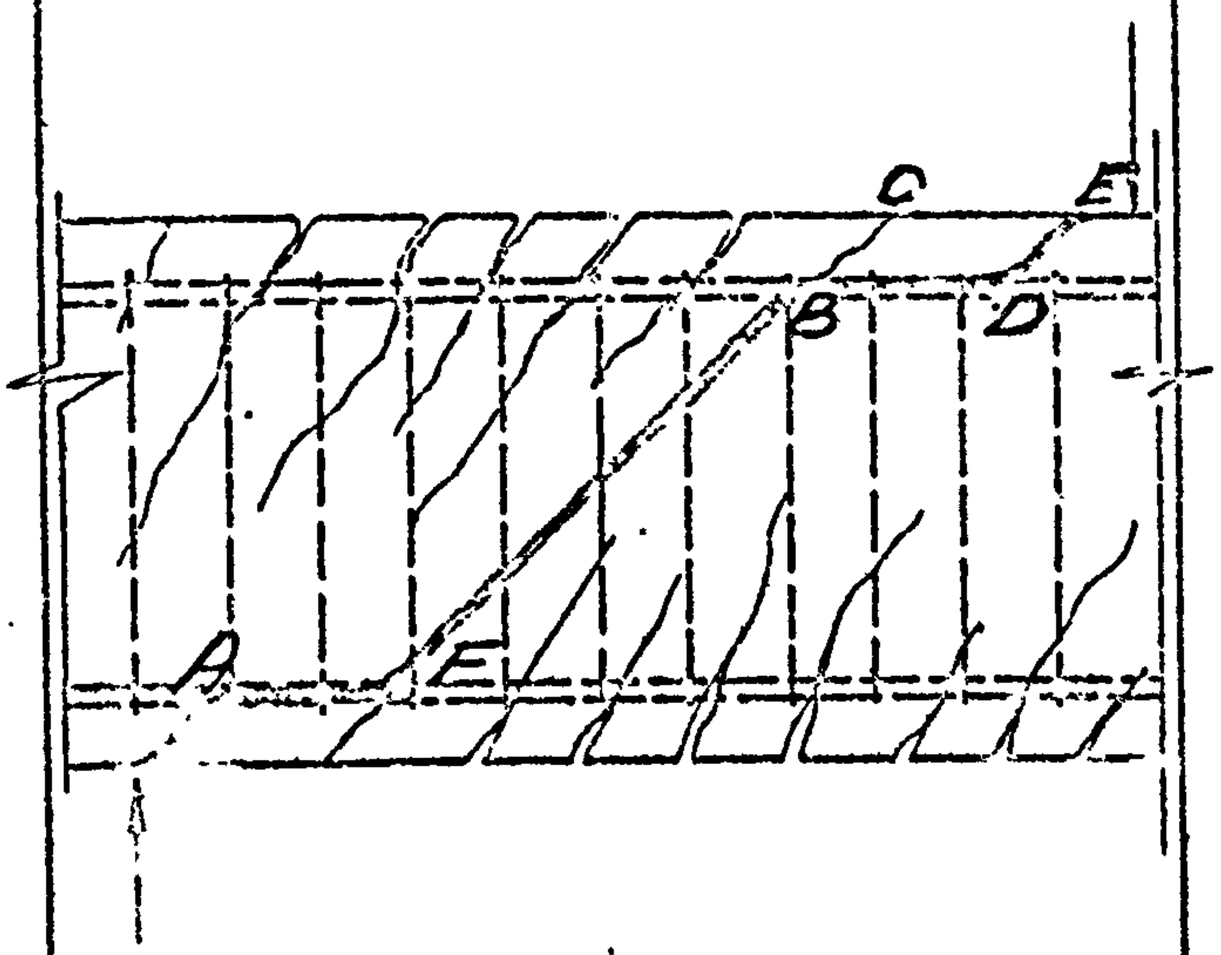
FLEXURAL STRAIN DISTRIBUTION

Fig. 6-1



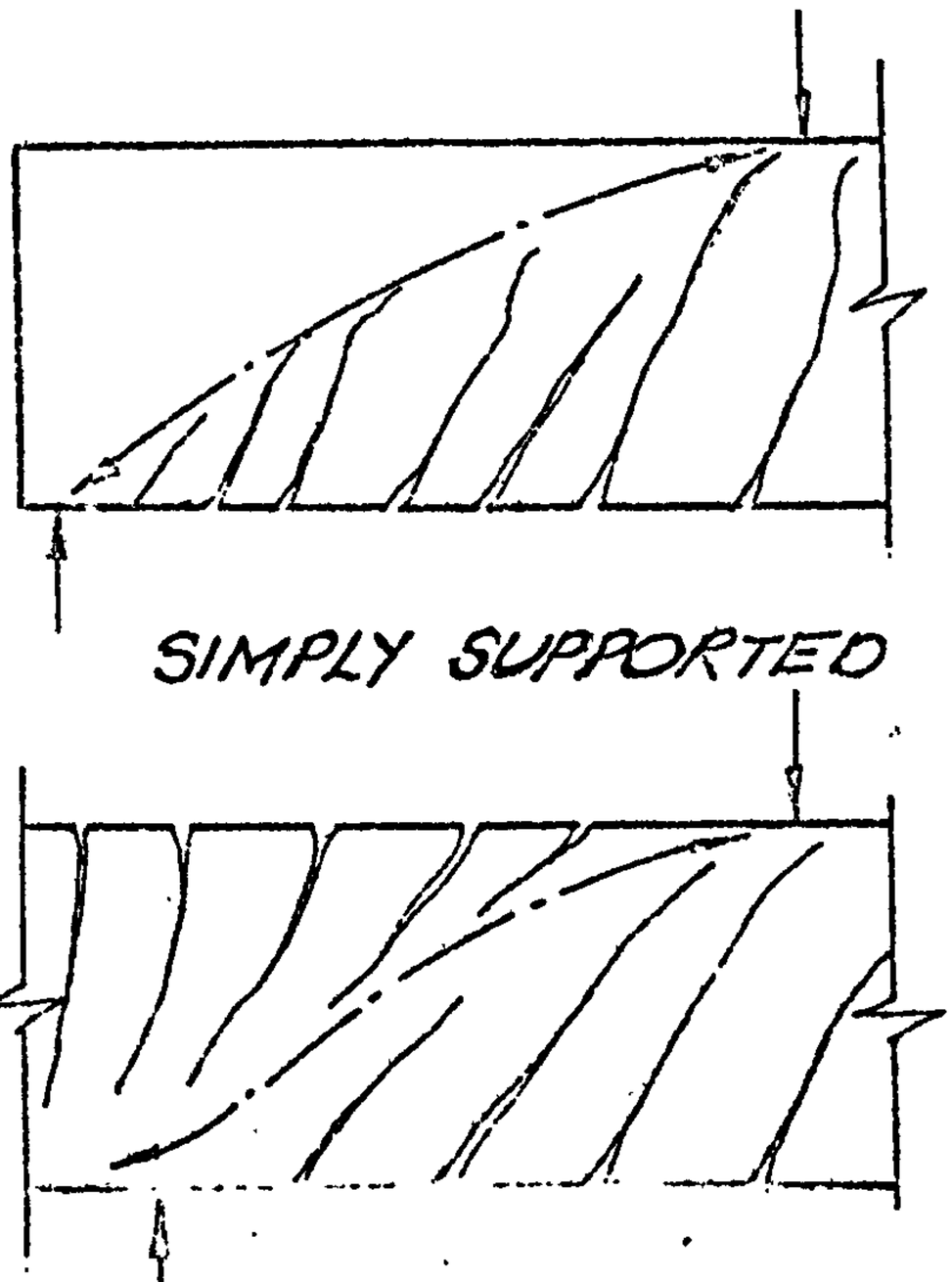
EQUILIBRIUM CONDITIONS AT A SHEAR CRACK

Fig. 6-2



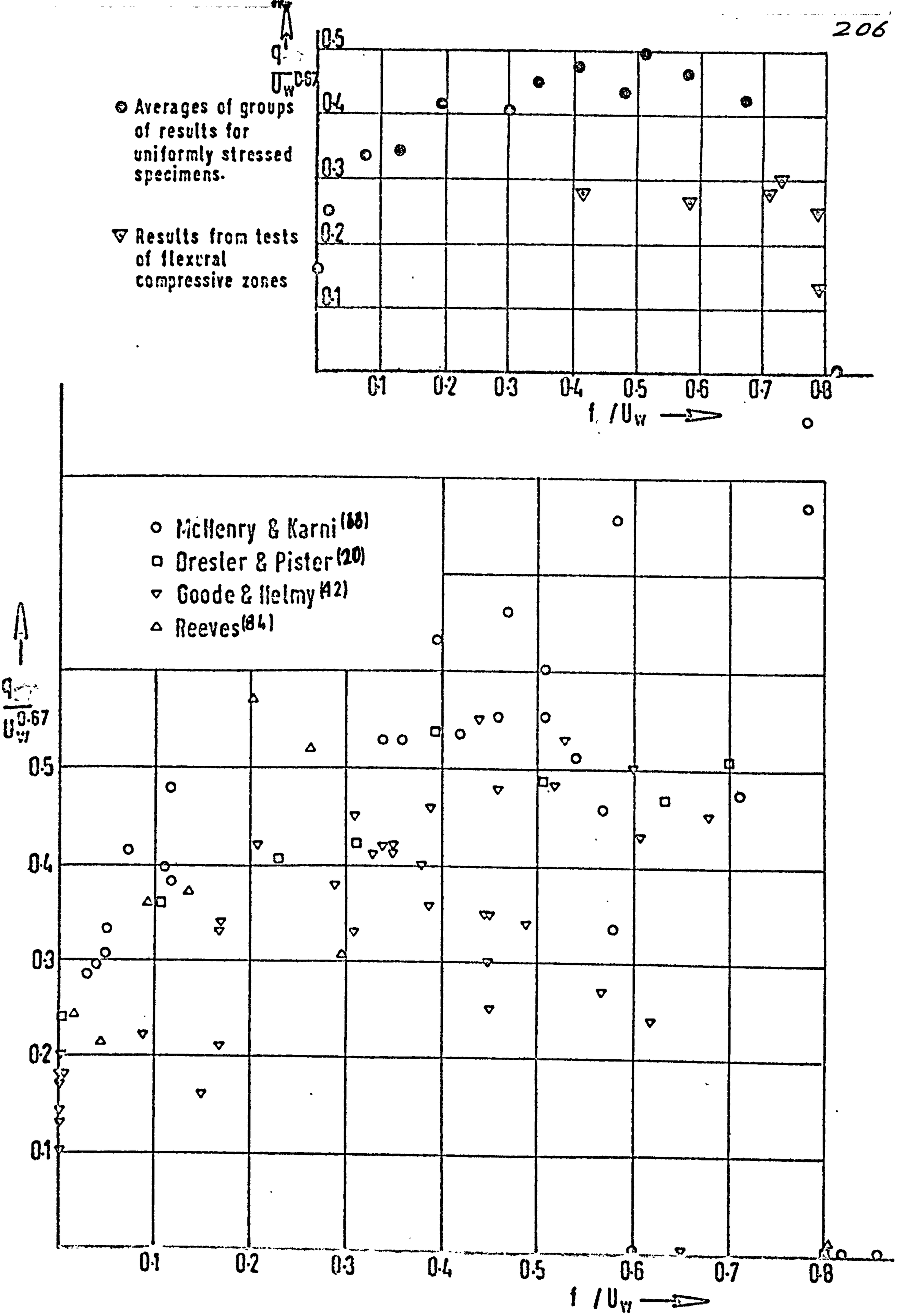
SHEARING FAILURE

Fig 6·3



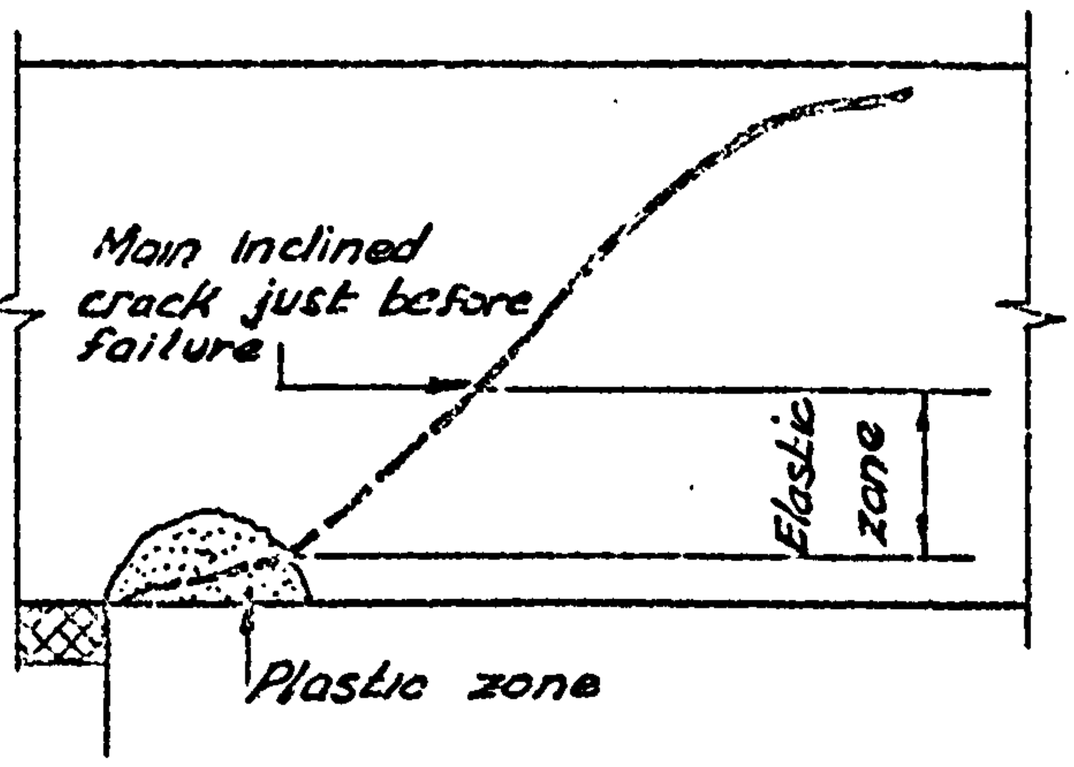
SUPPORT OF SHEAR BY INCLINED COMPRESSION.

Fig. 6·4.



FAILURE CRITERIA FOR CONCRETE – TEST RESULTS

FIGURE 6.5



SHEARING FAILURE THROUGH A PLASTIC HINGE

Fig. 6·6.

FIG. 6.7. ULTIMATE ROTATION AS A FUNCTION OF Z ON REYNOLD'S[35] TEST.

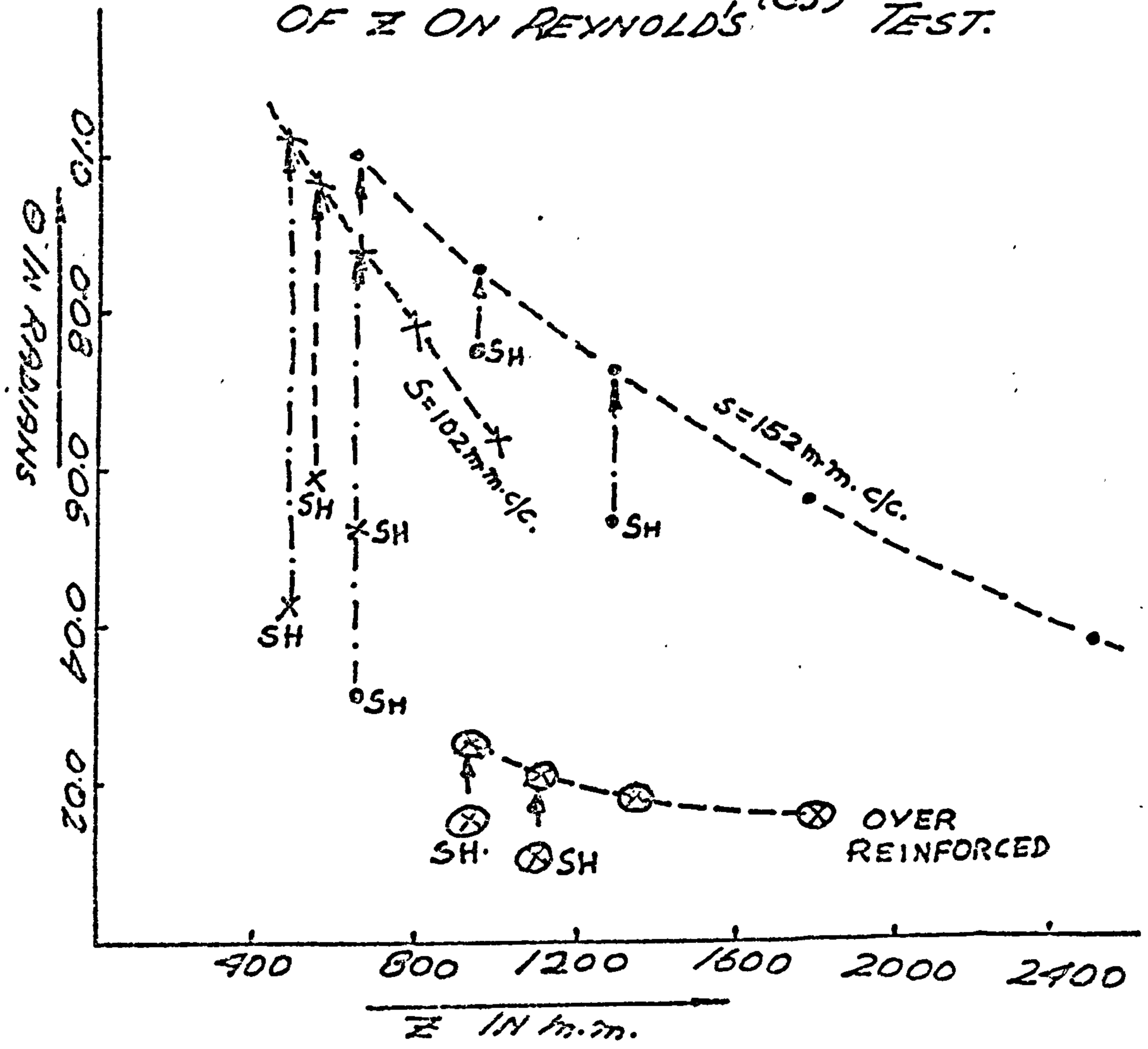


FIG. 6.8. REDUCTION Q_c DUE TO ROTATION.

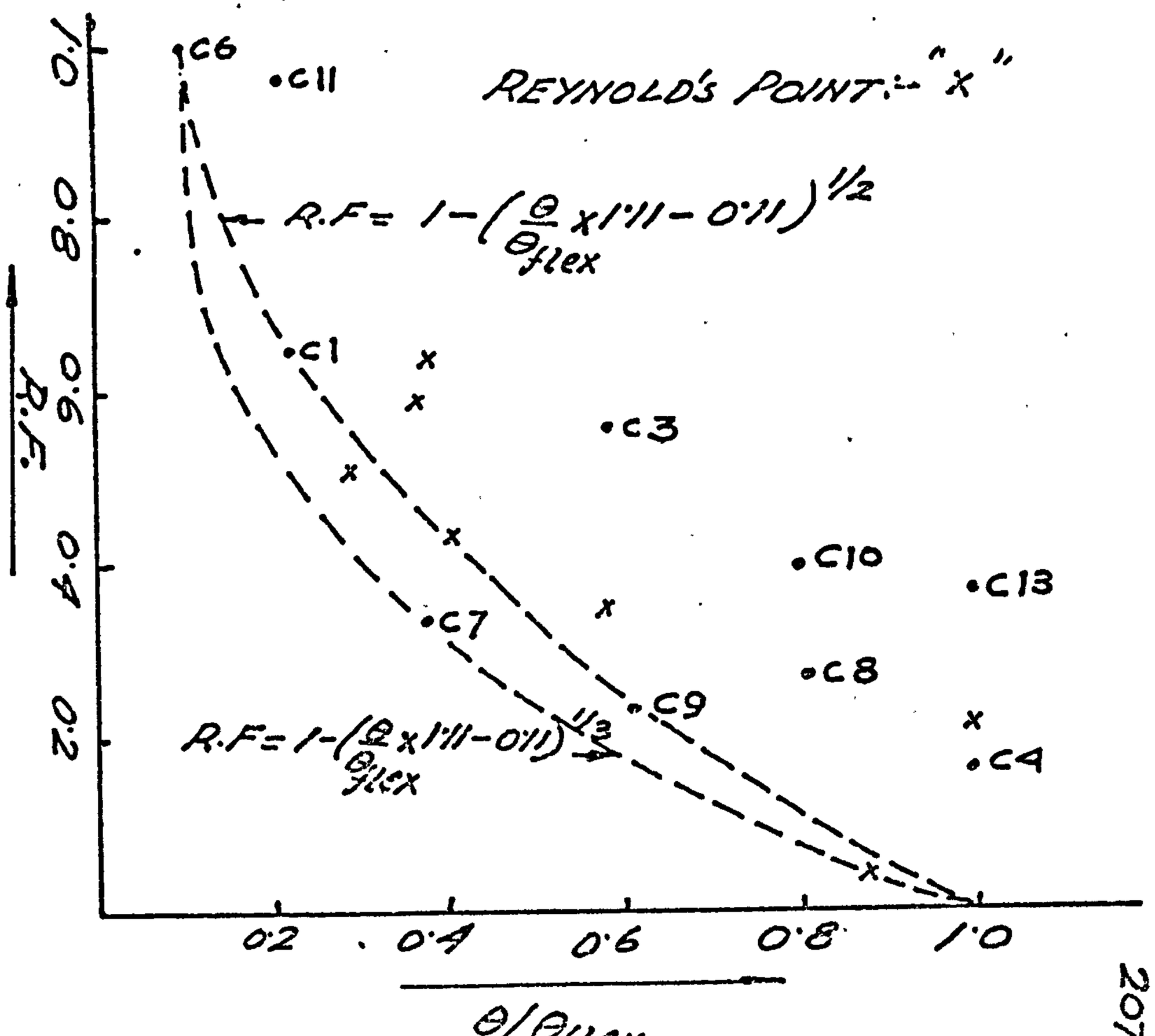


TABLE NO. 6.1

COMPARATIVE STUDY OF SHEAR STRENGTH AT MID-SUPPORT
FOR BEAMS FAILING IN SHEARING MODE.

Beam No.	U_w N/m.m^2	r_{st}%	r_{sc}%	$r_{sq}.f_{yq}$ N/m.m^2	M/Qd_1	$q_u$test N/m.m^2	Shearing equation $q_u$cal/$q_u$test	Remark
c3	51	0.545	-	1.075	2.0	2.11	0.83	Shear
c4	40.4	0.545	-	1.435	1.89	2.28	-	Flexure
c9	38.6	0.545	-	1.235	1.96	2.04	0.93	Flexure & Shear
c11	52.5	0.545	-	0.585	2.08	1.84	0.69	Shear
c1	39.4	1.465	-	1.615	2.64	3.21	0.85	Shear
c7	39.3	1.465	-	2.2	2.35	3.71	0.94	Shear
c8	41.8	1.465	-	2.49	2.22	4.07	0.94	Shear
c12	40.4	1.465	-	3.18	2.11	4.32	0.93	Flexure & Shear
*c6	46.5	0.545	-	0.585	2.15	1.81	0.98	Shear
*c10	54.6	0.545	-	1.615	1.85	2.79	0.89	Flexure & Shear
*c13	57.7	0.545	-	1.93	1.61	3.24	-	Flexure

* DENOTES SERIES NO. 2.

	Beam	U_w	r_{st}%	r_{sc}%	$r_{sq} f_{yq}$	q_u test	Remark	1.5 $r_{sq} f_{yq}$	$q_{c(test)}$	$(U_w r_{st})$	$U_w r_{st}$	$0.24(U_w r_{st})^{\frac{1}{3}}$	$\theta_{u.test}$	θ/θ_{flex}	Reduction Factor
Group I	(c3	51	0.545	-	1.073	2.11	Shear	1.60	0.51	27.8	3.78	0.91	0.031	0.586	0.56
	(c4	40.4	0.545	-	1.435	2.28	Flexure	2.15	0.13	22.0	3.44	0.83	0.053	1.00	0.16
	(c9	38.8	0.545	-	1.235	2.04	Flexure & shear	1.85	0.19	21.2	3.39	0.81	0.032	0.61	0.23
	(c11	52.5	0.545	-	0.585	1.84	Shear	0.88	0.96	28.6	3.82	0.92	0.011	0.21	1.0
Group II	(c1	39.4	1.465	-	1.615	3.21	Shear	2.42	0.79	57.7	5.06	1.21	0.0035	0.22	0.65
	(c7	39.3	1.465	-	2.2	3.71	Shear	3.30	0.41	57.6	5.06	1.21	0.006	0.38	0.34
	(c8	41.8	1.465	-	2.49	4.07	Shear	3.74	0.33	61.4	5.18	1.24	0.013	0.81	0.27
	(c12	40.4	1.465	-	3.47	4.32	Flexure & shear	5.21	-	59.2	5.12	1.23	0.016	-	-
Group III	(c6	46.5	0.545	-	0.585	1.76	Shear	0.88	0.88	25.4	3.65	0.88	0.0075	0.10	1.00
	(c10	54.6	0.545	-	1.615	2.79	Shear & Flexure	2.42	0.37	29.8	3.89	0.93	0.060	0.800	0.40
	(c13	57.7	0.545	-	1.93	3.24	Flexure & shear	2.89	0.35	31.5	3.96	0.95	0.075	1.00	0.37
Cranston θ_u at 5% drop of maxm. mom.	(1/1	24	0.9	0.161	0.615	0.35	Flexure	0.92	-	21.6	3.41	0.818	0.027	1.00	-
	(1/2	24	0.9	0.161	0.615	0.49	Flexure	0.92	-	21.6	3.41	0.818	0.051	1.00	-
	(1/3	24	0.9	0.161	0.615	0.67	Flexure	0.92	-	21.6	3.41	0.818	0.049	0.74	-
	(1/4	24	0.9	0.161	0.615	0.95	Fl. & shear	0.92	0.03	21.6	3.41	0.813	0.068	0.87	0.04
	(1/5	24	0.9	0.161	0.615	1.34	Shear	0.92	0.42	21.6	3.41	0.818	0.028	0.29	0.51
	(2/1	30	0.9	0.161	0.915	0.97	Flexure	1.37	-	27.0	3.74	0.896	0.056	1.00	-
	(2/2	30	0.9	0.161	0.915	1.17	Flexure	1.37	-	27.0	3.74	0.896	0.069	1.00	-
	(2/3	30	0.9	0.161	0.915	1.37	Flexure	1.37	-	27.0	3.74	0.896	0.047	0.57	-
	(2/4	30	0.9	0.161	0.915	1.68	Shear	1.37	0.31	27.0	3.74	0.896	0.059	0.58	0.35
	(2/5	30	0.9	0.161	0.915	1.94	Shear	1.37	0.57	27.0	3.74	0.896	0.036	0.38	0.64
	(3/1	35	2.1	0.166	0.615	0.89	Flexure	0.92	-	73.5	5.57	1.335	0.009	1.00	-
	(3/2	35	2.1	0.166	0.615	1.20	Shear	0.92	0.28	73.5	5.57	1.335	0.009	1.00	0.21
	(3/3	35	2.1	0.166	0.615	1.60	Shear	0.92	0.58	73.5	5.57	1.335	0.006	0.40	0.43
	(3/4	35	2.1	0.166	0.615	1.71	Shear	0.92	0.79	73.5	5.57	1.335	0.005	0.37	0.59

TABLE NO. 6.2

REDUCTION OF SHEAR STRENGTH DUE TO PLASTICITY

CHAPTER 7

CURTAILMENT OF LONGITUDINAL TENSION BAR

The effect of shear on the curtailment of longitudinal tension reinforcement has been studied by various research workers. Ferguson[41], Rusch[56], Leonhardt[56], Ramakrishnan[74], Placas[70] and Regan[76] have all attempted to investigate this problem. The details of code approaches are given in Chapter 2. It is commonly agreed that any curtailment of longitudinal tension reinforcement can result in a reduction of the shear strength of a reinforced concrete beam. The present codes of practice - A.C.I. & C.P., are inadequate to cope with this reduction of shear strength.

7.1 EFFECT OF SHEAR ON THE FORCES OF LONGITUDINAL TENSION BARS

In the following paragraphs a detailed study of the effect of shear on the longitudinal tension bars is attempted for beams with and without shear reinforcement.

7.1.1 Beams Without Shear Reinforcement

The variation of the force in the main longitudinal steel along the length of a shear crack is determined by the ability of the concrete below the shear crack to transmit the change of force to to the compression zone. The distance between the heads of shear and flexural cracks is very small, as shown in Fig. 7.1. Hence the resistance of the concrete above the flexural crack to bending is negligible. Thus in the absence of both shear reinforcement and dowel action, the steel force in the longitudinal tension reinforcement remains virtually constant along the length of the shear crack. That the strain in the longitudinal tension steel

under the critical shear crack becomes constant has been observed experimentally by Placas[70] and Ramakrishnan[74].

For beams failing upon formation of shear cracking, shear strength depends primarily on the ratio of main longitudinal steel and the strength of concrete. These two parameters determine the area of compression zone of concrete resisting the shear force and the widths of flexural cracks across which shear is transferred by interlock. Thus if the neutral axis factor at a particular section is n_1, and the area of tension reinforcement A_{st1}, and at some other section the area of steel were reduced to A_{st2}, the corresponding neutral axis factor would also be reduced to n_2, and the interlock action would be reduced correspondingly. Additionally if the neutral axis depth reduces in the direction of decreasing moment, the compressive force is inclined in the direction opposite to that which would support shear, i.e. l_a increases as n_1 decreases. This can cause some extra reduction of shear cracking resistance as found in tests by Baron[15].

7.1.2 Beams With Shear Reinforcement

When shear reinforcement is present, the forces it exerts on the concrete below the crack are balanced by the bond forces and inclined thrusts in the concrete. The strains in the steel have a lesser tendency to become uniform throughout the whole shear span than in the case of beams without shear reinforcement. Hence, although there is an increase of strain near the supports for simply supported beams or at the points of contraflexure for continuous beams, this increase is not as rapid as that of beams

without shear reinforcement. The rate of change depends upon the inclination of the thrust in the concrete
The strains in the steel along some distance from the load tend to be almost uniform. This produces higher stresses in the longitudinal steel than would be calculated from flexural considerations. In detailing, this must be taken into account.

To take this increase of stress in the longitudinal tension steel into account, various authors have suggested lateral translations of the steel force diagram (obtained by dividing the flexural moment diagram by the lever arm la at the section of maximum moment). Thus Leonhardt has suggested a lateral movement of $h = (1.2 - 0.9\beta)d_1 \geq 0.5d_1$ for vertical stirrups and $h = (1.2 - 1.2\beta)d_1 \geq 0.2d_1$ for inclined stirrups; Placas[70] by $1.5d^*$, and Rusch[56] by various degrees depending upon the inclination and ratio of the stirrups.

It has been observed from tests that when a critical shear crack crosses any stirrup, it yields the stirrup. Considering a strip of concrete below a shear crack - fig. 7.2, the equilibrium conditions relating the compression in the concrete to the tension in the vertical stirrup and the bond of the main steel gives,

$$r_{sq} \cdot f_{yq} \cdot b \cdot l = F_w \sin \theta_w$$

$$\text{and} \quad F_b \cdot l = F_w \cdot \cos \theta = r_{sq} \cdot f_{yq} \cdot b \cdot l \cdot \frac{\cos \theta_w}{\sin \theta_w}$$

$$\text{therefore} \quad F_b = r_{sq} \cdot f_{yq} \cdot b \cdot \cot \theta_w \qquad \ldots (7.1)$$

The maximum value of F_b possible is the flexural value obtained as follows:-

$$M_{flex} = F_{st} \cdot la \qquad \text{therefore} \ \frac{M_{flex}}{la} = F_{st} \qquad \ldots (7.1a)$$

therefore $F_b = \frac{d F_{st}}{dx} = \frac{d M_{flex}}{dx} \frac{1}{la} = \frac{Q}{la}$ ... (7.2)

The equivalent expression for stirrups inclined at an angle α to the horizontal is $F_b^* = r_{sq} . f_{yq} . b . \text{Sin } \alpha \ (\text{Sin } \alpha \ \text{Cot } \theta_w + \text{Cos } \alpha)$ ... (7.3)

7.2 STEEL FORCE DIAGRAM FOR R.C. RECTANGULAR BEAMS

7.2.1 Beams With Vert. Stirrups

In a reinforced concrete beam with vertical stirrups, failing in shear, the nature of shear cracks developed before failure is as shown in fig. 7.3. This is evident from tests reported in Chapter 3. The inclination of shear cracks before failure (i.e. θ_w) was observed to be approximately 26.5° (i.e. 2 to 1) to the horizontal. Placas[70] has also observed this in his tests. Bara's[14] beams which failed in shear also developed shear cracks inclined approximately at the same angle. During tests of beams failing in the shearing mode, Placas[70] noted that the critical crack rose higher than in cases of shear compression failure. Hence he suggested using 0.75d* as the height of the critical shear crack for the shearing mode of failure. For simplicity, assuming that the cracks near the load radiate from a height of 0.75d*, the horizontal distance along the main tension reinforcement from the section of maximum moment, i.e. main flexural crack to the first shear crack which forms 26.5° to the horizontal, becomes 0.75d* x 2 = 1.5d*. The bond force diagram is drawn in fig. 7.3 on the tension reinforcement, showing the variation of bond force per unit length. The steel force diagram is next

---

* see the Appendix for derivation.

plotted by dividing the flexural moment by the lever arm at the section of maximum moment. The bond force is imposed on this diagram, shown in fig. 7.3, by summation of unit bond forces over the distance in the following way.

From Fig. 7.3 $F_{st.x} = F_{st} - \sum_{x=0}^{x=1.5d^*}$ Bond Force ... (7.4)

when $x = 1.5d^*$ $F_{st.x} = F_{st} - \frac{1}{2} \times 1.5d^* \, r_{sq}.f_{yq}.b.\text{Cot } \theta_w$

$= F_{st} - 0.75d^* \, r_{sq}.f_{yq}.b.\text{Cot } \theta_w$

... (7.4a)

and $F_{st.\alpha}$ = i.e. at any section beyond $x = 1.5d^*$ at a distance y:-

$F_{st.\alpha} = F_{st.x} - r_{sq}.f_{yq}.b.y.\text{Cot } \theta_w$

... (7.5)

where $\theta_w = 26.5^\circ$ and

$r_{sq}.f_{yq}.b.\text{Cot } \theta_w \not> \frac{Q}{la}$.

7.2.2. Beams With Inclined Stirrups

From equation (7.3), it appears that the magnitude of bond force/unit length decreases with the decrease of the angle α, and thus that inclined stirrups would be inferior except for the greater force bonded in the radial zone of cracks (C.f. eqns. 7.4a & 7.5). However, in many practical cases F_b as given by equation 7.1 is greater than that given by equation 7.2 (the flexural rate), and also Cot θ_w is greater for 45° than for vertical stirrups again tending to bring bond back to the flexural rate. With the rate of bond thus equal to the flexural rate of equation 7.2 in the majority of beams designed to fail in flexure, inclined stirrups are preferable

to vertical ones on account of the lesser offset of the steel force diagram within the zone of radiating cracks. This superiority was confirmed by tests by Losberg (61) of beams with drastically curtailed main steel in which beams with inclined stirrups developed their flexural capacity while those with vertical stirrups failed prematurely. Placas found in his tests with 45° inclined stirrups that the length of cracks are approximately 2.25d*, making an angle of arc tan 0.33 to the horizontal. Thus for 45° inclined stirrups, the steel force diagram as shown in fig. 7.3 should be modified in such a way that the distance 1.5d* is replaced by 2.25d*, and the value of $\theta_w = 18.5^{\circ}$ in lieu of 26.5°. But as a note of caution it should be mentioned in this context that too few results are available to form a definitive opinion about inclined stirrups. Moreover those results which are available are mostly for stirrups inclined at 45° to the horizontal. To form a single equation, which would cover almost all cases of inclined stirrups, more test results are necessary.

<u>Referring to Fig. 7.3 modifying eqn. (7.4a) for 45° stirrups</u>

$$F_{stx} = F_{st} - \tfrac{1}{2} \times 2.25d^* \, r_{sq}.f_{yq}.b.\text{Cot}\,\theta_w$$

$$= F_{st} - 1.125d^* \, r_{sq}.f_{yq}.b.\text{Cot}\,\theta_w \qquad \ldots (7.4b)$$

and $F_{st.\alpha}$ at a section y from x = 2.25d*, i.e. equation (7.5) remains $F_{st.\alpha} = F_{st.\alpha} - r_{sq}.f_{yq}.b.y.\text{Cot}\,\theta_w$ where $\theta_w = 18.5$ and $r_{sq}.f_{yq}.b.\text{Cot}\,\theta_w \not> \frac{Q}{la}$.

7.3 STEEL FORCE DIAGRAM FOR R.C. T-BEAMS

7.3.1 Beams With Vertical Stirrups

Placas[70] in his series of tests on T-beams, has observed that in beams failing in the shearing mode of failure the maximum height of crack just before failure could be taken as (d* - ds). In T-beams, because of the large compressive resistance of the flange, shear-compression conditions are not critical. In his extensive series of T-beam tests, Placas[70] did not report any shear-compression failure of a T-beam. This fact was also supported by Ramakrishnan.[74] Hence the projection of the critical crack is 2 x (d* - ds). Therefore, replacing 1.5d* of fig. 7.3 by 2(d* - ds), equation (7.4a) reduces to:-

$$F_{st.x} = F_{st} - \tfrac{1}{2} \times 2(d^* - ds) r_{sq}.f_{yq}.b_r.\text{Cot } \theta_w$$

$$= F_{st} - (d^* - ds)\, r_{sq}.f_{yq}.b_r.\text{Cot } \theta_w \qquad \ldots (7.4c)$$

and Equation (7.5) remains

$$F_{st.\alpha} = F_{st.x} - r_{sq}.f_{yq}.b_r.\text{Cot } \theta_w\, y \qquad \ldots (7.5)$$

but applicable from a distance 2(d* - ds) from the face of flexural crack at the section of maximum moment,

where $\theta_w = 26.5^\circ$ and $r_{sq}.f_{yq}.b_r.\text{Cot } \theta_w \neq \frac{Q}{la}$.

7.3.2 Beams With Inclined Stirrups

Placas[70] tested a few beams with 45° inclined stirrups and the slope of the critical shear crack prior to failure for T-beams was observed to be similar to that for rectangular beams. Hence replacing 1.5d* from figure 7.3 by 3(d* - ds) and rewriting equation (7.4b):-

$$F_{st.x} = F_{st} - \tfrac{1}{2} \times 3(d^* - ds) r_{sq}.f_{yq}.b.\text{Cot } \theta_w$$

$$= F_{st} - 1.5(d^* - ds)\, r_{sq}.f_{yq}.b_r.\text{Cot}\,\theta_w \qquad \ldots (7.4d)$$

and $F_{st.\alpha}$ at a section y from $x = 3(d^* - ds)$.

$$F_{st.\alpha} = F_{st.x} - r_{sq}.f_{yq}.y.b_r.\text{Cot}\,\theta_w \qquad \ldots (7.5)$$

where $\theta_w = 18.5^\circ$ and $r_{sq}.f_{yq}.b.\text{Cot}\,\theta_w \not> \frac{Q}{1a}$.

The author is not aware of useful test results for different inclination of stirrups.

7.4 ANALYSIS OF RESULTS

The steel force diagrams at failure of the six beams tested by the author are given in fig. 7.6 & 7.7. The steel forces are obtained from the recorded strain readings of the slotted electrical strain gauges described in Chapter 3. Analysing the results of the tests presented in Chapter 3, it is observed that in Beams 1 & 2, both of which failed by shearing at the support (No. 2 at an earlier load) due to reduction of shearing strength by curtailment of longitudinal tension bars, the predicted values follow the shape of the steel force diagram and with a slight margin of safety. Beams 3 & 4 both failed at a much lower load, and the predicted results follow the pattern of the steel force diagram. In each of these beams, the nature of failure was shear in the span, hence the assumption of yielding of stirrups was justified, as is evident from the comparison between the theory and experimental results. Of the remaining beams, No. 5 failed by shearing at the support section at 330KN load on the span. The steel force diagram is for a load of 240 KN. At this load the shear cracks did not develop sufficiently to cause yielding

of stirrups. Hence the predicted values - based upon yielding of stirrups are slightly non-conservative in comparison with the actual steel force line. The same argument holds good for Beam 6, which failed predictably at a lower load. The nature of failure was flexure and shear in the span. There were many shear cracks, but no well defined "critical" shear cracks to govern the failure pattern. At a load of 240 KN, the shear cracks presumably did not cause complete yielding of stirrups.

7.5 DISCUSSION

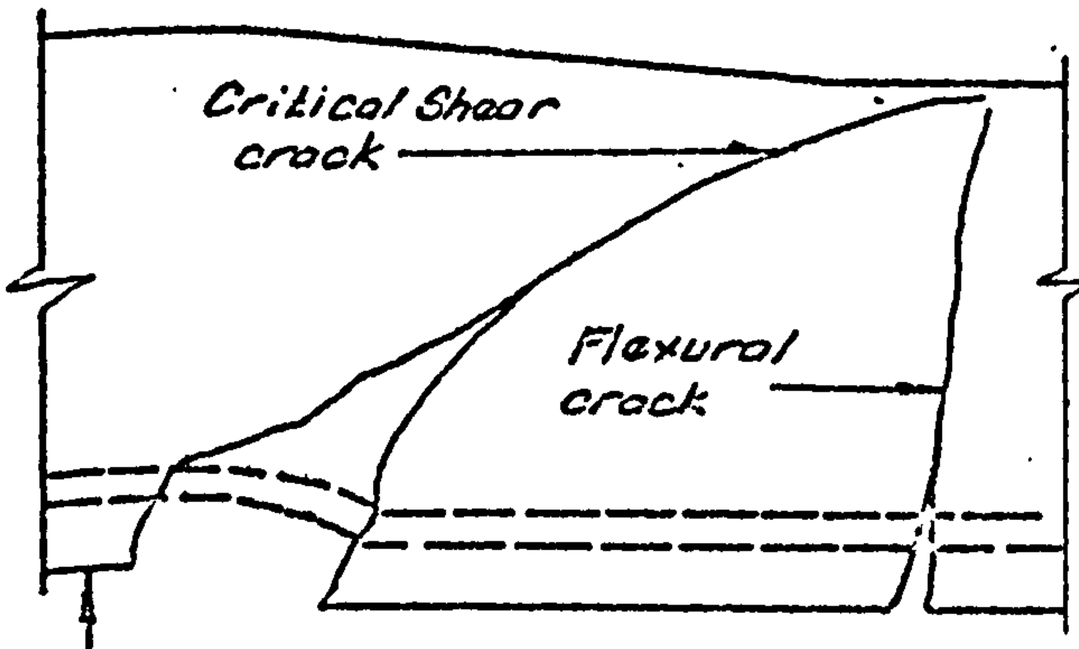
The proposed theory is an improvement on both Rusch's[56] and Leonhardt's rather empirical approach, primarily because it has a sound theoretical base. One point that could appear anomalous is that the predicted steel force does not necessarily follow the flexural steel force diagram - obtained by dividing the flexural moment by the lever arm, for all types of loading. Although this is strictly true, from a more careful scrutiny, it transpires that the larger the shear force the higher is the value of $r_{sq}.f_{yq}$, and thus the greater the reduction of steel force. Indirectly therefore, the predicted steel force diagram tends to follow the flexural steel force line.

From fig. 7.3, it appears that the higher the value of $r_{sq}.f_{yq}$, the steeper is the fall of steel force and vice versa. In other words, if there are adequate stirrups, the steel force reduces adequately and the resultant residual bond force becomes rather small, whereas, if there are inadequate stirrups or no stirrups at all, the reduction of steel force becomes minimal and the corresponding bond force becomes very large as shown in fig. 7.4..

Both Placas[70] & Ramakrishnan[74] have observed large forces near supports of a simply supported beam without stirrups.

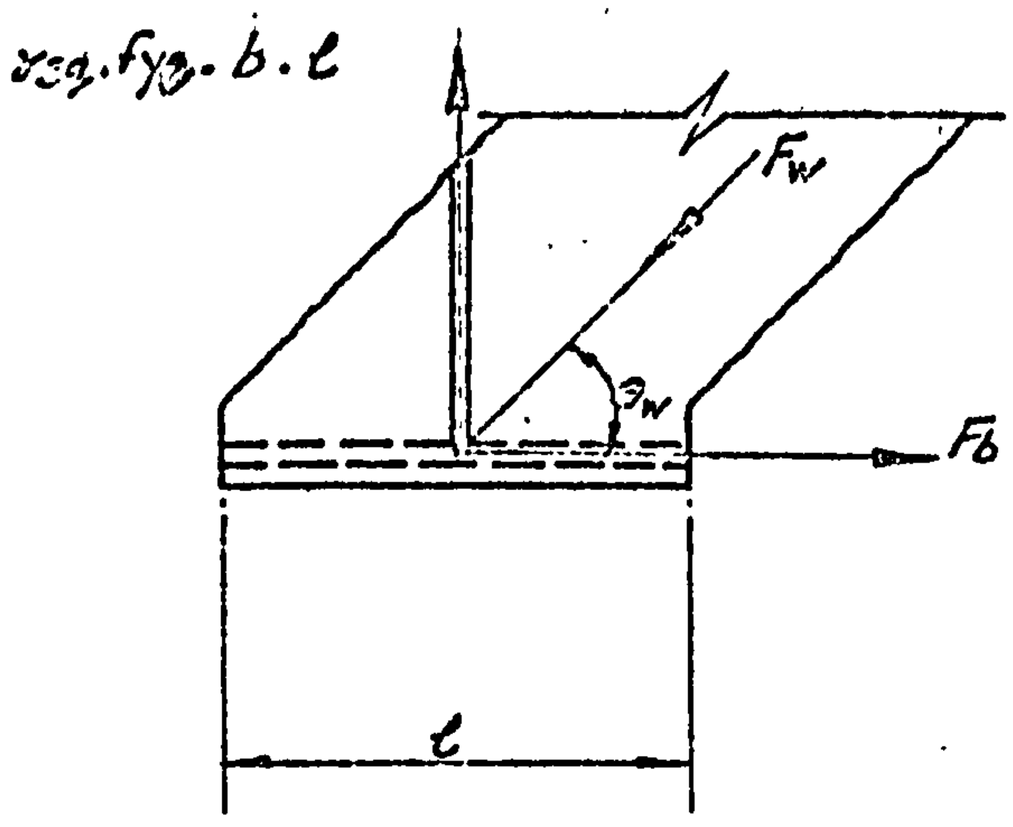
In a continuous point loaded beam, on either side of the point of contraflexure, i.e. to the support and to the applied load, the steel force diagram reduces from the section of maximum moment, depending upon the shear reinforcement, as shown in fig. 7.5. When the predicted steel force lines reach the point of contraflexure, considerable forces may remain to be reached, as shown in fig. 7.5. In the Author's beams B1 & B2, a number of longitudinal bars were cut off at the point of contraflexure as detailed in Chapter 3, weakening the shear strength of the structure at that section. Both these beams developed critical shear cracks at the mid-height at a load somewhat earlier than expected, and near to the point of contraflexure.

In order to detail a reinforced concrete beam, the steel force at the section of maximum moment is obtained by dividing the applied moment by the flexural lever arm. The effect of stirrups is next imposed on this diagram and a steel force diagram similar to fig. 7.3 is drawn, depending upon the type of stirrups, i.e. vertical or inclined, and the nature of beams, e.g. T-beams or rectangular beams. The bond force at any section is then read off from the figure, and the development length for this force is calculated from allowable bond stress in accordance with the current code of practice.



MAIN SHEAR AND FLEXURAL CRACKS

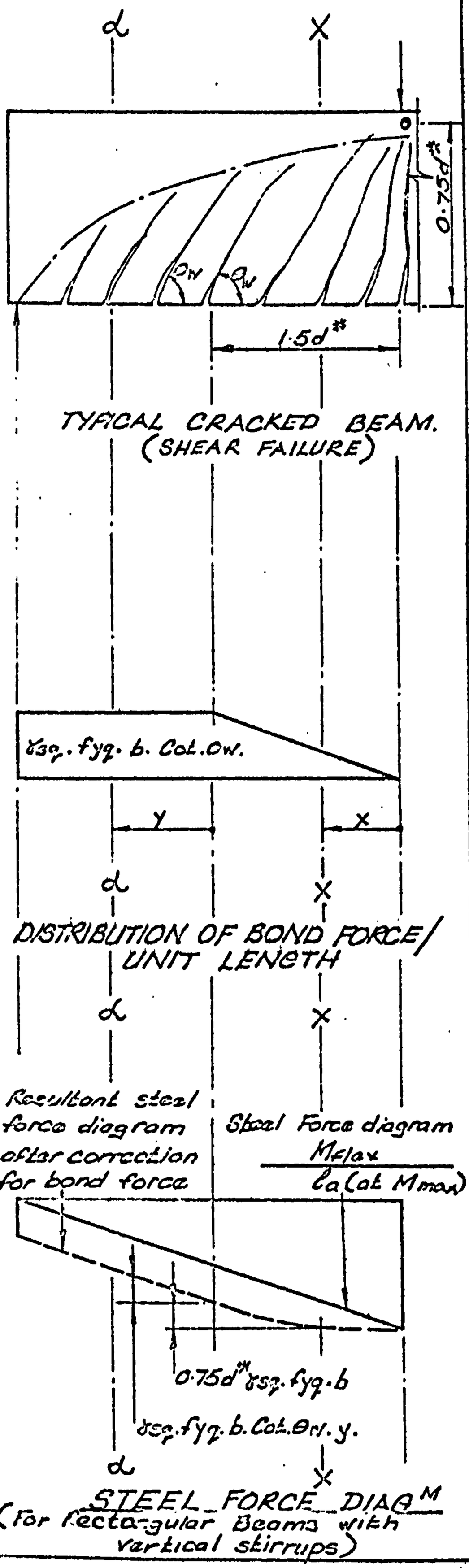
Fig. 7.1

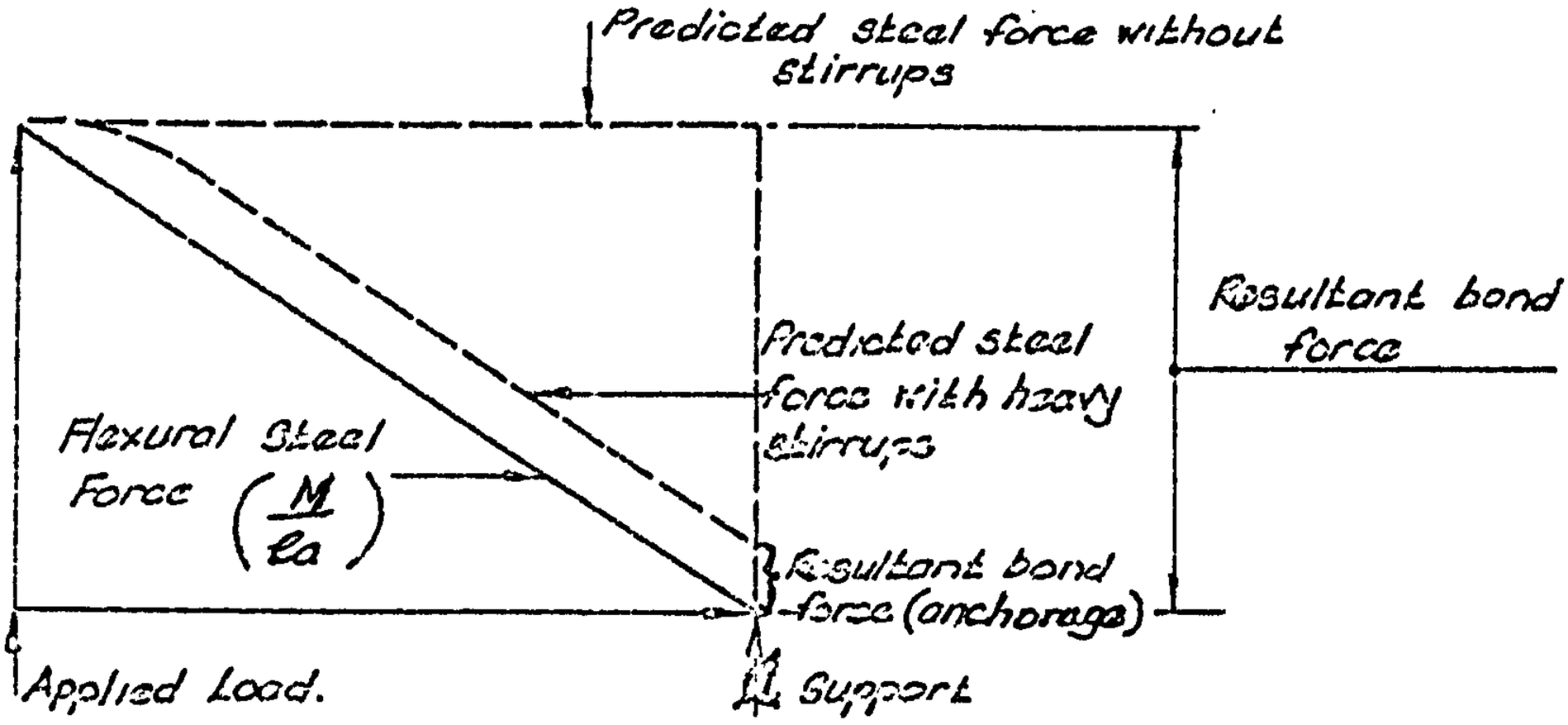


STRESS CONDITION AT MAIN STEEL

Fig. 7.2.

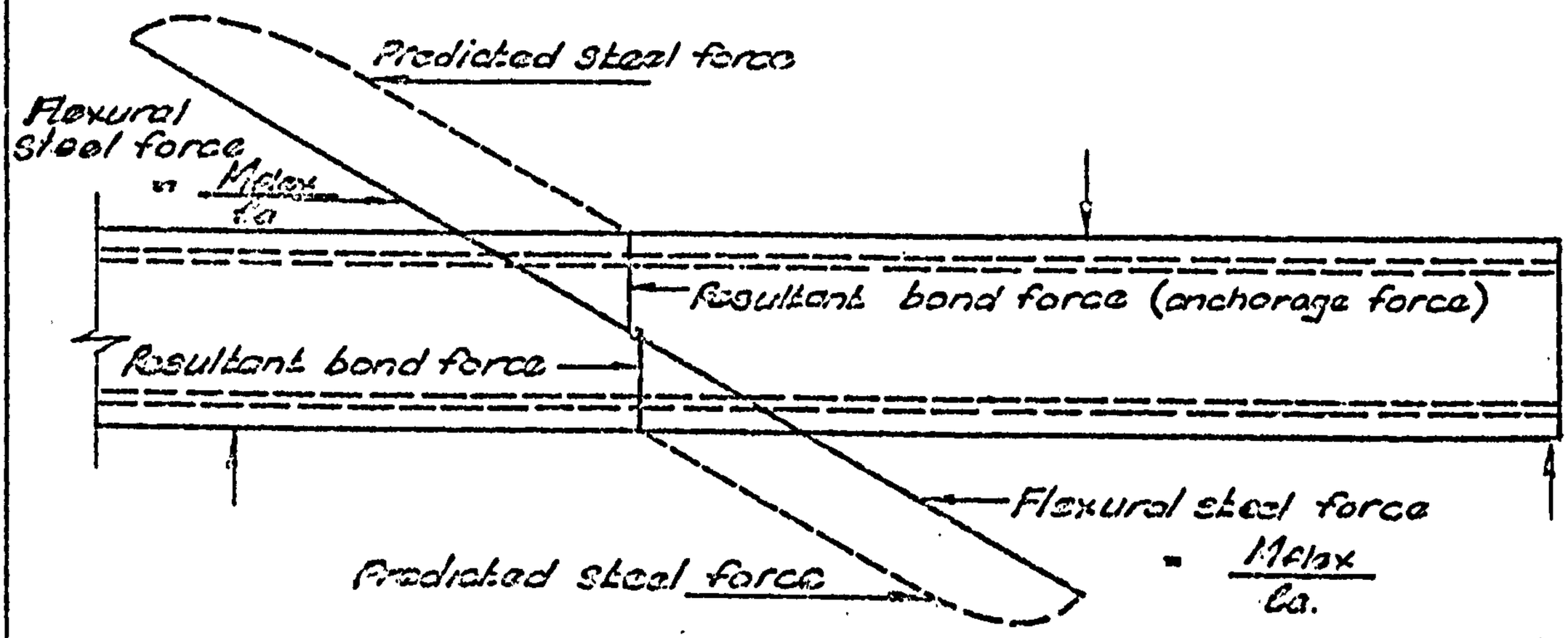
Fig. 7.3





RESULTANT BOND FORCE WITH DIFFERENT AMOUNTS OF STIRRUPS

Fig. 7.4.



STEEL FORCE DIAGRAM FOR A CONTINUOUS BEAM.

Fig. 7.5

FIG 7.6. STEEL FORCE DIAGRAM. (RESTRAINED BEAM)

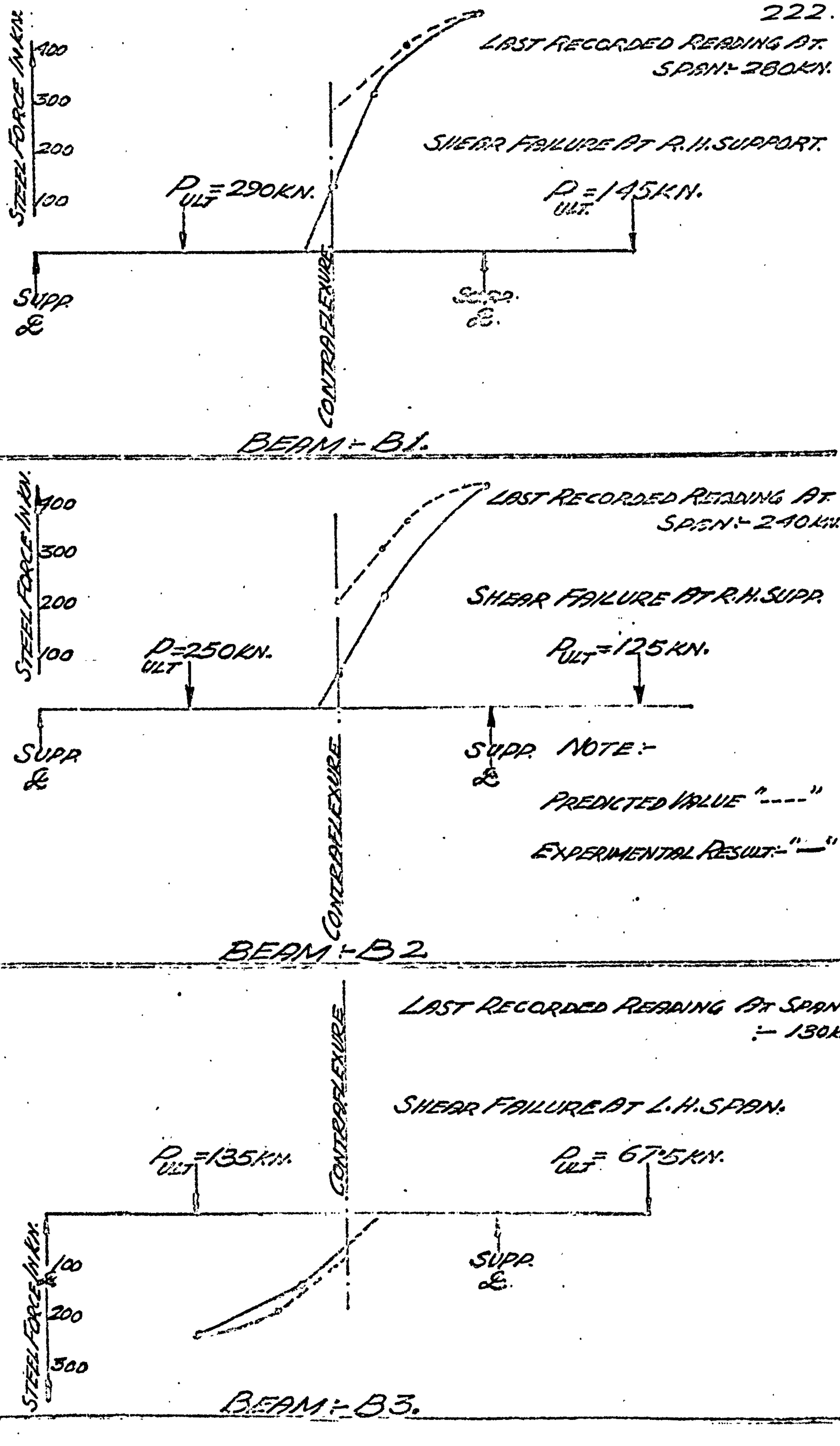
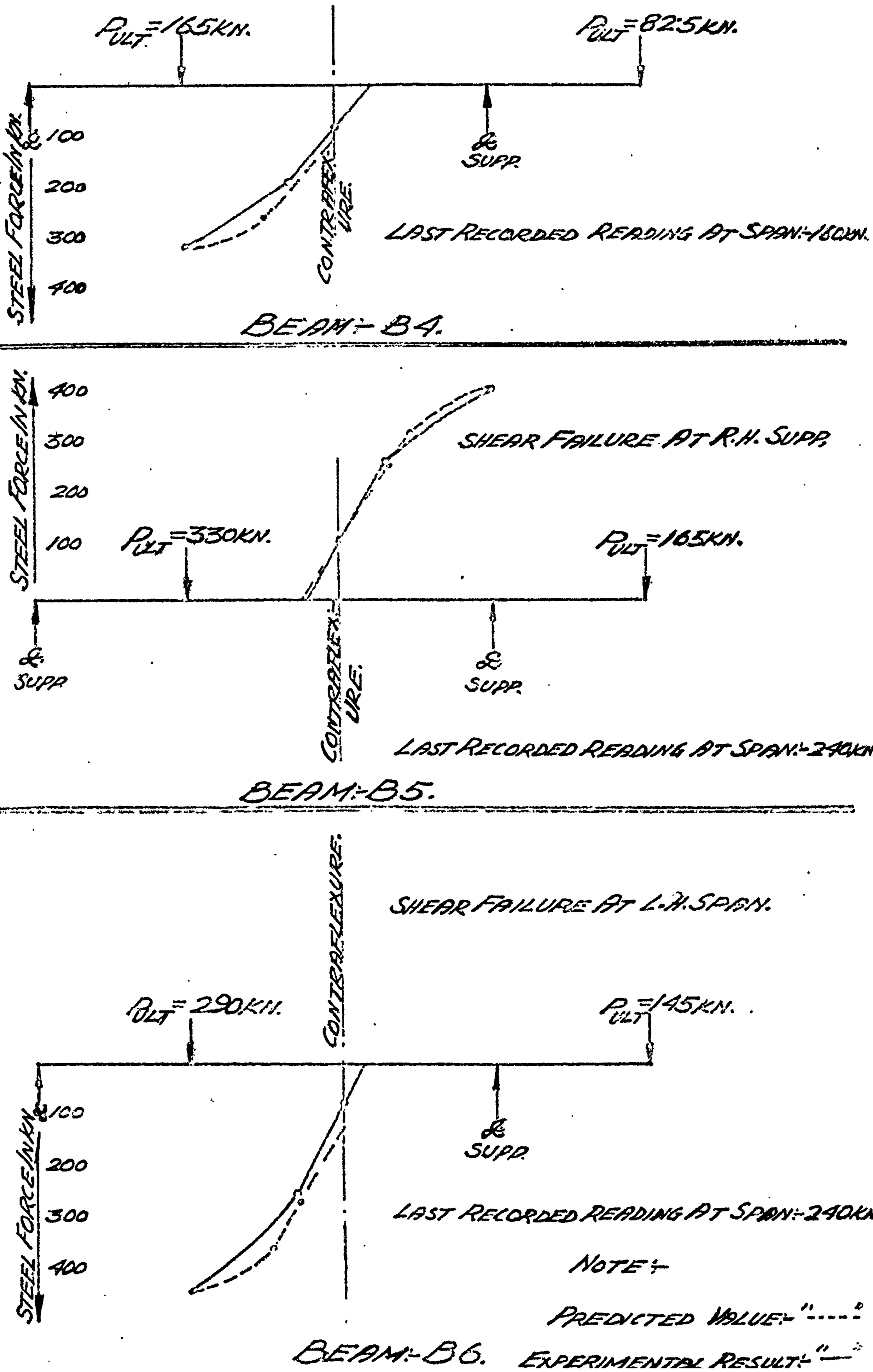


FIG. 7.7. STEEL FORCE DIAGRAM. (RESTRAINED BEAM)



CHAPTER 8

SERVICEABILITY

Service or working load criteria have been and always will be integral to the structural design process. The development and partial adoption of procedures utilising the post yield strength of reinforced concrete has in no way replaced these criteria. On the contrary, they have re-emphasised the importance of the pre-yield conditions and underlined the dual nature of the structural design problem. The service load as well as the over load condition must satisfy relevant behavioural and other design criteria.

In the design of continuous beams at serviceability limit the following factors have to be considered.

1. Crack widths, shear and flexural.
2. Deflections, due to superimposed loads which may render the structure unserviceable or physically unsound.
3. Excessive stress at critical sections under working load which gives rise to long term creep and deflection. The type of structure and the nature of the superimposed load would determine the maximum stress that could be allowed under working load conditions. This should be covered by limit state of local damage calculations which are beyond the scope of this thesis.

8.1 LIMIT CRACK WIDTH

The maximum tolerable crack width in structures, though an

important serviceability criterion, can only be described in relatively broad limits. However, it is known that the type of structure and the environment in which it is situated may influence the permissible width for cracks. For example, close to the sea or in an industrial area with corrosive waste gases, the atmospheric conditions may have adverse effects on the reinforcement if the crack widths are large enough to expose the reinforcement to weather. In the interior of structures, the maximum crack width may be limited by asthetic considerations. Depending upon the location of this structure, the allowable crack widths may vary from 0.1 mm to 0.4 mm in accordance with the C.E.B. recommendations[27], as given in Table 8.1 :-

TABLE 8.1

C.E.B. RECOMMENDATIONS ON ALLOWABLE CRACK WIDTHS

Structures in aggressive atmosphere	0.1 mm
Unprotected exterior of structure	0.2 mm
Protected structure or interior	0.3 mm
Limit of harmful cracks	0.4 mm

but is generally 0.3 mm according to the Draft British Code[38].

A review of the causes and the control of cracking has been produced by Reis, Mozer & Bianchini[79], and a collection of significant recent work is available in a special A.C.I. publication on cracking[5]. Many expressions exist for the prediction of crack widths and a comparative evaluation is not intended here. Invariably these expressions indicate that crack width is proportional to the stress in the steel and, as

such, proportional to the load factor.

8.1.1 Equations for Flexural and Shear Crack Widths

According to the Draft Unified Code[38], which is supported by extensive test data[22], the maximum crack width due to flexure is to be calculated from the following equation:-

$$w_f = 2.3\ c'.e \qquad \ldots (8.1)$$

where c' is the distance from the point considered either to the surface of the nearest longitudinal reinforcing bar or to the neutral axis, whichever is the lesser; and e is the apparent longitudinal tensile strain in the concrete at the point considered.

The position of the neutral axis and the magnitude of the calculated longitudinal strain (e calc.) should be found from the analysis of the section considered. To allow for the stiffening effect of the concrete in the tensile zone, the apparent longitudinal strain e is found from the following:-

$$e = e_{calc} - \frac{4b_r d_1 (d_c - d_n)}{A_{st}(d - d_n)} \times 10^{-6} \qquad \ldots (8.1a)$$

A negative value for e indicates that the section is uncracked.

The shear crack width formula proposed by Regan & Placas[78] is given by the following equation:-

$$w_{sh} = \frac{0.35 \sin\alpha}{10^4 r_{sq} (U_w)^{\frac{1}{3}}} \cdot \frac{Q - Q_{cr}}{b_r . d_1} \qquad \ldots (8.2)$$

where Q_{cr} = shear cracking force

$$\frac{Q_{cr}}{b_r d_1} = 0.25 \left(U_w . \frac{100\ A_{st}}{b_r d_1} \right)^{\frac{1}{3}} \leq 0.36 (U_w)^{\frac{1}{3}}$$

This formula has been established empirically by plotting crack widths against the parameters which they observed to influence the crack width.

8.1.2 Comparison with Test Results

No comparisons are made for flexural crack widths since as noted previously measurement of the widest flexural cracks (at the column stubs) was not practicable with the test arrangement used.

Figure 8.1 shows data for shear cracks as graphs of w_{sh} test & w_{sh} calc, for the continuous beams. As can be seen, the predictions of equation 8.2 are reasonably accurate for cracks in regions of sagging bending but very unsafe for those in support regions - the constant 0.3 of equation 8.2 would have to be increased to about 0.6 to give agreement for the latter cracks.

A possible explanation of this would be slip at the anchorages of the stirrups when they are in cracked tensile zones.

In an attempt to clarify this, use was made of crack width measurements by Leonhardt.[73] Unfortunately the only data given by him relates to the support regions and the outer (less stressed) regions of the span. Once again, the theory works adequately in the regions of positive bending and is non-conservative for the support zones. However, in this case, there is a possible alternative explanation in that the shear reinforcement was different in the two zones, being much more closely spaced near

the internal supports and it is possible that by involving both r_{sq} and s the equation overestimates the benefits to be obtained from close stirrup spacing. The use of the ratio $\sqrt{s/r_{sq}}$ in place of s/r_{sq} would resolve the difficulties with Leonhardt's results. None the less, the original explanation of anchorage is probably to be preferred in the case of the present beams since the detailing of the support and span regions was identical.

8.2 Limit Deflection

The deflection of beams under working load must be taken into account in view of the safety requirements of partition walls, plaster etc. and other conditions depending on the general utility of the structure (e.g. beams carrying crane loads etc.). Under these conditions, only the relative deflection due to the super-imposed load (without the use of over-load coefficients) need be considered as suggested by the C.E.B. Recommendations[27]. The initial deflection due to the permanent load takes place largely during construction and may be ignored as the major part generally occurs before the structure is put into use.

Load-deflection curves are also useful in studying the behaviour of beams at working loads and for estimating the range of acceptable working loads. Load deflection curves for beams failing in flexure are shown in Chapter 3.

Studying the test results for load/deflection curves away from support, it appears that these curves have three distict

stages.

Stage 1: This corresponds to that part of the curve before flexural cracking. In this stage the beam behaves elastically, and the curve is a straight line, the deflection being proportional to the load. The extent of this stage depends largely on the tensile strength of the concrete and the shear-span.

Stage 2: This represents that part of the curve between the beginning of the flexural cracking and the yielding of stirrups at a major inclined crack. After the appearance of flexural cracks, the deflection curve undergoes a change of curvature and deviates from the original straight line.

Stage 3: This stage usually forms for beams failing in shear, at or near the ultimate stage of loading. This is usually represented by a second change in the slope of the load-deflection curve because of the yielding of stirrups. The magnitude of these deflections is quite irrelevant to the use of deflection as serviceability criterion, since at working load level the stirrups will always be in the elastic range.

The three stages defined above, are not always distinguishable in the load-deflection curve, drawn from readings at reasonable load intervals. Because of the secondary nature of this problem, it was decided not to multiply the number of load stages in the present tests in order to obtain a better representation of the actual behaviour. It remains, however, that a better understanding of the beam deflection behaviour is obtained when the various load-deflection curves are viewed from the angle of the three load stages described above.

Specific limits for deflections are recommended by the Russian Structural Standard & Regulations[85].

The Draft British Standard Code of Practice[38] however, gives values in the form of span/effective depth ratios for different spans and end conditions, in addition to empirical formulae for determining deflections from known curvature values.

8.3 YIELD SAFETY

The maximum possible stress under working load is generally specified in relation to the yield stress of either the tension reinforcement or of concrete, as in the C.E.B. Recommendations[27], and it is generally assumed that there must be no plastic hinges in any part of the structures under working load conditions.

In practice, almost all beams are under-reinforced, i.e. tension reinforcement yields before concrete reaches maximum stress, hence the degree of safety against yield could be represented by the ratio of yield stress of the reinforcement to the maximum permissible stress at working load.

$$\text{i.e.} \quad \lambda_y = \frac{f_{yt}}{f_{st}} \qquad \ldots (8.3)$$

The C.E.B. recommendations suggest values of λ_y between 1 & 1$\frac{1}{3}$.

Since very little experimental information is available on the requirement of structures from the point of view of yield safety, this parameter may be assumed as a variable greater than unity whose value must be specified depending on the circumstances.

8.4 SERVICEABILITY PARAMETER

Flexural serviceability conditions can be expressed in terms of two parameters:

$$\lambda_u = \frac{P_u}{P_s}$$

where P_u = load at ultimate limit state, and P_s = load at serviceability limit state. According to the Draft British Code λ_u = 1.4 for dead and 1.6 for live loads.

$$\lambda_y = \frac{f_{yt}}{f_{st}} \approx \frac{M_y}{M_{service}}$$

So long as $\lambda y > 1$ at all sections (excluding over-reinforced sections without suitable compression reinforcement) no plastic hinges will form in the service stage and a beam will then perform as a fully continuous elastic member. The limiting span/depth ratio for deflection control can thus be determined adequately at the outset of a design from the tables of the Draft Code. Only the multiplying factor for reinforcement is strictly unknown and this can be estimated on the following basis.

The multiplier is intended to allow for the fact that the proportion of the span uncracked and therefore stiff at the service stage depends upon the ratio of the service moments to the flexural cracking moments. Viewing a span as a whole, this effect is not much altered by the proportions of top and bottom reinforcement within reasonable limits, so it should be reasonable to take the r_{st} value in the table as half that required for the free moment for internal spans and the full value for the free moment for external spans.

If the reduction of crack width caused by straining of the concrete is neglected, the draft code's equation for flexural crack widths is

$$w_f = 2.3\ c' e$$

If it is assumed that the widest parts of cracks will be at the tension surface (and this can be assured by the provision of longitudinal web reinforcement where necessary)

$$w_f = 2.3\ c' \frac{f_{st}}{E_{st}} \left(\frac{d - nd_1}{d_1 - nd_1}\right)$$

with $c' = \sqrt{2}t + 0.2D$ at a corner

$$\frac{d - nd_1}{d_1 - nd_1} \approx \frac{1.2 - 0.5}{1.0 - 0.5} = 1.4$$

$$w_f \leq 4.6t \cdot \frac{f_{st}}{E_{st}}$$

With the normal Draft Code limit $w_f \leq 0.3$ mm, $E_{st} = 200 kN/mm^2$ and $f_{yt} = 410\ N/mm^2$, the design condition becomes

$$t \leq 30\ mm/\lambda_{sy}$$

Even with $\lambda_{sy} = 1.0$ this condition is generally complied with from detailing requirements alone. It may be objected that the corner value of 'c' is not necessarily the maximum. However, where redistribution of moments is of interest the degree of reinforcement is relatively high and there will generally be at least one layer of bars spread across the tension surface. This being so and the beam being proportional so as not to have an excessive tensile zone of concrete, which is good practice, the corner position should be the critical one.

The last service condition is the control of widths of other cracks. This cannot be expressed in terms of λ_y and thus cannot be generalised. However, the most significant parameters in equation 8.2 are the spacing 's' of stirrups, and their working stress - reflected in the term $(Q_u - Q_c)/r_{sq}$. In practice if the design is not inadmissible on other grounds, shear crack widths can always be controlled by using mild steel stirrups and relatively close spacings.

From the above if the span/depth ratio is correctly chosen as for normal design the only limitation on redistribution imposed by service conditions is $\lambda_y \geq 1.0$, or to show the normal margin of safety for steel perhaps $\lambda_y \geq 1.15$. With the values of λ_u given above this means that the following percentage redistribution are permissible.

1) for dead loads 0.4/1.15 = 35%

2) for live loads 0.6/1.15 = 52%, or approx. 40% overall redistribution,

subject of course to the ultimate limit conditions on rotations given in Chapter 5.

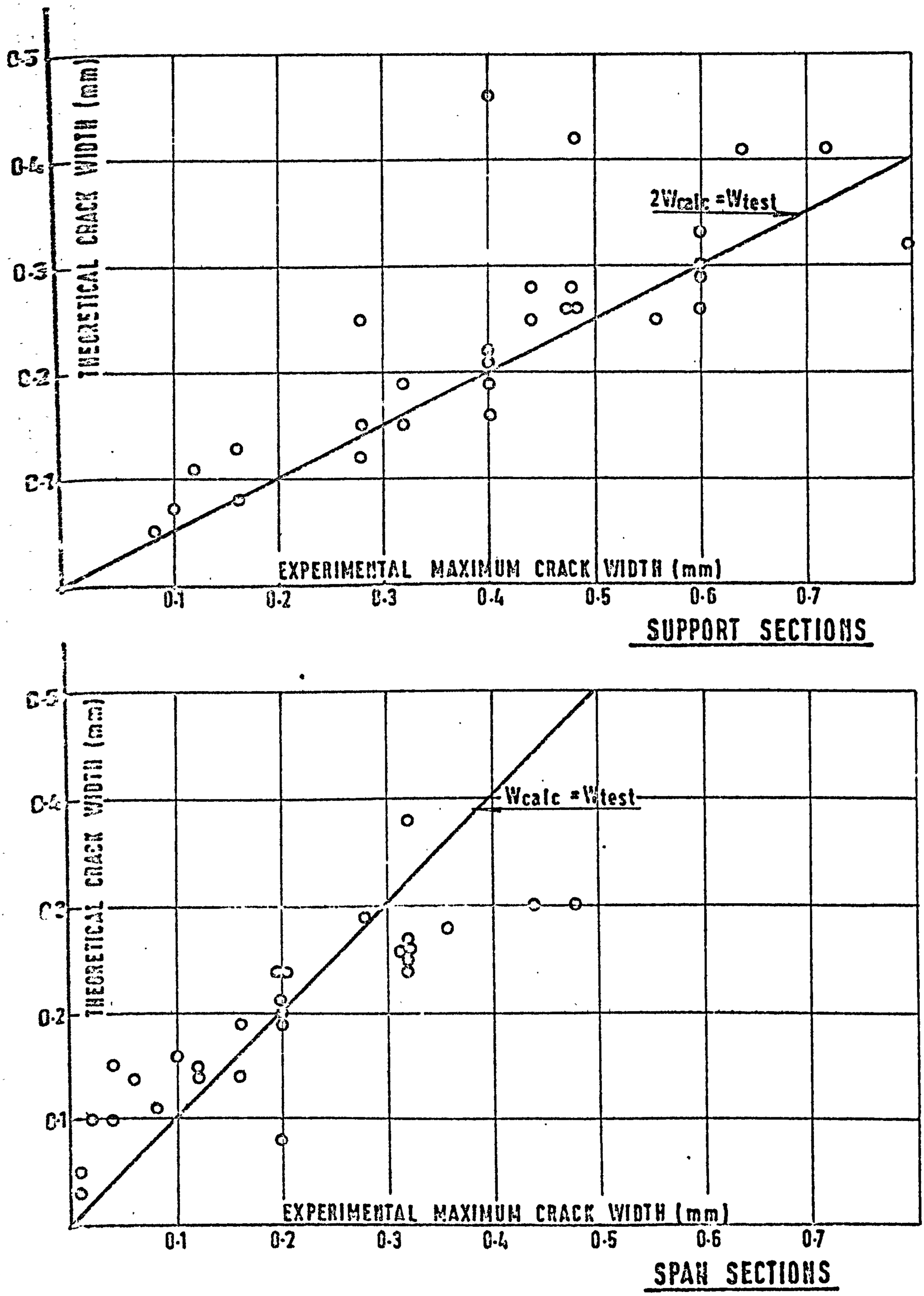


FIG. 8.1. COMPARISON OF CALCULATED & MEASURED SHEAR CRACK WIDTH.

CHAPTER 9

CONCLUSIONS, FUTURE RESEARCH & RECOMMENDATIONS FOR DESIGN.

9.1 CONCLUSIONS

From the research reported herein, the following conclusions are drawn:-

i) The prototype structural system with a uniformly distributed load can well be represented by a point load for the type of experiments the author has carried out, i.e. with the ratio $\bar{z}/d_1$ less than three.

ii) A simply supported point loaded system adequately models the behaviour of the critical section at the beam to column connection for a continuous system if the "arching effect" of the simply supported system is removed : by indirect loading or altogether avoided by using an M/Qd_1 ratio greater than three.

iii) "Shear Rotation" has clearly very little significance in a normal beam which develops plasticity in concrete, until at a very late stage of loading.

iv) For beams failing in flexure, a new method of approach - by trial-and-error - for determining inelastic rotation, is enunciated in Section 5.1, with examples given in Appendix B. A simplified version of it for practical design is given by equation (D.6) with its derivation in Appendix D.

v) For beams failing in shear after the formation of plasticity in the concrete, a new equation (6.11) is developed, which takes

into account the overall behaviour of a beam and the amount of rotation intended in the design as against its equivalent flexural limiting rotation, which comes mainly from the properties of the section.

vi) A radical approach is attempted for the evaluation of bond forces on the longitudinal tension steel. New formulae are suggested in Chapter 7, for drawing steel force diagrams for different inclinations and amounts of shear reinforcement. For curtailment of longitudinal tension steel, it has to be ensured that the bar, or bars, are extended for a distance equal to the development length for the steel force at the section considered.

9.2 FUTURE RESEARCH

9.2.1 Shear Rotation

The author has investigated this effect in beams - all of which failed either in the"shearing mode" or in flexure - after the formation of plasticity in the concrete compressive zone, i.e. after the yielding of longitudinal tension steel at the support section. The recording of the author's test data was in stages. No continuous recorder was used like the one suggested and used by both Mattock[63] & Corley[34]. The last recorded reading was invariably extrapolated to obtain the reading at failure.

It is therefore suggested that a fresh attempt be made to evaluate the effect of "Shear Deformation" on beams which fail before the yielding of longitudinal tension steel and beams which

develop other forms of failure, i.e. "Shear Compression" or "Web Crushing". It is also suggested that a continuous automatic recorder should be used to record the rotation of beams and the effect of "Shear Rotation" should be judged from the history of load-rotation diagrams of beams failing in flexure and in other modes.

9.2.2 Shear Strength After Yielding of Longitudinal Tension Steel

An attempt should be made to verify the equations suggested in Chapter 6, for the reduction of the "Shear Strength" of the concrete after the formation of plasticity by testing additional beams in the way tested by the author. If supported by more test results, a final new equation may be formulated or the less conservative equation suggested by the author be taken.

9.3 DESIGN RECOMMENDATIONS

In a design office, for a reinforced concrete rectangular beam under normal loading condition, i.e. without torsion, the parameters usually investigated are the flexural strength and the shear strength.

For a rectangular beam with vertical stirrups, the limiting flexural rotation and the ultimate moment can be derived from equations (D.6) & (5.10) respectively, if the properties of section are known. From the serviceability criteria for deflection, crack widths and yield safety the allowable extent of redistribution can be deduced. Hence with the known rotation, the shear strength of the concrete compressive zone can be calculated from equations (6.9) & (6.11) and the vertical stirrups needed to support the remainder of the ultimate shear force can be determined

from equation (6.11).

For detailing purposes, the cut-off lengths of longitudinal tension bars can be obtained by knowing the maximum steel force using equations (7.4) & (7.5) to determine bond forces. Full development lengths are then to be provided for the resultant steel forces.

REFERENCES

1. Abeles, P. W. & Turner, F.H. - Prestressed Concrete Designers' Handbook - Concrete Publications Ltd., London.

2. A.C.I. Standards Building Code 318-63.

3. A.C.I.-A.S.C.E. Committee 326 - Shear and diagonal tension - 1963.

4. A.C.I.-A.S.C.E. Committee 428 Report - Progress report on Code clauses for "Limit Design" - A.C.I. Journal, Sept., 1968.

5. A.C.I. - Causes, mechanism and control of cracking in concrete - A Symposium of twelve papers - A.C.I. publication, special 20, Detroit, A.C.I. 1968.

6. Amarakone, A. M. N. - Limit design of R.C. Skeletal Structures - Ph.D. Thesis; London University; July 1966.

7. Amarakone, A. M. N. - Limit design of R.C. Skeletal Structures - Research report, Imperial College; Civil Engineering Department; London, Aug. 1966.

8. Anson, M. - An investigation into a hypothetical deformation and failure mechanism for Concrete - Magazine of Concrete Research; June, 1964.

9. Arroyo, J. - Dowel action in Reinforced Concrete beams - D.I.C. Dissertation; Imperial College; 1964.

10. Baker, A. L. L. - A criterion of concrete failure - Proc. Institution of Civil Engineers, Feb. 1970.

11. Baker, A. L. L. - A plastic theory of ordinary reinforced concrete including moment distribution in continuous beams - Magazine of Concrete Research, No.2 - June 1949.

12. Baker, A. L. L. & Amarakone, A. M. N. - Inelastic hyperstatic frame analysis - Proceedings, International Symposium on flexural mechanics of reinforced concrete - Miami; Florida, Nov. 1964.

13. Baker, J. F., Horne, M. R. & Heyman, J. - The steel skeleton - Vol. II, Cambridge University Press, 1954.

14. Bara, H. C. - Investigation of the effect of axial loads in the shear strength of reinforced concrete beams. - Ph.D. Thesis; London University, April 1971.

15. Baron, M. J. - Shear strength of reinforced concrete beams at points of bar cut-off, A.C.I. Journal, Jan. 1966.

16. Base, G. D., Read, J. B., Beeby, A. W. & Taylor, H. P. J. - An investigation of the crack control characteristics of various types of bar in reinforced concrete beams - Research Report 18, parts 1 & 2, C & CA, Dec. 1966.

17. Baumann, T. - Versehe zum Studium der Verdubelungeswirkung der Biegezug bewehrung eines stahlbeton balken - Bericht Nr. 77, Malerialprufungsamt fur das Bauwesen der Technischen Hochschule Munchen, 1968.

18. Bremner, T. W. - The influence of the reincorcement on the Elastic and Inelastic properties of R. C. Members - M.Sc. thesis; London University, 1963.

19. Bresler, B. & Pister, K. S. - Failure of plain concrete under combined stresses - A.S.C.E. Proceedings, Vol. 81, April, 1955.

20. Bresler, B. & Pister, K. S. - Strength of concrete under combined stress - A.C.I. Journal; Sept. 1958.

21. Broms, B. - Crack width and crack spacing in reinforced concrete members - A.C.I. Journal, Vol. 62, No. 10; Oct. 1965.

22. Broms, B. & Lutz, L. - Effects of arrangement of reinforcement on crack width and spacing of reinforced concrete members. - A.C.I. Journal, Vol. 62, No. 11, Nov. 1965.

23. Burnett, E. F. P.- Limit design of R. C. beam - column connections - Ph.D. Thesis, London University, March 1969.

24. Burnett, E. F. P.- The ultimate load design of statically indeterminate structures - M.Sc.(Eng.) Thesis, London University, Dec. 1962.

25. Bryant, R. H., Bianchini, A. C., Rodriguez, J. J. & Kesler, C.E. - Shear strength of two span continuous R.C. beams with multiple point loading - T. & A.M. Report No. 194 - Dept. of Theoretical and Applied Mechanics, Univ. of Illinois.

26. C.E.B. Bulletin No. 40, Jan. 1964 - Muto, K. & Kokusho, S. - Contribution a l'etude de la resistance a l'effort tranchant des poutres forme dans diverse conditions de chargement.

27. C.E.B. Comite Europeen Du Beton - Federation International De La Precontrainte - Recommendations Internationals pour Le Calcul et L'Execution des ourages en beton, June 1970.

28. C.P. 114 - 1959 (Reset 1965).

29. Chan, W. W. L. - The rotation of reinforced concrete plastic hinges at ultimate load - Magazine of Concrete Research - Vol. 14, No. 41, July 1962.

30. Chan, W. W. L. - The ultimate strength and deformation of plastic hinges in R.C. frameworks - Magazine of Concrete Research - Vol. 7, No. 21, Nov. 1955.

31. Chan, W. W. L. - An investigation of the characteristics of plastic hinges in Reinforced Concrete - Ph.D. Thesis; London University, Feb. 1954.

32. Chinwah, J. G. C.- The strength and deformation characteristics of eccentrically loaded R. C. Columns - M.Sc.(Eng.) Thesis; London Univ., April 1967.

33. Clark, A. P. - Diagonal tension in R.C. beams - A.C.I. Journal, Oct. 1951.

34. Corley, W. G. - Rotational capacity of R.C. beams - Proceedings A.S.C.E. Journal, Struct. Div. Vol. 92, ST5, Oct. 1966.

35. Cranston, W. B. & Reynolds, G. C. - The influence of shear on the rotational capacity of R.C. beams - C & C.A. publication, T.R.A. 439, April 1970.

36. Dib, E. M. - Reinforced concrete deep beams - Ph.D. Thesis; London Univ., 1971 to be published.

37. Dilger, W. - Effect of shear on the rotational capacity of plastic hinges of reinforced concrete beams - Colloquium on Limit Design for structural concrete: Univ. of Waterloo, 1967.

38. Draft British Standard Code of Practice for the Structural Use of Concrete - BLCP 80, BSI, Sept. 1969.

39. Ernst, G. C. - Moment and shear redistribution - Journal A.C.I., Nov 1958.

40. Ferguson, P. & Thompson, J. N. - Diagonal tension in T-Beams without stirrups - A.C.I. Journal, March 1953.

41. Ferguson, P. M. & Hussain, S. I. - Strength effect of cutting off tension bars in concrete beams - Research Report No. 80, Centre for Highway Research, Univ. of Texas, June 1967.

42. Goode, C. P. & Helmy, M. A. - The strength of concrete under combined shear and direct stress - Magazine of Conc. Research, June 1967.

43. Guralnick, S. A. -.Shear Theory of R.C. beams - A.S.C.E. Journal, Structural Div., Jan. 1959.

44. Hanson, N. W. & Kurvits, O. A. - Instrumentation for structural testing - Journal of P.C.A., Vol. 7, No. 2, May 1965.

45. Hansen, E., Kielland, A., Nielsen, K.E.C. & Thaulow, S. - Compressive strength of concrete - Cube or cylinder - Nordisk Betong, 1960-4.

46. Hognestad, E.; Hanson, N. W; Magura; D. D; & Mass, M. A. - Shear strength of slender continuous reinforced concrete T-beams - Journal of the P.C.A. Research & Development Lab., Sept. 1963.

47. Hognestad, E. - High strength bars as concrete reinforcement - Journal of the P.C.A. Research and Development Laboratories, Vol. 3, No. 3, Sept. 1961.

48. I.C.E. Research Committee Report - Ultimate load design on the concrete structures - Profeedings Institution of Civil Engineers, Vol. 21, Feb. 1962.

49. Institution of Structural Engineers - The shear strength of R.C. beams - a report by the Shear Study Group, Jan. 1969.

50. Jones, L. L. - Ultimate load analysis of Reinforced and Prestressed Concrete structures - Chatto & Windus, London, 1965.

51. Jones, R. - The ultimate strength of reinforced concrete beams in shear - Magazine of Concrete Research, August 1956.

52. Gonnermann, H. F.- Effect of size and shape of Test specimen on compressive strength of concrete:Structural Research Laboratory, Chicago, Bulletin No. 16.

53. Kani, G. N. - A rational theory for the function of web reinforcement - A.C.I. Journal, March 1969.

54. Kesler, C. E. - Effect of length to diameter ratio on compressive strength of concrete - A.S.T.M. Proceedings, Philadelphia 1959.

55. Khan, M. H. - Shear strength of concrete beams reinforced with bent up bars - M.Phil. Thesis, London Univ., Oct. 1969.

56. Leonhardt, F. - La reduction de la conture d'effect tranchant dans les structures en beton arme - Interpretation des resultats d'essais a l'aide d'une generalisation de l'analogie du treillis - C. E. B. Bulletin d'Information No. 49, May 1965.

57. Leonhardt, F. & Walther, R. - The Stuttgart shear tests, 1961, contributions to the treatment of the problems of shear in reinforced concrete construction - London C. & C.A. 1964 (Translation No. 111). From Beton Und Stahlbetonban, V. 56, No. 12, 1961 & V. 51, Nos. 2,3,6,7 & 8, 1962.

58. Leonhardt, F., Walther, R. & Dilger, W. - Schubversuche an Durchlauftragern - Deutscher Ausschuss fur Stahlbeton - Heft 163, 1964.

59. Leonhardt, F. - Reducing the shear reinforcement in R.C. concrete beams and slabs - Magazine of Concrete Research, V. 17, No. 53, Dec. 1965.

60. Lichtenberg, S. - A statistical hypothesis for failure in concrete - Nordisk Betong 4/1959.

61. Losberg, A. - Nagra Undersokningar av. forankningsfragor som bakgrund till ny a Svenska betong bestam melser. (Investigation of anchorage problems as a background to the new Swedish Code) - Chalmers Tekniska Hogskola, Institutioner for Konstrucktions - teknik Nr. 69.7, 1969.

62. Macchi, G. - Elastic distribution of moments on continuous beams - Proceedings, International Symposium on the flexural mechanics of reinforced concrete - Miami, Nov. 1964.

63. Mattock, A. H. - Rotational capacity of hinging regions in R.C. beams - Proceedings International Symposium on flexural mechanics of reinforced concrete - Miami, Florida, Nov. 1964.

64. Murdock, J. W. & Kesler, C. E. - Effect of length to diameter ratio of specimen on the apparent compressive strength of concrete - A.S.T.M. Bulletin, Philadelphia, April, 1957.

65. McDonald, J. E. - The effect of confining reinforcement on the ductility of reinforced concrete beams - Technical Report C-69-5 - U.S. Army Engineers Waterways Experiment Station, Corps of Engineers, March 1969.

66. McHenry, D. & Karni, J. - Strength of concrete under combined tensile and compressive stress - A.C.I. Journal, April 1958.

67. Paulay, T. & Fenwick, R. C. - The nature of shear resistance in reinforced concrete beams - The Institution of Engineers, Australia; Civil Engineering Transactions, October 1967.

68. Poologasundaranayagam, K. - An analytical and experimental investigation of the formation and behaviour of plastic hinges in prestressed and reinforced concrete frames - Ph.D. Thesis; London Univ., Dec. 1959.

69. Placas, A. - La theorie de la plasticity applique au beton arme - M.A.Sc. Thesis, Ecole Polytechnique, University of Montreal, 1967.

70. Placas, A. - Shear strength of reinforced concrete beams - Ph.D. Thesis; London University, Nov. 1969.

71. Placas, A. & Regan, P. E. - Shear failures of reinforced concrete beams - A.C.I. Journal (to be published).

72. Rao, P. S. - Die Grundlagen zur Berechnung der bei Statisch Unbestimmten Stauhlbeton Konstruktion en im plastischen Bereich anftretenden Umlagerungem der Schnittkrafte - Deutscher Asschuss fur Stahlbeton No. 177, Berlin.

73. Rasch, C. - Spannungs - Dehnungs - Linien des Betous und Spannungsverteilung in der Biegedruckzone bei Konstanter Dehngeschwindigkeit - Deutscher Ausschuss fur Stahlbeton - Heft, 154. Berlin, 1962.

74. Ramakrishnan, V. - Behaviour and ultimate strength of reinforced concrete in shear - Publication of the P.S.C. College of Technology, Coimbatore, India, Jan. 1969.

75. Regan, P. E. - Shear in reinforced concrete - An analytical study - Report to C.I.R.I.A., April, 1971.

76. Regan, P. E. Combined shear and bending of R.C. members - Ph.D. Thesis; London University, March 1969.

77. Regan, P. E. & Placas, A. - Shear strength of R.C. beams - C.E.B. Bulletin d'Information, No. 70.

78. Regan, P. E. & Placas, A. - Limit state design criteria for shear in rectangular and T-beams - Magazine of Concrete Research, Dec. 1970.

79. Reis, E. E., Mozes, J. D., Bianchini, A. C. & Kesler, C, E. - Causes and control of cracks in concrete reinforced with high-strength steel bars - a review of research - Engineering Expt. Stn. Bulletin, No. 479, Univ. of Illinois.

80. Richart, F. E., Draffin, J. O., Olson, T. A. & Heitmann, R. H. - The effect of eccentric loading, slenderness ratio and their variables in R.C. Columns - Engineering Expt. Station Bulletin, No. 368, 1948, Univ. of Illinois.

81. Robinson, J. R. - L'adherence des barres groupess par deuse en contact annales de L'Institut Technique du batiment et des travaux publics No. 108, Dec. 1956.

82. Rodriguez, J. J., Bianchini, A. C., Viest, I. M. & Kesler - Shear Strength of two-span continuous R. C. beams - A.C.I. Journal, April 1959, Proceedings V. 55.

83. Roy, H. E. H. & Sozen, M. A. - The model to simulate the response of concrete to multi-axial loading. Civil Engineering Studies - Structural research series, No. 268; Univ. of Illinois.

84. Roy, H. E. H. & Sozen, M. A. - Ductility of Concrete - Proceedings International Symposium on the flexural mechanics on reinforced concrete, Miami, Florida, Nov. 1964.

85. Russian Structural Standards & Regulations - (Translation P.C.A.) - by Tal, K.E. - State publishing House, Moscow 1955.

86. Rusch, H. & Stockl, S. - Der Einfluss von Bugeln und Druckstaben auf das Verhalten der Biegedruckzone von Stahlbetonbalken - Deutscher Ansschuss fur Stahlbeton - Berlin, 1963.

87. Sahlin, S. & Nylander, H. - Undersokning Au Kontinuerliga Betongbalkar Vid langtaende Betongstuckning - Betong V. 40, 1955, No. 3.

88. Soliman, M. T. M.- Ultimate strength and plastic rotation capacity of R.C. members - Ph.D. Thesis, London Univ., July, 1966.

89. Soliman, M. T. M. & Yu, C. W. - The stress-strain relationship of concrete confined by rectangular transverse reinforcement - Magazine of Concrete Research, V. 19, No. 61, Dec. 1967.

90. Somes, N. F. - Compression tests on hoop-reinforced concrete - Proceedings of A.S.C.E. Structural Division, July, 1970.

91. Stockl, S. - Discussion of ductility of concrete - Proceedings, International Symposium on the flexural mechanics on reinforced concrete; Miami, Florida, Nov. 1964.

92. Stockl, S. - Das Unterschiedliche Verformungsverhalten der Rand - und Kernzonen Von Beton - Deutscher Ausschuss fur Stahlbeton - Berlin, 1966.

93. Szulczynski, T. & Sozen, M. A. - Load-deformation characteristics of concrete prisms with rectilinear transverse reinforcement - Civil Engineering Studies. Structural Series, No. 224, 1961, Sept.,Univ. of Illinois.

94. Taylor, R. - The design of Stirrups in reinforced concrete beams - C.E.B. Bulletin d'Information No. 41, April, 1964.

95. Taylor, R. - Some shear tests on R.C. beams without shear reinforcement - Magazine of Concrete Research, 1960.

96. Taylor, H. P. J. - Distribution of shear forces in reinforced beams carrying shear. - C. & C.A. Publication Nov. 1968 - International Conference on shear, torsion & bond in reinforced and prestressed concrete at P.S.G. College of Technology, Coimbatore, India.

97. Thaulow, S. - Apparent compressive strength of concrete as affected by height of test specimens and friction between the loading surfaces - Nordisk Betong, 1960-4.

98. Vitelmo, V., Bertero, W. & Ellippa, C. - Discussion of ductility of concrete by Roy & Sozen - Proceedings, International Symposium on the Flexural Mechanics on Reinforced Concrete, Miami, Florida, Nov. 1964.

99. Walther, R. - Calculation of the shear strength of reinforced and prestressed concrete beams by shear failure theory - London, C. & C.A. (Translation No. 110) - From Betou-Und-Stahlbetouban, V.57, No.11, Nov. 1962.

100. Yamashiro, R. & Siess, C.P. - Moment rotation characteristics of R.C. members subjected to bending, shear and axial load - Civil Engineering Studies, Structural Research Series, No. 260, Univ. of Illinois, Urbana, Dec. 1962.

A P P E N D I C E S

APPENDIX A

DETERMINATION OF STRESS-BLOCK PARAMETERS

A.1 Determination of K_1K_3:- (Fig. A.1)

$$F_{cc} = \tfrac{2}{3} f_o \, bnd_1 \left(\frac{e_o}{e_c}\right) + \left(\frac{e_c - e_o}{e_c}\right) . f_o \, bnd_1$$

or $$\frac{F_{cc}}{bnd_1} = \tfrac{2}{3} f_o . \left(\frac{e_o}{e_c}\right) + f_o . \frac{e_c - e_o}{e_c}$$

$$= f_o \left(1 - \tfrac{1}{3} \frac{e_o}{e_c}\right)$$

$$\frac{F_c}{f_o bnd_1} = K_1K_3 = \left(1 - \tfrac{1}{3} . \frac{e_o}{e_c}\right) \qquad \ldots (A.1)$$

A.2 Determination of K_2 & K_2/K_1K_3:- (Fig. A.1)

$$M = \tfrac{5}{8} . \frac{e_o}{e_c} . nd_1 . \tfrac{2}{3} . f_o \, bnd_1 + f_o \left(\frac{e_c - e_o}{e_c}\right) bnd_1 \left(\frac{e_o}{e_c} + \frac{e_c - e_o}{2e_c}\right) nd_1$$

$$M/f_o . b(nd_1)^2 = \frac{5}{12} \left(\frac{e_o}{e_c}\right)^2 + \left(\frac{e_c - e_o}{e_c}\right) \left(\frac{e_c + e_o}{2e_c}\right) \qquad \ldots (i)$$

$$\frac{M}{F_{cc}(nd_1)} = \frac{M/f_o b(nd_1)^2}{F_{cc}/bnd_1 f_o} = \frac{\frac{5}{12} \left(\frac{e_o}{e_c}\right)^2 + \left(\frac{e_c - e_o}{e_c}\right)\left(\frac{e_c + e_o}{2e_c}\right)}{\left(1 - \tfrac{1}{3} \frac{e_o}{e_c}\right)} \qquad \ldots (ii)$$

$$K_2 = 1 - M/F_{cc}(nd_1).$$

Thus the values of K_2 & $\frac{K_2}{K_1K_3}$ can be determined from equation (ii) and (A.1) above.

Table A.1 shows the values of the parameters K_1K_3, K_2 and K_2/K_1K_3 for different values of concrete strain.

TABLE NO. A.1

e_c	K_1K_3	K_2	K_2/K_1K_3
0.002	0.667	0.375	0.563
0.004	0.833	0.425	0.51
0.006	0.889	0.448	0.504
0.008	0.9167	0.46	0.502
0.01	0.9333	0.468	0.501
0.02	0.9667	0.483	0.50
0.03	0.9778	0.49	0.50
0.04	0.9833	0.492	0.50

APPENDIX B

TYPICAL CALCULATIONS FOR ROTATION & ULTIMATE MOMENT

B.1 Beam No. c.12:-

Compression reinforcement at support not effective.

$$K = \frac{f_o\ K_1K_3}{r_{st}e_c.E_{st}} = \frac{28.1 \times 0.667}{0.01465 \times 0.002 \times 0.2035 \times 10^6} = 3.14$$

$$n = \frac{-1 + \sqrt{1 + 4K}}{2K} = \frac{-1 + \sqrt{1 + 4 \times 3.14}}{2 \times 3.62} = \underline{0.427}$$

$$f_{st} = E_{st} \times e_c \times \frac{1 - n}{n} = 0.2035 \times 10^6 \times 0.002 \times \frac{0.573}{0.427}$$

$$= 0.545 \times 10^3 < 0.64 \times 10^3\ (f_{yt})$$

At $e_c = \underline{0.002}$

$$K_2n = 0.427 \times 0.375 = \underline{0.161}$$

Now $f_o = 2.35 \times (\frac{32.3}{0.8})^{\frac{2}{3}} = 28.1\ N/mm^2$

Approximate $l_p = \frac{600}{10} = 60$ mm < stirrups spacing

Therefore no additional stress due to links.

At <u>ultimate</u>, i.e. support section

Try $e_c = 0.035$

$$\left(\frac{n_u d_1 + b}{lp}\right)^2 \times 0.0035 = 0.035$$

or $$\left(\frac{n_u d_1 + b}{lp}\right) = \sqrt{10} = 3.165$$

$$f_o = 2.35\ U_w^{\frac{2}{3}} \left(\frac{n_u d_1 + b}{lp}\right)^{\frac{1}{3}} = 28.1 \cdot (3.165)^{\frac{1}{3}}$$

$$= 41.35\ N/mm^2$$

$$\frac{f_o bd_1}{F_{yt}} = \frac{41.35 \times 152.5 \times 272}{388 \times 10^3} = 4.42$$

$$\frac{K_2}{K_1 K_3} \times \frac{1}{f_o bd_1 / F_{yt}} = 0.5/4.42 = \underline{0.1132}$$

$$lp = \frac{(K_2 n)^{at\ 0.002} - (K_2/K_1K_3 \cdot F_{yt}/f_o bd_1)^{at\ ult}}{0.5 - \left(\frac{K_2}{K_1K_3} \cdot \frac{F_{yt}}{f_o bd_1}\right)^{ult}} \cdot (Z)$$

$$= \frac{0.161 - 0.1132}{0.387} \times 586 = \underline{71.0\ mm.}$$

$$(n_u d_1)^{at\ ult} = \frac{0.1132}{0.491} \times 272 = \underline{63\ mm.}$$

$\therefore$ average depth = <u>89.5 mm</u>

$$(nd_1)^{at\ 0.002} = 0.427 \times 272 = 116\ mm$$

<u>Check</u>:- $$\left(\frac{b + n'd_1}{lp}\right)^2 \times 0.0035 = \left(\frac{152.5 + 89.5}{71.0}\right)^2 \times 0.0035$$

$$= 0.0410 > 0.035.$$

Try 0.040:-

$$\left(\frac{n_u d_1 + b}{lp}\right) = \left(\frac{0.040}{0.0035}\right)^{\frac{1}{2}} = \underline{3.38}$$

$$f_o = 28.1 \times (3.38)^{\frac{1}{3}} = 42.10 \text{ N/mm}^2$$

$$lp = 600 \times \left(\frac{0.160 - 0.1112}{0.3888}\right) = \underline{73 \text{ mm}}.$$

$$\left.\begin{aligned} n_u d_1 &= \frac{0.1112}{0.49} \times 272 = 62 \text{ mm} \\ \& \; nd_1 &= 116 \text{ mm} \end{aligned}\right\} = \frac{178}{2} = \underline{89} \text{ mm } \underline{\text{average}}.$$

$$e_{cu} = \left(\frac{152.5 + 89}{73}\right)^2 \times 0.0035 = \underline{0.039}$$

Average $n'd_1$:- 89 mm & lp = 73 mm.

$$\theta_{cal} = \frac{0.039 \times 73}{89} \times \tfrac{3}{8} = \underline{0.012}$$

$$\theta_{cal}/\theta_{test} = 0.012/0.025 = \underline{0.480}$$

$$M_{ult_{cal}} :- \; 2.72 \times 388 \times \frac{10^3}{10^3}(1 - 0.1112) = 94{,}000 \text{ } \underline{\text{Nm}}$$

$$M_{ult_{test}} :- 101{,}800 \text{ Nm}$$

$$M_{cal}/M_{test} = \frac{94{,}000}{101{,}800} = \underline{0.92}$$

B.2 Corley's Test. Beam No:- M.5.

$$F_{yt} :- 2{,}270 \times 448 = 1{,}015{,}000 \text{ N}.$$

$$F_{yc} :- 142 \times 488 = \frac{69{,}500 \text{ N}}{945{,}500 \text{ N}}$$

$$\bar{z} = 1{,}830 \text{ mm}.$$

As before f_o = 26.1 + additional stress due to links (fig. B.2.1)

Assuming depth of N.A. = 26.1 + 0.48

$$= 26.58 \text{ N/mm}^2$$

$$0.1 \times p'' \times f_y = 0.1 \times 480 \times \frac{578 \times 71}{100.8 \times 152.5 \times 273}$$

$$= 0.48 \text{ N/mm}^2$$

From fig. B.2.2 :-

$$F_{cc} = 26.58 \times 0.667 \times 305 \times 179 \qquad 964{,}500 \text{ N}$$

$$F_{sc} = \frac{158.4}{179} \times 142 \times 0.002 \times 0.201 \times 10^6 = \underline{50{,}500} \text{ N}$$

$$1{,}015{,}000 \text{ N}$$

$$f_{st} = \frac{610 - 179}{179.0} \times 0.002 \times 0.201 \times 10^6 > 448 \text{ N/mm}^2$$

$$T = F_{yt} = 2{,}270 \times 448 = 1{,}015{,}000 \text{ N}$$

$$T = C.$$

K_2N at 0.002:- $\frac{179}{610} \times 0.375 = \underline{0.11}$

<u>At Ult</u>:-

$$\text{Try } e_{cu} = 0.025$$

$$\left(\frac{n_u d_1 + b}{lp}\right) = \sqrt{\frac{0.025}{0.0035}} = 2.68$$

$$f_o = 26.50 \times (2.68)^{\frac{1}{3}} + 0.48 = 36.25 + \frac{0.48}{36.73} \text{ N/mm}^2$$

$$\& \frac{f_o b d_1}{F_{yt}} = \frac{36.73 \times 305 \times 610}{945{,}500} = 7.21$$

$$lp = \frac{0.11 - \frac{0.5}{7.21}}{0.5 - \frac{0.5}{7.21}} \times 1{,}830 = \underline{173 \text{ mm}}$$

$$n_u d_1 = \frac{0.0693}{0.487} \times 610 = 87 \text{ mm}$$

Average neutral axis depth:- $\frac{179 + \frac{87}{266}}{2} = \underline{133 \text{ mm}}$

CHECK:- $e_{cu} = \left(\frac{305 + 133}{173}\right)^2 \times 0.0035 = \underline{0.0225}$

Try e_{cu} = 0.0233

As before:- f_o = 36.18 N/mm^2

$$lp = \frac{0.11 - 0.5/7.10}{0.5 - 0.5/7.10} \times 1,830 = \underline{160 \text{ mm}}$$

$n_u d_1$ = 88.0 mm

Average neutral axis depth:- $\frac{179.0 + 88.0}{267.0/2} = 133.50$

(In calculating effect of links this was assumed as 152.5 mm)

CHECK:- $e_{cu} = (\frac{305 + 133.50}{169})^2 \times 0.0035 = 0.0230$

$$\theta_{cal} = \frac{0.0230 \times 169}{133.50} \times \tfrac{3}{8} = 0.0110$$

$\theta_{cal}/\theta_{test}$ = 0.0110/0.009 = 1.18

$M_{ult_{cal}}$ = 945.5 x 610 x (1 - 0.07) + 65.5.589.4 + 7,800

= 585,000 N.m

$M_{ult_{test}}$ = 613,000 N.m

$M_{cal}/M_{test} = \frac{585,000}{613,000} = \underline{0.96}$

B.3 Mattock Test Beam No. D.4:-

z = 2790 mm

F_{yt} = 2,270 x 323 = 732,000 N

F_{yc} = 142 x 313 = = $\frac{45,400 \text{ N}}{686,600 \text{ N}}$

f_o = 24.7 + due to links = 24.7 + 0.69(say) = 25.39 N/mm^2

At e_{cu} = 0.002

Fig. D.4.2.

$$c = \begin{cases} F_{cc}:- & 152.5 \times 0.677 \times 266 \times 25.39 = 685{,}000 \text{ N.} \\ F_{sc}:- & \frac{254.4}{266} \times 142 \times 0.002 \times 0.1945 \times 10^6 \end{cases}$$

$$= 51{,}000$$

$$732{,}000 \text{ N}$$

$$f_{yt} = \frac{242}{266} \times 0.002 \times 0.1945 \times 10^6 = 354 \text{ N/mm}^2 > 323 \text{ N/mm}^2$$

$$T = F_{yt} = 732{,}000 \text{ N} = c$$

$$K_2 n = \frac{266}{508} \times 0.375 = 0.196$$

At ultimate:-

Try $e_{cu} = 0.01$

As before:- $f_o = 29.41 + 0.69 = 30.1 \text{ N/mm}^2$

$lp = 370$ mm $\quad (n' d_1 + b) \not> lp.$

average.

Try $e_{cu} = 0.008$

$f_o = 29.41 \text{ N/mm}^2$

$lp = 346$ mm $\quad n_u d_1 = 169$ mm

Average depth of NA $= 169 + \frac{266}{435/2}$

$= 217.5$ mm

Fig D.4.1.

$(\frac{217.5 + 152.5}{0.346})^2 \times 0.0035 < 0.008$

$2 \times (217.5 - 16) + 152.5 - 32$

$= \frac{403}{120.5}$

$(\frac{523.5 \times 71}{63.5 \times 120.5 \times 201.5}) = 0.0241 \times 0.1 \times 313 = \underline{0.75 \text{ N/mm}^2}$

Assumed 0.69 N/mm^2

$p'' = 2.41\%$ $\therefore$ $e_{cu} = \underline{0.008}$ min.

i.e. H/d 2.

$$e_{cu} = 0.35 \times 0.0241 \times \left(\frac{346}{63.5}\right)^{\frac{2}{3}} \times \frac{120.5 \times 201.5}{152.5 \times 217.5} \times \frac{22.5}{33.6}$$

$$= 0.01275$$

$$\theta_{cal} = \frac{0.01275 \times 346}{217.5} \times \frac{3}{8} = 0.0076$$

$$\theta_{cal}/\theta_{test} = \frac{0.0076}{0.0079} = 0.96$$

$$M_{ult(cal)} = 508 \times 0.847 \times 686.600 + 45.400 \times 488 + 7,700$$

$$= 324,000 \text{ Nm}$$

M_{test} = 315,000 Nm.

$$M_{cal}/M_{test} = \frac{324,000}{315,000} = 1.03$$

APPENDIX C

CALCULATION OF M_{ult} & θ_u FOR R.C. BEAMS BY OTHER METHODS

C.1 Corley's Method:-

Assumptions:- 1. At commencement of yield of the tension reinforcement, the concrete compressive stresses vary linearly from zero at the neutral axis to a maximum at the compression face of the beam, as shown in fig. c.1.

2. At ultimate strength, i.e. at maximum moment, the concrete compressive stresses are distributed in a nonlinear

manner as indicated in fig. c.2, and the magnitude and location of the resultant concrete compressive force can be expressed in terms of coefficients $K_1' K_2'$ & K_3' and the dimensions of the compressive zone.

3. Tensile strength of the concrete may be neglected.

4. The strain in the concrete at the various section levels may be assumed directly proportional to the distance from the neutral axis. Except in anchorage regions, strain in reinforcing bars is assumed equal to the tensile or compressive strain in the concrete at the same distance from the neutral axis as the centroid of each bar or group of bars considered.

5. The stress-strain curve for the tension reinforcing steel is assumed to be of tri-linear form, as shown in fig. c.3. For steel strains below the yield strain e_y, the steel stress is assumed equal to $E_s e_s$. For steel strains between commencement of yield and commencement of strain hardening, the steel stress is assumed constant and equal to the yield point stress f_y. For steel strains beyond the commencement of strain hardening, the steel stress is assumed equal to $f_o' + e_s E_s'$, as shown in fig. c.3.

6. At ultimate strength it is assumed that the compression reinforcement has yielded and that the stress in it is constant and equal to the yield point stress f_{yc}.

Conditions at Commencement of Yield:-

From a consideration of the properties of the transformed section it can be shown that:

$$n = \sqrt{\left\{r_{sc}(m-1) + m.r_{st}\right\}^2 + 2\left\{m.r_{st} + r_{sc}(1 - j_s)(m-1)\right\}} - \left\{r_{sc}(m-1) - m.r_{st}\right\} \qquad \ldots (c.1)$$

From the distribution of stresses of fig. c.1:-

$$f_{sc}/f_c = m(n + j_s - 1)/n \qquad \ldots (c.2)$$

From equilibrium of forces:-

$$f_c = \frac{r_{st} \cdot f_{yt}}{\frac{n}{2} + r_{sc} \cdot \frac{f_{sc}}{f_c}} \qquad \ldots (c.3)$$

Substituting for f_{sc}/f_c in equation (c.2) yields:-

$$f_c = \frac{r_{st} \cdot f_{yt}}{\frac{n}{2} + m.r_{sc}\left(\frac{n + j_s - 1}{n}\right)} \qquad \ldots (c.4)$$

Then the yield moment M_y is given by,

$$M_y = \tfrac{1}{2}.f_c.n\ bd_1^2\left(1 - \tfrac{n}{3}\right) + j_s.d_1A_{sc}.f_{sc} \qquad \ldots (c.5)$$

The curvature at commencement of yield ψ_y' is obtained from consideration of the distribution of strains:- (fig. c.1)

$$\psi_y = \frac{e_y}{d(1 - K)} \qquad \ldots (c.6)$$

Conditions at Ultimate Moment:-

$$K_1'K_3'.U_{cyl}.b.c' + f_{yc}.A_{sc} = f_{st}.A_{st}$$

$$c' = \frac{f_{st}.A_{st} - f_{yc}.A_{sc}}{b.K_1'K_3'.U_{cyl}} = d.\frac{r_{st}.f_{st} - r_{sc}.f_{yc}}{K_1'K_3'\ U_{cyl}} \qquad \ldots (c.7)$$

Ultimate moment of internal forces:-

$$M_{ult} = K_1'K_3'.U_{cyl}.b.c'(d_1 - K_2c') + f_{yc}.A_{sc}.j_s.d_1 \qquad \ldots (c.8)$$

Substituting the value of c':-

$$M_{ult} = bd_1^2\{(r_{st}.f_{st} - r_{sc}.f_{yc})\left(1 - \frac{K_2}{K_1'K_3'}.\frac{r_{st}.f_{st} - r_{sc}.f_{yc}}{U_{cyl}}\right) + r_{sc}.j_s.f_{yc}\} \qquad \ldots (c.9)$$

M_{ult} may be calculated if f_{st} is known.

From compatibility of strain:-

$$\frac{c'}{d_1} = \frac{e_{cu}}{e_s + e_{cu}} \quad \ldots (c.10)$$

From equilibrium of internal forces:-

$$\frac{c'}{d} = \frac{r_{st}.f_{st} - r_{sc}.f_{yc}}{K_1 K_3 . U_{cyl}} \quad \ldots (c.11)$$

Solving (c.10) & (c.11) yields:-

$$f_{st} = \frac{1}{r_{st}} \left\{ K_1 K_3 \, U_{cyl} \left(\frac{e_{cu}}{e_s + e_{cu}}\right) + r_{sc}.f_{yc} \right\} \quad \ldots (c.12)$$

Case 1: Stress in Tension Reinforcement below yield point.

$$e_s = f_{st}/E_s$$

Substituting for e_s in equation (c.12) and solving yields,

$$f_s = \sqrt{\tfrac{1}{4}\left(e_{cu}.E_s - \frac{r_{sc}}{r_{st}} . f_{yc}\right)^2 + \frac{e_{cu}.E_s}{r_{st}} \left(K_1 K_3 \, U_{cyl} + r_{sc}.f_{yc}\right)} - \tfrac{1}{2}\left(e_{cu}.E_s - \frac{r_{sc}}{r_{st}} . f_{yc}\right) \quad \ldots (c.13)$$

Case 2: Stress in Tension Reinforcement equal to yield point stress.

Then $f_{st} = f_{yt}$.

Case 3: Stress in Tension Reinforcement above yield point.

From fig. c.3:-

$$e_s = (f_{st} - f'_o)/E'_s \quad \ldots (c.14)$$

Solving equations (c.12) & (c.14) yields:-

$$f_s = \sqrt{\tfrac{1}{4}\left(e_{cu}.E'_s - f'_o - \frac{r_{sc}}{r_{st}}.f_{yc}\right)^2 + \frac{1}{r_{st}}\left(K_1 K_3 . U_{cyl} . e_{cu} . E'_s + r_{sc}.f_{yc}.E'_s - r_{sc}.f_{yc}.f'_o\right)} - \tfrac{1}{2}\left(e_{cu}.E'_s - f'_o - \frac{r_{sc}}{r_{st}}.f_{yc}\right) \quad \ldots (c.15)$$

In order to determine whether the reinforcement stress at ultimate is below, equal to, or above the yield point, the critical values of $(q - q')$ corresponding to $e_s = e_y$ & $e_s = e_{sh}$ must be calculated.

Solving equations (c.10) & (c.11) and transposing, yields:-

$$\frac{r_{st} \cdot f_{sy} - r_{sc} \cdot f_{yc}}{K_1' K_3' \cdot U_{cyl}} = \frac{e_{cu}}{e_s + e_{cu}} \qquad \ldots (c.16)$$

Now, when $e_s = e_y$ & e_{sh}, $f_{st} = f_{yt}$.

$$\frac{r_{st} \cdot f_{yt} - r_{sc} \cdot f_{yc}}{U_{cyl}} = \frac{K_1' K_3' \cdot e_{cu}}{e_s + e_{cu}}$$

$$\text{i.e. } (q - q') = \frac{K_1' K_3' \cdot e_{cu}}{e_s + e_{cu}} \qquad \ldots (c.17)$$

When $e_s = e_y$, balanced conditions occur at ultimate,

$$(q - q')_b = \frac{K_1' K_3' \cdot e_{cu}}{e_y + e_{cu}} \qquad \ldots (c.18)$$

When $e_s = e_{sh}$, strain hardening of the reinforcement is about to commence,

$$(q - q')_{st} = \frac{K_1' K_3' \cdot e_{cu}}{e_{sy} + e_{cu}} \qquad \ldots (c.19)$$

Hence if $(q - q') > (q - q')_b$, $f_{st} < f_{yt}$ at ultimate, i.e. Case 1.

If $(q - q')_b > (q - q') > (q - q')_{st}$, $f_{st} = f_{yt}$ at ult.i.e. Case 2.

If $(q - q')_{st} > (q - q')$, $f_{st} > f_{yt}$ at ultimate, i.e. Case 3.

The curvature at ultimate ψ_u, is obtained from a consideration of the distribution of strains (see fig. c.2).

For cases (1) & (3),

$$\psi_u = \frac{e_s + e_{cu}}{d_1} \qquad \ldots (c.20)$$

The value of e_s used in equation (c.20) will be the strain corresponding to the calculated steel stress at ultimate obtained from equation (c.13) or (c.14) as the case may be.

For case 2, where $f_{st} = f_{yt}$,

Substituting $f_{st} = f_{yt}$ in equation (c.11) yields,

$$c' = d_1\left(\frac{r_{st} \cdot f_{yt} - r_{sc} \cdot f_{yc}}{K_1 K_3 U_{cyl}}\right)$$

$$\text{i.e. } c' = \frac{d_1}{K_1 K_3}(q - q') \qquad \ldots (c.21)$$

Then, curvature at ultimate, $\psi_u = e_{cu}/c' \qquad \ldots (c.22)$

Values of e_{cu}, E_c & K_1, K_2 & K_3 used in calculations:

e_{cu} = the maximum concrete compressive strain at ultimate strength

$$= 0.003 + 0.02\frac{b}{z} + \left(\frac{p' \cdot f_{yh}}{20}\right)^2 \qquad \ldots (c.23)$$

where z is measured in inches.

E_c - the modulus of elasticity of the concrete was taken as:-

$E_c = 60{,}000\sqrt{U_{cyl}}$ E_c & U_{cyl} are in lbs/sq.inch

K_1 = 0.85 for strengths U_{cyl} up to 4000 p.s.i.

For U_{cyl} above 4000 p.s.i., K_1 is reduced continuously at a rate of 0.05 for each 1,000 p.s.i. of strength in excess of 4,000 p.s.i.

$K_2 = 0.425$ & $K_3 = 0.85$

Inelastic Rotation:-

The inelastic rotation θ_u occuring in a length of the beam equal

to half the effective depth and located adjacent to the section of maximum moment was calculated using the following equation obtained from a consideration of the relationship shown in Fig. c.4.

Inelastic rotation:-

$$\theta_u = \phi_u - \phi_y \cdot \frac{M_{ult}}{M_{yield}}$$

where $\phi_u = \psi_u \cdot \frac{d_1}{2}$ $\phi_y = \psi_y \cdot \frac{d_1}{2}$,

ψ_u & ψ_y being the curvatures at ultimate and at yield of the reinforcement.

C.2 I.C.E. Research Committee Report:-

Ultimate Moment

Calculations of the strength of sections in resisting bending for various grades of concrete and kinds of steel reinforcement are based on the following assumptions:-

i) The distribution of strain across the section is linear (except for influence of F when not equal to one).

ii) The ultimate distribution of compression stress in the concrete is parabolic (or an equivalent distribution).

iii) The moment/curvature relation for members is idealised as shown in fig. c.5. Limits L_1 & L_2 are defined by the characteristics of the concrete & steel, and values are assumed for the influential parameters to ensure that the calculated strength and deformation are safe as compared with test results.

At Ultimate:- (Fig. c.6)

$f_c = 0.85\ U_w$; $e_{cu} = 0.0035$; e_{su} = From test result at L_2;

$K_2 = \frac{3}{8}$; $n_u = \frac{A_{st} \cdot f_{yt} - A_{sc} \cdot f_{sc}}{\frac{2}{3} \times bd_1 \times f_c}$

& $M_{ult} = A_{st} \cdot f_{yt}(1 - K_2 n_u)d_1 + A_{sc} \cdot f_{sc} \cdot (d_1 - d_2)$ ... (c.24)

The stresses in compression steel are based on strain values, deduced from linear distributions of strain across the section, in conjunction with the stress/strain curve for steel.

Plastic Rotation

In idealised structures, hinge rotation occurs only in the plastic phase, and hence θ_u is the total ultimate rotation less the elastic rotation, within the plastic zone. For simplicity in order to simulate the rotational behaviour of a beam as obtained from tests to an equivalent beam, the curvature at a plastic hinge measured from tests is idealised to a constant curvature over a plastic length lp.

An empirical formula is given for plastic rotation based upon the concrete compressive strain, ultimate neutral axis depth and an equivalent plastic length as given below.

The length of plastic zone is $lp = K_4 K_5 K_6 (\frac{z}{d_1})^{\frac{1}{4}} d_1$ ... (c.25)

$$\theta_u = \frac{e_{cu} - e_o}{n_u d_1} \cdot lp \qquad \text{... (c.26)}$$

The values of e_{cu} & e_o are given as 0.0035 & 0.002, respectively. The value of $n_u d_1$ is obtained from the condition of equilibrium of forces at ultimate.

The values of K_4, K_5, K_6 are as follows.

K_4 = 0.7 for mild steel. K_4 = 0.9 for cold worked steel.

K_5 = 1 for members without axial load.

K_6 = 0.6 when U_w = 6,000 p.s.i & K_6 = 0.9 when U_w = 2,000 p.s.i.

(Intermediate values by proportion)

APPENDIX D

D.1 Simplified Equation for Rotation:-

For under-reinforced beams, which constitute the majority of beams in design, assuming yielding of the tension steel by a strain e_c = 0.002; equation (5.8) can be modified to

$$lp = \frac{M}{Q} \cdot \frac{\left\{ \left(\frac{K_2}{K_1K_3}\right)^{0.002} - \left(\frac{K_2}{K_1K_3}\right)^{ult} \right\} \frac{r_{st} \cdot f_{yt}}{2.35\ U_w^{\frac{2}{3}}}}{0.5 - \left(\frac{K_2}{K_1K_3}\right)^{ult} \frac{r_{st} \cdot f_{yt}}{2.35\ U_w^{\frac{2}{3}}}}$$

From Table A.1

$$lp = \frac{M}{Q} \cdot \frac{(0.56 - 0.50)\ \frac{r_{st} \cdot f_{yt}}{2.35\ U_w^{\frac{2}{3}}}}{0.5\left(1 - \frac{r_{st} \cdot f_{yt}}{2.35\ U_w^{\frac{2}{3}}}\right)}$$

$$= \frac{M}{Q} \cdot 0.05 \frac{r_{st} \cdot f_{yt}}{U_w^{\frac{2}{3}}} \Big/ 1 - 0.43 \cdot \frac{r_{st} \cdot f_{yt}}{U_w^{\frac{2}{3}}}$$

If $r_{st} \cdot f_{yt} / U_w^{\frac{2}{3}} = \psi$,

$$lp = \frac{M}{Q} \cdot \frac{\psi \cdot 0.05}{1 - 0.43\psi} \qquad \ldots (D.1)$$

From equation (5.9)

$$\theta_u = \frac{0.375 \cdot e_{cu} \cdot lp}{n'd_1}$$

$$= 0.375 \cdot 0.0035\left(\frac{b + nd_1}{lp}\right)^2 \cdot \frac{lp}{n'd_1}$$

$$\frac{0.0013 \cdot d_1(b/d_1 + n')^2}{lp \cdot n'} \qquad \ldots (D.2)$$

From Table A.1:-

$$n_{0.002} = \frac{r_{st} \cdot f_{yt}}{1.57\ U_w^{\frac{2}{3}}} = 0.64\ r_{st} \cdot f_{yt} \qquad \ldots (D.3)$$

& n_{ult} (say at a strain of 0.01) $= \dfrac{r_{st} \cdot f_{yt}}{2.19\ U_w^{\frac{2}{3}}}$

$$= 0.46\ r_{st} \cdot f_{yt} \qquad \ldots (D.4)$$

$$\text{Average } n' = \frac{n_{0.002} + n_{ult}}{2}$$

$$= 0.55\ \psi_l \qquad \ldots (D.5)$$

Putting the values of n' & lp in equation (D.2):-

$$\theta_u = \frac{0.0013 \cdot d_1 (\frac{b}{d_1} + 0.55\psi_l)^2}{\frac{M}{Q} \cdot \frac{0.05 \cdot \psi_l}{(1 - 0.43\psi_l)} \cdot 0.55\psi_l}$$

$$= \frac{0.0013 (\frac{Q \cdot d_1}{M}) \cdot (\frac{b}{d_1} + 0.55\psi_l)^2 \cdot (1 - 0.43\psi_l)}{0.0275\ \psi_l^2}$$

$$= \frac{0.047 \cdot (\frac{Qd_1}{M}) \cdot (\frac{b}{d_1} + 0.55\psi_l)^2 (1 - 0.43\psi_l)}{\psi_l^2} \qquad \ldots (D.6)$$

Plotting $\theta_u$cal as calculated from equation (D.6) against $\theta_u$test in figure D.1, it is observed that the correlation is reasonable. The value of the part of the equation dependent on ψ_l can be read from figure D.2.

APPENDIX E

EXPRESSION FOR BOND FORCE WITH INCLINED STIRRUPS

Resolving vertically:-

$$A_{sq} \cdot f_{yq} \cdot \frac{1}{s} \cdot \text{Sin}\,\alpha = f_{cw} \cdot b_r \cdot l \cdot \text{Sin}\,\theta_w^2$$

$$f_w \cdot b_r \cdot l = A_{sq} \cdot f_{yq} \cdot \frac{1}{s} \cdot \frac{\text{Sin}\,\alpha}{\text{Sin}^2\theta_w} = r_{sq} \cdot f_{yq} \cdot \frac{\text{Sin}^2\alpha}{\text{Sin}^2\theta_w}$$

Resolving horizontally:-

$$A_{sq}.f_{yq} \cdot \frac{1}{s} \cdot \text{Cos}\alpha + f_{cw} .b_r.l.\text{Sin}\ \theta_w.\text{Cos}\ \theta_w = f_b.l$$

$$\frac{A_{sq}.f_{yq}}{s\ \text{Sin}\alpha} = r_{sq}.f_{yq} \cdot \qquad \text{Hence :-}\ \frac{A_{sq}.f_{yq}}{s} = r_{sq}.f_{yq}\ \text{Sin}\alpha$$

$$\text{and } r_{sq}.f_{yq}.\text{Sin}\,\alpha\,.\text{Cos}\alpha + r_{sq}.f_{yq}.\frac{\text{Sin}^2\alpha}{\text{Sin}^2\theta_w} \cdot \text{Sin}\ \theta_w.\text{Cos}\ \theta_w = f_b$$

$$\text{Therefore } \underline{f_b = r_{sq}.f_{yq}\ (\text{Cos}\alpha + \text{Sin}\alpha\ .\text{Cot}\ \theta_w)\cdot}$$

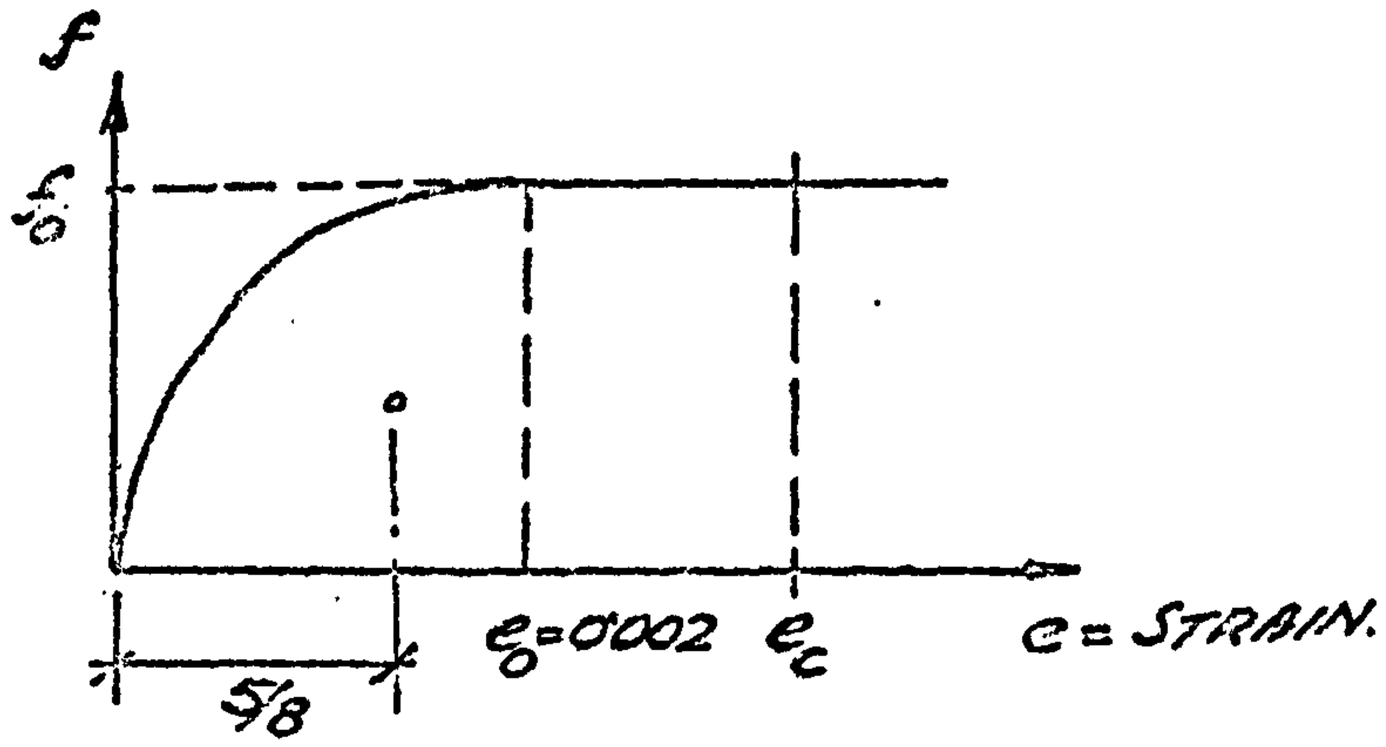


FIG. B.1. STRESS-BLOCK.

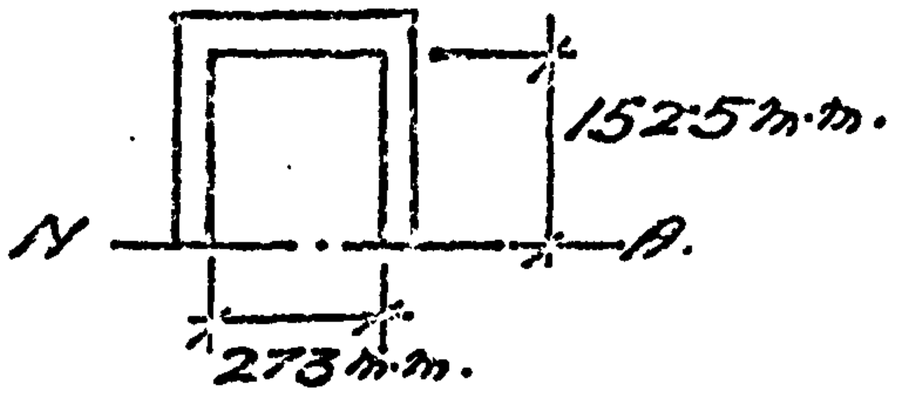


FIG. B.2.1.

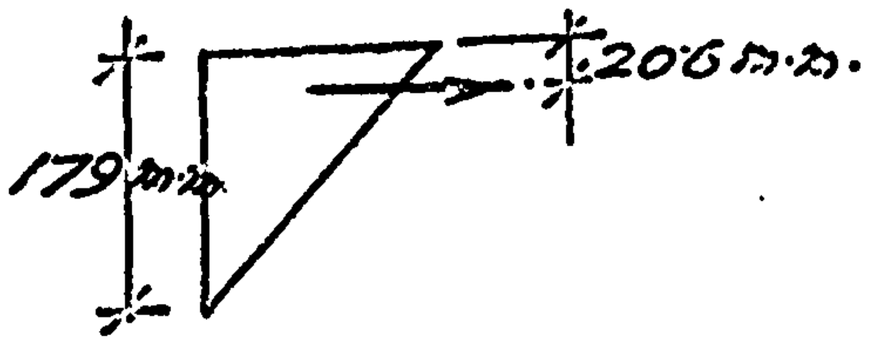


FIG. B.2.2.

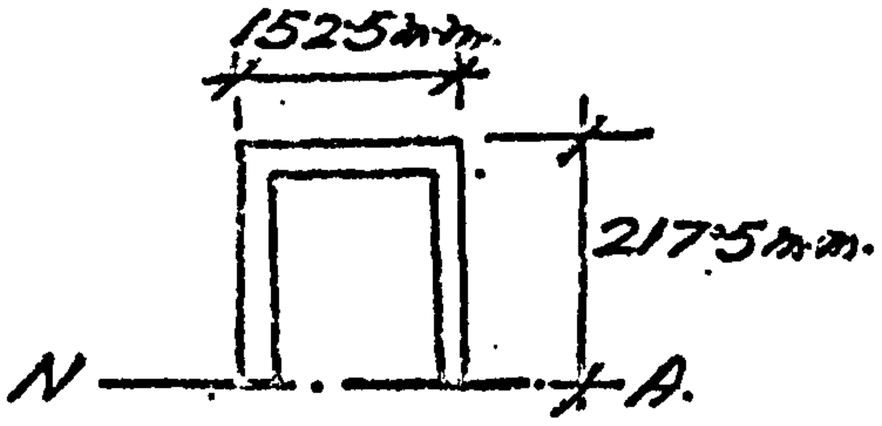


FIG. D.4.1.

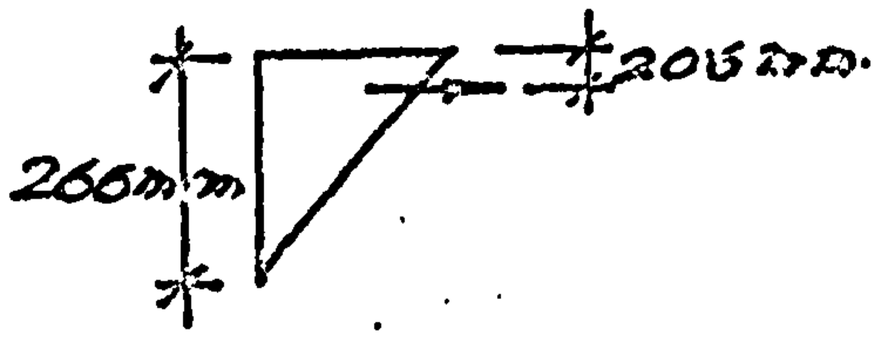


FIG. D.4.2.

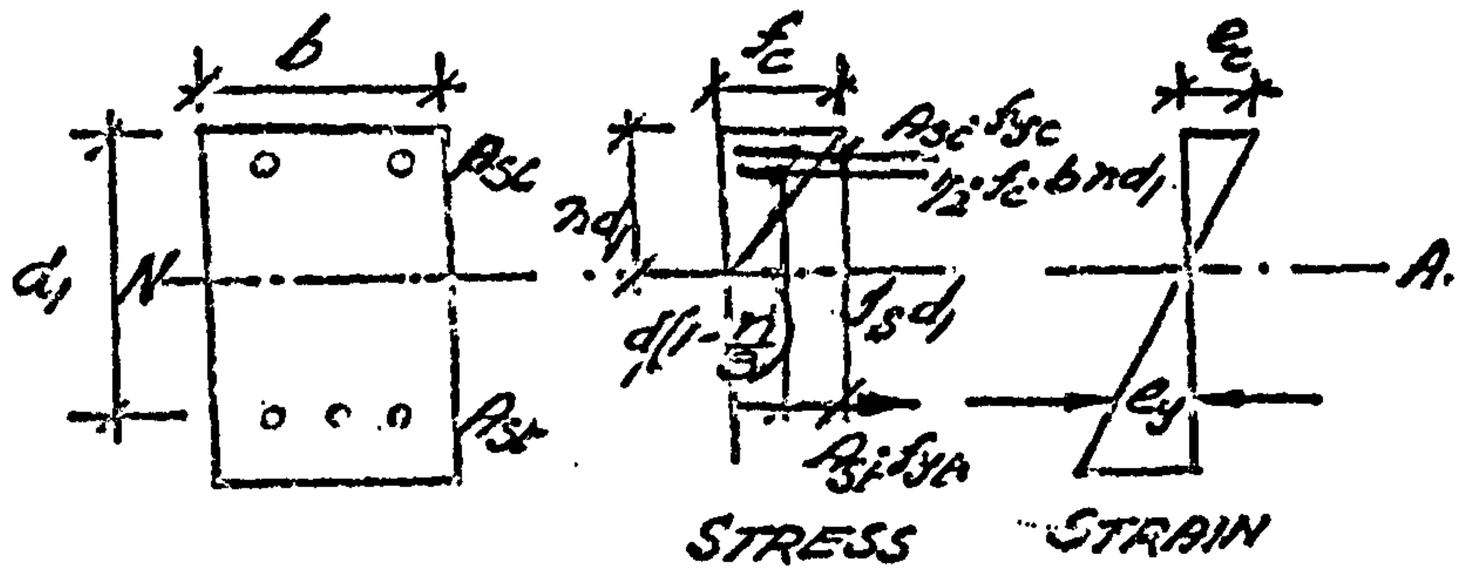


FIG. C.1. CONDITION AT YIELD OF TENSION REINF'T.

FIG. C.2. CONDITIONS AT ULTIMATE.

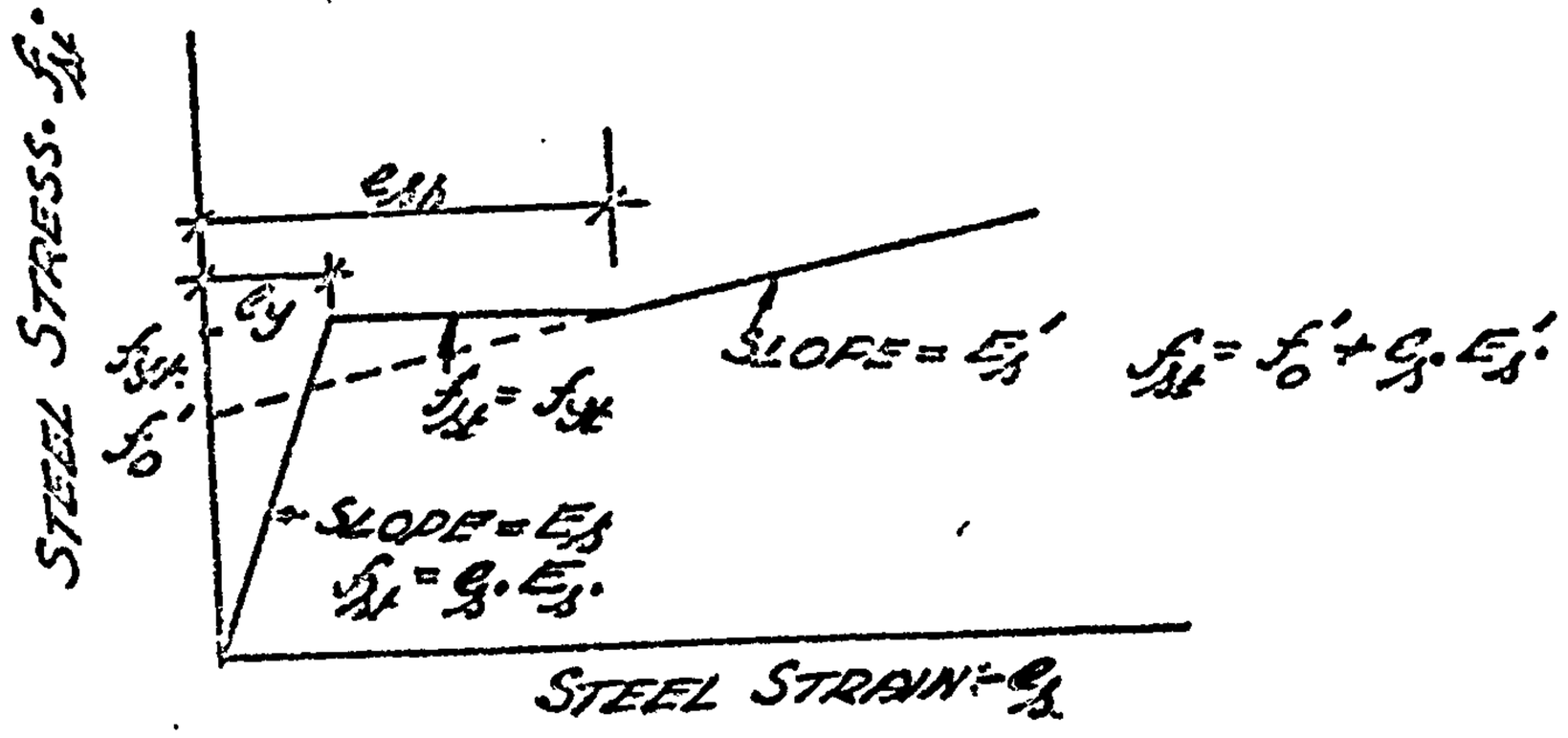


FIG. C.3. IDEALISED REINFORCEMENT STRESS-STRAIN CURVE.

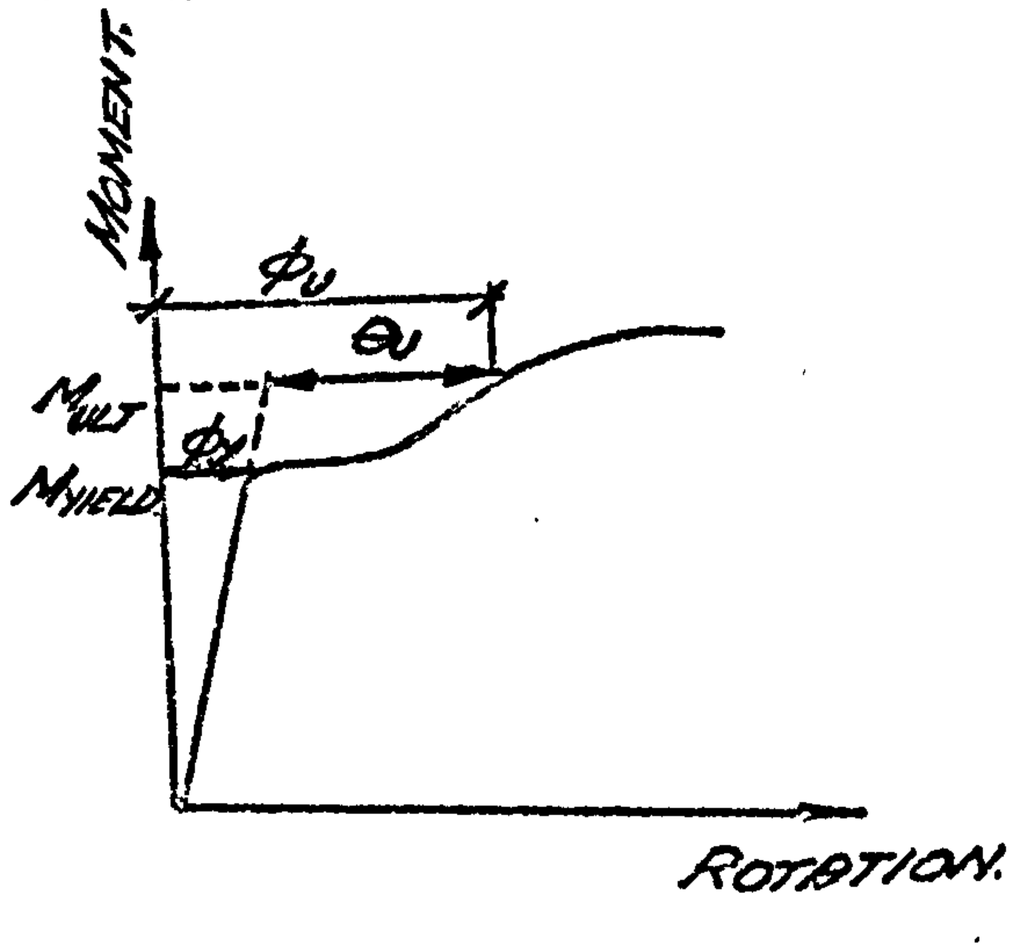


FIG. C.4. TYPICAL MOMENT/ROTATION CURVE.

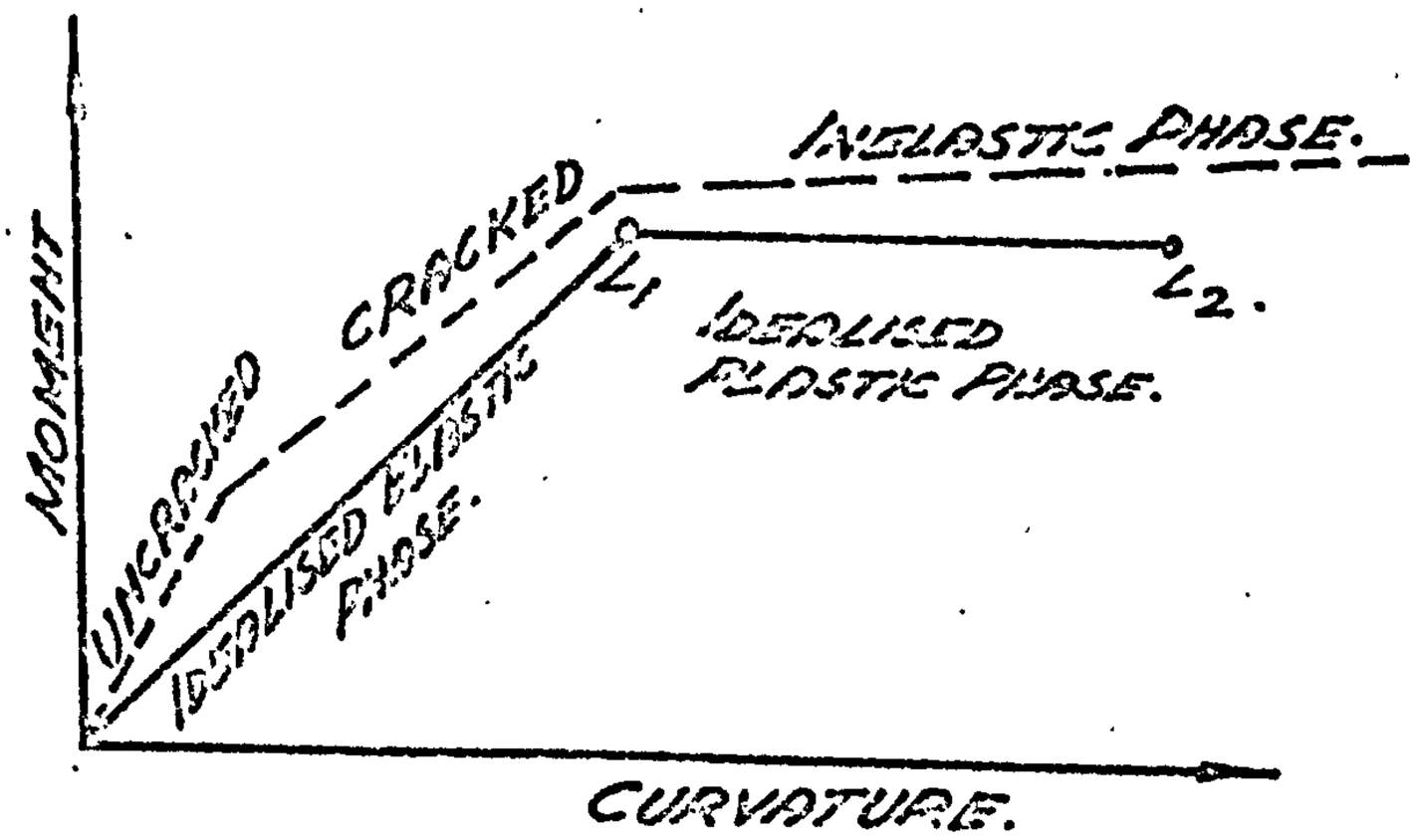


FIG. C.5. IDEALISED MOMENT/CURVATURE RELATION.

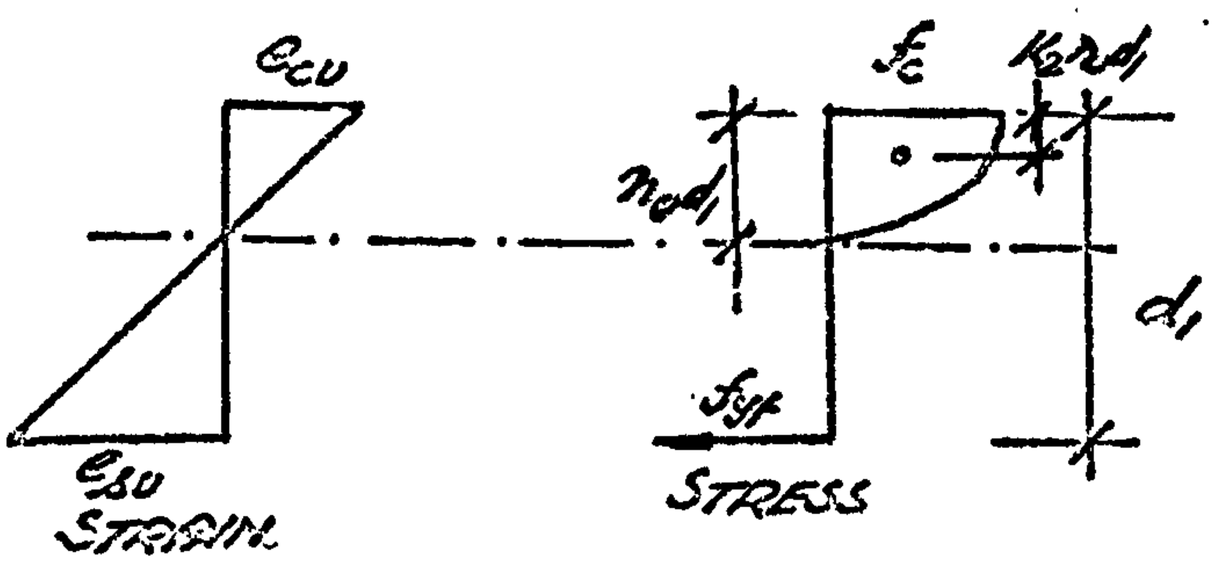


FIG. C.6. STRESS-STRAIN DISTRIBUTION AT ULTIMATE.

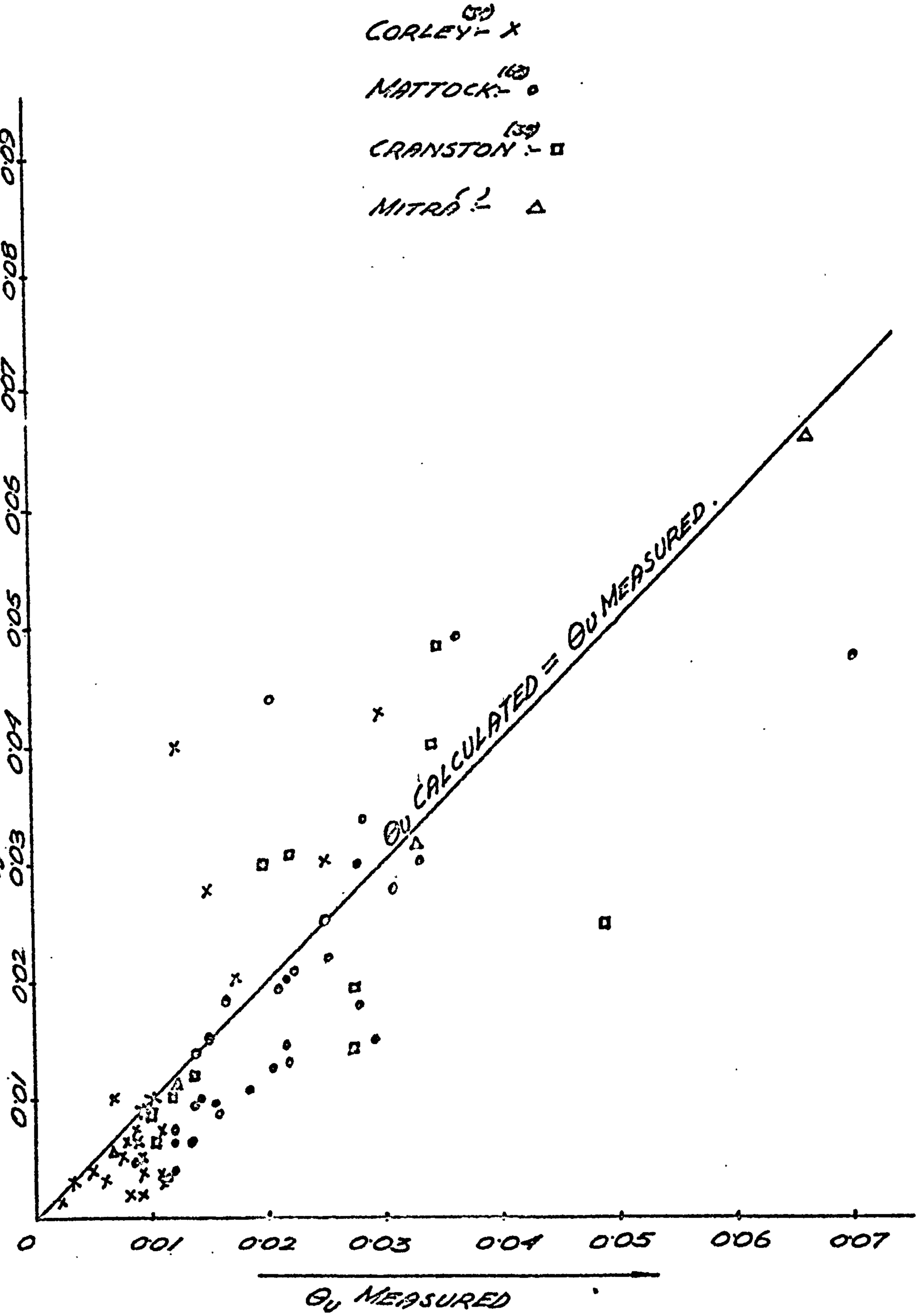


FIG. D.1. CALCULATED & MEASURED PLASTIC ROTATION.

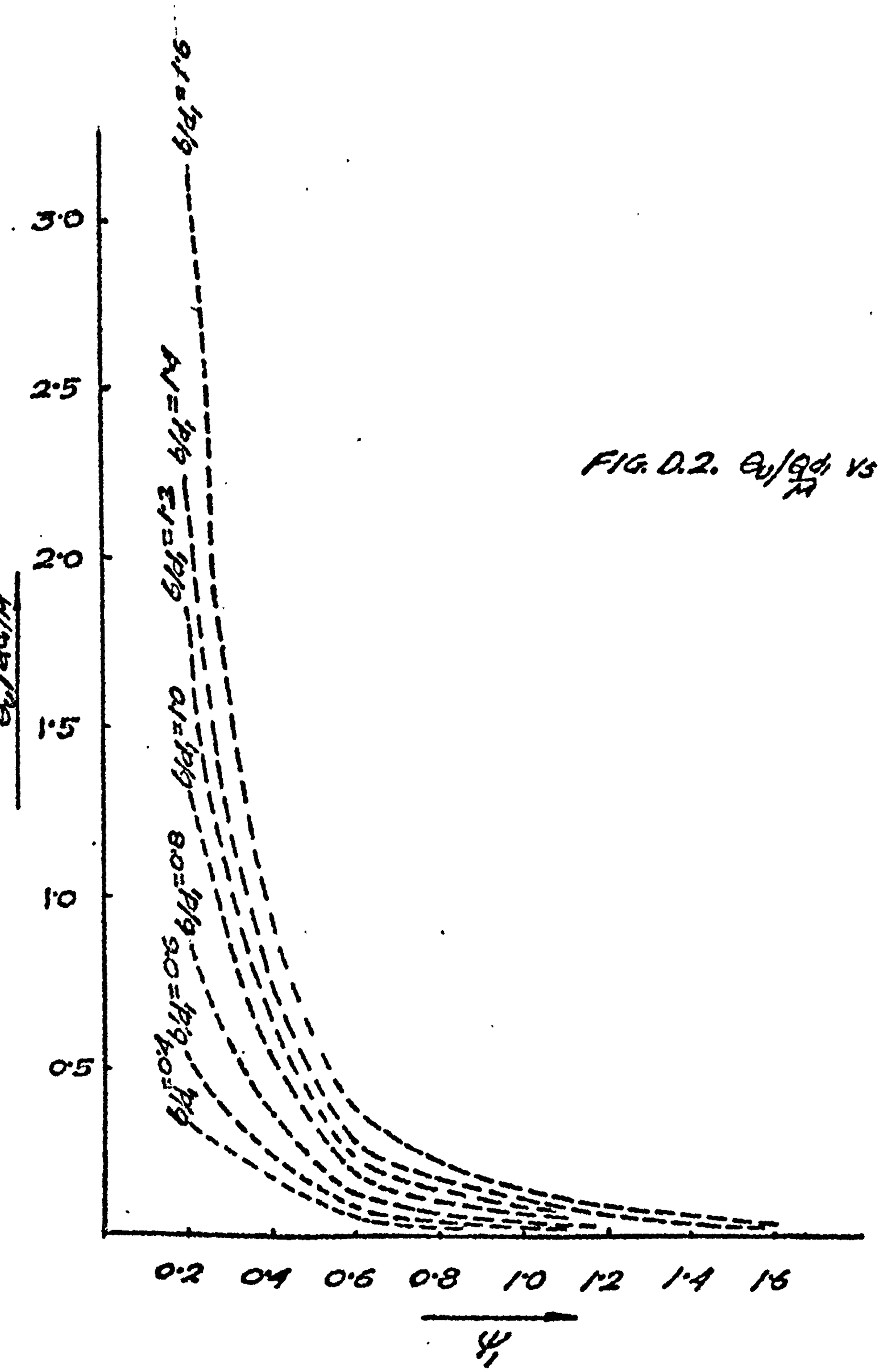


FIG. 0.2. $Q_M/Q_{d/M}$ vs H/H_1.